

ABSTRACT

Title of dissertation: THE SYNTHESIS OF A DIVERSE LIBRARY OF AI-2 ANALOGS TO INVESTIGATE BACTERIAL QUORUM SENSING

Jacqueline A.I. Smith, Doctor of Philosophy, 2011

Directed by: Assistant Professor Herman O. Sintim, Department of Chemistry & Biochemistry

Bacteria have evolved several mechanisms to promote their survival, which sometimes come at the cost of human health. They use toxins known as virulence factors to cause the symptoms associated with infections. They also form communities called biofilm, which allow them to thrive and resist attacks by the host's immune system. Conventional antibiotics fail to penetrate the biofilm matrix. The expression of virulence factors and formation of biofilm are both regulated by a phenomenon known as quorum sensing. Quorum sensing is a form of cell-to-cell communication, which allows bacteria to coordinate gene expression via the secretion of signaling molecules, known as autoinducers, and the subsequent detection of these molecules. The ultimate goal of this dissertation was to identify new small molecules that would be used to disrupt quorum sensing in bacteria. AI-2, which is a universal quorum sensing autoinducer, found in over 60 bacterial species, was targeted. In this study a new facile synthesis of AI-2 was achieved and this new methodology was adapted to the synthesis of a library of analogs.

These analogs were screened for their ability to modulate AI-2 mediated quorum sensing in *Vibrio harveyi*, *Escherichia coli*, *Salmonella typhimurium* and *Pseudomonas aeruginosa*. It was found that AI-2 analogs were able to cause synergistic agonism of bioluminescence in *V. harveyi*. Furthermore, several analogs were able to repress quorum sensing in *E. coli* yet very few analogs were active in the homologous quorum sensing system of *S. typhimurium*. These analogs were processed by the AI-2 processing enzymes in *E. coli*. Finally some AI-2 analogs were found to inhibit quorum sensing in *P. aeruginosa* in pure culture as well as in mixed cultures. These findings will provide the framework for the development of new small molecules which are able to modulate quorum sensing and thus act as tools in the inhibition of bacterial virulence and biofilm formation.

THE SYNTHESIS OF A DIVERSE LIBRARY OF AI-2 ANALOGS TO
INVESTIGATE BACTERIAL QUORUM SENSING

By

Jacqueline A.I. Smith

Dissertation submitted to the Faculty of the Graduate School of the
University of Maryland, College Park, in partial fulfillment
of the requirement for the degree of
Doctor of Philosophy
2011

Advisory Committee:
Assistant Professor Herman O. Sintim
Professor Philip DeShong
Professor Daniel Falvey
Assistant Professor Nicole LeBlanc-LaRonde

Copyright by
Jacqueline A.I. Smith
2011

Dedication

This dissertation is dedicated to my daughter Jasmine, my mom Phyllis and the entire
Smith and Watkins families.

In loving memory of my grandmother Mary Alice Watkins

Acknowledgements

I would like to thank God for blessing me with the ability to pursue this degree and for giving me strength and peace as I went through graduate school. Thank you Jesus! I would like to thank my advisor Dr. Herman Sintim for guiding my research and giving me insight into the scientific profession. I would also like to thank my family for supporting me; and all my friends, especially Kathy and Rey, for keeping me grounded as I went through this journey. I would like to thank my church Light of the World Family Ministries for their support and prayers. I thank the Meyerhoff Scholarship Program and my friends from UMBC for encouraging me to pursue my PhD and staying in contact with me over the years.

I would like to acknowledge my collaborators Dr. William E. Bentley (and the Bentley Lab), and Dr. Vincent Lee (and the Lee Lab). Special thanks goes to Varnika Roy for conducting the β -galactosidase screening, *in vitro* phosphorylation TLC and synthetic ecosystem experiments shown in Chapter 3. Also thanks to my labmate Jingxin Wang for help with characterization of the quinoxaline derivatives and Sonja Gamby for help with analogs in Chapter 2. I would like to acknowledge my dissertation committee members Dr. Philip DeShong, Dr. Nicole LaRonde-LeBlanc, Dr. Daniel Falvey, Dr. Sergei Sukarahev. I'd like to thank the NFS Bridge to the Doctorate Fellowship (2006-2008), GAANN Fellowship (2009-2010) and the Ann E. Wiley Dissertation Fellowship (Spring 2011) for financial support. Finally I would like to thank the entire staff of the University of Maryland Department of Chemistry and Biochemistry for their support.

Table of Contents

Dedication.....	ii
Acknowledgements.....	iii
Table of Content.....	iv
List of Tables.....	vi
List of Figures.....	vii
List of Schemes.....	xi
List of Abbreviations.....	xii
Chapter One: Introduction.....	1
1.1 New approaches to anti-infective chemotherapy.....	1
1.2 Quorum sensing in gram-negative and gram-positive bacteria.....	4
1.3 Quorum sensing inhibitors.....	6
1.4 Autoinducer-2 mediated quorum sensing.....	13
1.5 AI-2 inhibitors.....	22
1.6 Objective, hypothesis and specific aims.....	25
1.7 Dissertation outline.....	26
Chapter Two: Facile synthesis of AI-2 and a diverse library of analogs.....	27
2.1 Introduction: Discovering the chemical identity of AI-2.....	27
2.2 Previous syntheses of AI-2.....	28
2.3 Previous syntheses of AI-2 analogs.....	31
2.4 Results: New facile synthesis of AI-2.....	32
2.5 Synthesis of C1 analogs of AI-2.....	37
2.6 Synthesis of C4 and C5 analogs of AI-2.....	39
2.7 Discussion.....	41
2.8 Conclusion.....	42
Chapter Three: Biological evaluation of analogs in <i>V. harveyi</i>, <i>E. coli</i>, <i>S. typhimurium</i> and <i>P. aeruginosa</i>.....	43
3.1 Bioluminescence.....	43
3.2 Synergist agonism in <i>V. harveyi</i>	47
3.3 Discussion- <i>V. harveyi</i>	50
3.4 Quorum sensing in enteric bacteria.....	51
3.5 Inhibition and processing in enteric bacteria.....	52
3.6 Discussion- <i>E. coli</i> and <i>S. typhimurium</i>	59
3.7 <i>Pseudomonas aeruginosa</i>	62
3.8 <i>P. aeruginosa</i> pyocyanin production modulation.....	63
3.9 Discussion- <i>P. aeruginosa</i>	68
3.10 Ester-protected AI-2 and analogs.....	69
Chapter Four: Conclusions, Broader Impact and Future Work.....	76
4.1 Conclusion.....	76
4.2 Broader Impact.....	78
4.3 Future Work.....	79
Chapter Five: Experimental, supplementary figures and references.....	83
5.1 Methods of synthesis.....	83
5.2 Method of biological evaluation.....	85
5.3 Supplementary figures.....	87

5.4 NMR characterizations.....	98
5.5 Spectra.....	126
5.6 References.....	277

List of Tables

Table 1.1: Organisms which have the LuxS/AI-2.....	18
Table 3.1: <i>V. harveyi</i> strains and genotypes	47
Table 3.2: Enteric bacteria strains and genotypes	51
Table 3.3: <i>P. aeruginosa</i> strains and genotypes	63
Table 4.1: Inhibitory concentrations of select C1-analogs.....	77

List of Figures

Figure 1.1: Autoinducers used in quorum sensing.....	4
Figure 1.2: TraR bound to DNA and AHLs.....	5
Figure 1.3: Natural quorum sensing inhibitors and their synthetic derivatives.....	6
Figure 1.4: Methylthioadenosine nuclease (MTAN) inhibitors.....	8
Figure 1.5: AHL analogs.....	9
Figure 1.6: Analogs of AIP1 and AIP2.....	11
Figure 1.7: Compounds identified by high throughput screening.....	13
Figure 1.8: Crystal structure of S-THMF-borate bound to LuxPQ and R-THMF bound to LsrB.....	14
Figure 1.9: Quorum sensing in enteric bacteria.....	15
Figure 1.10: Quorum sensing in <i>V. harveyi</i>	16
Figure 1.11: LuxS inhibitors.....	22
Figure 1.12: Structural analogs of AI-2.....	23
Figure 1.13: Structurally unrelated inhibitors of AI-2.....	24
Figure 2.1: ^1H NMR of the equilibrium mixture of compounds derived from DPD.....	35
Figure 2.2: ^1H NMR of the quinoxaline derivatives of AI-2.....	36
Figure 2.3: Library of diverse C1-analogs of AI-2.....	37
Figure 3.1: Crystal structure of LuxPQ dimer.....	45
Figure 3.2: Bioluminescence induction in <i>V. harveyi</i> MM32 (at 8hrs) by addition of a mixture of 2 μM C1-analogs, 12nM AI-2 and 100 μM boric acid and 50 μM C1-analogs and 100 μM boric acid.....	49

Figure 3.3: AI-2 dependent β - galactosidase production in *E. coli* ZK126 pLW11 and *S. typhimurium* MET708 (both *luxS*⁺) in response to linear, branched and deoxy-analogs..54

Figure 3.4: Phosphorylation of DPD by LsrK in the presence of radio-label ATP and representative TLC analysis of the LsrK mediated phosphorylation. ATP alone, AI-2, butyl-DPD, isobutyl-DPD and deoxyl-isobutyl-DPD treated with LsrK for 2hrs.....55

Figure 3.5: AI-2 dependent β - galactosidase production in *E. coli* SH3 (LsrK⁻, LuxS⁻) and *E. coli* LW7 (LuxS⁻) in response to ethyl-DPD.....56

Figure 3.6: AI-2 dependent β - galactosidase in *E. coli* ZK126 (LsrR⁺) and *E. coli* LW8 (LsrR⁻) in response to methyl-DPD (AI-2), butyl-DPD, isobutyl-DPD and deoxy isobutyl-DPD.....57

Figure 3.7: AI-2 dependent β - galactosidase production in *S. typhimurium* MET708; AI-2 dependent bioluminescence production in *V. harveyi* BB170 and AI-2 dependent GFP induction in *E. coli* W3110 pCT6 (all strains are *luxS*⁺) in response to isobutyl-DPD and isopropyl-DPD.....58

Figure 3.8: Predicted tertiary structure of *S. typhimurium* and *E. coli* LsrR proteins.....61

Figure 3.9: *P. aeruginosa* virulence factor, pyocyanin63

Figure 3.10: Pyocyanin production in *P. aeruginosa* PAO1 in response to methyl-DPD, ethyl-DPD, heptyl-DPD, isobutyl-DPD, cyclopentyl-DPD and phenyl-DPD64

Figure 3.11: AI-2 dependent β - galactosidase production in *E. coli* LW7 and *S. typhimurium* MET715 (both *luxS*⁻) in response to a mixture of a) 40 μ M synthetic DPD and cyclic and b) synthetic DPD and aromatic analogs.....65

Figure 3.12: AI-2 dependent β - galactosidase production in <i>S. typhimurium</i> MET708; Pyocyanin production in <i>P. aeruginosa</i> PAO1; AI-2 dependent RFP induction in <i>E. coli</i> W3110 pCT6 dsRed (all strains are <i>luxS</i> ⁺) in response to isobutyl-DPD, phenyl-DPD and a cocktail of isobutyl-DPD and phenyl-DPD.....	67
Figure 3.13: Bioluminescence induction in <i>V. harveyi</i> MM32 in response to ester protected AI-2 and hexyl-DPD both in the absence and presence of exogenous AI-2.....	70
Figure 3.14: Bioluminescence induction in <i>V. harveyi</i> BB170 in response to ester protected AI-2 over time.....	71
Figure 3.15: β - galactosidase production <i>E. coli</i> LW7 in response to isobutyl-DPD, diacetate isobutyl, hexyl-DPD and diacetate hexyl in the presence of exogenous AI-2.....	72
Figure 3.16: Model pathway of ester protected AI-2 and analogs in <i>V. harveyi</i> and <i>E. coli</i>	73
Figure S1: β - galactosidase production in <i>E. coli</i> LW7 in response to AI-2, hexyl-DPD, isobutyl-DPD and their diacetate derivatives after 4 weeks of incubation at various temperatures.....	87
Figure S2: Bioluminescence induction in <i>V. harveyi</i> BB886 (LuxQ ⁻) in response to select C1-analogs.....	88
Figure S3: Bioluminescence induction in <i>V. harveyi</i> BB721 (LuxO ⁻) in response to C1-analogs.....	89

Figure S4: β - galactosidase production in <i>E. coli</i> LW7 and <i>S. typhimurium</i> MET715 (both <i>luxS</i> ⁻) in response to linear, branched and deoxy analogs.....	90
Figure S5: β - galactosidase production in <i>E. coli</i> LW9 (LsrB ⁻) in response to linear, branched and deoxy analogs of AI-2.....	91
Figure S6: Pyocyanin production in response to linear, branched, cyclic and aromatic C1-analogs.....	92
Figure S7: β - galactosidase production in <i>E. coli</i> LW7 and <i>S. typhimurium</i> MET715 (both are <i>luxS</i> ⁻) in response to cyclic and aromatic analogs.....	93
Figure S8: Effect of ester-protected AI-2 and analogs on <i>V. harveyi</i> growth.....	94
Figure S9: β - galactosidase production in <i>E. coli</i> LW7 in response to AI-2 and diacetate AI-2.....	95
Figure S10: Dose-response curves of C1 analogs in the presence of AI-2 measured by β -galactosidase in <i>E. coli</i> LW7 and <i>S. typhimurium</i> MET715(both are <i>luxS</i> ⁻).....	96
Figure S11: Phosphorelay used for signal transduction in the AI-2 mediated quorum sensing pathway of <i>V. harveyi</i>	97
Figure S12: Synergistic agonism of <i>V. harveyi</i> MM32 (LuxS ⁻) in the presence of various concentrations of AI-2 and Hexyl-DPD.....	97

List of Schemes

Scheme 1.1: Biosynthesis of AHLs.....	8
Scheme 1.2: Equilibrium mixture of AI-2 compounds.....	13
Scheme 1.3: Retrosynthetic analysis of AI-2.....	26
Scheme 2.1: Biosynthesis of 4,5-dihydroxyl-2,3-pentadiene (DPD).....	27
Scheme 2.2: Janda's synthesis of DPD.....	29
Scheme 2.3: Semmelhack's synthesis of DPD.....	29
Scheme 2.4: Vanderleyden's synthesis of DPD.....	30
Scheme 2.5: Doutheau's synthesis of DPD.....	31
Scheme 2.6: Synthesis of Trifluoromethyl-DPD.....	32
Scheme 2.7: A new synthesis of AI-2.....	33
Scheme 2.8: Resonance states of acyldiazo.....	34
Scheme 2.9: Condesation of DPD with 1,2-phenylenediamine to form quinoxaline.....	36
Scheme 2.10: New synthesis of diacetate AI-2 and diacetate analogs.....	39
Scheme 2.11: Synthesis of deoxy-AI-2 analogs.....	40
Scheme 3.1: Mechanism of bioluminescence production with riboflavin as the luciferin.....	44

List of Abbreviations

AB= Autoinducer Bioassay

Ac= Acetate

AcOH= Acetic Acid

ACP= Acyl-carrier protein

AHL= Acyl homoserine lactone

AIP= Autoinducing peptide

AI-2= Autoinducer 2

ATP= Adenosine triphosphate

CAI-1= *Cholerae* Autoinducer-1

DABCO= 1,4-Diazabicyclo[2.2.2]octane

DBU= 1,8-Diazobicyclo[5.4.0]undec-7-ene

DCM= Dichloromethane

DMSO= Dimethyl sulfoxide

DMS= Dimethyl sulfide

DPD= 4,5-Dihydroxyl-2,3-pentadione

EtOH= Ethanol

GFP= Green fluorescent protein

HAI-1= *Harveyi* Autoinducer-1

HSL= Homoserine lactone

LDA= Lithium diisopropylamide

LM= Luria Marine

MeCN= Methyl acetonitrile

MeI= Methyl iodide

MeOH= Methanol

MRSA= Methicillin-resistant *Staphylococcus aureus*

MTA= Methylthioadenosine

MTAN= Methylthioadenosine nuclease

MTR= Methylthioribose

nBuLi= (Normal) Butyl Lithium

ONPG= *O*-nitrophenyl-galactoside

PQS= *Pseudomonas* quinolone signal

R-DHMF= R-dihydroxymethyl furanone

RLU= Relative light units

R-THMF= R-tetrahydroxymethyl furanone

SAH= S-adenosylhomocysteine

SAM= S-adenosylmethionine

S-DHMF= S-dihydroxymethyl furanone

SRH= S-ribosehomocysteine

S-THMF= S-tetrahydroxymethyl furanone

TBAF= Tetrabutylammoniafluoride

TBS= Tertbutyldimethylsilyl

THF= Tetrahydrofuran

VRE= Vancomycin-resistant *Enterococcus*

VRSA= Vancomycin-resistant *Staphylococcus aureus*

Chapter One

Introduction

1.1 New approaches to anti-infective chemotherapy

Over the last two decades the treatment of bacterial infections has become non-trivial due to the rapid development of resistance and the emergence of multi-drug resistant organisms.¹ By 2003, 50% of all hospital infections were caused by methicillin-resistant *Staphylococcus aureus* (MRSA).¹ In 2007, 70% of all hospital-acquired infections were resistant to at least one or more antibiotic.² Today, community-acquired MRSA as well as vancomycin-resistant *S. aureus* (VRSA) and vancomycin-resistant *Enterococci* (VRE) are less susceptible to newer drugs such as daptomycin and linezolid.¹ Since antibiotics are designed to be lethal to bacteria (bactericidal) or inhibit their growth (bacteriostatic), evolutionary pressure is placed on the organism to develop mechanisms of resistance.²⁻³ Such mechanisms include alteration of the drug target, degradation of the drug molecule or rapid expulsion of the drug out of the cell.²⁻³ Progress has been made in developing anti-infective agents which have novel targets including riboswitches, fatty acid synthesis, and programmed cell death.³ However, since these processes are vital for the survival of bacteria it is inevitable that resistance will soon develop.³

Bacteria communicate through the secretion and detection of small molecules in a process known as quorum sensing.^{3a, 4} Once a critical population is reached bacteria coordinate the expressions of genes required for processes such as virulence, biofilm formation, and bioluminescence.⁴ Virulence factor expression is responsible for the symptoms associated with bacterial infections whereas biofilm formation accounts for the

persistence of infections as well as difficulties encountered when trying to kill bacteria with antibiotics.²⁻³

Virulence is accomplished through the secretion of factors such as toxins and proteases, which directly affect host cell function.² Bacteria only express these factors when the population is large enough to be effective.² It has been shown that quorum sensing regulates the expression of these virulence genes.⁵ As bacteriocidal drugs put enormous pressure on bacteria to develop resistance, it has been suggested that strategies such as quorum sensing inhibition, which attenuate bacterial virulence but do not kill bacteria, might lead to less resistance development.²⁻³

Biofilm is a community of bacteria encapsulated in a polysaccharide matrix; this matrix can form on surfaces such as living tissues or medical devices.⁶ Once incorporated in a biofilm matrix, bacteria are resistant to traditional antibiotics and are rarely cleared by the host immune system.⁶⁻⁷ Also the biofilm environment increases the probability of antibiotic-resistant plasmid being transferred between bacteria.^{6b} Biofilm is involved in over 60% of bacterial infections.^{3a, 6a} However there is currently no anti-biofilm drug in clinical use.^{3a, 6a} Since quorum sensing has been shown to be involved in biofilm formation, anti-quorum sensing agents may provide a mean to clear biofilm infections.

Although not proven clinically there are several reasons why attenuating virulence and biofilm formation by interfering with quorum sensing is less likely to cause resistance. Firstly mutation of quorum sensing proteins in order to overcome the action of anti-quorum sensing agents would cause the organism to be unresponsive to the natural signaling molecules. Therefore it would not be able to detect when a threshold concentration of bacteria is present. Secondly, since quorum sensing is a community-

dependent behavior, mutating a quorum sensing protein will cause the organism to be “out of sync” with the other bacteria. Although the mutated organism will be able to overcome the action of the anti-quorum sensing agents its neighbors will not. Thus the mutated organism will turn quorum sensing “on” independently. Ultimately its efforts to conduct processes such as biofilm formation and virulence expression will be inadequate and the host immune system can easily clear these lone mutants. Finally there is no growth advantage in developing anti-quorum sensing-resistance like that of antibiotic-resistance where mutation allows the organism to thrive and replicate. If a mutation of quorum sensing proteins does occur, the forementioned discussions suggest that this mutant may be at a growth disadvantage. Therefore targeting quorum sensing as a new means of anti-infective treatment is less likely to cause rapid resistance.

1.2 Quorum sensing of gram-negative and gram-positive organism

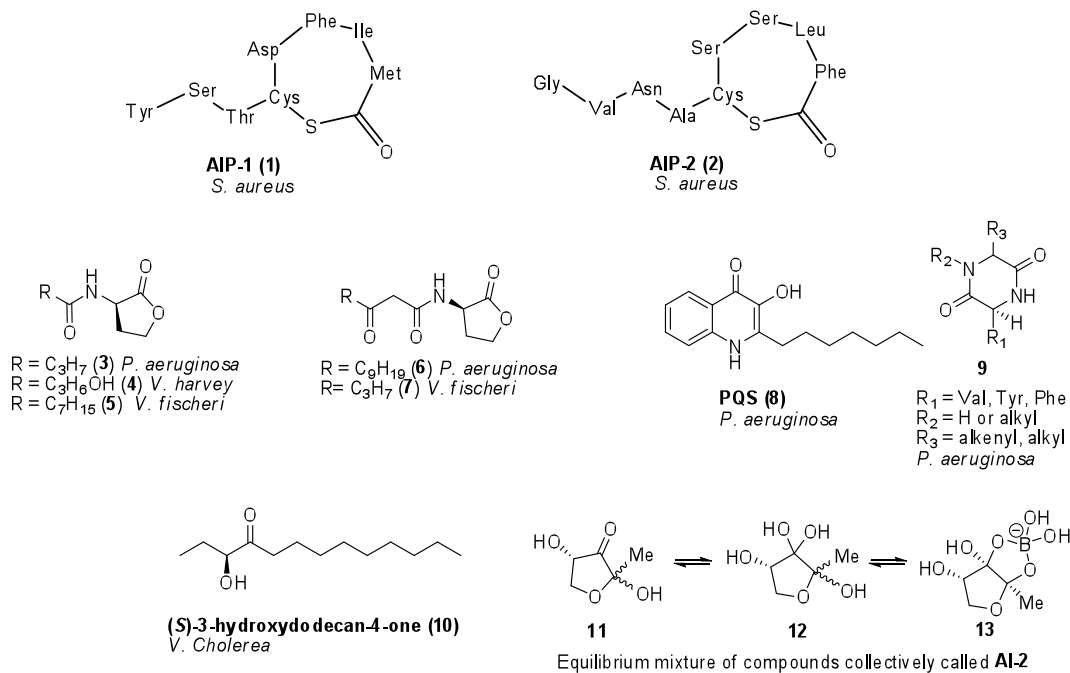


Figure 1.1: Autoinducers used in quorum sensing^{3a}

Quorum sensing involves the release of signaling molecules called autoinducers. Generally gram-negative bacteria use acylhomoserine lactones (AHLs) with varying acyl-chain lengths (3-7; Figure 1.1) whereas gram-positive species use oligopeptides, which may be post-translationally modified (1-2; Figure 1.1) for intra-species communication.^{4a,8} In gram-negative bacteria, such as *Vibrio fischeri* and *Pseudomonas aeruginosa*, AHLs are produced by a LuxI-type synthase proteins and detected by a LuxR-type cytoplasmic receptor proteins, which bind to DNA in order to activate or repress genes (See Figure 1.2).^{3a, 4a, 9}

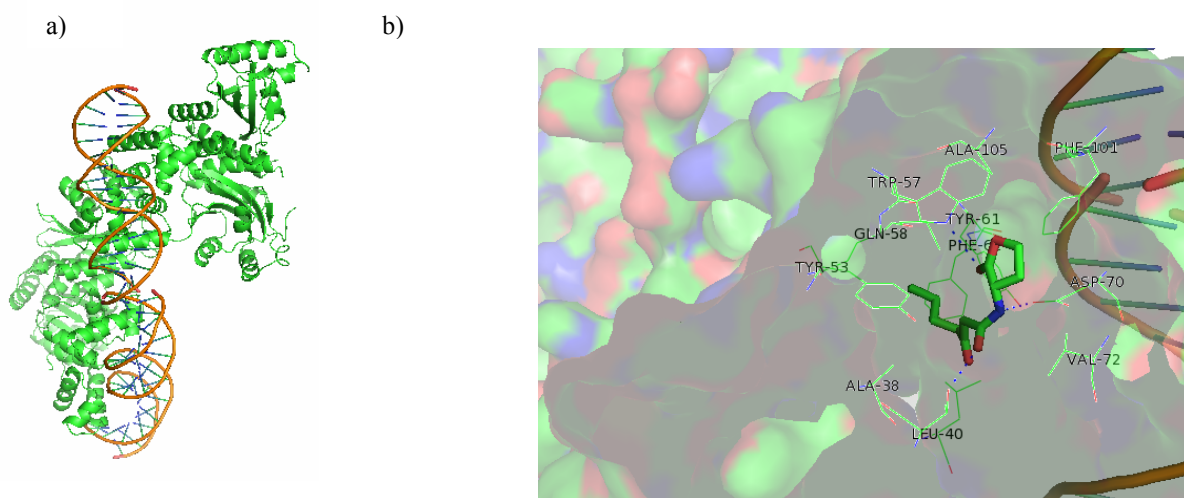


Figure 1.2: a) crystal structure of TraR bound to DNA b) AHL in binding site of TraR

The bioluminescent marine bacterium, *V. fischeri*, uses 3-oxo-hexanoyl-homoserine lactone (3OC6-HSL; **7**) and *N*-octanoyl-homoserine lactone (C8-HSL; **5**) for intraspecies communication.^{3a, 10} The opportunistic organism *P. aeruginosa* uses two AHLs: *N*-butyryl-homoserine lactone (C4-HSL; **3**) and *N*-3-oxo-dodecanoyl-homoserine lactone (3OC12-HSL; **6**) in a dual quorum sensing system.^{3a, 4a, 10} 3OC12-HSL is produced by LasI and detected by LasR while C4-HSL is produced by RhlI and is detected by RhlR.^{3a, 4a} The *las* system controls the *rhl* system as well as several virulence factors.^{3a, 4a} *P. aeruginosa* also secrete other signaling molecules including 2-heptyl-3-hydroxyl-4-quinolone (*Pseudomonas quinolone signal*; (PQS), **8**) and piperazines (**9**).^{3a, 4a} Other *Vibriosis* such as *V. cholerae* and *V. harveyi* use parallel quorum sensing signals.¹¹ In *V. cholerae*, the signaling molecules are S-3 hydroxydodecan-4-one (CAI-1; **10**) and AI-2 (**11-13**).^{3a, 4a, 11} CAI-1 and AI-2 are synthesized by CqsA and LuxS, respectively and then detected by the membrane bound proteins CqsS and LuxPQ, respectively.^{3a, 4a, 11} In *V. harveyi*, a third signal HAI-1 (3OHC4-HSL; **3**) is synthesized by LuxM and detected

by LuxN.^{3a, 11} Enterohaemorrhagic *E. coli* (EHEC) use an unidentified compound known as AI-3 for signaling along with the hormones epinephrine and norepinephrine.^{4b, c, 12} AI-3 binds the membrane bound protein QseC, which initiates a phospho-relay and triggers the expression of genes responsible for attaching and effacing lesions.^{4b, c, 12} The quorum sensing systems of the bacteria described above are well understood and attempts to target these organisms for anti-infective chemotherapy have been pursued.^{10, 13}

1.3 Quorum sensing inhibitors

Researchers have found that in nature bacteria target the quorum sensing communication system of other organisms in competition for resources. This is accomplished through quorum quenching enzymes (i.e. lactonases and acylases)¹⁴ which degrade the signaling molecules before they are able to initiate quorum sensing. Unfortunately anti-quorum sensing chemotherapies are unlikely to use proteins due to their potential to cause an immune system response. Instead small molecules are better candidates for anti-quorum sensing studies.

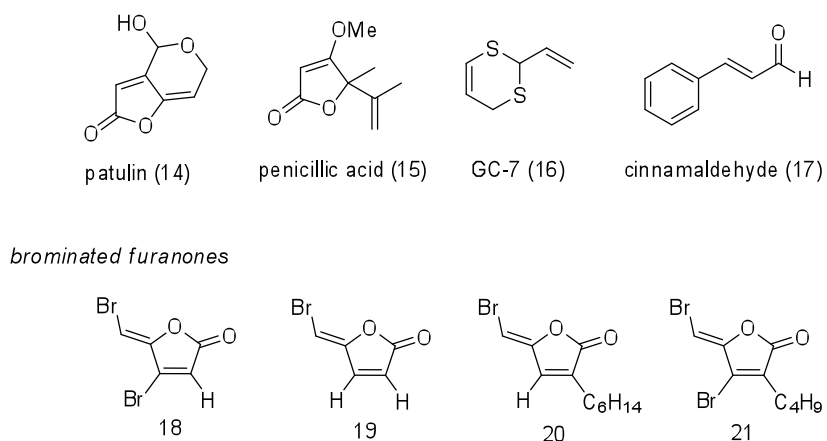
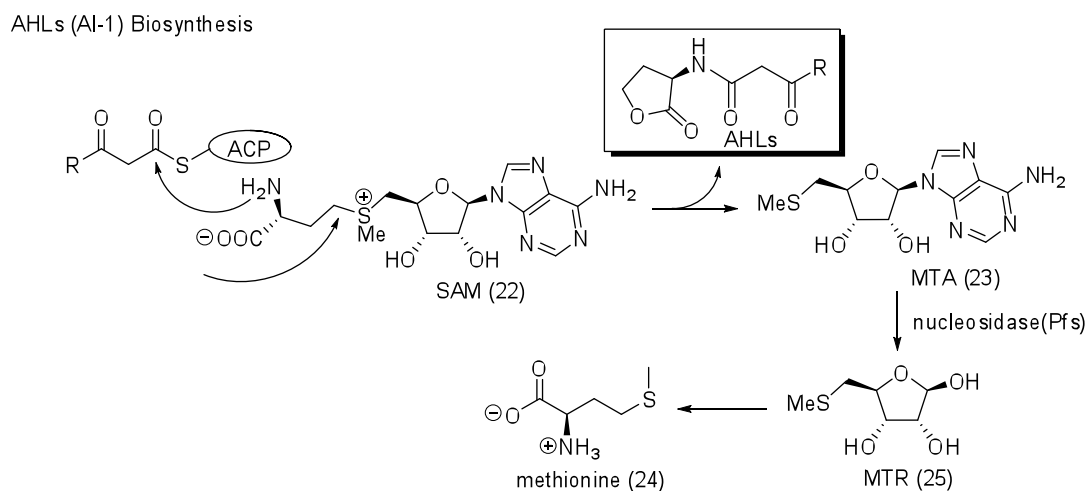


Figure 1.3: Natural quorum sensing inhibitors and their synthetic derivatives

Nature provides several examples of small molecules that interfere with quorum sensing (Figure 1.3). For example, patulin (**14**) and penicillic acid (**15**), present in the broth of *Penicillium*, were able to down regulate gene expression in *P. aeruginosa*.¹⁵ A component of garlic extract, GC-7 (**16**), was able to inhibit *V. fischeri* signaling systems.^{3a} The food additive cinnamaldehyde (**17**) was found to be a potent inhibitor of AI-2 mediated quorum sensing in several *Vibrios*.¹⁶ Derivatives of cinnamaldehyde were also screened however only 4-NO₂-cinnamaldehyde was more active than the parent compound, but it suffered from toxicity.¹⁶ The mechanism of inhibition of cinnamaldehyde was found to be due to binding to the master regulator LuxR found in *V. harveyi*.¹⁶

The most well known natural inhibitors of quorum sensing are the brominated furanones, which are produced by red algae.¹⁷ Brominated furanones have been found to inhibit biofilm formation in *S. typhimurium* and *P. aeruginosa*.¹⁸ Synthetic derivatives of these brominated furanones (**18** and **19**) have demonstrated inhibition of *P. aeruginosa* biofilm formation *in vitro* as well as *in vivo* on mice models.¹⁷⁻¹⁸ Both natural (**20**) and synthetic brominated furanones (**21**) are able to reduce biofilm formation in *S. typhimurium*.^{18b} Though the synthetic analog (**21**) was slightly less active, it had a lower toxicity.^{18b} Initial studies found that brominated furanones inhibit quorum sensing by targeting LuxR.^{17, 19} However, a recent study found that these compounds can covalently modify LuxS.²⁰ These examples confirm that small molecules can indeed effect quorum sensing *in vivo* and *in vitro*.^{22, 18b}

Taking lead from nature, synthetic molecules have been developed to block the synthesis, binding or other downstream signaling events caused by autoinducers using structural analogs or compounds identified by high throughput screening.¹³



Scheme 1.1: Biosynthesis of AHLs^{3a} (ACP= acyl-carrier proteins)

In the biosynthesis of AHLs, LuxI-type enzymes catalyze the reaction of the fatty acid portion of acyl carrier proteins with S-adenosylmethionine (SAM (**22**)) to form AHLs and methylthioadenosine (MTA, **23**; see Scheme 1.1).^{3a, 10, 21} The nucleosidase, Pfs then converts MTA into methylthioribose (MTR; **24**), which forms methionine (**25**).^{3a, 10, 21}

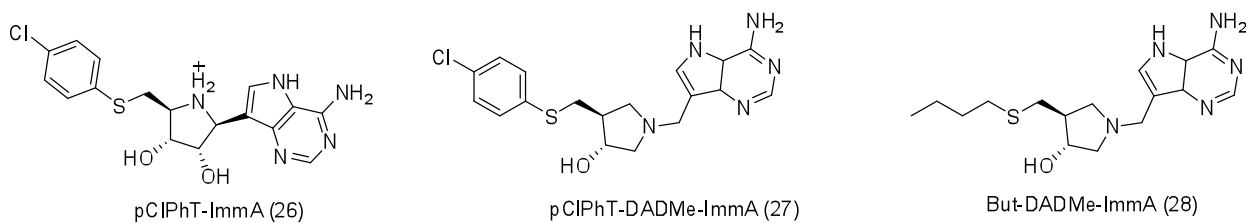


Figure 1.4: Methylthioadenosine nucleoside (MTAN) inhibitors

Recent work by Schramm involved the synthesis of a library of transition state analogs of MTA as inhibitors of the methylthioadenosine nuclease (MTAN, (Pfs); See Figure 1.4).²² Originally, early stage transition state analogs were designed and *p*-chlorophenylthio-ImmA (pClPhT-ImmA; **26**) was found to be the tightest binder of Pfs.²² A newer generation of analogs were designed to mimic late stage transition states; in this series *p*-chlorophenylthio-DADMe-ImmA (**27**) was also the best binder.²² Additionally But-DADMe-ImmA (**28**) was able to effect biofilm formation in *V. cholerae* and *E. coli* O157:H7.²³ Although this approach has given promising results, MTANs are vital for polyamine synthesis, methyl transfer and methionine synthesis in human cells as well as in bacteria.²³ Therefore these molecules are likely to be toxic due to their potential to interfere with important metabolic process in human cells.

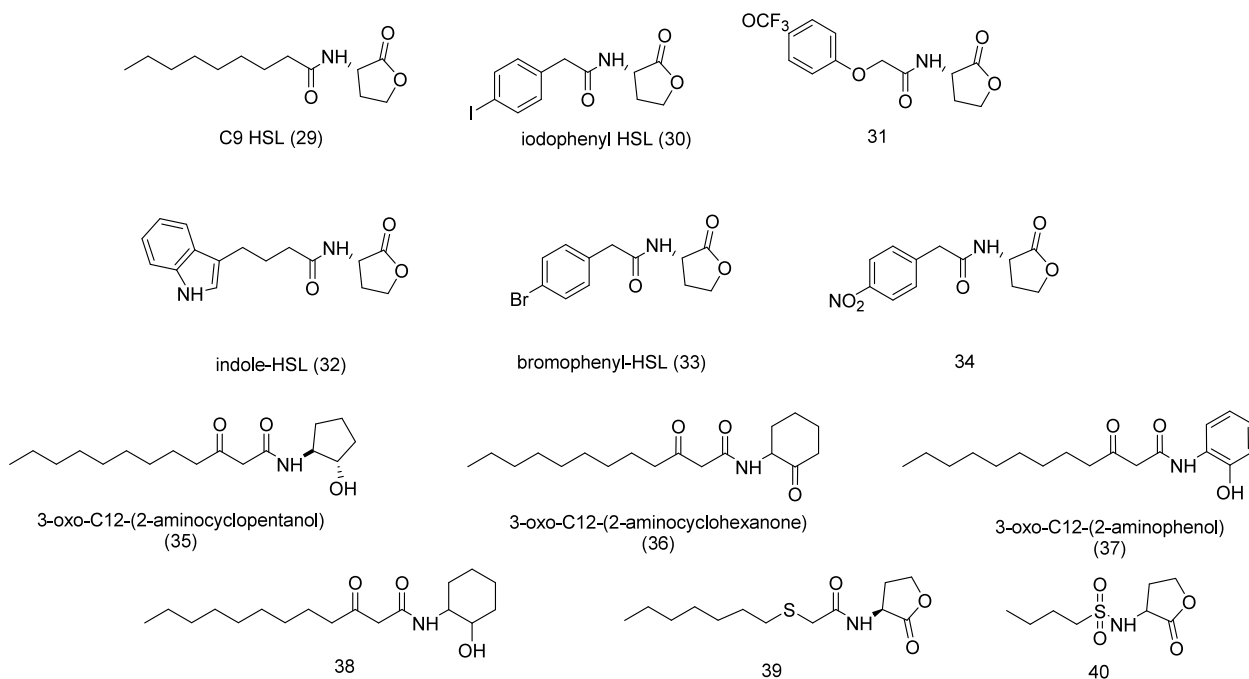


Figure 1.5: AHL analogs

Structural analogs of AHLs are the most widely explored set of small molecule modulators of quorum sensing (Figure 1.5).¹⁰ As previously described, AHLs of different chain lengths are used for signaling between specific species of bacteria.^{4a, 10} Early studies showed that alteration of the structure of the AHL often resulted in reduced agonism or in some cases antagonism via competition with the natural ligand for binding to LuxR-type proteins.²⁴ Initial results showed that C9-AHL (**29**), which is only one carbon longer than the natural AHL, was a potent inhibitor of LuxR mediated bioluminescence in *V. fischeri*.²⁴ Following the introduction of a new synthetic route, over 90 analogs with non-native AHLs have been synthesized and evaluated in *A. tumefaciens*, *P. aeruginosa* and *V. fischeri* by Blackwell.²⁵ Out of this library several analogs were found, including iodophenyl HSL, **30** and compound **31**, to be antagonists against all three bacteria.²⁵ Additionally, bromophenyl HSL (**33**) and indole-HSL (**32**) were found to reduce biofilm formation of *P. aeruginosa*.²⁶ Interestingly **34** acted as a potent agonist in *V. fischeri* although most other aryl analogs acted as antagonists.²⁵ Despite these successes AHLs are susceptible to hydrolysis by lactonases.^{14a} Therefore analogs that lack the lactone moiety are more desirable. Suga has synthesized analogs which have the lactone ring replaced with other cyclic structures.²⁷ The cyclohexanone (**36**), cyclopentanol (**35**) and phenol (**37**) derivatives of 3-oxo-C12-HSL all acted as antagonist while cyclohexanol (**38**) was found to be an agonist of *P. aeruginosa*.^{27b} Other structural alterations, for instance replacing the amide functionality with an amino-sulfonyl group or sulfide, afforded antagonists **40** and **39**.²⁸

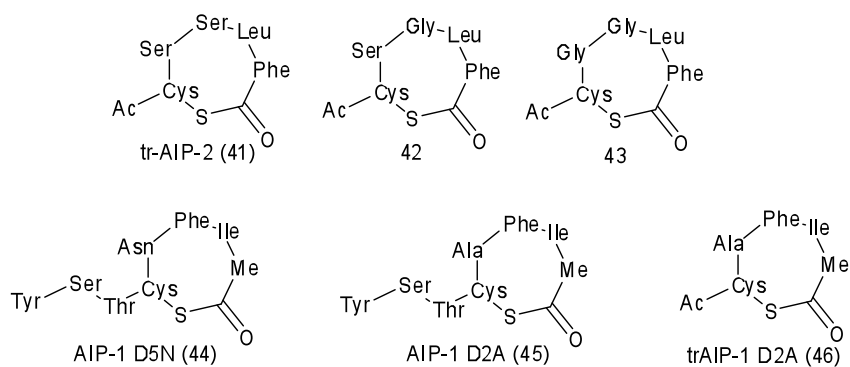


Figure 1.6: Analogs of AIP1 and AIP2

Analogs of quorum sensing in gram-positive bacteria have primarily targeted *S. aureus*. In this system oligopeptides are modified, cyclized and transported out of the cell. These autoinducing peptides (known as AIPs) then bind the membrane bound protein AgrC which induces a phosphorelay mechanism and controls virulence expression. In *S. aureus*, four groups of AIPs are produced by different strains and are detected by specific AgrCs.²⁹ It has been shown that AIPs of different groups bind and inhibit the response of the natural AIP.²⁹ This cross-inhibition stimulated the evaluation of structural analogs of AIPs across groups (i.e. AIP-II analogs were tested on AgrC-1; Figure 1.6).^{29a} Initial replacement of aspartate with alanine (AIP-1 D5A; **45**) resulted in a potent inhibitor of all 4 AgrCs.³⁰ Other variations such as **44** gave an inhibitor of AgrC-2 and AgrC-4 only.³⁰ Truncation of AIP-1 D5A (trAIP-1 D2A; **46**) provided an equally potent inhibitor of AgrC-1-4.³⁰ Likewise truncated AIP-II (**41**) was found to be a potent inhibitor across all four groups.³⁰ Structure activity relationship (SAR) studies of this compound uncovered two additional derivatives, **42** and **43**, which are more potent against AgrC-1 and AgrC-2.³¹

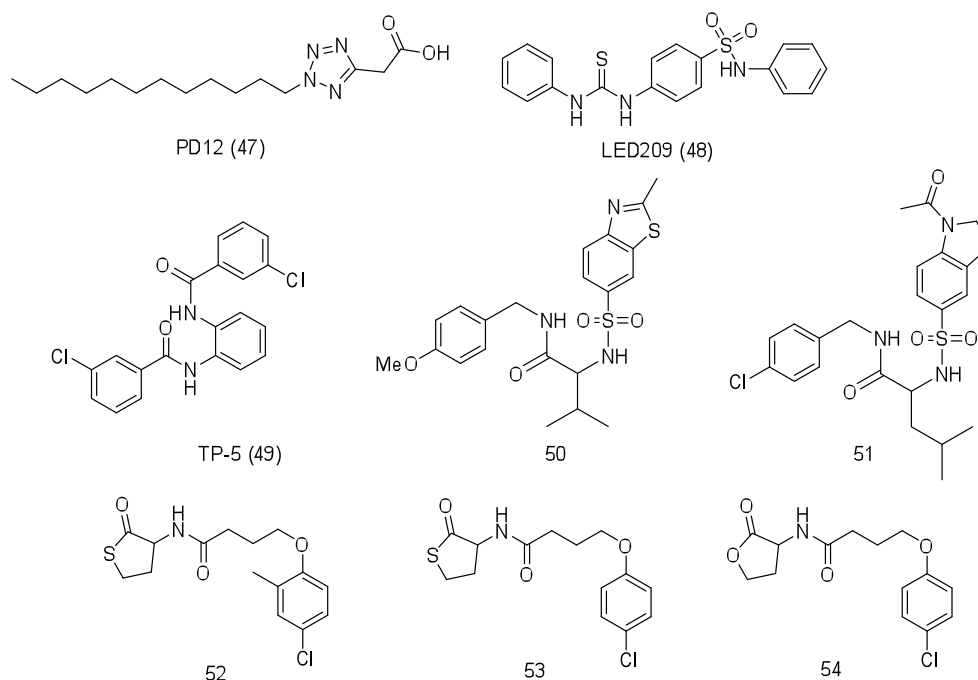


Figure 1.7: Compounds identified by high throughput screening

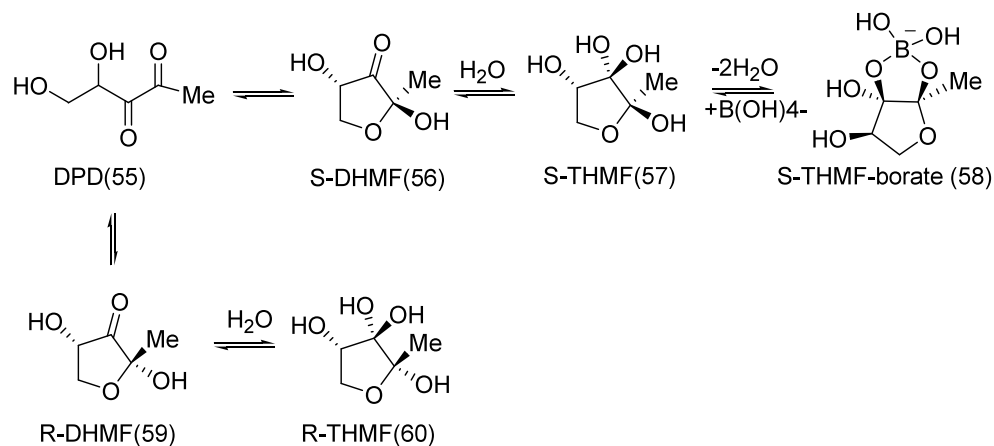
Other modulators of quorum sensing have been found by high throughput screenings (Figure 1.7). PD12 (47) and TP-5 (49) are inhibitors of AHL signaling in *P. aeruginosa*.³² TP-5 was the only antagonists amongst a series of structurally similar compounds all of which acted as agonists.^{32b} LED209 (48) was found through high throughput screenings to inhibit Enterohaemorrhagic *E. coli* through binding to the membrane bound receptor QseC (for further details see p.6 and the indicated references).³³ Competition with AHLs for binding to the membrane bound receptor protein, LuxN, in *V. harveyi* has recently been investigated by Bassler.³⁴ Out of the 30,000 compounds screened, 15 non-toxic candidates were identified most of which were structurally unrelated to AHLs (50 and 51).³⁴ In a subsequent study, Bassler screened these LuxN inhibitors for activity against LuxR-type proteins owing to the fact the AHLs

have the capacity to bind both membrane bound and cytoplasmic proteins.³⁴ Chlorothiolactone (**52**) was identified as an inhibitor of a human pathogen *Chromobacterium violaceum*, which uses the CviR as the LuxR-type cytoplasmic receptor.³⁵ Further studies on chlorothiolactones, **53** and chlorolactone, **54**, revealed that inhibition can occur through binding to CviR and inhibiting transcription or by preventing binding of CviR to DNA which also inhibits transcription.³⁵

Though it has been shown that anti-quorum sensing chemotherapy is possible, the challenge to find a common target among many bacteria still remains.

1.4 Autoinducer-2 mediate quorum sensing

Most autoinducers are species-specific but there exists a universal autoinducer, AI-2, which has been detected in several species of bacteria.³⁶



Scheme 1.2: Equilibrium mixture of AI-2 compounds

AI-2 is not a single compound but a collection of inter-converting compounds **55-60** (Scheme 1.2).³⁷ Once formed, DPD undergoes spontaneous rearrangements to give a mixture of compounds; (2S, 4S)-2,4-dihydroxy-2-methyldihydroxyfuran-3-one (S-

DHMF; **56**), (2R, 4S)-2,4-dihydroxy-2-methyldihydroxyfuran-3-one (R-DHMF; **59**), (2S, 4S)-2-methyl-2,3,3,4-tetrahydroxytetrahydrofuran (S-THMF; **57**) and (2R, 4S)-2-methyl-2,3,3,4-tetrahydroxytetrahydrofuran (R-THMF; **60**).³⁸ In the presence of borate salts, S-THMF can form S-THMF-borate (**58**).³⁷ It has been shown that different species of bacteria recognize different forms of DPD (See Figure 1.8); *S. typhimurium* detects R-THMF (**60**)³⁸ whereas *V. harveyi*, which is found in marine environments detects S-THMF-borate (**59**).³⁷

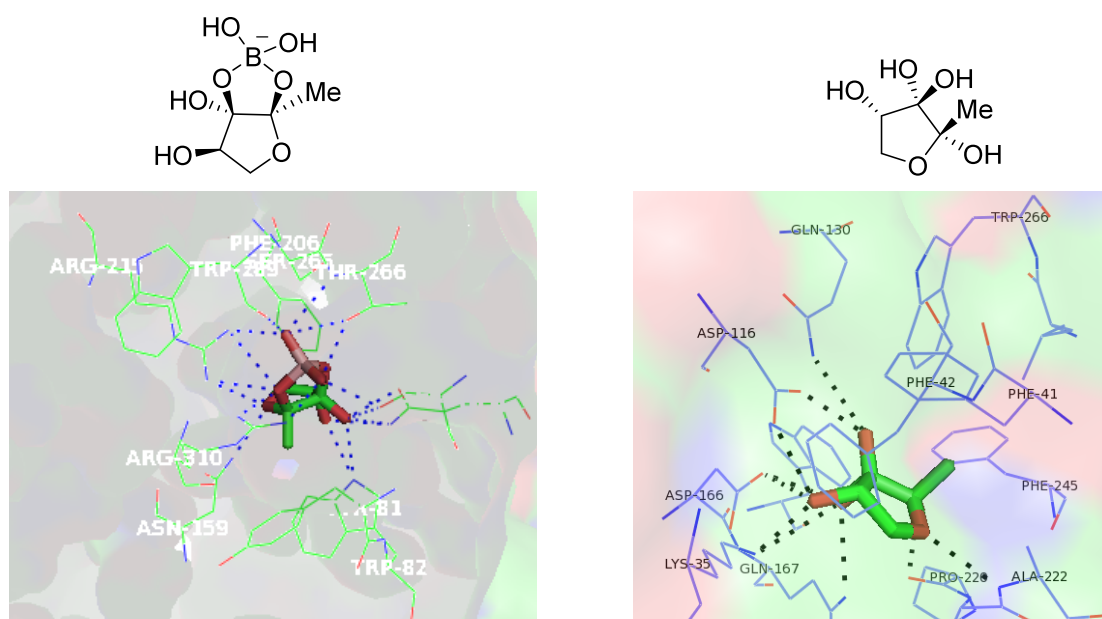


Figure 1.8: Crystal structure of a) S-THMF-borate bound to LuxPQ and b) R-THMF bound to LsrB

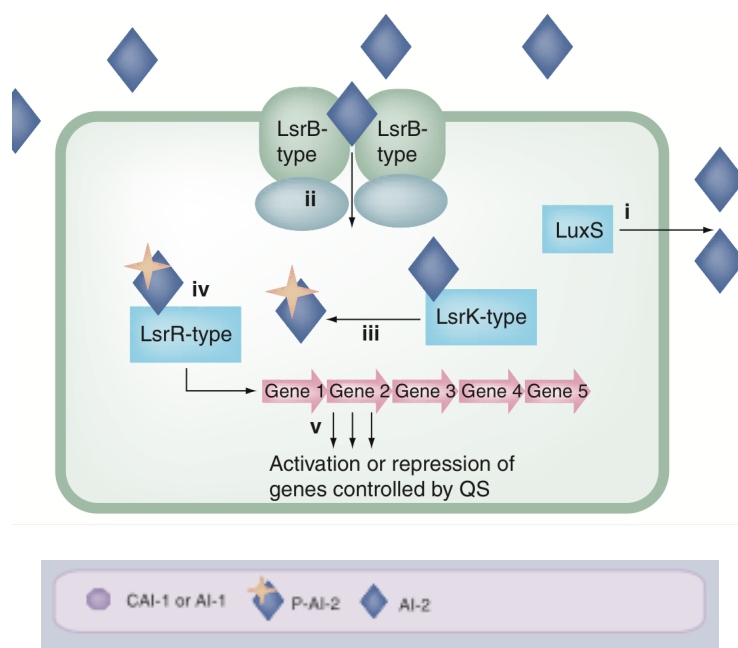


Figure 1.9: Quorum sensing in enteric bacteria^{3a}

In enteric bacteria, AI-2 is internalized through the LsrABC transporter and phosphorylated by LsrK (Figure 1.9).³⁹ Phosphorylated AI-2 (P-AI-2) acts as a substrate of the LsrR protein.³⁹ In a non-quorum sensing state, LsrR represses the *lsr* operon.⁴⁰ When P-AI-2 binds to LsrR, the *lsr* operon is derepressed and the LsrR-regulated genes are expressed.³⁹ LsrG, an enzyme encoded by the *lsr* operon, catalyzes the degradation of P-AI-2 into phosphoglycolic acid (PG) and an unknown C3 compound.⁴¹ It has been shown that the internalization of AI-2 by enteric bacteria interferes with the quorum sensing process of other bacteria.⁴² Similar internalization of AI-2 is executed in *A. actinomycetemcomitans* by the ribose binding protein, RbsB.⁴³ In this organism phosphorylated AI-2 interacts with a two-component system consisting of QseBC, which controls biofilm formation and iron uptake.⁴³ *S. meliloti* also internalizes AI-2 through a LsrB homolog although this organism does not have LuxS.⁴⁴

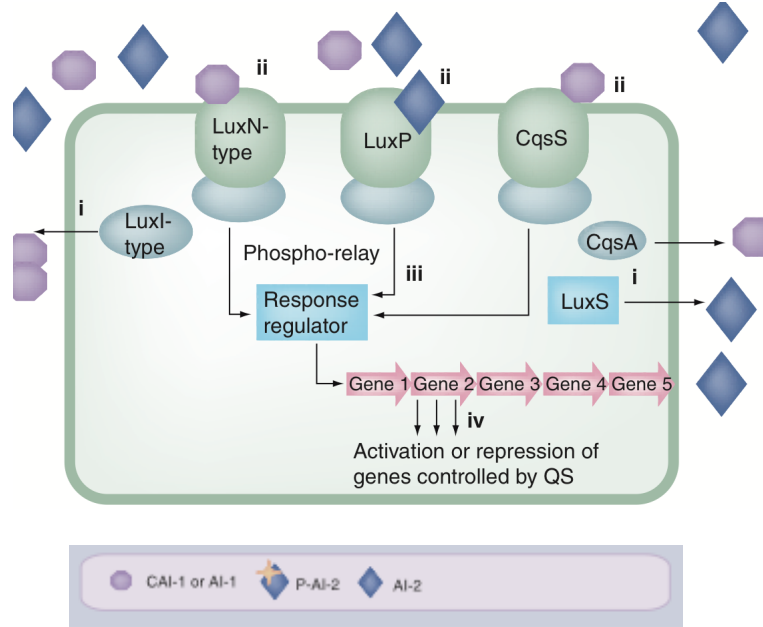


Figure 1.10: Quorum sensing in *V. harveyi*^{3a}

As previously mentioned, *V. harveyi*, a marine bacterium also uses AI-2 for signaling.⁴⁵ *V. harveyi* uses quorum sensing to encode genes, which control bioluminescence and virulence.⁴⁶ Under normal conditions (low cell density), LuxPQ acts as a histidine-kinase and initiates the phosphorylation of LuxU which subsequently phosphorylates LuxO (Figure 1.10).⁴⁷ LuxO along with σ^{54} activates five small regulatory RNAs (sRNAs).^{11 48} These sRNAs along with the Hfq chaperone destabilize the transcriptional regulator, LuxR preventing its production.⁴⁹ LuxR regulates the expression of genes responsible for bioluminescence and virulence.⁵⁰ Therefore under normal conditions, LuxR is not present to induce the expression of genes responsible for bioluminescence and virulence factor production.⁵⁰ In the quorum sensing state (high cell density), when AI-2 binds, LuxPQ acts as phosphatase and dephosphorylates LuxU and LuxO.¹¹ This results in the inactivation of the sRNAs and ultimately allows LuxR to

activate bioluminescence and virulence genes.⁴⁹ A similar phospho-relay is initiated upon AI-2 binding in *V. cholerae* but HapR, the homologue of LuxR, represses biofilm formation.⁵¹

4, 5-Dihydroxy-2, 3-pentanedione (DPD; **55**), the linear precursor of AI-2, is synthesized by the LuxS protein, which is highly conserved in both gram-positive and gram-negative bacteria.^{36, 45} Therefore it has been suggested that AI-2 functions as an interspecies signal unlike the intraspecies AHLs and oligopeptides.^{4a, 8} The *luxS* gene is present in over 60 species of bacteria and AI-2 production has been reported in many of these organisms.^{52, 3} Table 1.1 outlines a subset of these organisms and LuxS/AI's role. Therefore drugs which target the LuxS/AI-2 quorum sensing system could have the potential to have broad-spectrum anti-quorum sensing activity.

Table 1.1: Organisms which have the LuxS/AI-2 system

Bacteria	Observed phenotype in LuxS mutants	Complementation mode	Ref
Oral pathogens			
<i>Streptococcus oralis</i>	Reduced mutualistic biofilm growth	Synthetic DPD; Plasmid containing <i>luxS</i> gene	53
<i>Streptococcus gordinii</i>	Downregulation genes required for carbohydrate metabolism; Reduced mixed biofilm formation	Plasmid containing <i>luxS</i> gene	54
<i>Aggregatibacter actinomycetemcomitans</i>	Reduced biofilm growth	Partially purified DPD; Plasmid containing <i>luxS</i> gene	43, 55
<i>Porphyromonas gingivalis</i>	Reduced mixed biofilm growth;	Synthetic DPD; Plasmid containing <i>luxS</i> gene	54
<i>Streptococcus mutans</i>	Attenuated biofilm formation	AI-2 producing bacterial strains	56
<i>Actinomyces naeslundii</i>	Reduced mutualistic biofilm growth	Synthetic DPD; Plasmid containing <i>luxS</i> gene	53
Food-borne pathogens			
<i>Salmonella typhimurium</i>	Inactive AI-2 internalization	<i>In vitro</i> synthesized AI-2; Plasmid containing <i>luxS</i> gene	57
<i>Clostridium perfringens</i>	Reduced toxin production	Culture supernatant	58
<i>Campylobacter jejuni</i>	No differentiation of genes (via microarray analysis)	<i>In vitro</i> synthesized AI-2	59
<i>Bacillus cereus</i>	Normal biofilm formation	<i>In vitro</i> synthesized AI-2*	60
<i>Listeria monocytogenes</i>	Increased biofilm formation	<i>In vitro</i> synthesized AI-2**	61
<i>Vibrio cholerae</i>	Increased biofilm formation	Synthetic DPD*	62
<i>Vibrio anguillarum</i>	Pigmentation	Synthetic DPD	63
<i>Vibrio ichthyoenter</i>	No change in biofilm formation or virulence	N/A	64
<i>Vibrio vulnificus</i>	Decreased protease and increased haemolysin production	Plasmid containing <i>luxS</i> gene	65
<i>Edwardsiella tarda</i>	Reduced biofilm formation, type III secretion system gene expression and virulence	Culture supernatant containing AI-2	66
<i>Vibrio harveyi</i>	Reduced bioluminescence	Synthetic DPD	46a
Opportunistic pathogens			
<i>Staphylococcus aureus</i>	Increased virulence factor synthesis	Synthetic DPD	67
<i>Staphylococcus epidermidis</i>	Increased biofilm and enhanced virulence	Plasmid containing <i>luxS</i> gene; Culture supernatant containing AI-2*	68, 69
<i>Streptococcus intermedius</i>	Increased antibiotic susceptibility	Synthetic DPD	70
<i>Streptococcus anginosus</i>	Increased antibiotic susceptibility	Synthetic DPD	71
Symbiotic bacteria			
<i>Escherichia coli</i>	Reduced biofilm formation	<i>In vitro</i> synthesized AI-2	66
<i>Lactobacillus reuteri</i>	Increase biofilm thickness	Purified AI-2**	72
<i>Lactobacillus rhamnosus</i>	Decreased metabolism and biofilm formation	Culture supernatant; Synthetic DPD**	73
Human pathogens			
<i>Neisseria meningitidis</i>	Metabolic byproduct	Culture supernatant	74
<i>Helicobacter pylori</i>	Lost of motility	Plasmid containing <i>luxS</i> gene; <i>In</i>	75

		<i>in vitro</i> synthesized AI-2	
<i>Proteus mirabilis</i>	No effect on virulence or motility	N/A	⁷⁶
<i>Borrelia burgdorferi</i>	No effect	N/A	⁷⁷

*addition of *in vitro* synthesized AI-2 caused a reduction in biofilm; **Failed to effect biofilm formation

Despite the ubiquitous nature of AI-2 there is still some debate as to whether it is indeed used for signaling in all organisms which possess LuxS or if it simply acts as a metabolic byproduct of the methyl cycle.^{78, 79} In addition to DPD, LuxS also produces homocysteine, which is converted to cysteine and used in the biosynthesis of the essential amino acid, methionine.⁸⁰ Studies using LuxS mutants often show alterations in biofilm formation/architecture and/or virulence factor expression but due to the role of LuxS in metabolism it is often difficult to determine whether these alterations are the result of interfering with quorum sensing or due to the disruption of the active methyl cycle.^{78 79} Previous studies have relied on complementation of LuxS mutant strains with, plasmids containing *luxS*, culture supernatant containing AI-2, or *in vitro* synthesized DPD, partially purified AI-2 or synthetic DPD in attempts to decipher the role of the LuxS/AI-2 system in bacteria.^{78, 79}

In some organisms the role of AI-2 in pathogenesis is now clear.⁷⁹ A *luxS* mutation in *Vibrio vulnificus*, an organism responsible for septicemia and wound infections, caused aberrant expression of virulence factors.⁶⁵ Upon addition of culture supernatant containing AI-2, these virulence factors were restored to basal levels.⁶⁵ In *luxS* mutants of *Clostridium perfringens*, the gram-positive pathogen responsible for gangrene, toxin production was restored to wild-type levels when culture supernatant containing AI-2 was added.⁵⁸ However, this complementation strategy can be misleading since other components in culture supernatant cannot be ruled out as effecting virulence expression. *Helicobacter pylori*, the gram-negative organism responsible for peptic

ulceration, gastric cancer and some types of gastric lymphoma, is controlled by AI-2 mediated quorum sensing.⁷⁵ Complementation with synthetic DPD in a *luxS* mutant restored motility through flagellar transcription whereas complementation with cysteine did not restore this phenotype.⁷⁵ In addition to phenotypes, transcriptome analysis has also been used to identify genes which are modulated in the presence of AI-2. Transcriptome analysis in *Staphylococci* reveals AI-2's importance in metabolism and virulence.^{67, 69, 68} Transcriptome analysis in *S. aureus* revealed that deletion of the *luxS* gene affected several metabolic enzymes as well as genes responsible for the production of capsular polysaccharide (CP), a virulence factor on bacteria cell walls which allow cells to evade phagocytes of the host immune system.⁶⁷ Similarly transcriptome analysis of *S. epidermidis luxS* mutants showed metabolic genes being modulated but also modulation of pro-inflammatory and immune evasion factors.^{69, 68}

In addition to virulence factor expression, AI-2 has also been shown to control biofilm formation in several bacteria.⁷⁴ A *luxS* mutant strain of *Streptococcus oralis* was unable to produce biofilm and grow mutualistically with *Actinomyces naeslundii*.⁵³ This malfunction was restored by the addition of synthetic AI-2. Another oral pathogen responsible periodontal disease, *Aggregatibacter actinomycetemcomitans*, also lacked the ability to form biofilm and cause virulence in *luxS* mutant strains; partially purified AI-2 was able to restore this activity.⁵⁵ Finally biofilm formation and architecture was restored by *in vitro* synthesized AI-2 in *Escherichia coli*.⁶⁶ In some organisms such as *Vibrio cholerae*, a human pathogen responsible for the gastrointestinal disease cholera⁶² and *B. cereus*, AI-2 signaling results in the repression of biofilm formation.⁶⁰ Other phenotypes, which are modulated by AI-2 include antibiotic susceptibility and production. For

example, antibiotic susceptibility was restored in a *luxS* mutant of *Streptococcus anginosus*⁷¹ and *Streptococcus intermedius*⁷⁰ after addition of synthetic DPD.

A few examples point to AI-2 as a by-product of metabolism.^{81, 78, 79} Studies with the probiotic, *Lactobacillus rhamnosus*, reveal that neither growth nor biofilm formation was restored to wild type levels in *luxS* mutants with culture supernatant containing AI-2 or with chemically synthesized DPD.⁷³ Though cysteine was successfully able to significantly restore growth and biofilm formation.⁷³ Additionally, purified AI-2 was unable to restore biofilm in *luxS* mutants of *Lactobacillus reuteri*⁶⁷ and *Listeria monocytogenes*.⁶¹ Transcriptome analysis in a *luxS* mutant of the human pathogen, *Campylobacter jejuni*, revealed that the differentiation of genes associated with metabolism, rather than quorum sensing, was responsible for this organism's loss of motility.⁵⁹ Also the addition of *in vitro* synthesized AI-2 had no effect on gene expression in this analysis, indicating that motility is affected by metabolic disturbance rather than quorum sensing.⁵⁷ Similar transcriptional analysis using DNA microarrays in *Neisseria meningitides* indicated that the attenuation of virulence observed in *luxS* mutant was not due to quorum sensing as addition of culture supernatant containing AI-2 did not affect gene expression.⁸¹ Finally, the role of AI-2 in *S. typhimurium* has been questioned owing to the fact that complementation with chemically synthesized DPD was not able to restore biofilm formation.⁸² Cysteine and the other components of the active methyl cycle were also ineffective at restoring biofilm.⁸² Therefore it is unclear what caused biofilm perturbation in *S. typhimurium*.⁸² The relevance of quorum sensing in *S. typhimurium* has also been questioned because of the similarities in AI-2 processing with sugar metabolism (i.e. binding, internalization and phosphorylation) and the lack of function of

AI-2 in *S. typhimurium* other than internalization.⁷⁹ Other organisms for example *Borrelia burgdorferi*⁷⁷ and *Proteus mirabilis*⁷⁶ exhibit no difference in wild type versus *luxS* mutant strains indicating that LuxS may be present only for its role in the active methyl cycle. The aforementioned examples reveal that not all organisms, which contain LuxS and produce AI-2 use it for quorum sensing.

Though LuxS is important for metabolism and in some cases AI-2 has been shown to be a by-product of metabolism, it is clear that AI-2 can modulate virulence factor expression, biofilm formation and antibiotic susceptibility in several bacteria.^{74, 53, 71} Additionally, some organisms which do not have LuxS have been able to respond to exogenously added AI-2.^{44, 83} This could suggest that over time AI-2 as a by-product of metabolism became an indicator for some bacteria that other bacteria were present in their surroundings. Furthermore, AI-2 has been shown to form independently of LuxS from ribulose-5-phosphate.⁸⁴ Therefore the designation of AI-2 as an interspecies signaling molecule is still valid as no other single molecule has been shown to be relevant to as many organisms as AI-2.⁸

1.5 AI-2 inhibitors

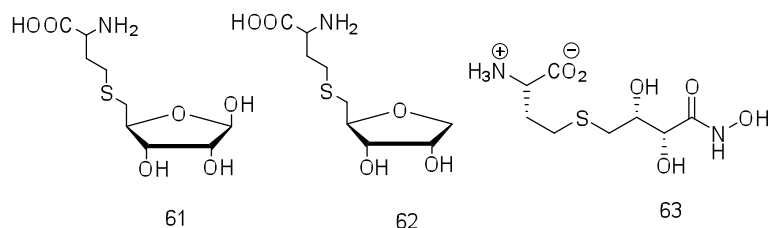


Figure 1.11: LuxS Inhibitors⁸⁵

AI-2 is ubiquitous and chemotherapies which target this molecule could provide a broad-spectrum anti-infective agent. Though inhibitors of the AI-2 mediated quorum sensing systems have not been rigorously pursued until recently. Initial attempts to inhibit AI-2 synthesis have involved the construction of analogs of the natural substrate of LuxS S-ribosylhomocysteine (Figure 1.11).^{78, 84} Studies by Zhou revealed two active analogs: S-anhydroribosylhomocysteine, **61** and S-homoribosylcysteine, **62**.^{85a} These analogs were found to inhibit AI-2 synthesis but no other biological tests were conducted.⁸⁴ Other acyclic analogs of SRH (i.e., **63**) were found to bind differently to the LuxS of different organisms including *B. subtilis*, *V. harveyi* and *E. coli*, although to varying extents.^{85b} LuxS inhibition would not be a useful target for anti-quorum sensing therapies though due to the fact that other metabolic processes are controlled by LuxS⁸⁰ and the biological response of inhibitors could be the result of interfering with these processes rather than quorum sensing.^{78, 79}

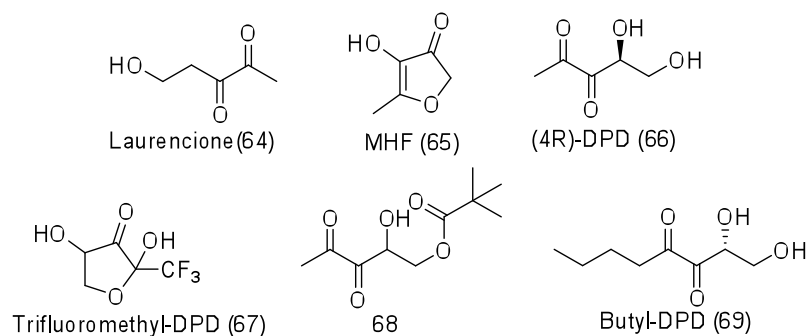


Figure 1.12: Structural analogs of AI-2^{79, 86, 87, 88}

The inhibition of AI-2 via competition for receptors or processing enzymes has been pursued through the synthesis of structural analogs of AI-2 (Figure 1.12).^{79, 86, 87, 88}

Initial studies looked at the natural compounds laurencione (**64**) and MHF (**65**) due to the structural similarities with the linear and cyclic forms of AI-2, respectively.⁸⁶ Although both showed some activity they were not as effective at causing bioluminescence induction as AI-2 in *V. harveyi*.⁸⁶ Synthetic efforts by Janda found that the enantiomer (4R)-DPD (**66**) was also less active than the natural molecule.⁸⁶ Eventually new synthetic routes were published allowing for variations on the hydroxyl moieties of AI-2 analogs (**68**).⁸⁷ Unfortunately, no biological tests have been reported for this analog although similar acetylated analogs were found to act identical to AI-2.⁸⁹ An analog which replaced the hydrogens in the C1 methyl group of DPD with fluorines (trifluoromethyl-DPD; **67**) was found to be more active than the natural compounds (**64**, **65**) or the enantiomer of DPD (**66**) in inducing bioluminescence in *V. harveyi*.⁸⁸ With these initial results it became clear that AI-2 analogs often acted as less potent agonist of AI-2 mediated processes rather as antagonists. Subsequent studies by Janda identified butyl-DPD (**69**) as a good inhibitor of β -galactosidase transcription in *S. typhimurium* although the mechanism of this inhibition was not revealed.⁹⁰ Although butyl-DPD as well as propyl-DPD acted as antagonist in *S. typhimurium* they were also found to cause synergist agonism in *V. harveyi*.⁹⁰

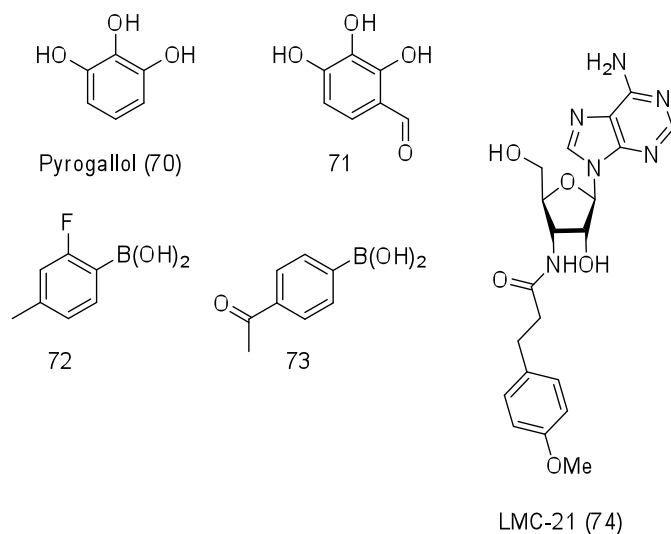


Figure 1.13: Structurally unrelated inhibitors of AI-2 QS^{91, 92, 63}

Other compounds have been screened which are structurally unrelated to AI-2 (Figure 1.13).^{91, 92, 63} The commercial compound pyrogallol (**70**) and its derivative (**71**) have been identified as a potent inhibitor of quorum sensing controlled-bioluminescence.⁹¹ Likewise various boronic acids (**72** and **73**)⁹² inhibit bioluminescence at low concentrations although the toxicity of both the pyrogallol and boronic acid will likely prevent clinical use. A new structural class of phenothiazine derivatives also have been found to inhibit AI-2 quorum sensing.⁹³ Recently, a new set of compounds were screened for activity against *V. harveyi* and other vibrios. LMC-21 (**74**)⁶³ was found to be a potent inhibitor of biofilm formation in *V. anguillarum* and *V. vulnificus* as well as block *V. harveyi* infection of Artemia shrimp.⁶³ Although structurally similar to SAM and SAH, the mode of inhibition of this nucleoside was found to be through blocking the LuxPQ receptor.⁶³

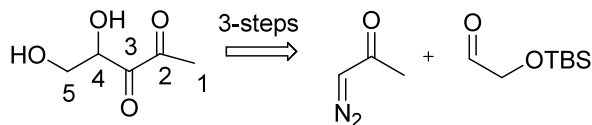
From the forementioned discussion of AI-2 inhibitors it is evident that there is a need for a more extensive development of structural analogs of AI-2 as these molecules are more likely to modulate quorum sensing in a diverse set array of bacteria.

1.6 Objective, hypothesis and specific Aims

The objective of this dissertation is to create a superior synthesis of AI-2 which facilitates the design of a large library of analogs. Our hypothesis is that structural analogs will allow for probing into the promiscuity or specificity of quorum sensing proteins. Also since AI-2 is a universal signaling molecule we hypothesize that analogs of AI-2 will have broad range applicability as modulators of quorum sensing or probes to identify new AI-2 receptors.

The specific aims are as follows:

1. To develop a new synthesis of AI-2 and construct analogs.



Scheme 1.3: Retrosynthetic Analysis of AI-2

2. To compare analog activities to AI-2 activity in several organisms by monitoring:
 - a. Bioluminescence induction/inhibition in *V. harveyi*
 - b. β -galactosidase production/inhibition in *E. coli* and *S. typhimurium*
 - c. Pyocyanin production/inhibition in *P. aeruginosa*
3. To monitor the effect of AI-2 and analogs in mixed bacteria cultures which mimic real life scenarios where bacteria co-habit in an ecosystem with other organisms.

1.7 Dissertation Outline

Chapter 2 describes the newly developed synthesis of AI-2. This chapter will demonstrate the ability of this new synthesis to obtain a library of diverse C1 analogs as well as C4 and C5 analogs.

Chapter 3 describes the evaluation of the newly developed analogs on *V. harveyi*, *E. coli*, *S. typhimurium* and *P. aeruginosa*. This chapter also describes the evaluation of AI-2 and analogs on mixed cell cultures.

Chapter 4 will outline the conclusions, broader impact and future direction of this research

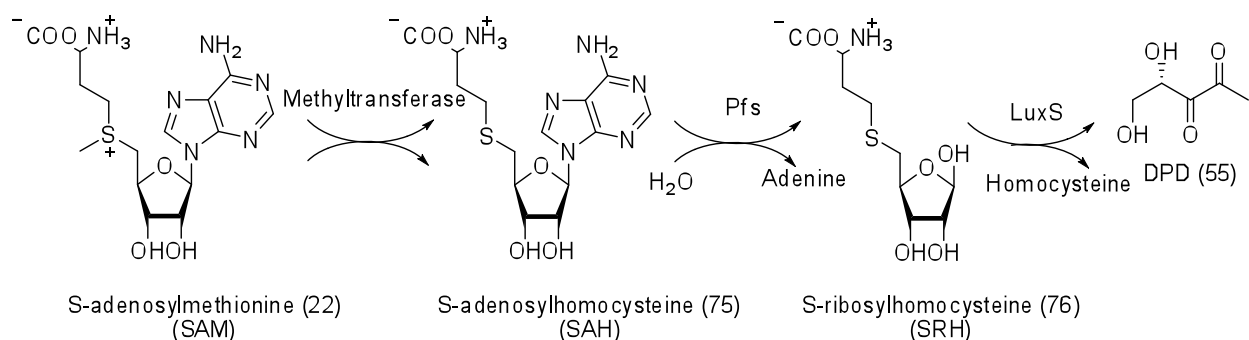
Chapter 5 provides the experimental procedure, spectroscopic characterization and biological protocols used.

Chapter Two

Facile synthesis of AI-2 and a diverse library of analogs

2.1 Introduction: Discovering the chemical identity of AI-2

AI-2 is now considered a universal quorum sensing molecule. Initial genetic studies found that *E. coli*, *S. typhimurium*, *V. cholerae*, *V. harveyi* and *E. faecium* all contained the *luxS* gene which encodes for LuxS, the synthase enzyme for AI-2.⁴⁶ The *luxS* gene is located near *metK* and *Pfs*, genes encoding proteins known to be involved in the active methyl cycle.³⁶



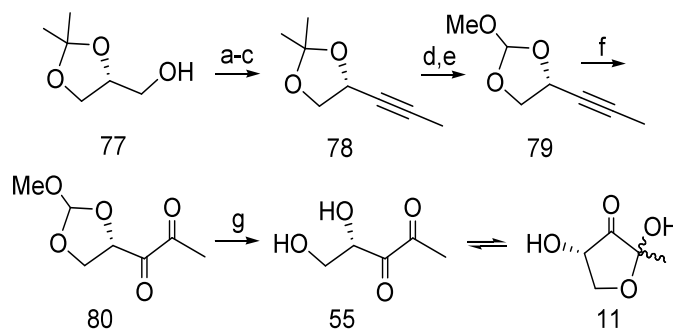
Scheme 2.1: Biosynthesis of 4,5-dihydroxyl-2,3-pentadiene (DPD)

The active methyl cycle is an important S-adenosylmethionine (SAM; **22**) metabolic pathway which produces DPD and cysteine (Scheme 2.1).⁸⁰ A methyltransferase removes a methyl group from the methionine moiety of SAM to form S-adenosylhomocysteine (SAH; **75**).³⁶ Next, the Pfs enzyme removes the adenine group producing S-ribosylhomocysteine (SRH; **76**).³⁶ SRH is the substrate which is subsequently degraded by LuxS to produce 4,5-dihydroxyl-2,3-pentadione (DPD; **55**) and

homocysteine.³⁶ As homocysteine is known to be recycled to become cysteine and then methionine, it was proposed that DPD was an interspecies autoinducer responsible for light production in many organisms in addition to *V. harveyi* whereas HAI-1 (see Figure 1.10; p. 4) is a species-specific signaling molecule.⁴⁶ AI-2 can be synthesized *in vitro* using purified proteins (Pfs and LuxS) and the required substrate (SAH; which is converted to SRH by Pfs).³⁶ It can also be isolated as partial purified AI-2 using chloroform-methanol extraction or a boron affinity column.⁹⁴ Despite these efforts a chemical synthesis of DPD, the precursor to AI-2, was needed to provide spectroscopic confirmation of the structure of AI-2.³⁶ Ultimately a chemical synthesis of AI-2 would also provide the means to make analogs of AI-2, which could be used to perturb AI-2 signaling in bacteria.

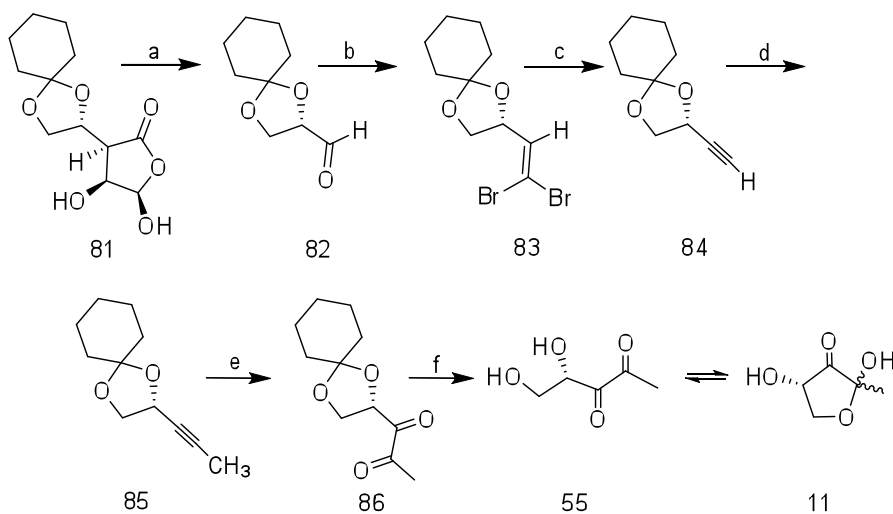
2.2 Previous syntheses of AI-2

Several groups were interested in chemical synthesis of AI-2/DPD^{80, 87, 92} yet despite its fairly simple framework, DPD is highly functionalized, prone to hydration and polymerization and is unstable to column chromatography.⁹⁵ Therefore the chemical synthesis of this molecule is non-trivial.



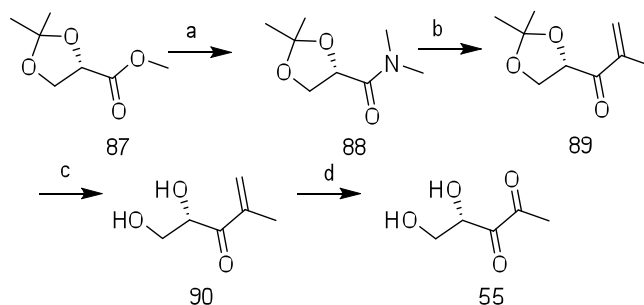
Scheme 2.2: Janda's Synthesis of DPD Reagents and conditions: a) oxalyl chloride, DMSO, CH₂Cl₂; then Et₃N; b) CBr₄, Ph₃P, CH₂Cl₂; c) tBuLi, MeI, THF; d) 60% AcOH; e) CH(OMe)₃(neat), H₂SO₄(cat.); f) KMnO₄, acetone, buffer(aq); g) H₂O, pH 6.5 (K₂HPO₄/KH₂PO₄ (0.1 M), NaCl (0.15M)), 24 hr.⁹⁵

The first synthesis of AI-2, published by Janda in 2004, required seven steps (Scheme 2.2).⁹⁵ The key step of Janda's synthesis is a Corey-Fuch reaction to prepare alkyne **78**.⁹⁵ It was later observed that the acetal protecting group was difficult to deblock therefore compound **78** was converted to compound **79** and a subsequent potassium permanganate oxidation of alkyne **79** afforded diketone **80** (Scheme 2.2).⁹⁵ Acidic cleavage of **80** was monitored by NMR and confirmed for the first time that AI-2 indeed existed as a mixture of the linear, DPD and cyclic products.⁹⁵ The Mallaird reaction of the dione moiety of DPD and 1,2-phenylene diamine gave one single compound confirming that linear and cyclic species were in equilibrium with each other.⁹⁵



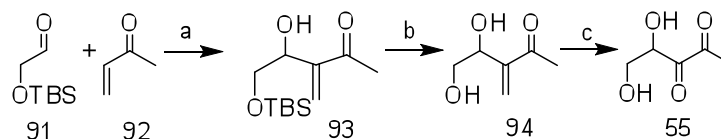
Scheme 2.3: Semmelhack's Synthesis of DPD; Reagents and conditions: a) KIO_4 , K_2CO_3 , $\text{H}_2\text{O}/\text{CH}_2\text{Cl}_2$ (76% yield) b) Ph_3P , CBr_4 (67%) c) i. $n\text{BuLi}$ ii. H_2O (79%) d) i. $n\text{BuLi}$ ii. CH_3I (64%/99%) e) cat. RuCl_2 , NaIO_4 (70%) f) $\text{pH } 1.5$ (100%).⁹⁶

In 2005, Semmelhack reported a synthesis of AI-2, which was similar to what Janda had reported.⁹⁶ However Semmelhack utilized a cyclohexylidene protecting group for the diol instead of an acetal group that was used by Janda (Scheme 2.3).⁹⁶ Also, in Semmelhack's synthesis, rhodium acetate/sodium periodate was used to oxidize the alkyne moiety into the diketone functionality instead of the harsher potassium permanganate reagent used by Janda.⁹⁶ The major drawbacks of both Semmelhack's and Janda's syntheses are two-fold: 1) They both require several chromatographic separation steps which would not facilitate the rapid generation of analogs; 2) because the diol remains protected throughout their syntheses, the synthesis chemical probes of AI-2 whereby one or both of the alcohol groups are functionalized is not possible by these methods.



Scheme 2.4: Vanderleyen Synthesis of DPD a) $\text{NH}(\text{CH}_3)_2$, EtOH; b) $\text{CH}_2=\text{C}(\text{CH}_3)\text{MgBr}$, Et_2O , THF; c) DOWEX 50X8-100, MeOH; d) O_3 , MeOH, Me_2S .⁸²

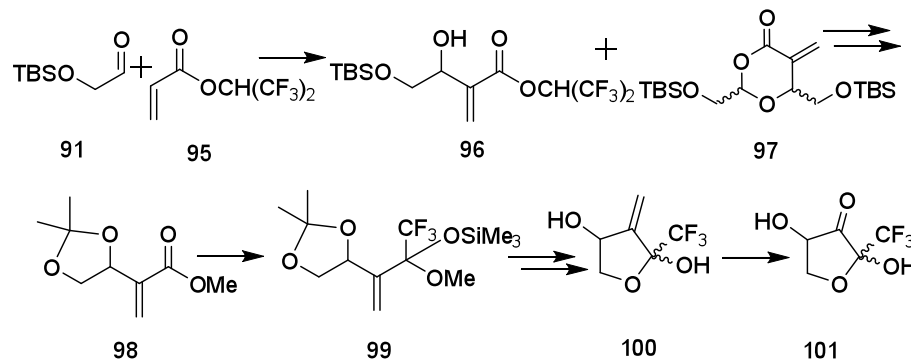
Two additional syntheses of AI-2 were reported in 2005.⁸² The synthesis reported by Vanderleyden required five steps (Scheme 2.4).⁸² Key steps of Vanderleyden's synthesis are the nucleophilic addition of a Grignard reagent to amide 88 and a subsequent ozonolysis to access the dicarbonyl functionality of DPD (Scheme 2.4).⁸² Cleavage of the acetal was performed using DOWEX resin.⁸²



Scheme 2.5: Doutheau Synthesis. Reagents and conditions: (a) THF, DABCO (0.25 equiv), 0°C (b) TBAF (1 equiv), THF, rt. (c) O_3 , MeOH, -78°C , then DMS, -78°C to rt.⁸⁹

Lastly, Doutheau reported a three step synthesis of AI-2 using a Baylis-Hilman reaction and ozonolysis as key steps to access AI-2.⁸⁹ Although the Doutheau synthesis is shorter than the previously reports, for AI-2 analogs whereby the starting material enone is not commercially available several steps are required to make the starting material, *vide vida*.

2.3 Previous syntheses of AI-2 analogs

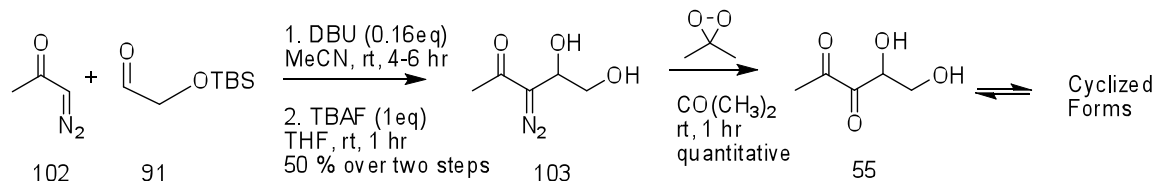


Scheme 2.6: Synthesis of Trifluoromethyl-DPD.⁸⁸

Despite the obvious need for AI-2 analogs for biological testing, only a handful of AI-2 analogs had been synthesized and investigated for biological activities prior to this work.⁸⁸ In 2006 Doutheau synthesized trifluoromethyl-DPD in six steps.⁸⁸ In this work, the key Baylis-Hillman reaction was shown not to be widely applicable, as it resulted in an inseparable mixture of the desired product **96** and the aldehyde dimer **97** (Scheme 2.6).⁸⁸ Doutheau has also reported that the bis-(O)-acetylated AI-2 derivative is a stable analog of AI-2.⁸⁷ In biological media the ester groups of this analogue are cleaved to release active AI-2.⁸⁷ Additionally an AI-2 analog with a tertbutyl ester group was synthesized as well as ethyl-DPD and a 4,5-dihydroxyl-2,3-hexandione compound but these analogs were not tested for biological activity.⁸⁹

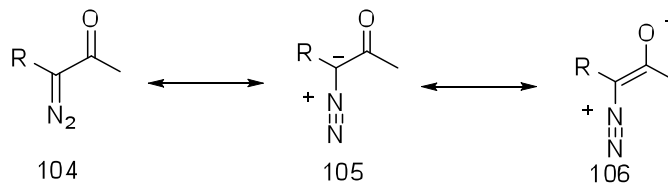
From the foregoing discussions about AI-2's synthesis and adaptation of the reported methodologies toward the synthesis of AI-2 analogs, it was evident that there was the need for a much simpler synthesis of AI-2 that will be amenable to the rapid synthesis of a large library of diverse AI-2 analogs.

2.4 Results: New facile synthesis of AI-2



Scheme 2.7: A new synthesis of AI-2.⁹⁷

We have developed a very simple synthesis of AI-2, which is amenable to analog synthesis.⁹⁷ Our synthesis of AI-2 (Scheme 2.7) begins with the condensation of acyldiazomethane (**102**) with commercially available 2-(tert-butyl dimethylsilyloxy)acetaldehyde (**91**).⁹⁷ The acyldiazomethane was formed via the reaction of acetyl chlorides with diazomethane.⁹⁸ Nucleophilic addition of diazo compounds to aldehydes has previously been achieved through deprotonation of the diazo functionality by a strong base such as LDA or NaOH.⁹⁹ Our initial attempts using LDA to deprotonate acyldiazomethane proved problematic, presumably due to the decomposition of the lithiated diazo intermediate. Purification of the product was also challenging because several side products were formed. In search of a milder method, we employed the DBU-catalyzed condensation of diazo compounds and aldehydes, first reported by Wang.¹⁰⁰ This facile conversion was conducted at room temperature and gave the TBS-protected hydroxydiazo: 5-(tert-butyl dimethylsilyloxy)-3-diazo-4-hydroxypentan-2-one in 58% yield (not shown).



Scheme 2.8: Resonance states of acyldiazo

Subsequently a TBAF deprotection of the silyl group was conducted to give the diazodiol **103**.⁹⁷ Analysis by ¹³C NMR indicated that this diol remained in the linear form; there was an absence of signal between 100 and 120 ppm, which is indicative of lactols and a ketone peak at 192 ppm (See Experimental Section). This is most likely due to the fact that the diazo carbonyl is less electrophilic because of resonance contributor **106** (Scheme 2.8). Also an IR stretch of 2135 cm⁻¹ indicated that the diazo functionality remained intact after treatment with TBAF. During the course of our research we learned that we could conduct the TBAF deprotection without purification of the nucleophilic addition product. We therefore performed the nucleophilic addition and deprotection successively and obtained a yield of 50% over two steps.⁹⁷ The formation of compound **103** set the stage for a facile oxidation to DPD.

Due to its instability to column chromatography, in any successful synthesis of AI-2, the last step must involve the use of reagents that are readily removed. For the oxidation of diazodiol **103** to DPD, we strategically chose the highly reactive dioxirane because it is volatile and easily removed.⁹⁷ Dioxirane was prepared as a concentrated solution in acetone and added to the diazodiol **103**.⁹⁷ Upon disappearance of starting material, the excess reagent and acetone were evaporated.⁹⁷ ¹H NMR showed an

equilibrium mixture of compounds, as expected for the interconverting isomers of AI-2
 (See Figure 2.1).⁹⁷ Our NMR data for synthetic AI-2 is identical to literature data.^{80, 87, 92}

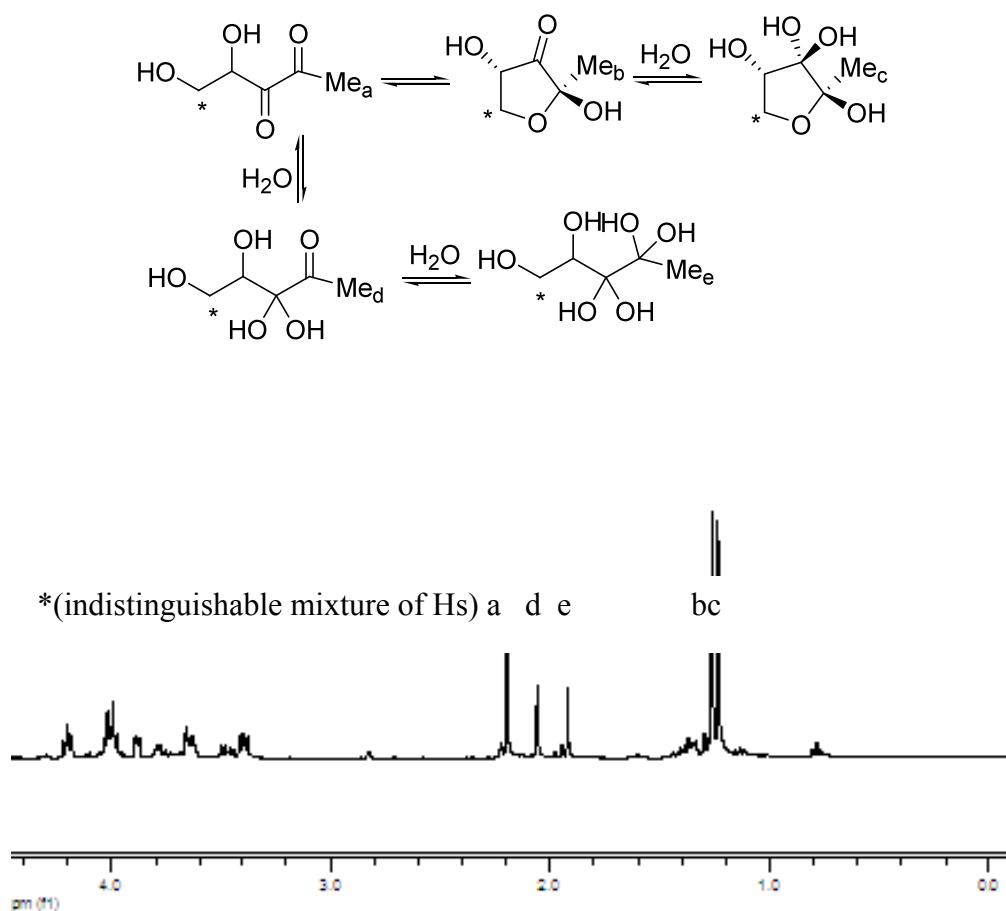
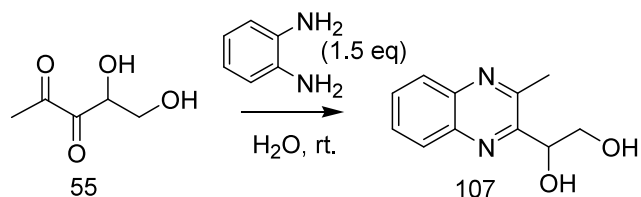


Figure 2.1: ¹H NMR of equilibrium mixture of compounds derived from DPD



Scheme 2.9: Condensation of DPD with 1,2 phenylenediamine to form quinoxaline

Finally the reaction of our synthetic AI-2 with 1, 2-phenylenediamine gave quinoxaline **107** as one species in ^1H NMR (See Figure 2.2).⁹⁷

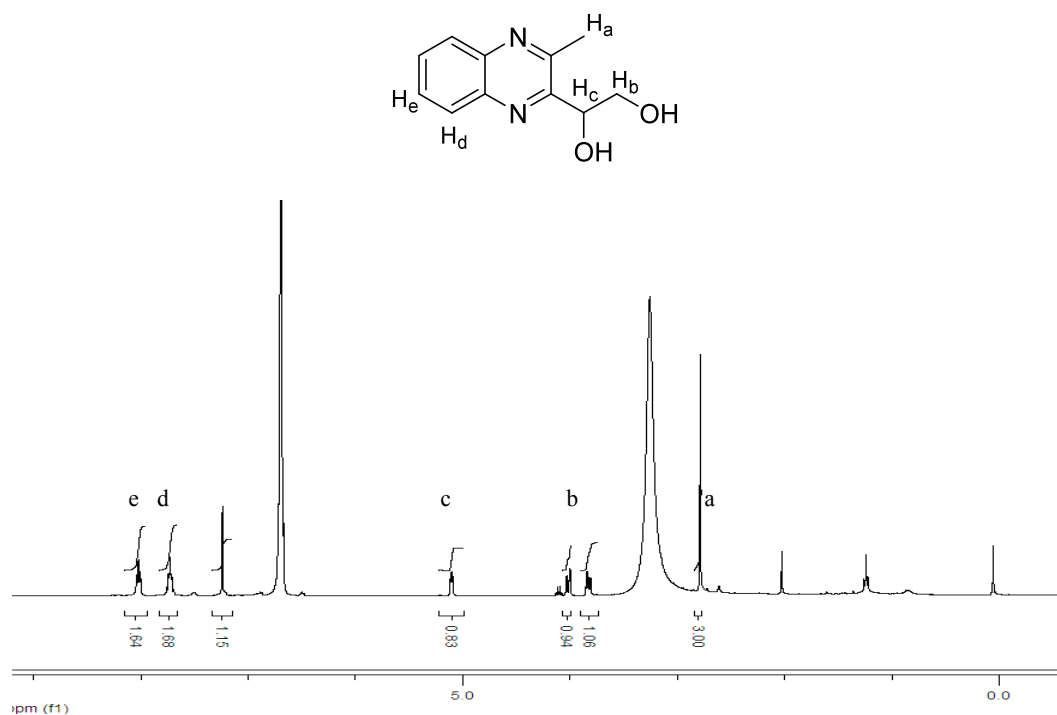


Figure 2.2: ^1H NMR of quinoxaline derivative of AI-2

Our concise synthesis differs from all other published approaches due to the clean final step.⁹⁷ DPD synthesized using this method was stable at room temperature for at least 4 weeks and stable upon refrigeration for several months.

2.5 Synthesis of C1 analogs of AI-2

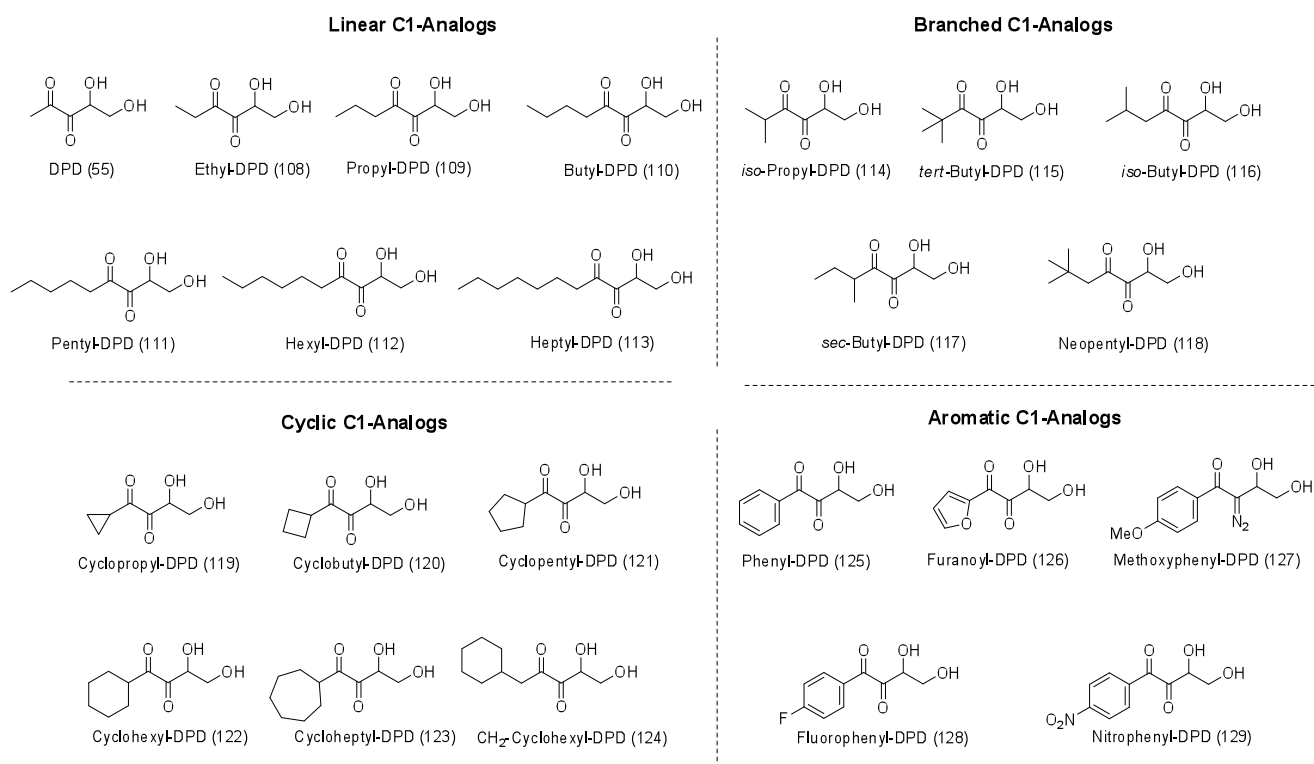


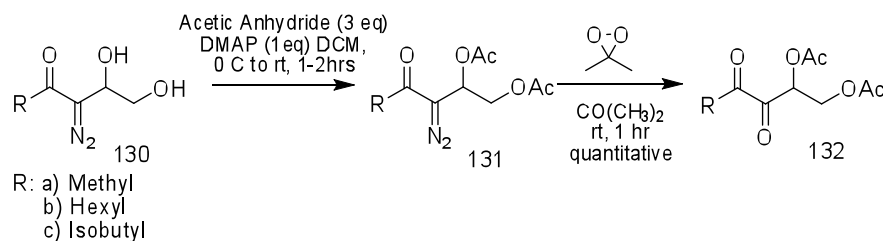
Figure 2.3: Library of diverse C1- analogs of AI-2.^{97, 101}

With this facile synthesis in hand, we proceeded to synthesize 22 AI-2 analogs with branched, cyclic and aromatic as well as linear alkyl groups at the C1 position (**108-129**; Figure 2.3).⁹⁷ Janda's AI-2 synthesis is not amenable to the synthesis of analogs with branched alkyl groups due to the difficulty of alkylation with secondary or tertiary groups.⁹⁰ AI-2 analogs with branched and cyclic alkyl groups could provide important insights into the constraints of the active site in AI-2 receptor proteins such as LuxP and LsrB as well as other known processing enzymes (LsrK and LsrR).⁴¹ Since there are

several commercially available acid chlorides, we were able to prepare diazo carbonyls with various alkyl groups via the reaction of diazomethane and acid chlorides.⁹⁸ Desired alkyl groups whose acid chlorides were not commercially available were obtained from the carboxylic acid compounds. After the diazo carbonyl was acquired, synthesis of this diverse set of analogs followed the previously described method.^{97, 101}

Our new synthesis of AI-2 provided the route needed to access C1 analogs of AI-2 (Compounds **108-129**, see Figure 2.3). These were synthesized using various commercially available acid chlorides without difficulty and without the need for any alterations in our synthetic strategy. The one-pot condensation-deprotection step was accomplished with moderate yields for analogs (**108-129**). NMR analysis of these analogs (**108-129**) showed an equilibrium mixture of linear and cyclic analogs with exceptions being observed with neopentyl-DPD (**118**) and isobutyl-DPD (**116**). The proton NMR of both neopentyl-DPD (**118**) and isobutyl-DPD (**116**) in D₂O indicated that these analogs existed predominantly as linear forms. Also a single species was observed in H¹ NMR of DPD analogs in chloroform. Differences in the equilibrium ratios of DPD and cyclic forms of different analogs may have the potential to affect the biological profile of analogs.

2.6 Synthesis of C4 and C5 analogs of AI-2

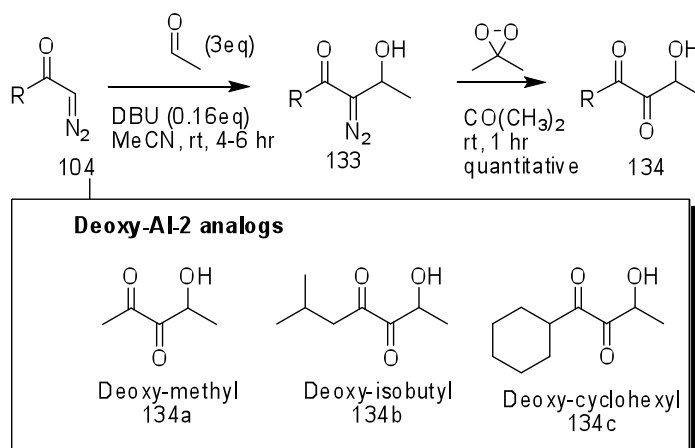


Scheme 2.10: New synthesis of diacetate AI-2 and analogs

Although our synthesis of AI-2 is mild, due to the chemical reactivity of AI-2, purification cannot be achieved. Therefore we endeavored to synthesize ester-protected AI-2 and analog derivatives, since this modification would allow purification to be preformed on silica gel. Using our new methodology, we are able to synthesize the diacetate analog of AI-2 by treating diazodiol **130** with acetic anhydride to give **131** (Scheme 2.10). Dioxirane oxidation of this compound gave diacetate DPD analog (**132a**) which remained in the linear confirmation. Acetate protection was also conducted using select analogs (hexyl (**132b**) and isobutyl (**132c**)). These analogs would be used to observe the effect of protecting the diol on biological activity (See Section 3.10). Also protection of AI-2 (methyl-DPD; **55**) and hexyl-DPD (**112**) with different ester groups were also conducted (see Supplementary S8). Biological activity of these variants was also investigated (Section 3.10).

NMR analysis of ester-protected analogs was much cleaner than free DPD analogs. As expected blocking the C4 and C5 hydroxyl groups prevents cyclization, therefore only one species was observed in both H¹ and C¹³ NMRs spectra of the compounds.

Since AI-2 is known to dimerize at high concentrations, these ester-protected analogs could also provide a way to store AI-2 and analogs for prolonged periods without dimerization. To test this hypothesis, ester analogs of AI-2 were stored at different temperatures for up to four weeks and biological testing was conducted on analogs to determine their stability under these conditions. Results showed that both free and ester-protected analogs maintained their biological profile after 4 weeks. However, these acetate analogs were found to be slightly less active than free analogs (See Supplementary Figure S1). Therefore the instability of AI-2 may be the result of harsh preparation methods by different synthetic routes or concentration.



Scheme 2.11: Synthesis of deoxy-AI-2 analogs.¹⁰¹

Additional variations of the aldehyde used with our method provided 5-deoxy-analogs of DPD (Scheme 2.11).¹⁰¹ Briefly diazocarbonyls were reacted with acetaldehyde to give **133**.¹⁰¹ Dioxirane oxidation of **133** gave **134** as deoxy-analogs of DPD.¹⁰¹ Although deoxy-analogs are essential “locked” in the linear form, ¹H NMR revealed that

the two carbonyl groups are readily hydrated. Synthesis of deoxy-AI-2 as well as other select analogs allowed the biological probing of the importance of the C5 hydroxyl group to be conducted (see Section 3.5).¹⁰¹

2.7 Discussion

Six syntheses of AI-2 have been presented since 2004, yet several years lapsed before this research lead to the introduction of a library of analogs of AI-2. This is evidence that published syntheses are too lengthy and do not provide easy access to AI-2 or analogs. Elaboration of the C1 position of AI-2 using either the Janda or Semmelhack protocol requires an alkylation step via an S_N2 displacement reaction.⁹⁰ This places some constraints on the type of C1 analogs that can be readily obtained via these methods. Furthermore both Janda and Semmelhack's methods protect the diol unit in AI-2 with an acetal protection and this does not allow easy variation at the C4 or C5 position. Additionally as evident in Janda's synthesis the acidic cleavage of the diol moiety is not always straightforward.⁹⁵ In Semmelhack's synthesis although the cyclohexanone by-product is shown not to effect cell growth; it remains to be seen if this by-product effects bioluminescence or can be internalized and/or processed by quorum sensing proteins.⁹⁶ Finally Doutheau's synthesis though concise and keeps the diols free, requires starting enones that are not readily available.⁸⁹ Moreover the Baylis-Hillman reaction can be problematic when attempting to synthesize analogs.⁸⁸ Other recently published syntheses require several chromatographic separation steps (>3) and have not be demonstrated to produce analogs.⁸⁹

2.8 Conclusion

In conclusion, our new synthesis of AI-2 is short and the most amenable to analog synthesis.¹⁰¹ Access to analogs of various shapes and sizes will allow the specificity or promiscuity of quorum sensing proteins to be deduced. Not only does our synthesis allow for the rapid development of a large library of C1 analogs, but is also capable of constructing analogs with variations at the C4 and C5 position. Furthermore this synthesis is shown to make stable AI-2 and analogs have been shown to remain active at various temperatures. (See Supplemental Figure S1) This new synthesis has and will continue to aid in the discovery of new protein targets for anti-quorum sensing chemotherapies.¹⁰¹

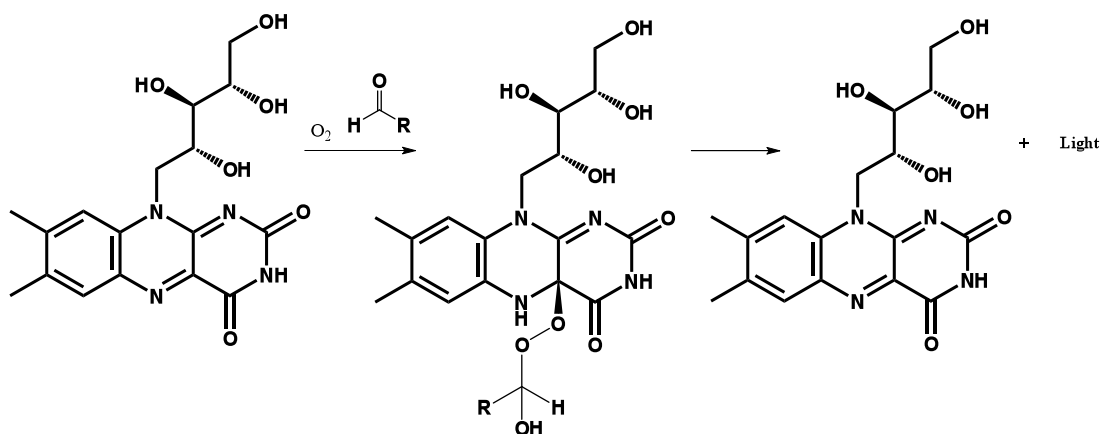
Chapter Three: Biological evaluation of analogs in *V. harveyi*, *E. coli*, *S. typhimurium*
and *P. aeruginosa*

3.1 Bioluminescence

Quorum sensing was first discovered in the marine bacterium *V. fischeri*, which produces light when in a symbiotic association with the Hawaiian Bobtail squid.^{4a} It was observed that light production, known as bioluminescence, was highly dependent on cell density and researchers soon discovered that bacteria could coordinate gene expression through the detection of signaling molecules. This phenomenon was termed quorum sensing.¹⁰²

Bioluminescence is caused by an enzyme-catalyzed reaction, which is controlled by the *lux* (luciferase) gene operon.^{46b} Light is produced by the oxidation of a reduced flavin mononucleotide (FMNH₂) reacting with molecular oxygen and a fatty aldehyde.^{46b} This reaction results in the emission of blue-green light at 490 nm.^{46b} Bioluminescence occurs in several other species of the *Vibrio* genera as well as the *Xenorhabdus*, *Photobacterium*, and *Shewanella* genera.^{46b} Different substrates and proteins control light production in each bioluminescent organism with the only similarity being the use of molecular oxygen.^{46b} The *lux* operon is usually made up of *luxCDABE* genes required for the synthesis of the luciferase (*luxAB*) and aldehyde substrate.^{46b} The aldehyde substrate is formed via a fatty acid reductase encoded by *luxCDE* required to convert polypeptides to the fatty aldehyde.^{46b} The *lux* operon of *V. fischeri* consists of *luxRICDABEG* with the additional genes: *luxR*, *luxI* and *luxG*.^{46b} *luxG* has been proposed to encode the flavin reductase responsible for synthesizing the reduced flavin

mononucleotide.^{46b} We now know that *luxI* and *luxR* encode the synthase (LuxI) and receptor (LuxR) of the AHL autoinducer.⁹ After quorum sensing was first discovered in *V. fischeri*, researchers sought to understand the quorum sensing process in other organisms.



Scheme 3.1: Mechanism of bioluminescence production with riboflavin as the luciferin

V. harveyi, another marine organism which uses quorum sensing to regulate bioluminescence, uses a quorum sensing system that greatly differs from that of *V. fischeri* and other gram-negative bacteria. In *V. harveyi* the *lux* operon consists of *luxCDABEGH*, with the additional gene *luxH* encoding for the synthesis of the riboflavin precursor, 3,4-dihydroxy-2-butanone-4-phosphate.^{46b} This indicates that riboflavin is the luciferin (luciferase substrate) in *V. harveyi*.^{46b} Interestingly, the *lux* operon of *V. harveyi* does not contain genes encoding for LuxI and LuxR.¹¹ This is due to the fact that *V. harveyi* does not use the LuxI-LuxR system for quorum sensing like *V. fischeri*.¹¹ Instead a region separate from the *luxCDABEGH* operon has been identified in *V. harveyi*, which also controls the luminescence phenotype. This region contains the regulatory gene *luxR* (which has no homology to the *luxR* of *V. fischeri*),^{47b} which is a key transcriptional

factor required for expression of the *luxCDABEGH* operon.^{46b} LuxR acts as both an activator and repressor of quorum sensing-controlled processes; it activates bioluminescence, while repressing type III secretion factors.^{11, 45a} LuxR is controlled by a phosphorelay mechanisms involving a series of proteins which are switched on at high cell density (See Section 1.4).¹¹

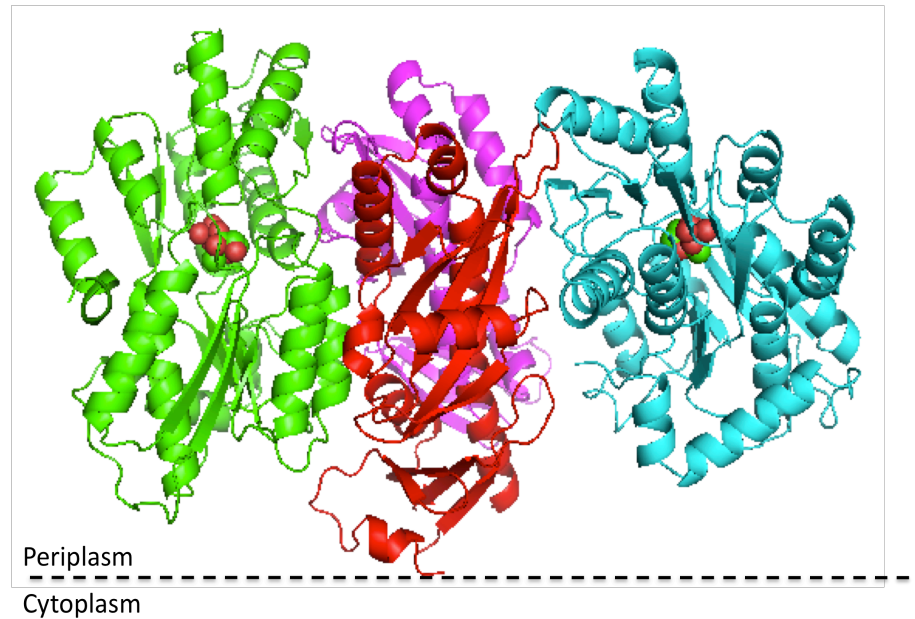


Figure 3.1: Dimer of 2 LuxPQ complexes bound to 2 molecules of AI-2 (LuxP (green) bound to AI-2 and periplasmic domain of LuxQ (red); LuxP' (cyan) bound to AI-2 and periplasmic domain of LuxQ' (magenta))

As previously described, the S-THMF-borate isomer is the active AI-2 found bound to LuxP in *V. harveyi*.³⁷ The presence of boron is likely due to the marine environment in which *V. harveyi* resides, where boron concentrations can reach up to 0.4 mM.¹¹ The AI-2 pathway of *V. harveyi* is quite unique because its receptor exists as a dimer (LuxPQ).^{47a} Crystallography and mutagenesis of this LuxPQ complex have been studied and much insight is now known about the role of this interesting pair in controlling quorum sensing. It is known that LuxQ is in a complex with LuxP even at

low cell density.^{47a} Also certain contacts intrinsically exist between LuxQ and LuxP, which inhibits the conversion of LuxQ from kinase to phosphatase.^{47a} These contacts are disrupted upon binding of AI-2.^{47a} Additionally, it has been revealed that two LuxPQ dimers merge in the presence of AI-2 and exist at a 140 degree angle to each other.¹⁰³ The formation of this tetramer results in the release of LuxQ, switching it from kinase to phosphatase, and therefore turning quorum sensing “on”.¹⁰³ Since these conformational changes are vital for AI-2 to mediate quorum sensing, it may be possible to design small molecules which interfere with these changes and perturb the signaling pathway.

LuxP and analogous phosphorelay mechanisms are found in most *Vibrios*¹¹ Also LuxR homologs have been discovered in *V. cholera* (HapR)¹⁰⁴, *V. anguillarum* (VanT)¹⁰⁵, *V. parahaemolyticus* (OpaR)¹⁰⁶, *V. vulnificus* (SmcR)¹⁰⁷ and *V. fischeri* (LitR)¹⁰⁸. It is likely that homologous proteins exist in organisms in which quorum sensing circuits have not yet been defined. Therefore investigations into how small molecules modulate the bioluminescence production of *V. harveyi* by targeting LuxR and other proteins could have applications in other human and fish pathogens.

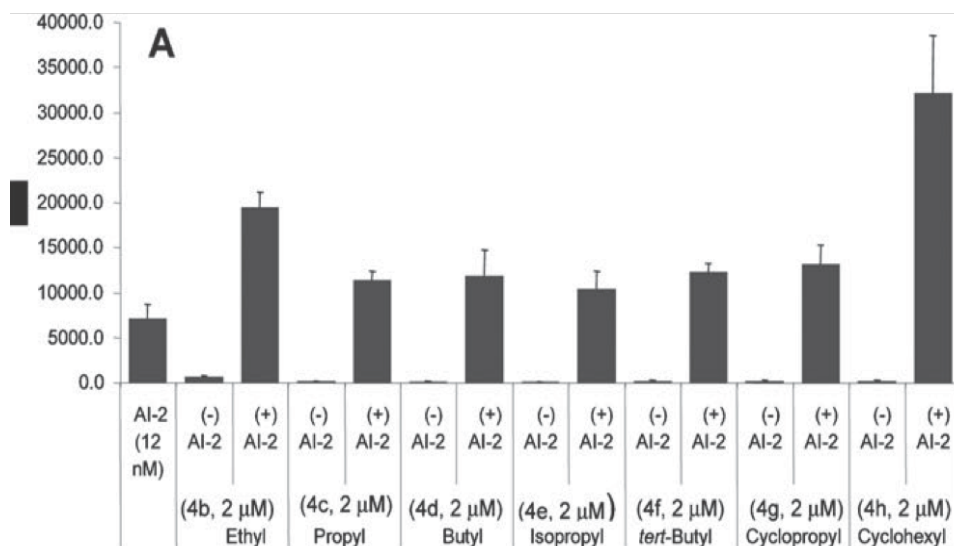
3.2 Synergistic agonism in *V. harveyi*

Table 3.1: *V. harveyi* strains and genotypes^{47b,102}

<i>V. harveyi</i> strains	Relevant genotype and/or property
BB120	Wild type
BB170	Wild type <i>luxN::Tn5</i> (sensor 1 ⁻ , sensor 2 ⁺); AI-1 ⁺ , AI-2 ⁺
MM32	<i>luxN::Tn5; luxS::Tn5</i> (sensor 1 ⁻ , sensor 2 ⁺); AI-1 ⁺ , AI-2 ⁻
BB886	Wild type <i>luxPQ::Tn5</i> Kan
BB721	Wild type <i>luxO::Tn5</i>

V. harveyi bioluminescence induction is often used as a reporter of AI-2 signaling activity.¹⁰² After the development of our facile synthesis, we sought to investigate how C1 analogs of different sizes and shapes modulate the quorum sensing circuit of *V. harveyi* through the monitoring of bioluminescence induction.⁹⁷ Initial screenings for bioluminescence induction in *V. harveyi* were conducted on a diverse subset of the entire C1 analog library created.⁹⁷ Since the LuxN/HAI-1 pathway is the dominant signaling pathway in *V. harveyi*¹⁰⁹ it is important to suppress detection of HAI-1 by LuxN. Also in order to control the amount of AI-2 in this model system, AI-2's synthase, LuxS, must be inactivated. Therefore a LuxN, LuxS double mutant strain (designated MM32) was used for testing. At high concentrations (50 μ M) only ethyl-DPD (**108**; Figure 2.3) and cyclopropyl-DPD (**119**; Figure 2.3) were able to induce bioluminescence after 8 hours albeit to a 10-fold lower degree than AI-2 (Figure 3.1a).⁹⁷ The other analogs tested were not able to induce luminescence even at this high concentration.⁹⁷ At lower

concentrations (2 μ M) none of the analogs significantly induced bioluminescence (Figure 3.1b).⁹⁷ Ironically in the presence of 12nM AI-2, analogs were found to synergize the action of AI-2.⁹⁷ Ethyl-DPD (**108**; Figure 2.3) and cyclohexyl-DPD (**122**; Figure 2.3) gave the most pronounced synergistic agonism causing 4.3-fold and 9.1-fold activation, respectively.⁹⁷ The remaining analogs gave moderate enhancement: propyl-DPD (**109**; 2.6 fold), butyl-DPD (**110**; 2.7 fold), isopropyl-DPD (**114**; 2.4 fold), *tert*-butyl-DPD (**115**; 2.9 fold) and cyclopropyl (**119**; 3.1 fold) (See Figure 2.3 for structures).⁹⁷ Other researchers^{90, 110} have reported similar synergistic agonism however the observation of synergism in analogs of a range of shapes and sizes suggest promiscuity in the quorum sensing proteins responsible for bioluminescence induction in *V. harveyi*.⁹⁷



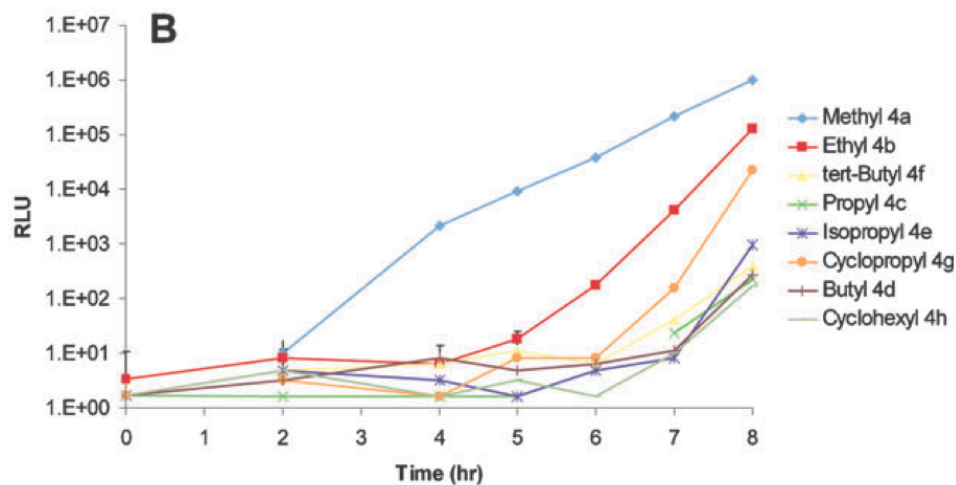


Figure 3.2: a) Bioluminescence induction in *V. harveyi* MM32 (at 8hrs) by addition of 2 μ M analog, 12nM AI-2 and 100 μ M boric acid b) Bioluminescence induction in *V. harveyi* MM32 by addition of 50 μ M analogs and 100 μ M boric acid.⁹⁷

In order to shed light on the mechanism of synergistic agonism by AI-2 analogs, bioluminescent strains with deletions in select proteins involved in signal transduction in *V. harveyi* have been tested (For a detailed scheme of the AI-2 signaling pathway in *V. harveyi* see Supplementary Figure S11, p121). *V. harveyi* BB886 is a LuxQ mutant strain which cannot respond to AI-2.¹⁰² Therefore any modulation observed in this strain would be the result of analogs acting on the AI-1 pathway. Since analogs were not able to induce bioluminescence in this strain, it is probable that synergistic agonism is derived in the AI-2 pathway. (See Supplemental Figure S2) Another possible target of synergistic bioluminescence is the transcriptional regulator LuxR. Small molecules have been shown to bind LuxR and destabilize its interaction with the *lux* operon.¹⁶ Therefore it is plausible to suggest that C1 analogs could also bind LuxR, and enhance stabilization,

resulting in synergism with AI-2. *V. harveyi* BB721, is a LuxO mutant strain and since LuxO indirectly represses luminescence through LuxR this strain is always bright.^{47b} If C1 analogs target proteins downstream of LuxO, incubation with *V. harveyi* BB721 should give the same synergistic response in this mutant (BB721). No synergism was observed with C1 analogs in this strain (See Supplemental Figure S3). Although these observations suggest that the target of C1 analogs is upstream of LuxO, more experimentation is needed to definitively determine the mechanism of synergistic agonism.

3.3 Discussion-*V. harveyi*

Synergistic agonism by C1 analogs of AI-2 provides further insight into the well known quorum sensing circuit of *V. harveyi*. Mutant bioluminescent strains showed that deletion of LuxQ abolished the observed synergisms. Also a lack of response following the mutation of the response regulator, LuxO, suggests that analogs do not bind LuxR. These findings point to the action of C1 analogs being at the LuxPQ level. Analogues are unable to induce bioluminescence on their own. This may lead to the assumption that these molecules do not bind LuxPQ effectively. However it is possible that analogs bind LuxPQ allosterically and sensitize LuxP to AI-2. Mutagenesis at the LuxP:LuxQ interface resulted in sensitizing LuxP to lower AI-2 concentrations.^{47a} Therefore, it is possible that C1 analogs similarly bind to one active site of the LuxPQ dimer while AI-2 binds to the other active site. The conformational change that results from this hetero-ligand binding probably leads to a more efficient kinase activity by LuxQ. Future investigations are needed to determine the actual origin of synergistic agonism.

3.4 Quorum sensing in enteric bacteria

Table 3.2: Enteric bacteria strains and genotypes^{101,39}

<i>E. coli</i> strains	Relevant genotype and/or property
W3110	Wild type
LW7	W3110 $\Delta lacU160-tna2$ $\Delta luxS::Kan$
ZK126	W3110 $\Delta lacU169-tna2$
LW8	ZK126 $l srR::Kan$
LW9	ZK126 $\Delta(l srACDBFG)::Kan$
SH3	W3110 $\Delta lacU160-tna2$ $\Delta luxS \Delta l srK ::Kan; Cm$
<i>S. typhimurium</i> strains	
MET708	$rpsl putRA :: Kan-l sr-l acZYA luxS::T-POP$
MET715	$rpsl putRA :: Kan-l sr-l acZYA$

In addition to bioluminescence induction in *Vibrios*, the AI-2 signaling pathways of enteric bacteria (i.e. *E. coli* and *S. typhimurium*) are well characterized.⁴¹ The *l srACDBFGE* operon controls the expression of the proteins involved in the transport and processing of AI-2 in these organisms.³⁹ The *l sr* operon is AI-2-dependent hence the designation LuxS-regulated (*l sr*).³⁹ In addition to transport proteins, the *l sr* operon divergently transcribes genes which encode LsrK, the AI-2 kinase and LsrR, the transcriptional repressor.³⁹ LsrR plays a vital role in the biofilm architecture of *E. coli*.¹⁰⁸ It was reported that a LsrR mutant strain of *E. coli* produced biofilm which was structurally different from biofilm produced in the wild-type strain.^{74, 108} Investigations

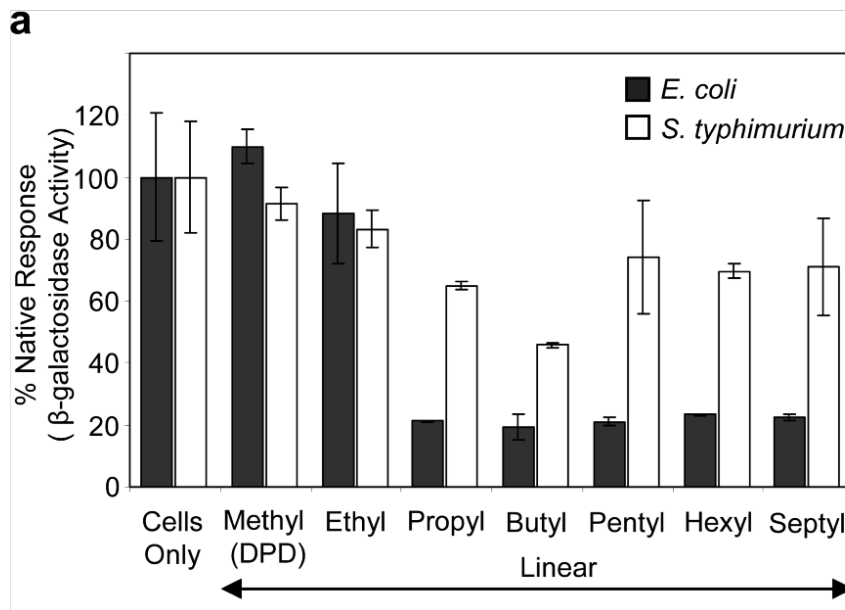
into quorum sensing controlled expression of the *lsr* operon could contribute to the development of anti-biofilm treatments through small molecules which target LsrR.

3.5 Inhibition and processing in enteric bacteria

In addition to *V. harveyi* bioluminescence, we investigated the effect of diverse linear and branched C1 analogs on the uptake and processing of AI-2 in enteric bacteria.¹⁰¹ Since *lsr* is under AI-2 mediated- quorum sensing control, we used *lsr-lacZ* reporter strains to observe modulation of β -galactosidase production by AI-2 analogs. The *lacZ* gene expresses the enzyme β -galactosidase, which in nature cleaves lactose into glucose and galactose. *lacZ* is often fused to gene operons where an analog of lactose, called *o*-nitrophenyl- β -galactoside (ONPG), is used as a colometric indicator of operon activity.¹¹¹ Once the target operon is activated and *lacZ* is expressed, β -galactosidase is produced.¹¹¹ If ONPG is introduced into the system, it is cleaved and generates *o*-nitrophenol.¹¹¹ *O*-nitrophenol is yellow and has a UV absorbance at 420 nm.¹¹¹ Therefore the intensity of *o*-nitrophenol detected is proportional to the amount of β -galactosidase produced. Since the *lsr* operon is under quorum sensing control, bacterial strains containing the *lsr-lacZ* fusion, produces β -galactosidase in response to AI-2. Conversely small molecules which interrupt AI-2 mediate *lsr* expression will not produce β -galactosidase.

Initial results using LuxS mutant strains in both *E. coli* and *S. typhimurium* showed that only ethyl-DPD (**110**; Figure 2.3) was able to activate transcription of *lsr* on its own¹⁰¹ (See Supplementary Figure S5). Next we tested our analogs for their ability to antagonize the AI-2 signaling.¹⁰¹ In bacterial strains which produced their own AI-2

(LuxS⁺) several analogs were able to compete with AI-2 in *E. coli* including all linear analogs with chain-length greater than 2-carbons (propyl-DPD (**109**), butyl-DPD (**110**), pentyl-DPD (**111**), hexyl-DPD (**112**), and heptyl-DPD (**113**); see Figure 2.3 for structures) and several branched analogs (isopropyl-DPD (**114**), isobutyl-DPD (**116**), secbutyl-DPD (**117**), neopentyl-DPD (**118**)).¹⁰¹ Ironically in the LuxS⁺ *S. typhimurium* reporter strain, fewer linear analogs (butyl-DPD; **110** and to a lesser extent propyl-DPD; **109**) and a single branched analog (isobutyl-DPD; **116**) were able to antagonize AI-2 signaling.¹⁰¹ Therefore isobutyl-DPD (**116**) was identified as a potent inhibitor of both *E. coli* and *S. typhimurium* quorum sensing.¹⁰¹ Identical results emerged when exogenous AI-2 was added to LuxS mutant strains in the presence of the C1 analogs.¹⁰¹



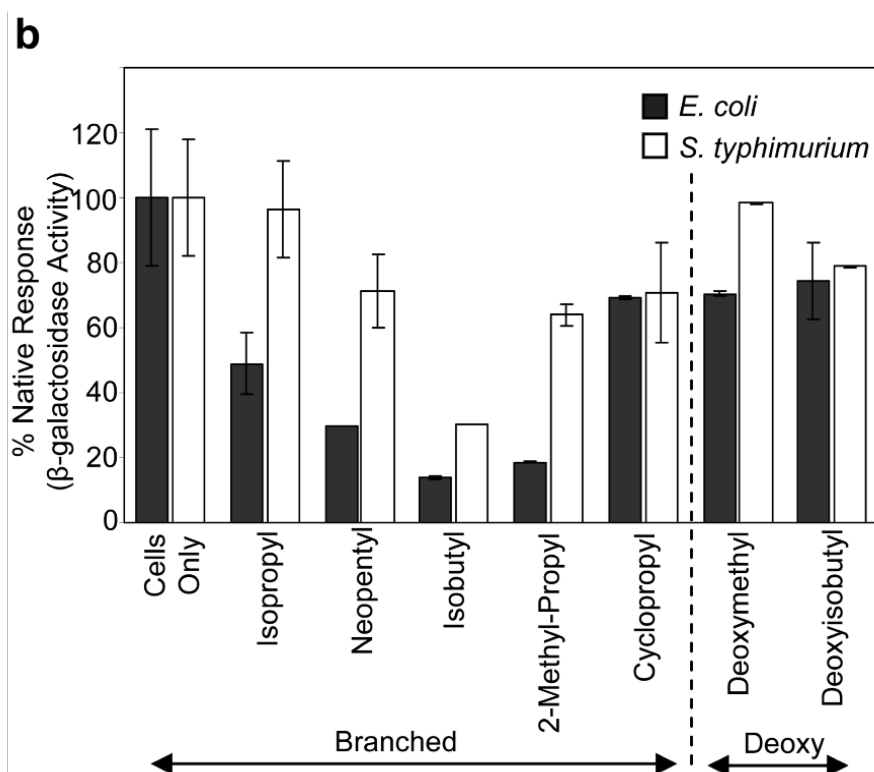


Figure 3.3: AI-2 dependent β -galactoside production in *E. coli* ZK126 pLW11 and *S. typhimurium* MET708 (both *luxS*⁺) in response to a) linear analogs and b) branched and deoxy analogs.¹⁰¹

To further understand the mechanism by which analogs cause inhibition of quorum sensing, we tested their ability to be processed by the AI-2 internalization and phosphorylation proteins, LsrB and LsrK, respectively.¹⁰¹ A *lacZ* reporter strain lacking the transporter, LsrB, was tested for activity in the presence of AI-2 and analogs in *E. coli*.¹⁰¹ Ironically, both agonists (methyl-DPD; **55** and ethyl-DPD; **108**) and antagonists (C3 and greater linear; branched analogs) remained effective in modulating quorum sensing in the absence of the AI-2 transporter (See Supplementary Figure S6).¹⁰¹ It is possible that analogs are able to freely diffuse into the cell or use alternative transporters. Also *in vitro* phosphorylation of AI-2 and analogs using radio-labeled ATP were

conducted to test whether analogs were able to be phosphorylated by LsrK.¹⁰¹ TLC shows that all DPD-analogs are phosphorylated whereas deoxy-analogs, which lack a hydroxyl group at the C5 position (See Section 2.6 for structure of deoxy-analogs) are not phosphorylated (Figure 3.4).¹⁰¹ This confirms Bassler's assignment of phospho-AI-2 as having the phosphate group on the C5 hydroxyl rather than the C4 hydroxyl.⁴¹ Interestingly, even analogs which do not antagonize AI-2 signaling are able to be phosphorylated by LsrK.¹⁰¹ Therefore phosphorylation must not be the only determinant which controls inhibition of the *lsr* operon.

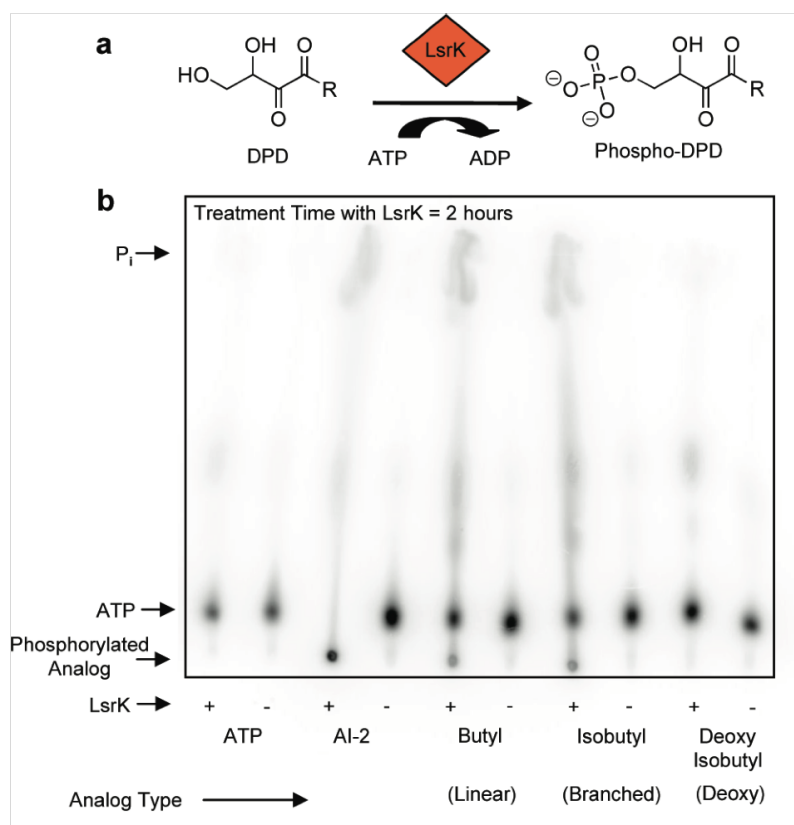


Figure 3.4: a) Phosphorylation of DPD by LsrK in the presence of ATP b) Representative radioactive TLC analysis of LsrK mediated phosphorylation. ATP, AI-2, Butyl-DPD, Isobutyl-DPD and deoxy-Isobutyl treated with LsrK for 2hrs.¹⁰¹

Binding of phospho-AI-2 to the transcriptional repressor, LsrR is key to the expression of genes in the quorum sensing system of enteric bacteria.^{41, 110} Phospho-AI-2 has been shown to bind LsrR and subsequently destabilize its interaction with the *lsr* operon promoter region therefore de-repressing the operon.¹¹² We predict that it is the phosphorylated form of ethyl-DPD (**108**), which causes agonism through destabilization of the LsrR-operon complex. To support this notion, reporter strain lacking LsrK did not show agonism (Figure 3.5).¹⁰¹

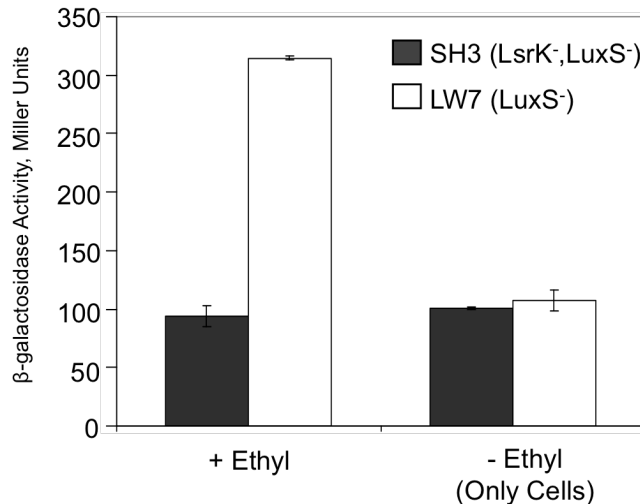


Figure 3.5: AI-2 dependent β -galactoside production in *E. coli* SH3 (LsrK⁻, LuxS⁻) and *E. coli* LW7 (LuxS⁻) in response to ethyl-DPD.¹⁰¹

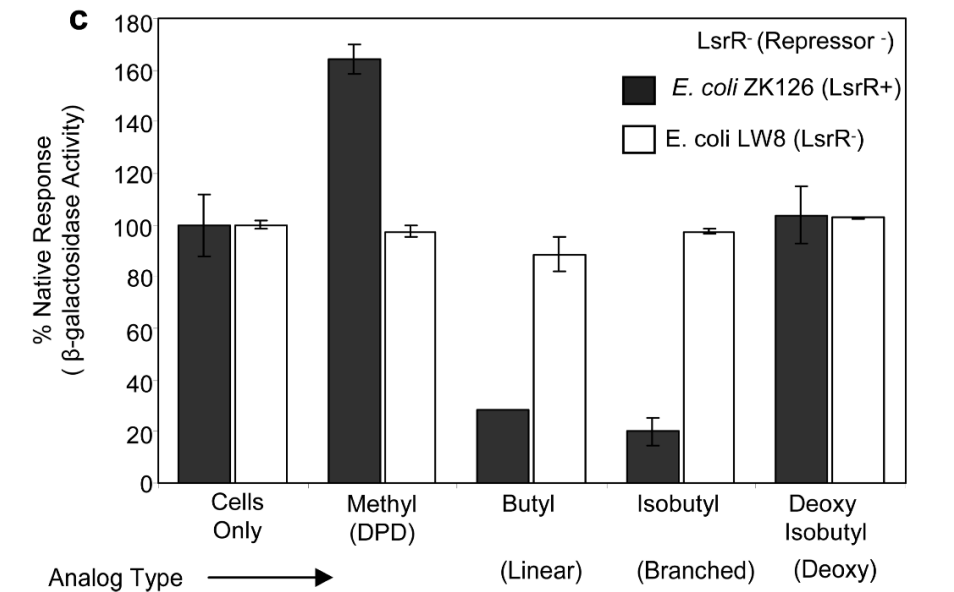


Figure 3.6: AI-2 dependent β -galactoside production in *E. coli* ZK126 (LsrR⁺) and *E. coli* LW8 (LsrR⁻) in response to methyl-DPD (AI-2), butyl-DPD, isobutyl-DPD and deoxy-isobutyl-DPD.¹⁰¹

Likewise, phosphorylated forms of antagonists probably bind LsrR and stabilize its interaction with the *lsr* operon, sustaining its repression of quorum sensing-controlled genes. Screening of the most potent inhibitors (butyl-DPD; **110** and isobutyl-DPD; **116**) in strains lacking the LsrR repressor revealed that inhibition was not observed (Figure 3.6).¹⁰¹ This indicates that inhibition of the *lsr* operon occurs through LsrR.

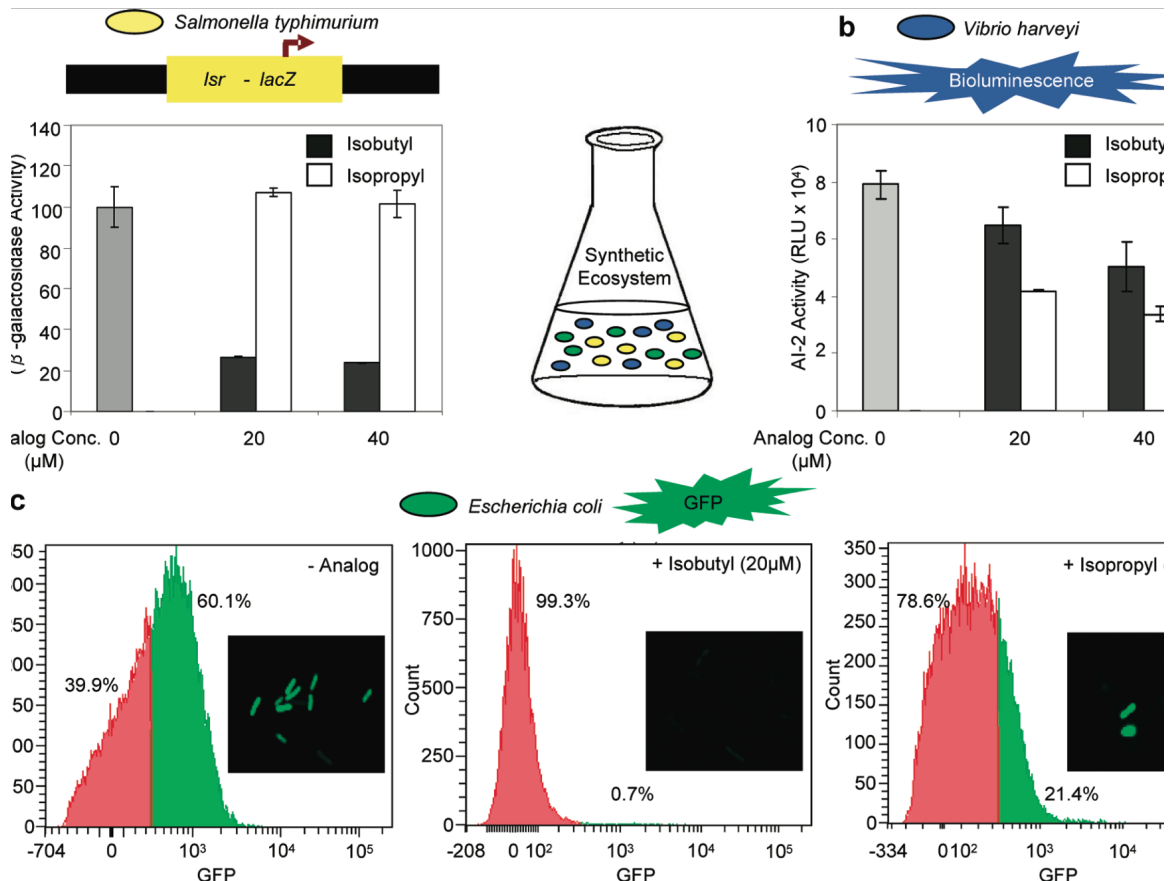


Figure 3.7: a) AI-2 dependent β -galactoside production in *S. typhimurium* MET708 b) AI-2 dependent bioluminescence production in *V. harveyi* BB170 and c) Flow cytometry analysis of AI-2 dependent GFP induction in *E. coli* W3110 pCT6 (all strains are *luxS*⁺) in response to isobutyl-DPD and isopropyl-DPD.¹⁰¹

It is well known that AI-2 signaling in one species can be detected and interfere with the quorum sensing network of another unrelated species.⁴² Thus we postulated that inhibitors of AI-2 signaling would be able to perturb several quorum sensing systems simultaneously. To test this hypothesis, we examined our most potent analog isobutyl-DPD (**116**), in a tri-species synthetic ecosystem.¹⁰¹ This synthetic ecosystem was strategically designed so that the response of each organism to AI-2 was uniquely identifiable and could be quantified separately.¹⁰¹ The following responses were utilized:

β -galactoside production in *S. typhimurium* MET708, GFP induction in *E. coli* W3110 pCT6, and bioluminescence induction in *V. harveyi* BB170.¹⁰¹ As anticipated isobutyl-DPD (**116**) was a potent inhibitor of *E. coli* GFP induction and *S. typhimurium* β -galactosidase production in the synthetic ecosystem (Figure 3.7a and 3.7c).¹⁰¹ Surprisingly isobutyl-DPD (**116**) was also able to inhibit *V. harveyi* bioluminescence (Figure 3.7b).¹⁰¹ Although C1 analogs of AI-2 are known to cause synergistic agonism of bioluminescence in AB media⁹⁷, it has been shown that once a quorum is already formed they act as antagonists.¹⁰¹ This antagonism is only observed in LM media.¹⁰¹ Since bioluminescence is highly dependent on environment, we assume that components of the media may change the observed effect of analogs. Therefore isobutyl-DPD (**116**) has emerged as a broad-spectrum inhibitor of quorum sensing.

While isobutyl-DPD (**116**) showed broad inhibition, isopropyl-DPD (**114**) was found to be a selective inhibitor of *E. coli* which did not effect *S. typhimurium* (Figure 3.7a and 3.7c).¹⁰¹ Selectivity is of great benefit when pathogenic bacteria exist in a niche where symbiotic organisms exist. Similar to isobutyl-DPD, isopropyl-DPD was also found to inhibit *V. harveyi* bioluminescence (Figure 3.7b).¹⁰¹ Therefore we have found both a broad and a selective inhibitor which were effective in a mixed culture environment.¹⁰¹

3.6 Discussion- *E. coli* and *S. typhimurium*

Three proteins have been identified as key AI-2 signaling in enteric bacteria, LsrB, LsrK and LsrR and may act as checkpoints when AI-2-like molecules are introduced into the system.¹⁰¹ For the first checkpoint, we've shown through an LsrB

mutant that analogs are able to enter the bacterial cell through diffusion or alternative transporters.¹⁰¹ AI-2 has been shown to be transported by the ribose binding protein RbsB in other organisms.⁵⁵ Therefore it is plausible that AI-2 analogs also use this apparatus as an alternative entry into the cell or perhaps they can freely diffuse into the cell.¹⁰¹ For the second checkpoint, *in vitro* phosphorylation was shown in all analogs.¹⁰¹ Moreover deoxy-analogs were not phosphorylated indicating that the hydroxyl group on the C5 position is necessary for phosphorylation.¹⁰¹ Also we've confirmed that phosphorylation is required for gene expression, as the LsrK mutant was unable to activate the *lsr* operon.¹⁰¹ From this observation we can assume that it is the phosphorylated form of analogs which cause agonism or antagonism of the *lsr* operon.¹⁰¹ Finally lack of inhibition in LsrR mutants indicate that LsrR is the target of C1 analogs and the various biological profiles of the analogs are likely due to varying binding affinities for LsrR. We predict that the C1 alkyl chains interact with LsrR and cause the protein to bind to the DNA promoter region of the *lsr* operon to different extents.¹⁰¹ Since a minimum 3-carbon chain length is required for antagonism we can assume the side chain binds to a hydrophobic region and causes a stronger LsrR-DNA complex to form.¹⁰¹ In contrast to AI-2 (methyl-DPD; **55**) and ethyl-DPD (**108**) cause LsrR not to bind and therefore de-represses the operon.¹⁰¹

The differences observed in quorum sensing modulation in *S. typhimurium* and *E. coli* indicate that subtle differences may exist which make the *S. typhimurium* system more robust. Interestingly several linear and branched analogs were able to repress *lsr* transcription in *E. coli* while only butyl- and isobutyl-DPD were effective in *S. typhimurium*.¹⁰¹ These findings were unexpected since the two quorum sensing systems

are homologous.¹⁰¹ Alignment studies have shown that LsrK and LsrR proteins in these organisms share 82% and 77% homology, respectively.¹⁰¹ Also the *E. coli* LsrR binding site showed 83% homology to the *S. typhimurium* promoter region.¹⁰¹ In addition predicted secondary and tertiary structures show similar folds for these organisms (Figure 3.8).¹⁰¹ Further studies are needed to determine why these systems show divergent response to C1-analogs.

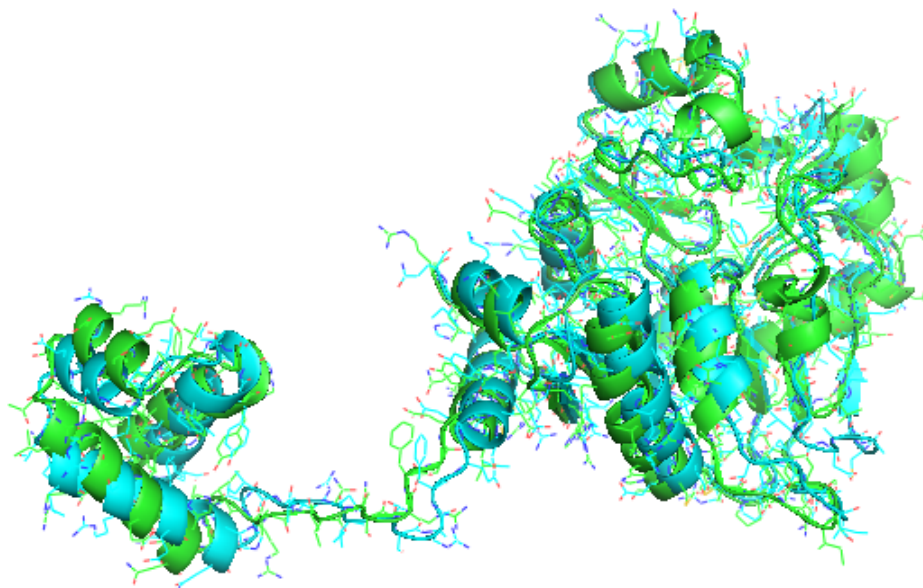


Figure 3.8: Predicted tertiary structures of the LsrR proteins of *S. typhimurium* (green) and *E. coli* (cyan) provided by ESyPred3D¹⁰¹

The observation that analogs of AI-2 can be either broad- or selective-inhibitors in mixed cultures is medically relevant since bacteria rarely exist in isolation.¹¹³ Therefore quorum sensing targets which remain effective in mixed cultures that most resembles natural environments are valuable. Overall, linear and branched analogs gave much insight into the ability of AI-2 like molecules to be processed by the AI-2 machinery of enteric bacteria.

3.7 *Pseudomonas aeruginosa*

P. aeruginosa is an opportunistic pathogen which causes biofilm-related lung infections in cystic fibrosis patients.¹¹⁴ *P. aeruginosa* quorum sensing uses the typical LuxI-LuxR-type system found most often in gram-negative bacteria.⁷ Quorum sensing has been shown to control biofilm in this organism as mutant strains with alterations in the quorum sensing pathway are deficient in biofilm formation.¹¹⁴ Biofilm formation was restored upon addition of the signaling molecule, *N*-3-oxo-dodecanoyl-homoserine lactone (See Figure 1.1; **6**).¹¹⁴ This observation suggests that *N*-3-oxo-dodecanoyl-homoserine lactone (**6**) is vital for biofilm formation and that small molecules which can compete with this signaling molecule may be able to prevent biofilm formation.¹¹⁴ Several small molecules analogs of AHLs have been identified which modulate *Pseudomonas* biofilm formation yet they face solubility and stability issues.²⁵⁻²⁶ Therefore there is a need for structurally diverse small molecules which target quorum sensing and are able to clear *P. aeruginosa* associated biofilm infections.

AI-2 is not synthesized in *P. aeruginosa* nor have any AI-2 receptors been identified in this organism.⁸³ Genetic analysis has shown that AI-2 up-regulates some genes required for *Pseudomonas* pathogenesis.⁸³ This is an interesting phenomenon as AI-2 has been suggested to be a universal signaling molecule and therefore able to be sensed by an array of bacteria. C1 analogs of AI-2 contain side chains which resemble the side chains found in AHLs. It has been suggested that these analogs freely diffuse through the cell in a manner similar to how AHLs diffuse into the cells and directly bind the LuxR-type transcription proteins required for quorum sensing in gram-negative bacteria. If AI-2

analogs are AI-1-like and therefore able to affect the AI-1 pathway of gram-negative bacteria in addition to the AI-2 pathway of enteric bacteria, this dual action is another means of universally affecting quorum sensing.

3.8 *P. aeruginosa* pyocyanin production modulation

Table 3.3: *P. aeruginosa* strains, genotypes and references

<i>P. aeruginosa</i> strains	Relevant genotype and/or property
PAO1	Wild type

AHL analogs of various shapes and sizes have been found to modulate quorum sensing and biofilm formation in *P. aeruginosa*.¹⁰ Likewise we decided to screen our entire library of C1 analogs including cyclic and aromatic (See Figure 2.3; **108-129**) on *P. aeruginosa*.

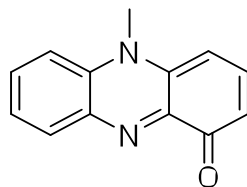


Figure 3.9: *P. aeruginosa* virulence factor pyocyanin

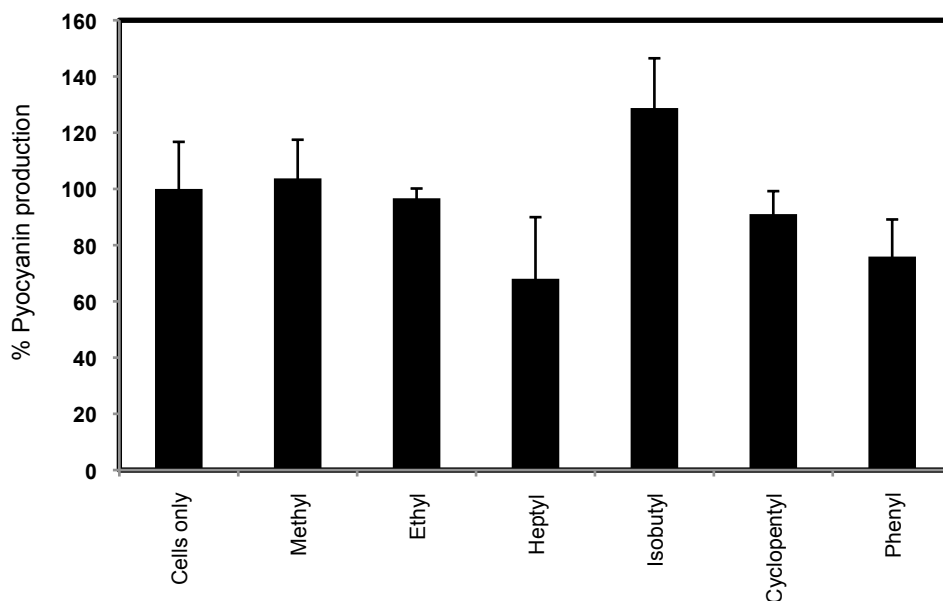
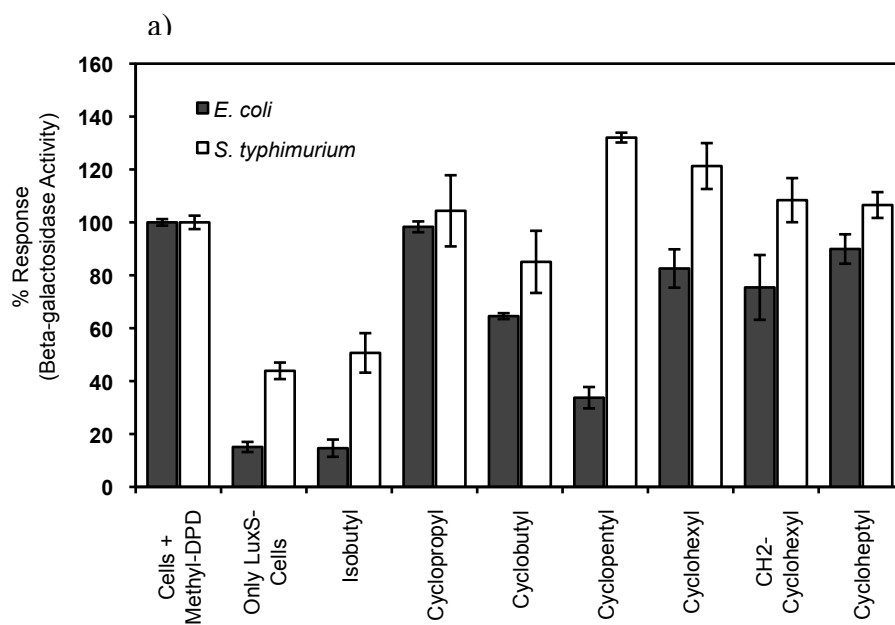


Figure 3.10: Pyocyanin production in *P. aeruginosa* PAO1 in response to methyl-DPD, ethyl-DPD, heptyl DPD, isobutyl-DPD, cyclopentyl-DPD and phenyl-DPD

The effect of analogs on the production of a virulence factor, pyocyanin, is an interesting method to evaluate the effect of small molecules on this quorum sensing-controlled process. Pyocyanin is an aromatic compound which absorbs at 540 nm and produces a blue-green pigment (Figure 3.9).¹¹⁵ In the wild-type strain PAO1, only a few C1 analogs were found to reduce pyocyanin production. Several linear analogs moderately inhibit pyocyanin production while some cyclic and aromatic analogs are more effective. A panel of analogs are shown in Figure 3.10. Heptyl-DPD (**112**), cyclopentyl-DPD (**121**) and phenyl-DPD (**125**) (see Figure 2.3 for analog structures) were the most effective modulators of pyocyanin production (See Supplementary Figure S6 for biological profile of analogs in *P. aeruginosa*).

In addition the cyclic and aromatic analog subsets were screened in *E. coli* and *S. typhimurium* for their ability to effect the *lsr* operon. Initial agonism assays showed that

none of the cyclic or aromatic analogs were able to induce gene expression on their own (See Supplementary Figure S7). Next the analogs were screened in the presence of synthetic DPD in order to determine if any analogs act as antagonists.



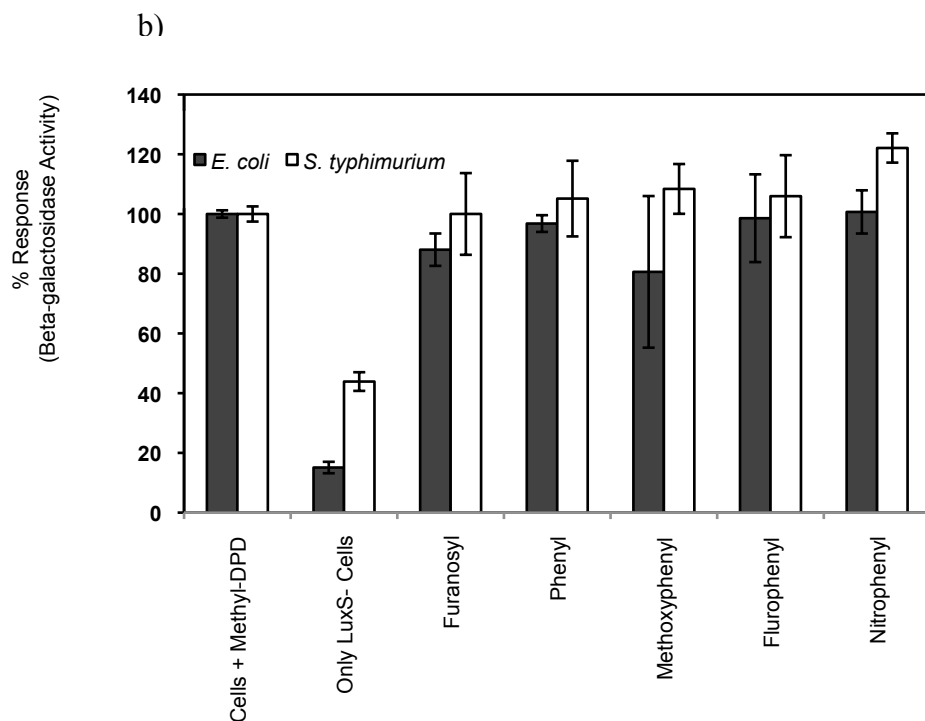


Figure 3.11: AI-2 dependent β -galactoside production in *E. coli* LW7 and *S. typhimurium* MET715 (both *luxS*⁻) in response to 40 μ M synthetic DPD and a) cyclic analogs and b) aromatic analogs.

Of the cyclic analogs only cyclopentyl-DPD (**121**) significantly antagonized AI-2 activity while cyclobutyl-DPD (**120**) gave minimal inhibition in *E. coli* (see Figure 3.11). Larger cyclic analogs (cyclohexyl-DPD (**122**), CH₂-cyclohexyl-DPD (**124**) and cycloheptyl-DPD (**123**); see Figure 2.3) all did not give significant knockdown. Therefore AI-2 processing enzymes may be unable to accommodate large groups at the C1 position greater than cyclopentyl-DPD (**121**). Also since 5-membered rings are more flexible than 3- and 4- membered rings, a desired conformation may be required for inhibition that is inaccessible to the more strained cyclopropyl-DPD (**119**) and cyclobutyl-DPD (**120**) analogs. None of the aromatic analogs were able to modulate quorum sensing in *E. coli*

or *S. typhimurium* including the 5-membered aromatic analog, furanoyl-DPD. It is likely that some degree of flexibility is required at the C1 position for analogs to be processed, which the flat aromatic compounds lack. Cyclopentyl-DPD (**121**) was not effective at inhibiting *S. typhimurium* *lsr* expression. This is consistent with our previous finding that the two enteric bacteria show differing levels of susceptibility.¹⁰¹ Further studies and molecular modeling will be conducted to determine if cyclic and aromatic groups are incompatible with AI-2 processing enzymes due to their bulkiness and rigidity.

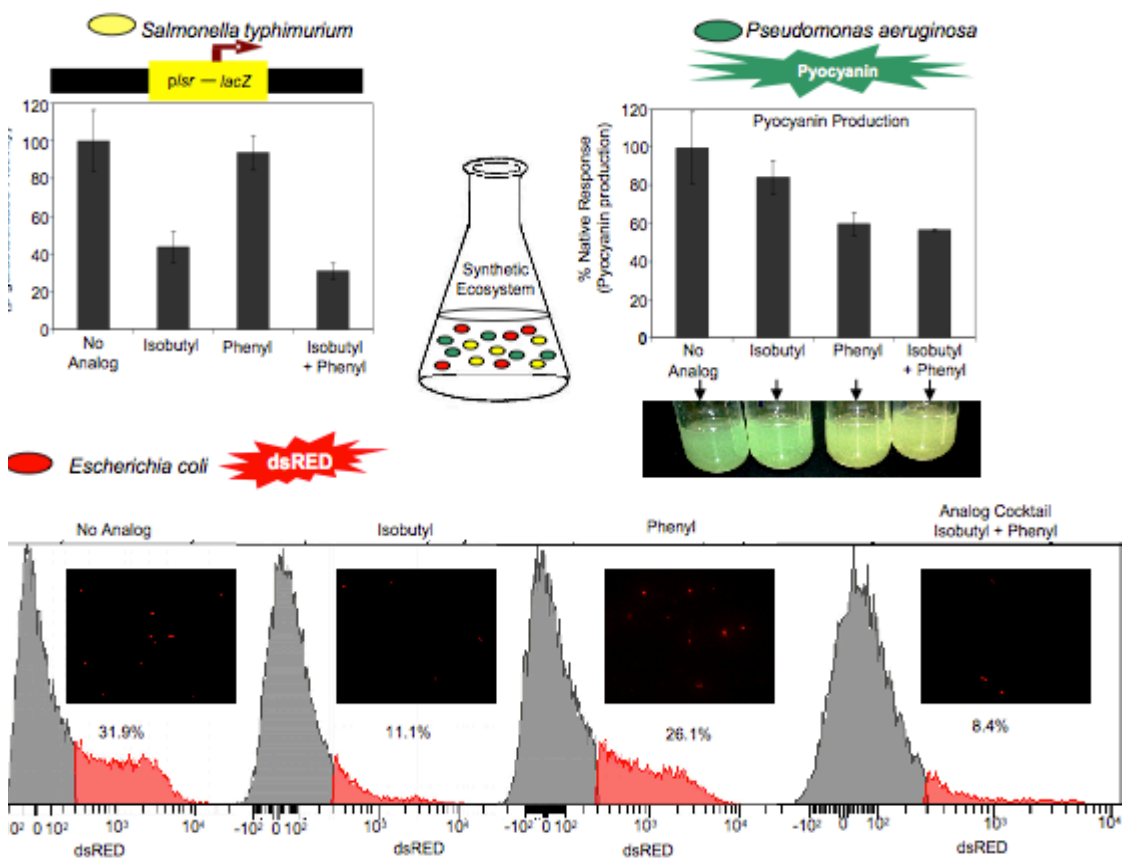


Figure 3. 12: a) AI-2 dependent β -galactoside production in *S. typhimurium* MET708 b) Pyocyanin production in *P. aeruginosa* PAO1 and c) Flow cytometry analysis of AI-2 dependent RFP induction in *E. coli* W3110 pCT6 dsRed (all strains are *luxS*⁺) in response to isobutyl-DPD, phenyl-DPD and a cocktail containing both isobutyl-DPD and phenyl-DPD.

A new synthetic ecosystem was constructed using *E. coli*, *S. typhimurium* and *P. aeruginosa*. As previously discussed, in order to decipher the response of each bacterium different reporters were used: AI-2 induced β -galactoside production in *S. typhimurium* MET708, pyocyanin production in *P. aeruginosa* PAO1 and AI-2 dependent RFP induction in *E. coli* W3110 pCT6 dsRed. Previously isobutyl-DPD (**116**) was found to be an inhibitor of *E. coli*, *S. typhimurium* and *V. harveyi* yet it is not able to inhibit pyocyanin production. Phenyl-DPD (**125**) is a potent inhibitor of pyocyanin production, therefore we developed a cocktail containing these two complementary analogs. This cocktail was able to knockdown quorum sensing in all three organisms of this new synthetic ecosystem. The analog cocktail approach is a new avenue to simultaneously perturbing the quorum sensing system of several organisms to be further explored.

3.9 Discussion- *P. aeruginosa*

These results show that expanding the diversity of groups at the C1 position of AI-2 to include cyclic and aromatic groups allow for diverse bacteria to be targeted. In addition to the 3-carbon length minimum previously identify for *E. coli* inhibition, cyclic analogs reveal that a five-membered ring (cyclopentyl-DPD; **121**) may be the optimal ring size able to effect AI-2 processing enzymes. Also smaller rings and aromatic analogs suggest that some degree of flexibility is required for inhibition.

Although *P. aeruginosa* is a part of the human microflora, lung infections caused by these pathogens are difficult to treat due to robust biofilm.¹¹⁵ AHL analogs which have been shown to perturb quorum sensing regulated biofilm formation are known to have solubility issues and are susceptible to quenching by acylases, lactonases as well as other

native defense enzymes.^{14b, 116} AI-2 analogs, which are able to interfere with the AI-2 pathway in enteric bacteria as well as the AI-1 signaling pathway in organisms such as *P. aeruginosa*, would be a valuable addition to the arsenal of quorum sensing small molecules currently available.

3.10 Ester-protected AI-2 and analogs

Although ester-protection may be desired for the stability and purification of AI-2 and analogs, it remains to be seen if these derivative will behave similarly in biological systems. Acetate-protected AI-2 has been shown to induce bioluminescence in a manner similar to free AI-2.⁸⁷ It is therefore hypothesized that analogs of AI-2 with ester protecting groups would also act in a manner synomonous to the free DPD analog. Also different ester protecting groups may offer varying levels of bioactivity. Ester protected pro-drugs of AI-2 and hexyl-DPD were synthesized and first screened in *V. harveyi* MM32 (LuxN-, LuxS-). Also ester-protected analogs did not inhibit bacterial growth (see Supplementary Figure S8). We found that ester analogs of AI-2 were able to induced bioluminescence to a significant extent (Figure 3.13a; black bars) were as ester-protected hexyl analogs were not able to induce bioluminescence in their own (Figure 3.13b; white bars). This would be expected since C1 analogs do not induce bioluminescence on its own (with the exception of ethyl-DPD; **108**).

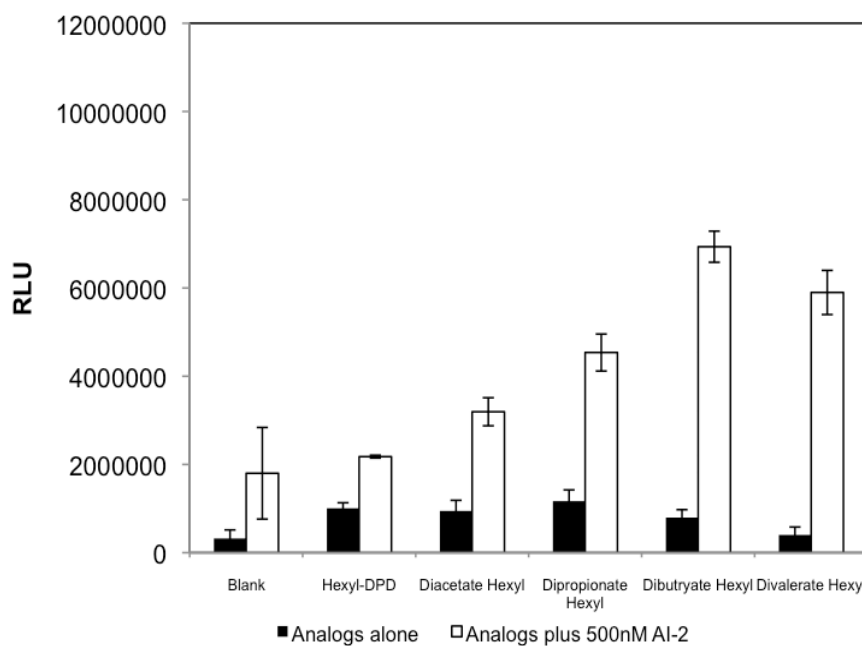
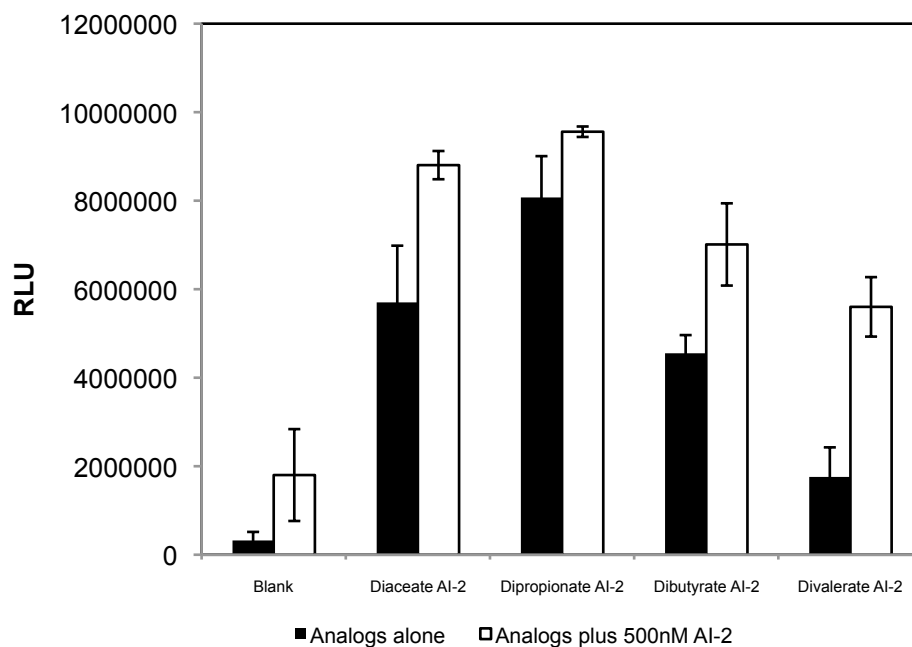


Figure 3.13: Bioluminescence induction in *V. harveyi* MM32 (LuxS⁻) in response to various ester protections on AI-2 and hexyl-DPD

Next, analogs were screened for synergistic agonism. Synergistic agonism was observed in *V. harveyi* MM32 (LuxS⁻) in response to ester protected hexyl analogs in the presence

of exogenous 500nM AI-2 (Figure 3.13b; light gray bars). Surprisingly ester-protected analogs caused more synergism than free hexyl-DPD. Similarly AI-2 prodrugs were also tested in the presence of 500nM AI-2 (Figure 3.13a).

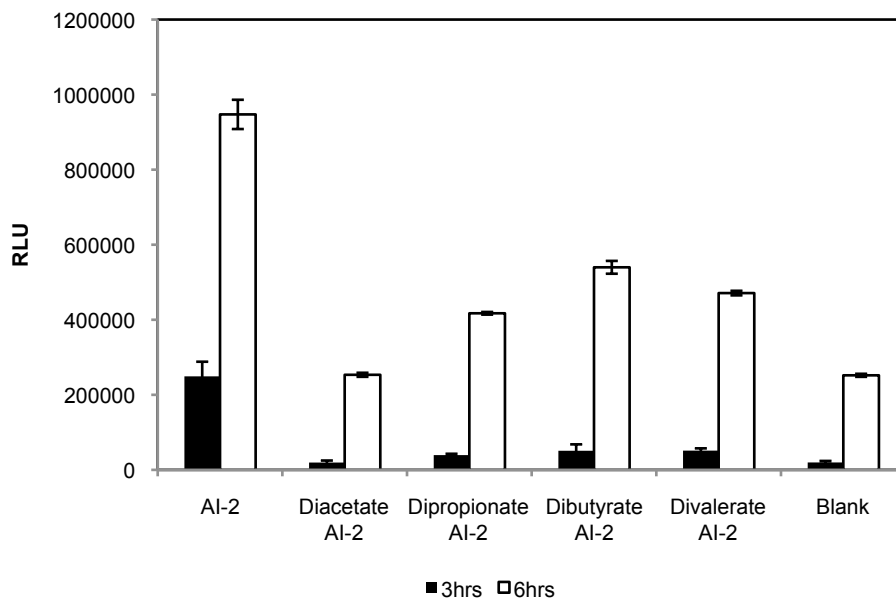


Figure 3.14: Bioluminescence induction in *V. harveyi* BB170 (LuxS⁺) in response to various AI-2 prodrugs over time

Although ester protected AI-2 derivatives were active they did not cause bioluminescence to the degree to which free AI-2 induced (Figure 3.14a) in *V. harveyi* BB170 (LuxS⁺). It is possible that these analogs are limited by the time needed for cleavage of the ester groups. As Figure 3.14 shows the activity of ester protected AI-2s increased significantly from 3hrs to 6hrs. This suggests that these analogs may have a time-dependent response.

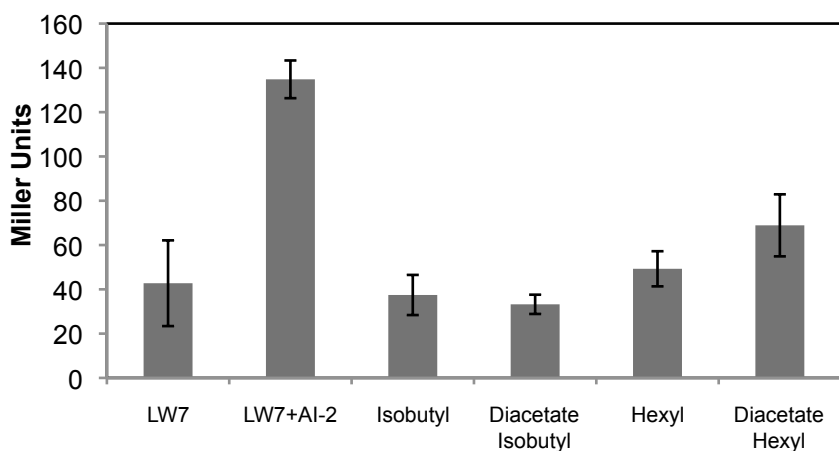


Figure 3.15: AI-2 dependent β -galactoside production in *E. coli* LW7 (LuxS⁻) in response to isobutyl, diacetate isobutyl, hexyl and diacetate hexyl in the presence of AI-2 (1:1 ratio)

Finally ester protected analogs were screened for activity in *E. coli*. Since isobutyl-DPD was identified as the best inhibitor in *E. coli*, this analog and diacetate isobutyl (**132c**) was compared for antagonism of β -galactosidase production in the presence of exogenous AI-2. Hexyl-DPD (**111**) and diacetate hexyl (**132b**) were also tested. Results showed that the ester protected inhibitors were able to compete with AI-2 as well as the free analogs (Figure 3.15). Similarly diacetate AI-2 (**132a**) was able to induce β -galactosidase production although to a lesser extent than AI-2 (Supplementary Figure S9).

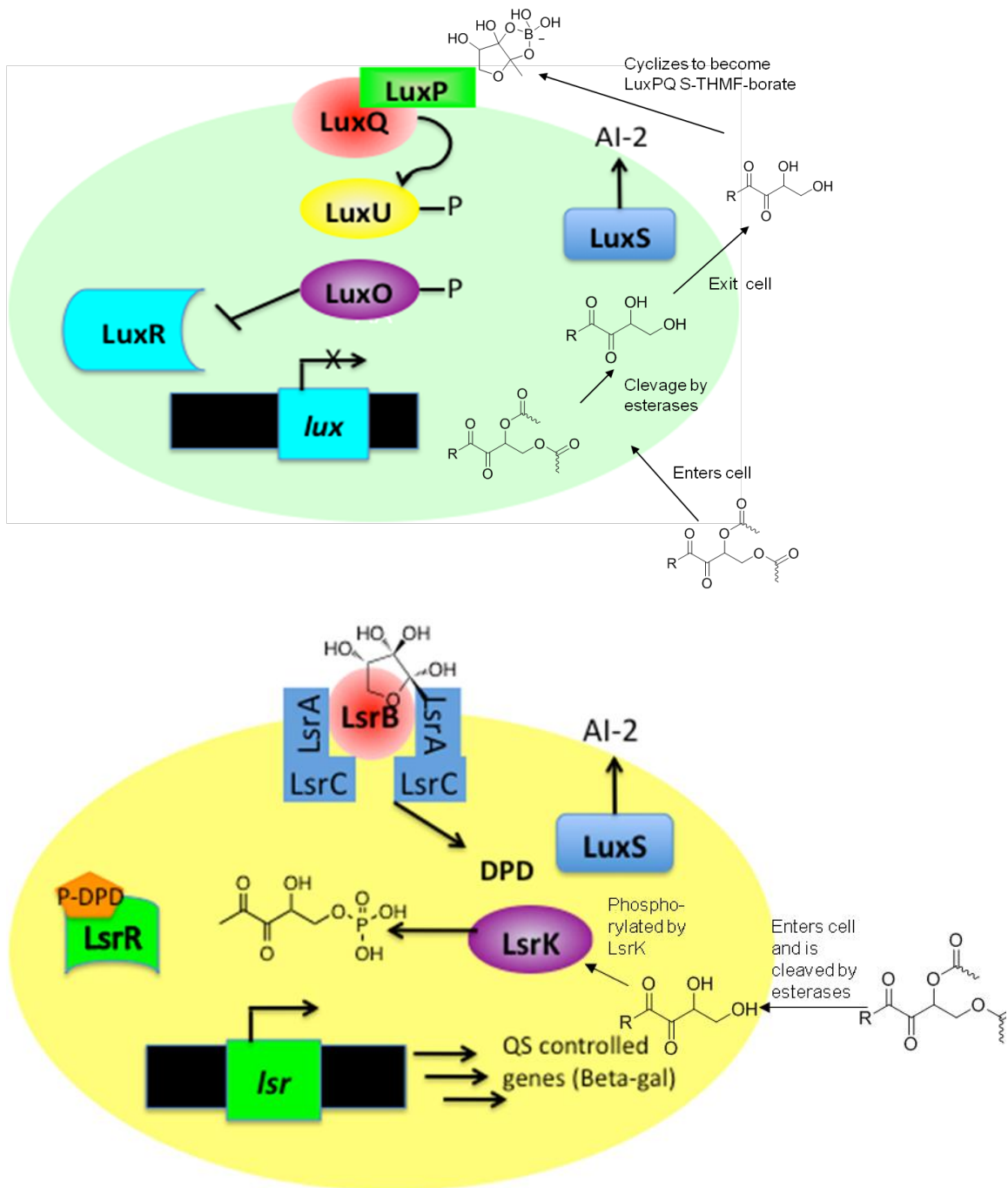


Figure 3.16: Models of biological activity of ester protected; a) Required entry and exit of ester analogs suggests time-dependent activity in *V. harveyi*; b) Required entry only suggests non-time-dependent activity in *E. coli*

In conclusion although ester protected AI-2 and analogs have similar bioactivity as the free DPDs there seem to be a dependence on time for bioluminescence induction. This would be expected since these analogs need to be cleaved before they can obtain the active cyclic forms of AI-2 (and presumably analogs). This time dependence is not observed in the case of β -galactosidase production in *E. coli*. Figure 3.16 provides models of the proposed path of ester protected AI-2 in these two systems. It has been suggested that AI-2 and analogs can traverse cell membranes through passive diffusion. Therefore it is plausible that in the case of *V. harveyi*, ester protected analogs must first diffuse into the cell where it can be cleaved by esterases. Free analogs then must exit and cyclize into the active form (S-THMF-borate) to induce bioluminescence by binding LuxPQ. In *E. coli* ester protected analogs likely have a more direct path to initiating activity. Once inside the cell, ester protected analogs can be cleaved and get directly phosphorylated by LsrK. Since AI-2 binding proteins exist inside the cell in *E. coli* there is no need for the cleaved products to exit and re-enter through LsrB. Since there are several transport pathways in *E. coli* further studies are needed to confirm this model. These models suggest that the *V. harveyi* system is more sensitive to the time required for ester analogs to become fully active.

Chapter Four

Conclusions, Broader Impact and Future Work

4.1 Conclusion

The development of a new synthesis of AI-2 has enabled the construction of a large library of analogs with diverse groups at the C1 position.^{93, 97} Linear, branched, cyclic and aromatic analogs of AI-2 have been synthesized which allow for probing into the length, bulk and electronic requirements of the C1 position.^{97, 101} In addition, variations at the C4 and C5 positions have been made which also give insight into the structural requirements of AI-2 for signaling and stability.

Since AI-2 is a universal signaling molecule, access to this library of analogs has allowed for the perturbation of AI-2 signaling in several quorum-sensing systems.¹⁰¹ In *V. harveyi* AI-2 analogs of various shapes and sizes all caused synergistic agonism of AI-2 induced bioluminescence.⁹⁷ In *E. coli*, linear analogs with chain lengths of three carbons or greater as well as branched analogs were shown to antagonize the *lsr* based AI-2 response.¹⁰¹ Ironically in *S. typhimurium*, which is known to have homologous quorum sensing proteins as *E. coli*, only butyl-DPD (**110**) and isobutyl-DPD (**116**) were found to be inhibitors.¹⁰¹ Overall several potent inhibitors were identified many of which are active in more than one organism. Isobutyl-DPD (**116**) is the most potent inhibitor of enteric bacteria while butyl-DPD (**110**) and cyclopentyl-DPD (**121**) are also very potent inhibitors in *E. coli* (see Table 4.1). Additionally in *P. aeruginosa*, although AI-2 is not produced in this organism, C1 analogs moderately reduced pyocyanin production.

Table 4.1: Inhibitor Concentration (IC₅₀) of the most potent C1-inhibitors

	Inhibitory Concentrations (IC₅₀/μM)			
	<i>E. coli</i>	Standard Error (logIC ₅₀)	<i>S. typhimurium</i>	Standard Error (logIC ₅₀)
Isobutyl-DPD	0.1073	0.1813	40	0.1164
Butyl-DPD	5.934	0.1927	>40	ND
Cyclopentyl-DPD	4.885	0.1464	>40	ND
Heptyl-DPD	31.87	0.244	>40	ND
Phenyl-DPD	>40	ND	>40	ND

Finally individual AI-2 analogs were found to be both broad- and selective-inhibitors of mixed culture synthetic ecosystems.¹⁰¹ Also a “cocktail” of analogs including isobutyl-DPD (**116**) and phenyl-DPD (**125**) were found to simultaneously affect diverse organisms in a synthetic ecosystem.

The versatility of this new synthesis is demonstrated not only the construction of C1 analogs but also C4 and C5 analogs. Deoxy-analogs lacking the hydroxyl group on C5 allowed for investigations into the importance of phosphorylation on inhibition in enteric bacteria. Also ester-protection at both the C4 and C5 position offer the advantage of silica purification. Moreover ester-protected antagonists, isobutyl diacetate (**132c**) and hexyl diacetate (**132b**), showed the same activity as free analogs in *E. coli*. Although agonist, methyl diacetate (**132a**), demonstrate slightly lesser activity. A slow-releasing mechanism involving cell entry and cleavage by the ester analogs has been proposed. This may allow sustained modulation of quorum sensing processes in *V. harveyi* or other organism. Overall the conciseness and versatility of this new synthesis has provided new insights in the quorum sensing system of several organisms.

4.2 Broader Impact

The broader impact of this unique body of work is quite diverse. In addition to a new synthetic route to AI-2, which is amenable to several variations (i.e. C1 alkyl groups, C4 and C5 groups), the preliminary biological work presented opens the field for massive exploration. Not only has possible anti-quorum sensing therapeutic targets been identified, these findings have illuminated new aspects of the universal nature of AI-2 (i.e., *P. aeruginosa* inhibition, cocktail approach in mixed cultures, synergistic agonism).

The ability of AI-2 to respond to an organism in which it is not produced is an interesting phenomenon.⁸³ The flexibility of this new synthesis would allow analogs to be designed containing functional groups capable of “tagging” proteins with which it interacts. Using this strategy, new AI-2 receptor proteins can be identified in organisms where the AI-2 signaling pathway is not well understood.

Although much research has been done in recent years to better understand how AI-2 effects pathogenesis, a detailed understanding only exists in a handful of organisms.^{42, 74} *V. harveyi* bioluminescence induction is a typical reporter of AI-2 activity and synergistic agonism by analogs have wide reaching implications. Recently it has been found that the quorum sensing regulator, LuxR, represses type III secretion in *V. harveyi* in addition to activating bioluminescence.^{46a} Therefore synergistic agonists may enhance the suppression of type III secretion in this organism. Similarly in *V. cholerae*, AI-2 (and CAI-1) activated gene expression results in repression of biofilm formation and virulence.⁵¹ Thus, synergistic agonists may inhibit pathogenesis in this organism as well. Furthermore, as previously mentioned several other *Vibrios*, which are fish pathogens

have homologues quorum sensing systems as *V. harveyi*.^{44a, 60, 97, 111} It remains to be seen how C1 analogs will affect quorum sensing controlled processes in these organisms.

Additionally the role of AI-2 mediated quorum sensing in biofilm formation is not fully understood in many organisms.⁷⁸ The recent discovery that biofilm architecture in *E. coli* is affected by LsrR (and AI-2), is key to understanding how organisms control biofilm.¹⁰³ Our finding that C1 analogs are processed by AI-2 enzymes in *E. coli* and likely bind LsrR will be useful in understanding what effect altering the C1 position of AI-2 has on biofilm formation and architecture in *E. coli*. The potential insights obtained from these studies could then be extended to understand biofilm formation on a more global platform.

Moreover our finding that AI-2 analogs are effective in a variety of mixed culture environments is extremely relevant to oral microbes which often are involved in mixed culture biofilm formation.^{43, 53} The ability of our analogs to either selectively or broadly disturb these organisms' quorum sensing network could be useful in dental care.

4.3 Future Work

This research has revealed and defined the structural requirements of AI-2 signaling pathways. Although synergistic agonism is observed among all analogs in *V. harveyi*, it is known that the cyclic form of AI-2 is the active form in *V. harveyi*. Therefore synthesis of “locked” cyclic analogs may provide enhanced synergistic effects especially if side chains which showed more pronounce effects in this work are incorporated. Likewise in enteric bacteria our *in vitro* phosphorylation suggested that it is the phosphorylated forms which bind to LsrR in *E. coli*. The varying levels of

inhibition among C1 analogs observed in this organism could be due to some analogs more readily adapting the linear conformer and thus being more efficiently phosphorylated by LsrK than analogs which may prefer to exist in the cyclic conformer. Therefore synthetic design of stable, cell permeable-phospho-analogs may be more potent inhibitors than the unphosphorylated C1 analogs identified in this work. Since preferred C1 side chains have been found which effect *E. coli* and *S. typhimurium*, new analogs could be designed to be selective or broad-spectrum based on the side chain installed.

In addition to structural insights, biological insights have also been gained. In *V. harveyi* the absence of synergistic agonism in mutant strains strongly suggest that this effect is caused by allosteric binding of analogs to LuxPQ. The complex interactions between LuxP and LuxQ have been proven to effect AI-2 sensitivity (see Section 3.1).^{47a} However direct binding assays could be problematic since AI-2 most likely has a much higher binding affinity for LuxPQ than analogs. Therefore a fluorescence-based sensor may be a more effective method to monitor binding of analogs to LuxPQ. Pei has constructed a LuxPQ which contains a fluorophore and quencher at the LuxQ hinge of LuxP.¹¹⁷ Therefore monitoring the behavior of this LuxPQ-probe in the presence of C1 analogs may be more beneficial since fluorescence is highly sensitive. Any subtle changes which the analogs cause could be detected and analyzed to understand their synergistic effect. Other methods including orthogonal chemical genetics have also been used to explore the affect of small molecules on proteins such histidine kinases.¹¹⁸

The different responses observed in *lsr* expression in *E. coli* and *S. typhimurium* is quite intriguing. These systems have been assumed to be homologous based on the

presence of identical proteins involved in AI-2 processing in both organisms.⁴⁰ Our C1 analogs have revealed that subtle variations exist which alter *S. typhimurium*'s susceptibility. C1 analogs in this manner could be used as actual probes to decipher where biological variations originate. For example *E. coli* transporter mutants were tested and it was found that alternative transport into the cell exists. This alternative pathway may not exist in *S. typhimurium* therefore testing our C1 inhibitors in a transporter mutant strain for this organism could show a difference. Another possible approach would be to compare the substrate specificity of LsrK in the two organisms. LsrK of *S. typhimurium* has been shown to be substrate specific not being able phosphorylating glucose or ribose.³⁸ Thus the conclusions made from *in vitro* phosphorylation using *E. coli* LsrK may not directly correlate to *S. typhimurium*. Finally binding assays of C1 analogs using purified LsrR from *E. coli* and *S. typhimurium* may show that the divergent biological effects of analogs is due to different binding affinities for LsrR. Ultimately the wide variety of C1 analogs available will allow the underlying dissimilarities of these enteric bacteria to be unraveled in the future.

Additionally the biological relevance of AI-2 internalization and processing in enteric bacteria is thought to be a method of quenching the AI-2 signal of other bacteria in its niche.^{40, 106} To prove this theory it is necessary to conduct a more exhaustive study of synthetic ecosystems. A concentration-dependent effect of exogenous AI-2 and analogs on the response of an organism in the presence and absence of various other organisms could give valuable insights on the role of AI-2 in mixed culture environments.

The observation that AI-2 and analogs are able to perturb quorum sensing in *P. aeruginosa* is fascinating yet the idea that such effects are due to AI-1 likeness requires further investigation. The effect of analogs on other quorum sensing process in *P. aeruginosa* could be tested such as elastase B production. Also screening with mutant strains are needed to identify what pathway AI-2 and analogs are acting on to effect quorum sensing in *P. aeruginosa* (i.e., *las*, *rhl*, etc.). Additionally analogs should be screened in other AI-1 dominate pathways such as *V. cholerae* to see if similar effects are observed. Once a thorough understanding of AI-2/analog's role in effecting the quorum sensing circuitry of these unlikely organism, combination therapies maybe desired which incorporated AI-2 analogs with other known quorum sensing inhibitors.

Chapter Five

Experimental, Supplemental Figures and References

5.1 General Methods of Synthesis

Air and moisture sensitive reactions were carried out in oven-dried glasswares sealed with rubber septa under a positive pressure of dry argon or nitrogen, unless otherwise indicated. Reactions were stirred using Teflon-coated magnetic stir bars. Organic solutions were concentrated using a Büchi rotary evaporator with an aspirator pump. Dry tetrahydrofuran was obtained using PureSolvent™ prior to use. Dry acetonitrile was distilled from CaH₂ prior to use. Thin-layer chromatography (TLC) was performed on Merck Kieselgel 60 F254 plates with a 365 nm fluorescent indicator. The TLC was visualized by ultraviolet light and acidic *p*-anisaldehyde stain followed by gentle heating. The crude reaction mixtures were purified by flash chromatography on silica gel (230-400 mesh).

NMR spectra were measured on Bruker AV-400, Bruker DRX-400 (¹H at 400 MHz, ¹³C at 100MHz), Bruker DRX-500 (¹H at 500 MHz, ¹³C at 125MHz) or Bruker AVIII-600 (¹H at 600 MHz, ¹³C at 150MHz). Data for ¹H -NMR spectra are reported as follows: chemical shift (ppm, relative to residual solvent peaks or indicated external standards; s = singlet, d = doublet, t = triplet, q = quartet, dd = doublet of doublets, td = triplet of doublets, m = multiplet), coupling constant (Hz), and integration. Data for ¹³C -NMR are reported in terms of chemical shift (ppm) relative to residual solvent peak. Mass spectra (MS) and high resolution mass spectra (HRMS) were recorded by JEOL AccuTOF-CS (ESI positive, needle voltage 1800~2400 eV). Infrared spectra (IR) were recorded by a ThermoNicolet IR200 Spectrometer.

Synthesis of Diazodiols: To a solution of the diazocarbonyl in anhydrous acetonitrile (0.2M) was added DBU (0.16-0.20 eq) and the requisite aldehyde (2-(*tert*-butyldimethylsilyloxy)) acetaldehyde or acetaldehyde) (1-1.5 eq). The reaction was stirred at room temperature under nitrogen for 4-8 hours and monitored by TLC. Upon disappearance of starting material, the reaction was quenched with sodium bicarbonate. The organic layer was extracted with dichloromethane (3 x 20 mL) and dried with magnesium sulfate. The solvent was evaporated under reduced pressure. To a solution of crude product in anhydrous tetrahydrofuran (0.2M) TBAF was added (1-2 eq) at 0° C. The solution was allowed to warm to room temperature and stirred for 1-3 hours under nitrogen. The solvent was evaporated and the crude product was purified by column chromatography. The product eluted as yellow oil with 1:3 to 3:2 ethyl acetate:hexane.

Synthesis of DPDs: To a solution of diazodiol (1 eq) in acetone (1-2 mL) was added dioxirane (15-20 mL) in acetone dropwise. The reaction was allowed to stir at room temperature (1-2 hrs) until complete disappearance of starting material as indicated by TLC (loss of UV activity). Solvent and excess reagent was evaporated under reduced pressure. NMR was taken without further purification.

Synthesis of Quinoxaline Derivatives: To a solution of DPD-analog was added 1, 2- phenylenediamine (1.5 eq). The reaction was stirred at room temperature for 10 minutes and then the reaction mixture was washed with (2M) HCl. The crude mixture was purified on silica.

5.2 Methods of Biological Evaluation

Bacterial Strains and Growth Condition

S. typhimurium and *E. coli* strains were cultured in Luria-Bertani medium (LB, Sigma) at either 30°C or 37°C with vigorous shaking (250 rpm) unless otherwise noted. The *V. harveyi* strains were grown in AB or LM medium. Antibiotics were used for the following strains: (60 or 100 µg ml⁻¹) kanamycin for *S. typhimurium* MET715, (50 µg ml⁻¹), ampicillin for *E. coli* LW7 pLW11. (50 µg ml⁻¹) ampicillin and (50 µg ml⁻¹) kanamycin for *E. coli* MDAI-2 pCT6 and *E. coli* SH3 pLW11 along with (20 µg ml⁻¹) chloramphenicol for the latter and (20 µg ml⁻¹) kanamycin for *V. harveyi* BB170.

Modulation of bioluminescence in *V. harveyi*

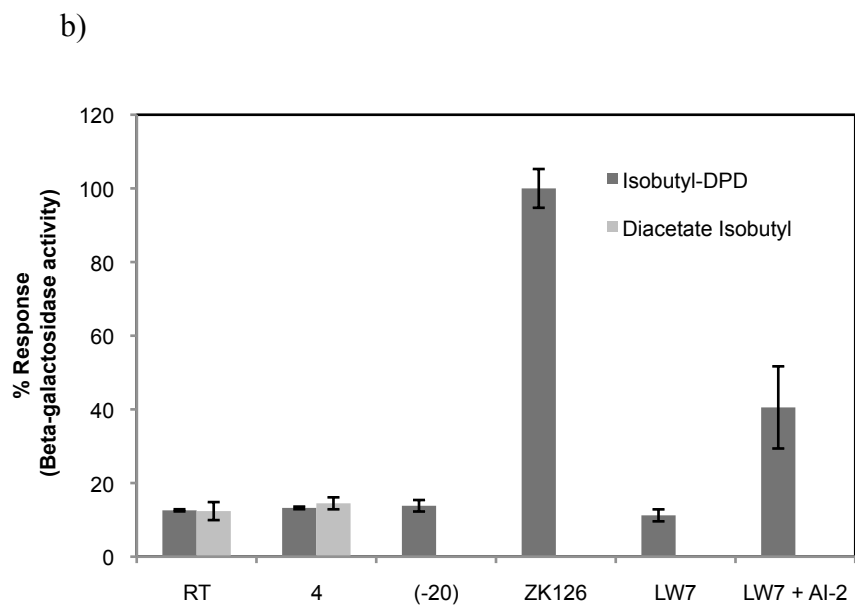
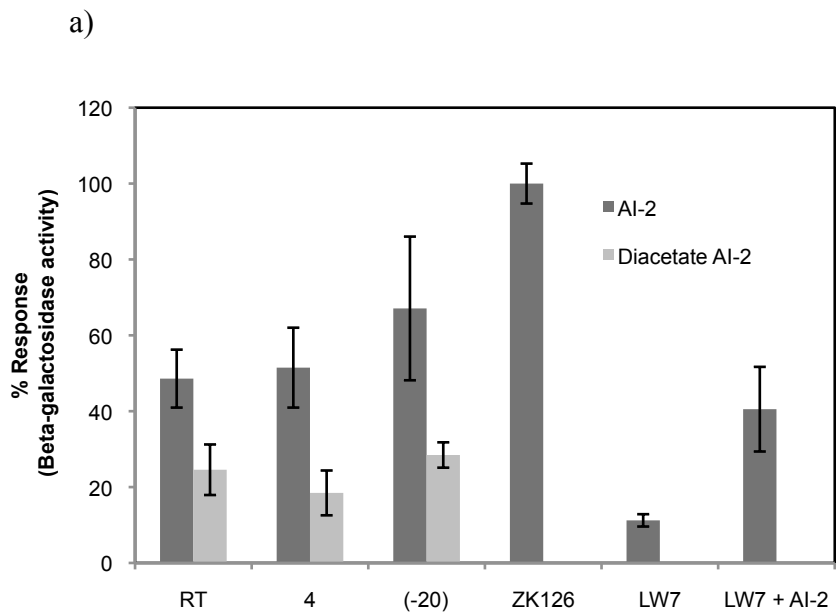
The test compounds were evaluated for their (ant) agonistic activity in *V. harveyi* following reported protocol. Briefly, *V. harveyi* strain BB170 or MM32 was grown for 18 h at 30 °C in AB (or LM) medium and then diluted 1:500 into fresh AB medium. Aliquots of analogs (and AI-2) were added to cells in a 96-well plate. Bioluminescence was taken at either 30 min or 1 h intervals.

Measurement of β -galactosidase production in *E. coli* and *S. typhimurium*. The QS response indicated by *lsr* gene expression was analyzed in pure culture studies by culturing *E. coli* LW7 pLW11, *E. coli* ZK126 pLW11 and *S. typhimurium* MET708, *S. typhimurium* MET715 overnight in LB medium supplemented with appropriate antibiotics as stated previously. These cells were then diluted into fresh LB medium (with

antibiotics) and grown to an OD₆₀₀ of 0.8 - 1.0 at 30 °C, 250 rpm. Cells were then collected by centrifugation at 10,000 xg for 10 minutes, and resuspended in 10 mM phosphate buffer. AI-2 (40 μM) and the respective analog (40 μM) were added to the *E. coli* or *S. typhimurium* suspension for 2 hours at 37 °C. AI-2 dependent β-galactosidase production was quantified by the Miller assay.¹¹¹

Measurement of pyocyanin production. Pyocyanin was extracted from culture supernatants of wild type PAO1, and measured as described by Essar et al.¹¹⁰ Briefly, 2 mL of chloroform was added to 2 mL of culture supernatant, taken from 19 h cultures grown in the presence of DPD analog. After extraction, 1 mL of the chloroform layer was transferred to a fresh tube and mixed with 180 μL of 0.2 M HCl. After centrifugation, the aqueous (top) layer was separated and its absorption measured at 520 nm.

Supplementary Figures



c)

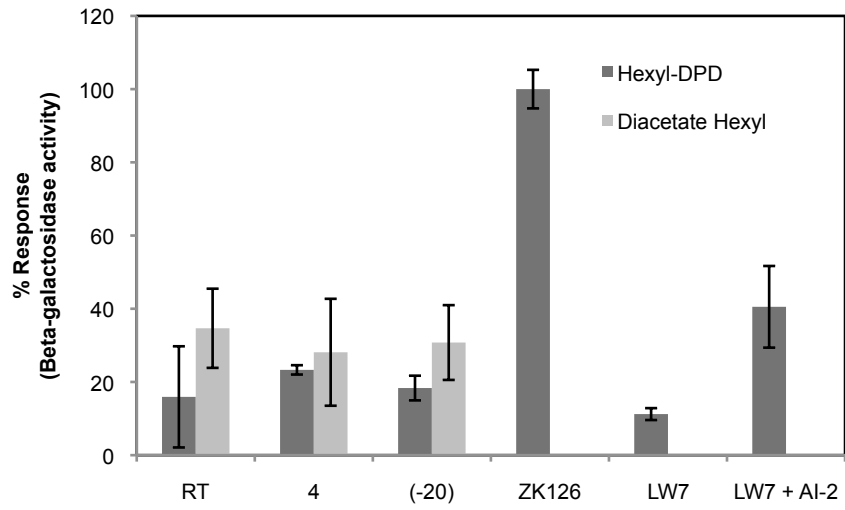


Figure S1: β -galactoside production in *E. coli* LW7 (LuxS⁻) in response to a) AI-2, b) hexyl-DPD, c) isobutyl-DPD and their diacetate derivatives in the presence of exogeneous AI-2 stored for 4- weeks at various temperatures

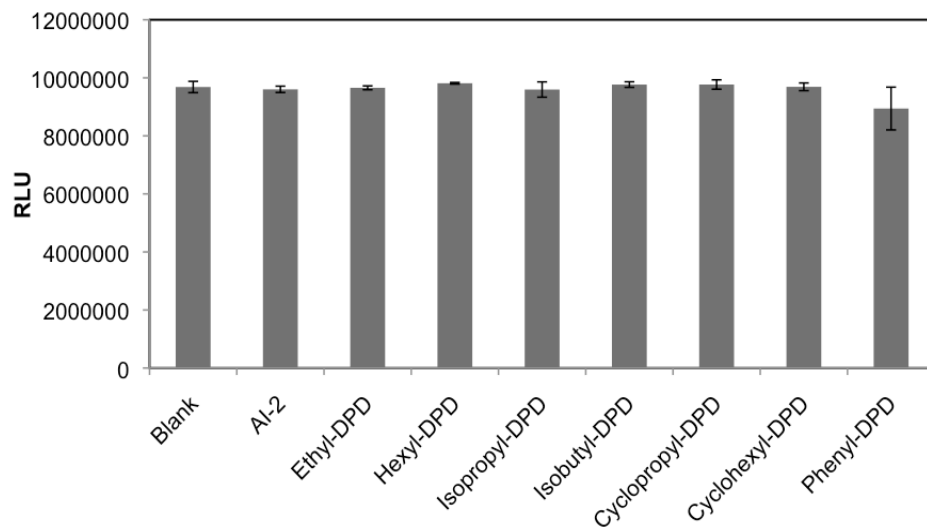


Figure S2: Bioluminescence induction in *V. harveyi* BB886 (LuxQ⁻) in response to select C1 analogs

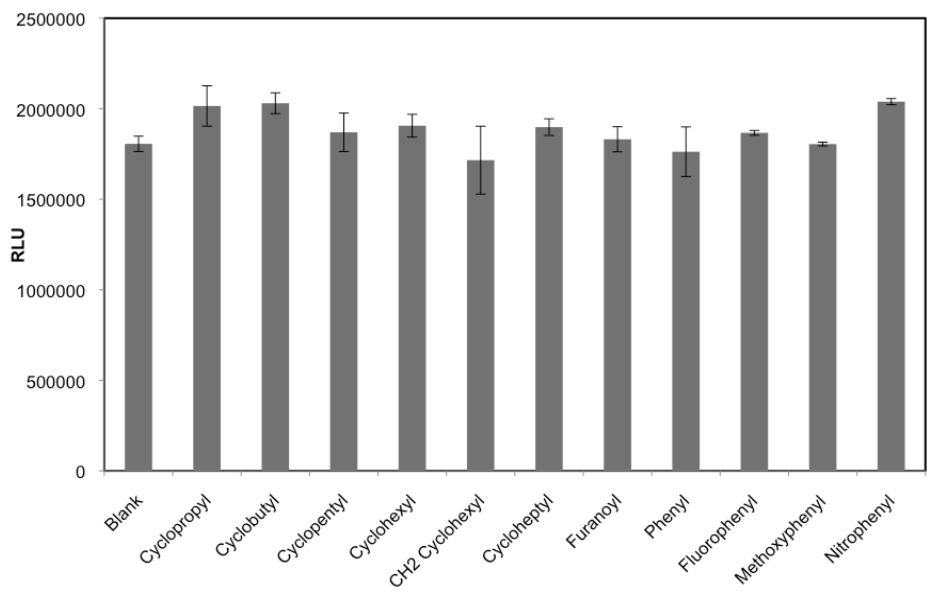
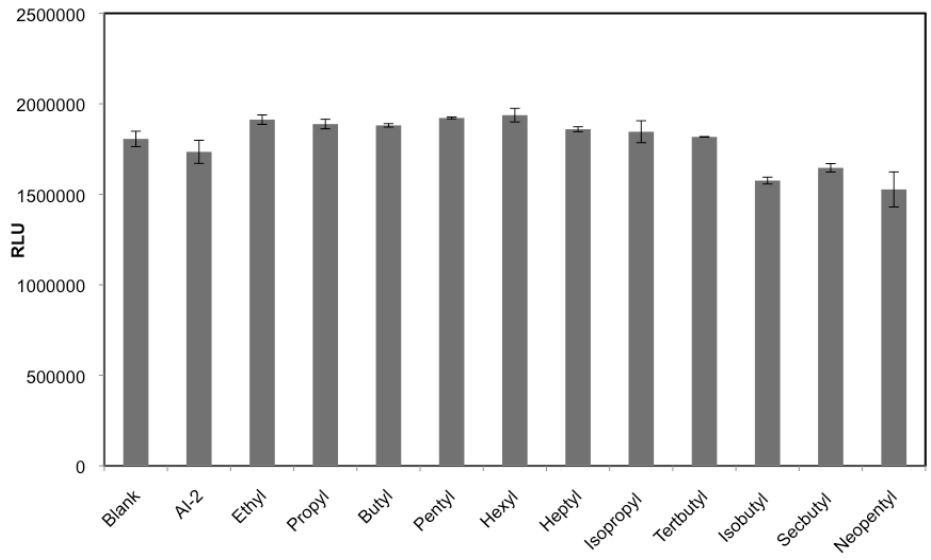


Figure S3: Bioluminescence induction in *V. harveyi* BB721 (LuxO) in response to C1 analogs

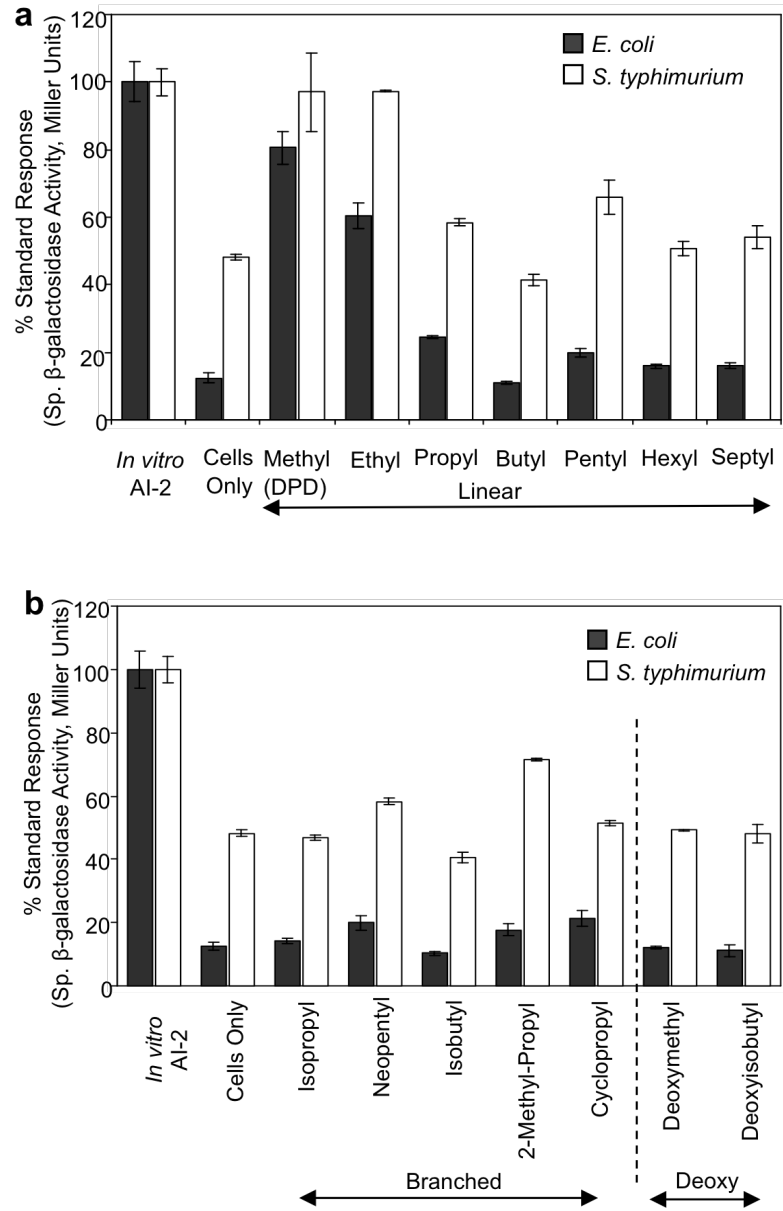


Figure S4: β -galactoside production in *E. coli* LW7 and *S. typhimurium* MET715 (both *luxS*⁻) in response to a) linear analogs and b) branched and deoxy analogs.

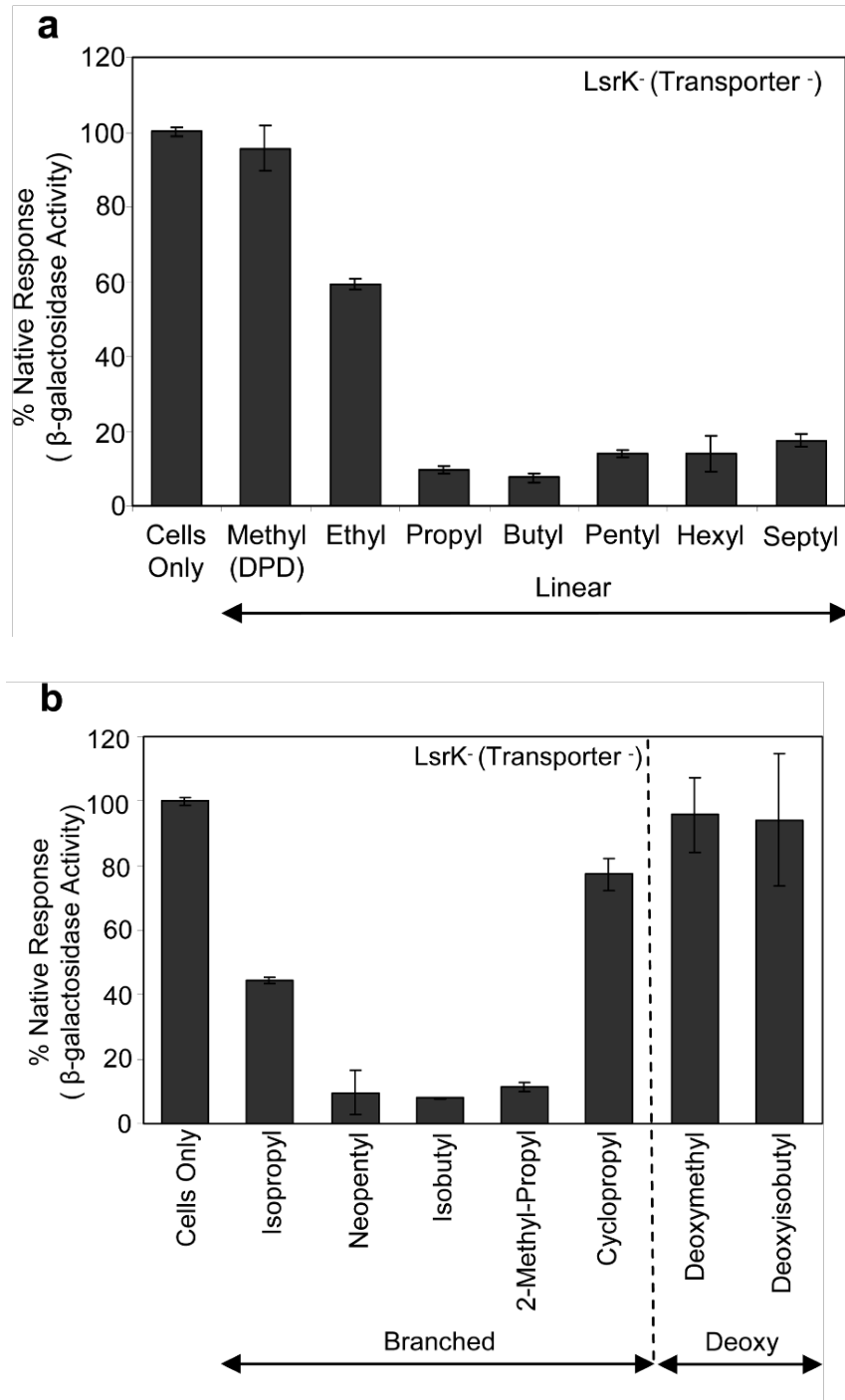
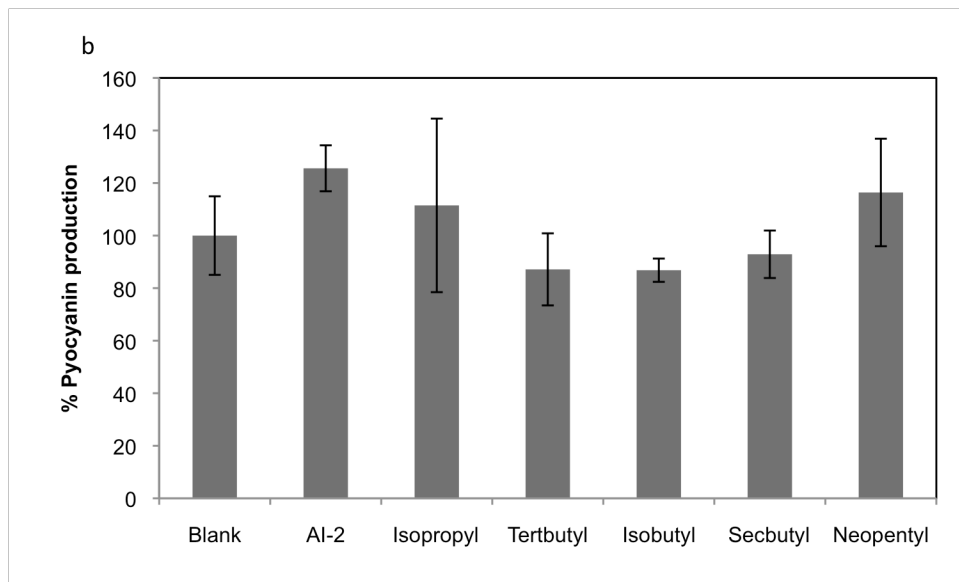
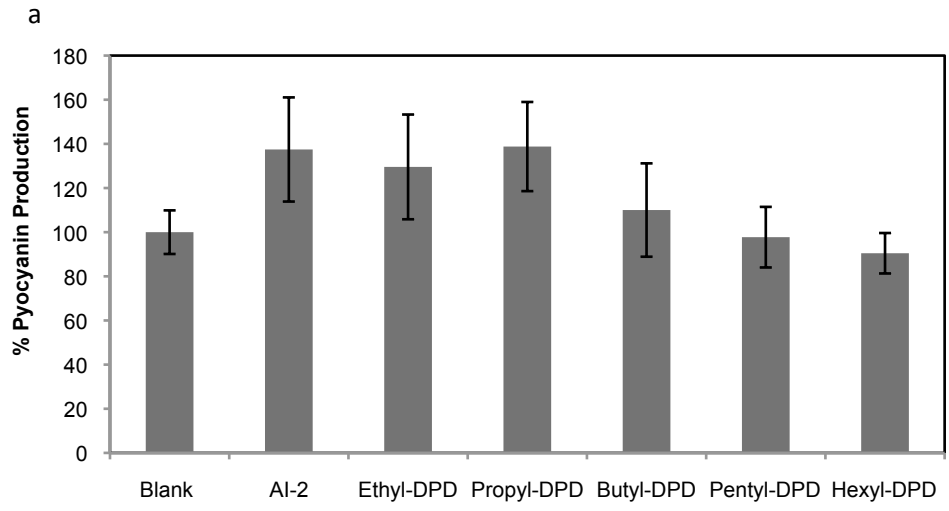


Figure S5: β -galactoside production in *E. coli* LW9 (LsrB⁻) in response to a) linear analogs and b) branched and deoxy analogs¹⁰¹



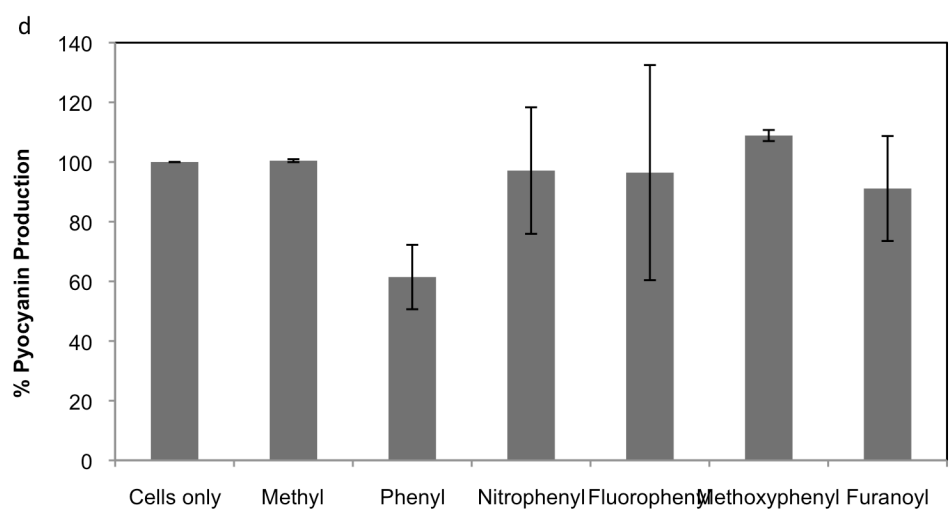
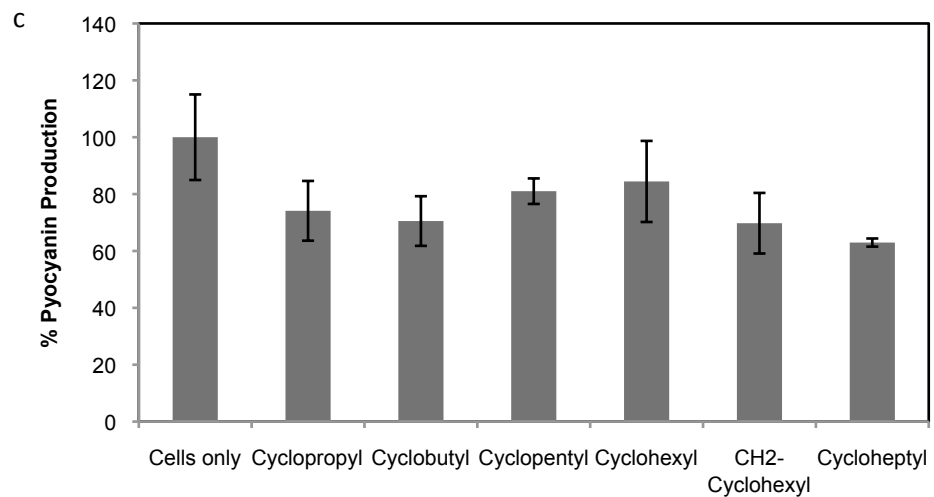


Figure S6: Pyocyanin production in response to a) linear b) branched c) cyclic and d) aromatic C1 analogs of AI-2

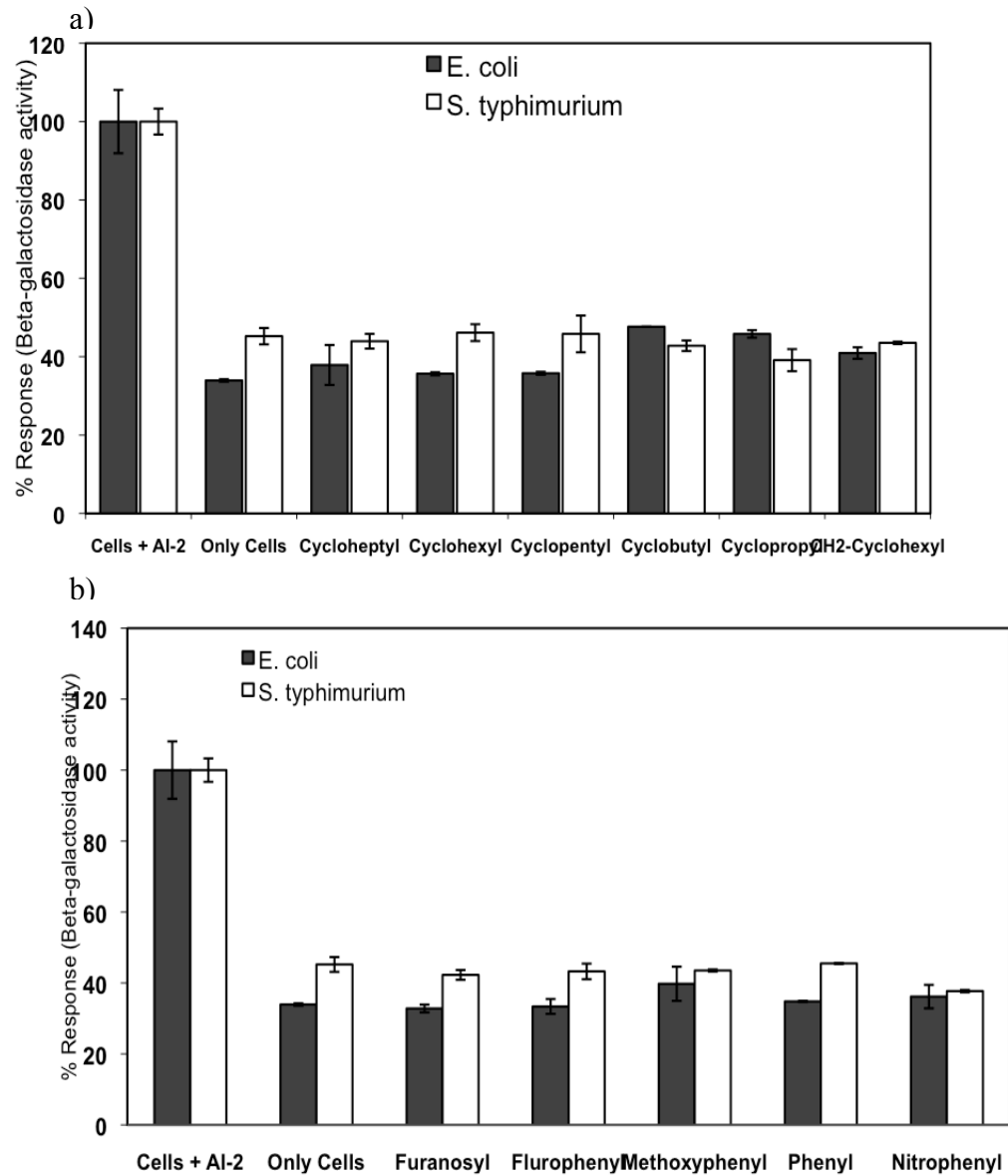


Figure S7: β -galactoside production in *E. coli* LW7 and *S. typhimurium* MET715 (both are LuxS⁺) in response to a) cyclic and b) aromatic analogs

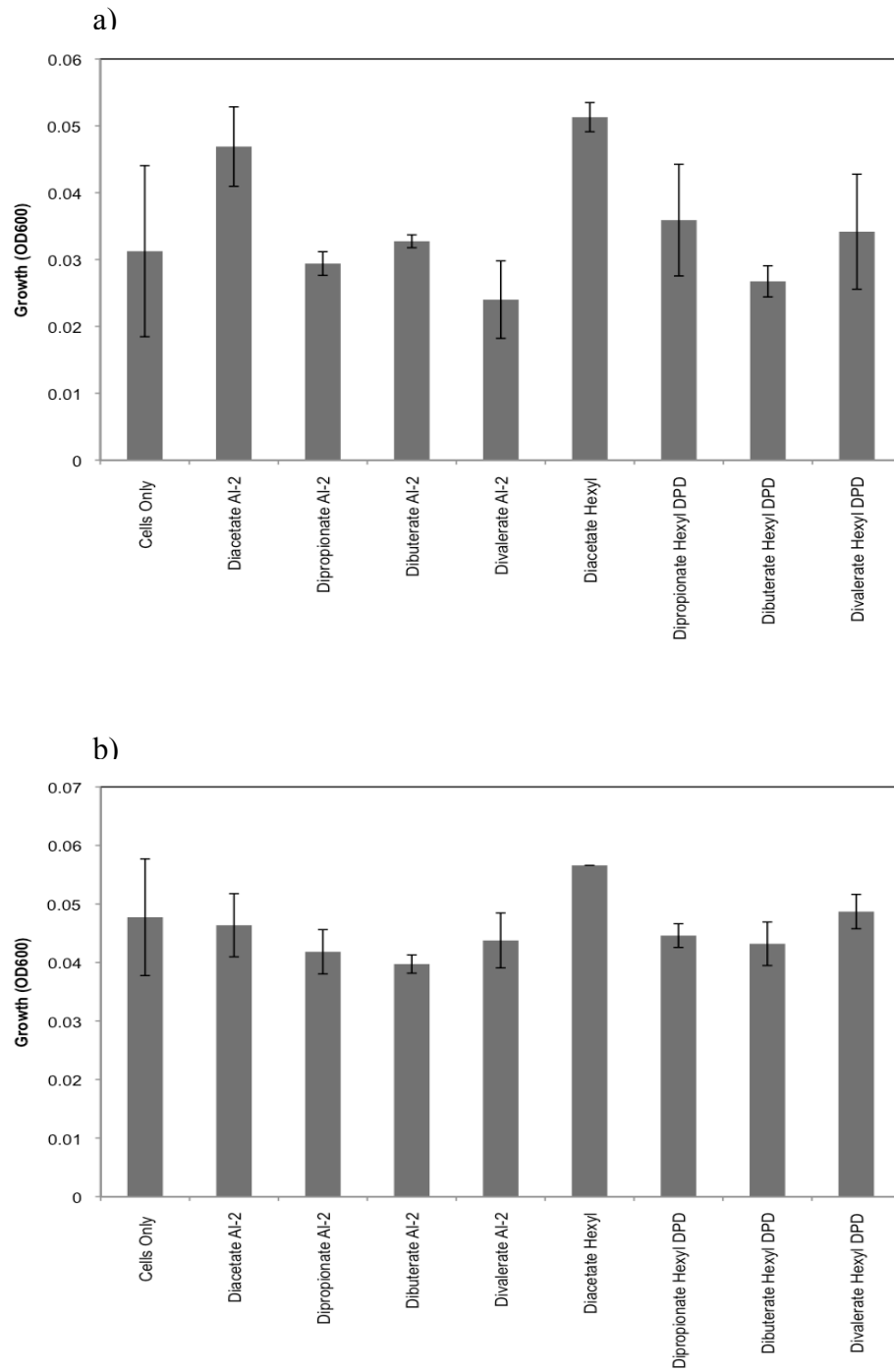


Figure S8: Effect of ester-protected AI-2 and analogs growth in *V. harveyi* a) MM32 and b) BB170

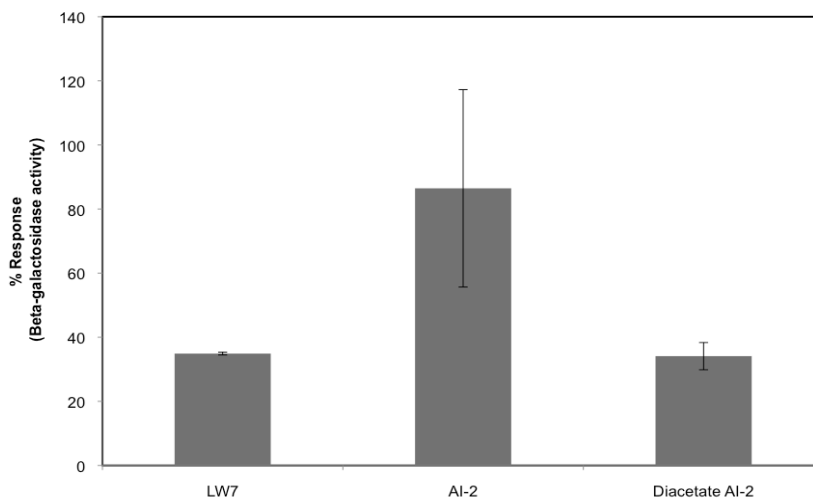
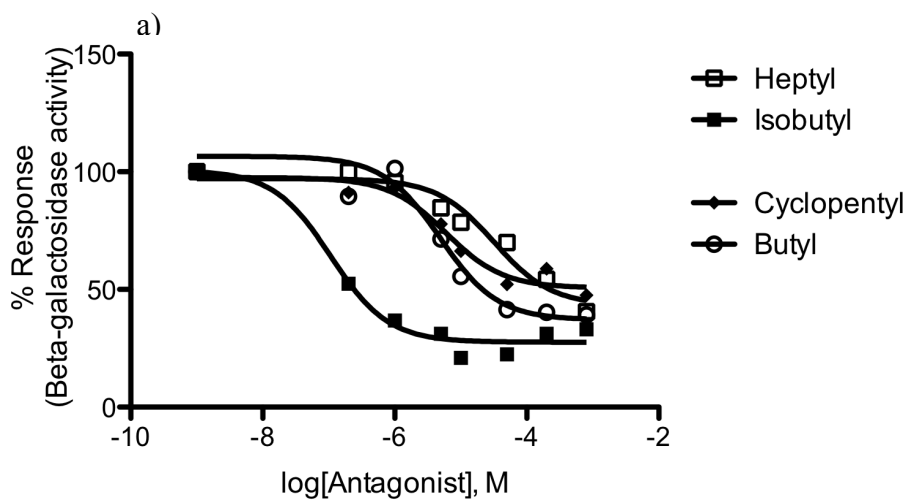


Figure S9: β -galactosidase production in response to AI-2 and diacetate AI-2 in *E. coli* LW7 (LuxS⁻)



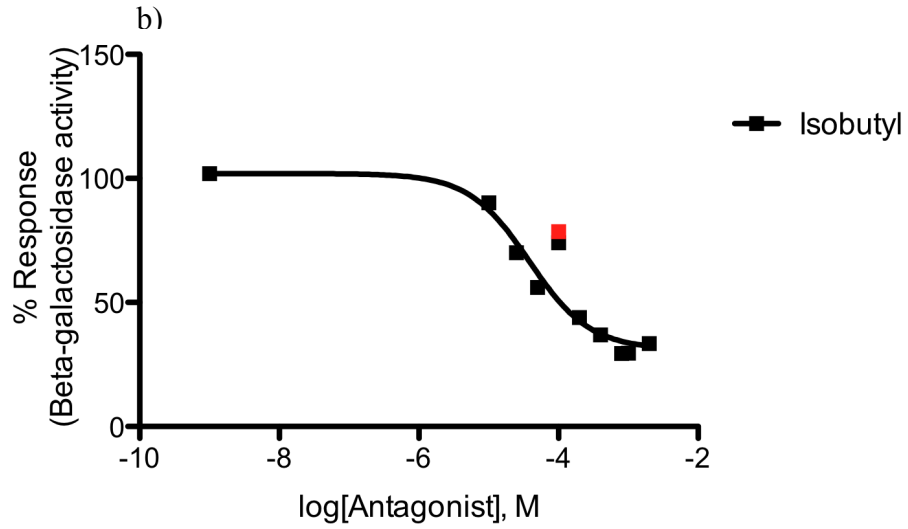
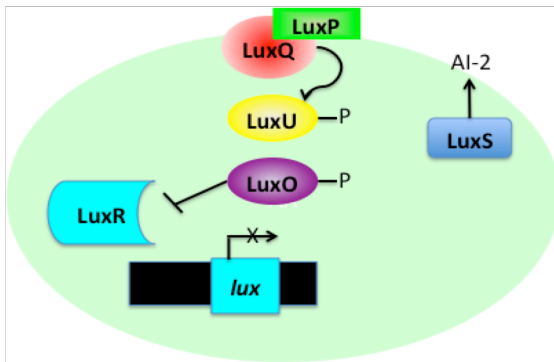


Figure S10: Dose-response curve of C1 inhibitors in the presence of AI-2 in a) *E. coli* and b) *S. typhimurium*

Quorum Sensing "Off"



Quorum Sensing "On"

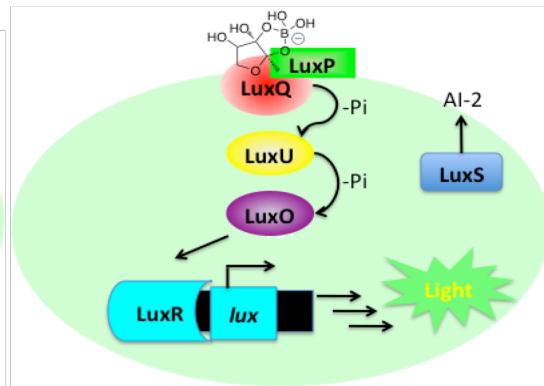


Figure S11: Phosphorelay used for signal transduction in the AI-2 mediated quorum sensing pathway of *V. harveyi*

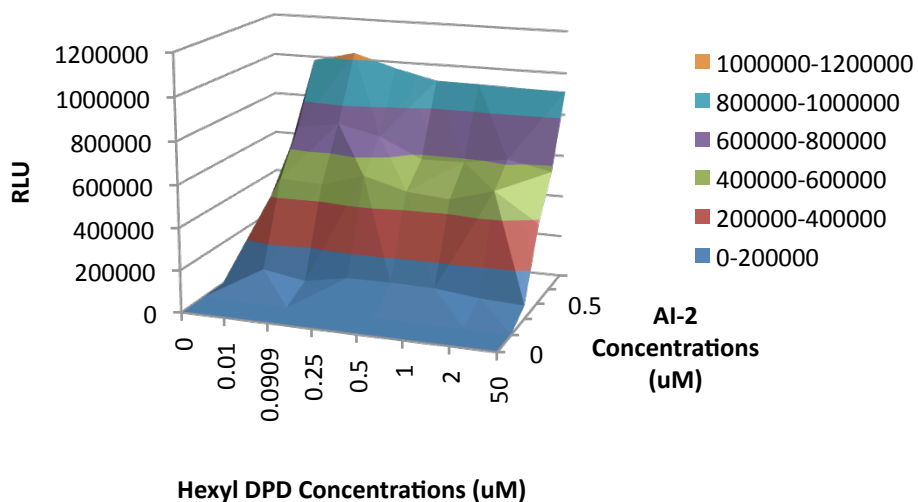
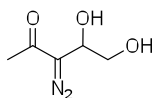
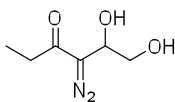


Figure S12: Synergistic agonism of *V. harveyi* MM32 (LuxS⁻) in the presence of various concentrations of AI-2 and Hexyl-DPD

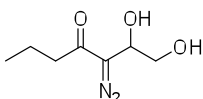
5.2 NMR Characterizations



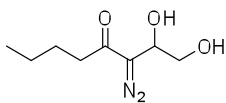
3-diazo-4, 5-dihydroxypentan-2-one (S1): ¹H NMR (400 MHz, CDCl₃) δ ppm 4.76 (1H, m), 3.85 (1H, dd, *J* = 11.4, 3.2 Hz), 3.75 (1H, dd, *J* = 11.4, 3.2 Hz), 3.46 (1H, s, br), 2.69 (1H, s, br), 2.26 (3H, s). ¹³C NMR (100 MHz, CDCl₃) δ ppm 191.7, 66.3, 64.2, 25.6. IR: 3349, 2361, 2338, 2092, 1607 cm⁻¹. Yield: 50% (over 2 steps)



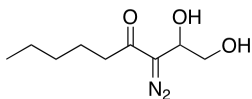
4-diazo-5,6-dihydroxyhexan-3-one (S2): ^1H NMR (400 MHz, CDCl_3) δ ppm 4.75 (1H, m), 4.48 (1H, br), 4.21 (1H, br), 3.81-3.79 (1H, m), 3.72-3.70 (1H, m), 3.44 (1H, br), 2.50 (2H, q, $J = 7.4$ Hz), 1.13 (3H, t, $J = 7.4$ Hz); ^{13}C NMR (100 MHz, CDCl_3) δ ppm 195.2, 65.9, 64.1, 31.2, 8.2; IR: 3365, 2980, 2940, 2084, 1607 cm^{-1} . Yield 33% (over 2 steps)



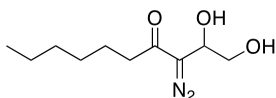
3-diazo-1,2-dihydroxyheptan-4-one (S3): ^1H NMR (400 MHz, CDCl_3) δ ppm 4.75 (1H, m), 4.08 (1H, br), 3.81 (1H, dd, $J = 11.2, 3.4$ Hz), 3.70 (1H, dd, $J = 11.2, 5.4$ Hz), 3.35 (1H, br), 2.45 (2H, t, $J = 7.4$ Hz), 1.68-1.63 (2H, m), 0.94 (3H, t, $J = 7.4$ Hz). ^{13}C NMR (100 MHz, CDCl_3) δ ppm 195.3, 66.6, 64.8, 40.5, 18.6, 14.1. IR: 3395, 2964, 2935, 2876, 2082, 1605 cm^{-1} . Yield: 52% (over 2 steps)



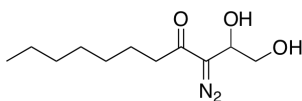
3-diazo-1,2-dihydroxyoctan-4-one (S4): ^1H NMR (400 MHz, CDCl_3) 4.75 (1H, br), 3.83 (1H, dd, $J = 3.9, 11.5$ Hz), 3.72 (1H, dd, $J = 5.3, 11.5$ Hz), 3.02 (1H, s, br), 2.45-2.49 (2H, m), 1.95 (1H, s, br), 1.57-1.65 (2H, m), 1.30-1.40 (2H, m), 0.91 (3H, t, $J = 7.3$ Hz) ^{13}C NMR (100 MHz, CDCl_3) δ ppm 194.9, 66.2, 64.1, 37.7, 26.5, 22.1, 13.6. IR: 3334, 2959, 2872, 2082, 1607 cm^{-1} . Yield: 48% (over 2 steps)



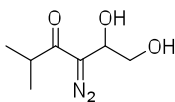
3-diazo-1,2-dihydroxynonan-4-one (S5): ^1H NMR (CDCl_3 , 400 MHz) δ 4.78 (1H, t, $J=$ 4.4 Hz), 3.83-3.85 (1H, m), 3.73 (1H, dd, $J=$ 16.8, 5.6 Hz), 2.49 (2H, t, $J=$ 7.6 Hz), 1.65 (2H, t, $J=$ 7.2 Hz), 1.32-1.33 (4H, m), 0.89-0.93 (3H, m); ^{13}C NMR (CDCl_3 , 100 MHz) δ 195.9, 96.3, 67.1, 64.9, 39.1, 31.9, 24.9, 23.1, 14.5. IR: 3377, 2957, 2931, 2872, 2085, 1710, 1609 cm^{-1} Yield: 25% (over 2 steps)



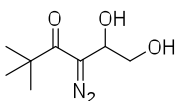
3-diazo-1,2-dihydroxydecan-4-one (S6): ^1H NMR (CDCl_3 , 400 MHz) δ 4.75 (1H, br), 3.77-3.79 (1H, m), 3.68 (1H, dd, $J=$ 13.6, 4.8 Hz), 2.47 (2H, t, $J=$ 6.4, 5.6 Hz), 1.58-1.64 (2H, m), 1.26-1.35 (6H, m), 0.87-0.91 (3H, m); ^{13}C NMR (CDCl_3 , 100 MHz) δ 195.2, 70.5, 65.9, 64.5, 38.5, 31.7, 29.0, 24.8, 22.6, 14.2. IR: 3394, 2956, 2928, 2959, 2086, 1610 cm^{-1} Yield: 49% (over 2 steps)



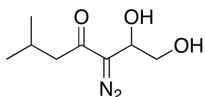
3-diazo-1,2-dihydroxyundecan-4-one (S7): ^1H NMR (CDCl_3 , 400 MHz) δ 4.78 (1H, br), 3.86-3.89 (1H, m), 3.77 (1H, dd, $J=$ 15.2, 4.4 Hz), 3.54 (1H, br), 2.77 (1H, br), 2.50 (2H, t, $J=$ 7.6 Hz), 1.66 (2H, q, $J=$ 7.2 Hz), 1.27-1.32 (8H, m), 0.91 (3H, t, $J=$ 6.8, 7.2 Hz); ^{13}C NMR (CDCl_3 , 100 MHz) δ 195.8, 67.1, 64.8, 38.7, 32.0, 29.6, 29.4, 25.0, 23.0, 14.5. IR: 3393, 2926, 2857, 2084, 1610 cm^{-1} Yield: 61% (over 2 steps)



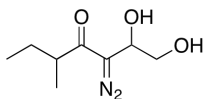
4-diazo-5,6-dihydroxy-2-methylhexan-3-one (S8): ^1H NMR (400 MHz, CDCl_3) δ ppm 4.74-4.76 (1H, m), 3.81 (1H, dd, $J = 11.5, 3.9$ Hz), 3.70 (1H, dd, $J = 11.5, 5.6$ Hz), 2.79-2.86 (1H, m), 1.12 (6H, d, $J = 6.8$ Hz). ^{13}C NMR (100 MHz, CDCl_3) δ ppm 199.5, 66.7, 64.8, 36.5, 19.1. IR: 3357, 2971, 2929, 2362, 2084, 1738, 1609 cm^{-1} . Yield: 25% (over 2 steps)



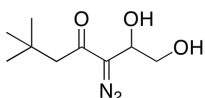
4-diazo-5,6-dihydroxy-2,2-dimethylhexan-3-one (S9): ^1H NMR (400 MHz, CDCl_3) δ ppm 4.78 (1H, t, $J = 4.9$ Hz), 3.83 (1H, dd, $J = 4.2, 11.5$ Hz), 3.74-3.70 (1H, m), 1.23 (9H, s). ^{13}C NMR (100 MHz, CDCl_3) δ ppm 200.6, 67.8, 64.0, 44.3, 26.6. IR: 3358, 2971, 2361, 2338, 2077, 1702, 1602 cm^{-1} . Yield: 20% (over 2 steps)



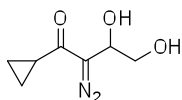
3-diazo-1,2-dihydroxy-6-methylheptan-4-one (S10): ^1H NMR (CDCl_3 , 400 MHz) δ 4.79 (1H, br), 4.18 (1H, br), 3.83 (1H, dd, $J = 11.2, 3.6$ Hz), 3.72 (1H, dd, $J = 11.6, 5.6$ Hz), 2.36 (2H, d, $J = 6.8$ Hz), 2.12-2.19 (1H, m), 0.97 (6H, d, $J = 6.8$ Hz); ^{13}C NMR (CDCl_3 , 100 MHz) δ 195.1, 71.3, 66.6, 64.8, 47.5, 26.3, 22.9. IR: 3377, 2960, 2873, 2087, 1708, 1609 cm^{-1} Yield: 22%



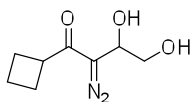
3-diazo-1,2-dihydroxy-5-methylheptan-4-one (S11): ^1H (CDCl_3 , 400MHz) δ 4.80 (1H, br), 3.83 (1H, dd, $J= 15.6, 4.4$ Hz), 3.73 (1H, dd, $J= 16.4, 4.8$ Hz), 2.65-2.70 (1H, m), 1.69-1.77 (1H, m), 1.44-1.51 (1H, m), 1.14-1.16 (3H, d, $J= 6.8$ Hz), 0.92-0.96 (3H, m); ^{13}C (CDCl_3 , 100 MHz) δ 199.5, 67.2, 64.8, 43.6, 27.3, 17.1, 12.3. IR: 3405, 2967, 2935, 2878, 2084, 1755, 1605 cm^{-1} Yield: 54% (over 2 steps)



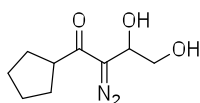
3-diazo-1,2-dihydroxy-6,6-dimethylheptan-4-one (S12): ^1H NMR (CDCl_3 , 400 MHz) δ 4.77--4.79 (m, 1H), 3.82-3.85 (m, 1H), 3.72-3.75 (m, 1H) 2.36 (s, 2H), 1.05 (s, 9H); ^{13}C NMR (CDCl_3 , 100 MHz) 194.8, 71.8, 66.9, 64.7, 50.9, 32.9, 30.0. IR: 3387, 2955, 2870, 2082, 1602, 1467 cm^{-1} Yield: 53% (over 2 steps)



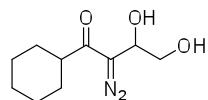
1-cyclopropyl-2-diazo-3,4-dihydroxybutan-1-one (S13): ^1H NMR (400 MHz, CDCl_3) δ ppm 4.81 (1H, s, br), 3.87-3.92 (1H, m), 3.79-3.83 (1H, m), 3.38 (1H, s, br), 2.62 (1H, s, br), 1.94-2.01 (1H, m), 1.13-1.17 (2H, m), 0.92-0.97 (2H, m); ^{13}C NMR (100 MHz, CDCl_3) δ ppm 193.5, 66.4, 63.7, 16.4, 9.5. IR: 3401, 2929, 2362, 2088, 1690, 1612 cm^{-1} . Yield: 28% (over 2 steps)



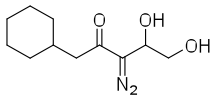
1-cyclobutyl-2-diazo-3,4-dihydroxybutan-1-one (S14): ^1H (CDCl_3 , 400MHz) ppm δ 4.75 (1H, br), 3.72-3.83 (2H, m), 2.32-2.34 (2H, m), 2.16-2.17 (2H, m), 1.97-2.00 (2H, m), 1.86-1.91 (2H, m); ^{13}C (CDCl_3 , 100MHz) ppm δ 196.9, 67.0, 64.7, 42.5, 24.9, 18.3 IR: 3376, 2944, 2867, 2085, 1754, 1697, 1603 cm^{-1} . Yield: 21% (over 2 steps)



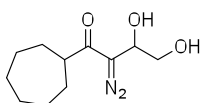
1-cyclopentyl-2-diazo-3,4-dihydroxybutan-1-one (S15) : ^1H NMR (400 MHz, CDCl_3) δ ppm 4.75-4.77 (1H, m), 4.21 (1H, br), 3.77-3.81 (1H, m), 3.67-3.71 (1H, m), 3.50 (1H, br), 1.77-1.80 (4H, m), 1.86-1.89 (2H, m), 1.55-1.59 (2H, m) ^{13}C NMR (100 MHz, CDCl_3) δ ppm 198.4, 66.6, 64.9, 47.0, 29.8, 26.4 IR 3376, 2952, 2869, 2360, 2082, 1607 cm^{-1} Yield: 19% (over 2 steps)



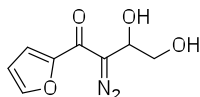
1-cyclohexyl-2-diazo-3,4-dihydroxybutan-1-one (S16): ^1H NMR (400 MHz, CDCl_3) δ ppm 4.75 (1H, t, $J = 4.6, 4.6$ Hz), 3.85 (1H, dd, $J = 4.1, 11.5$ Hz), 3.75 (1H, dd, $J = 4.9, 11.5$ Hz), 3.41 (1H, s, br), 2.58 (1H, s, br), 2.49-2.56 (1H, m), 1.74-1.83 (3H, m), 1.68-1.70 (1H, m), 1.42-1.51 (2H, m), 1.22-1.32 (3H, m). ^{13}C NMR (100 MHz, CDCl_3) δ ppm 198.4, 66.7, 64.3, 46.3, 28.8, 25.5. IR: 3399, 2975, 2932, 2362, 2085, 1616 cm^{-1} . Yield: 36% (over 2 steps)



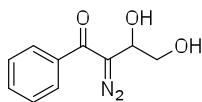
1-cyclohexyl-3-diazo-4,5-dihydroxypentan-2-one (S17): ^1H (400MHz, CDCl_3) ppm
 δ : 4.77 (1H, br s), 3.87-3.84 (1H, m), 3.75 (1H, dd, $J = 10.8, 6.8$ Hz), 2.35 (2H, d, $J = 7.2$ Hz), 1.66-1.79 (6H, m), 1.22-1.33 (4H, m), 0.99-1.05 (2H, m); ^{13}C (100MHz, CDCl_3)
 ppm δ : 195.8, 97.1, 64.7, 46.3, 35.6, 33.5, 26.4



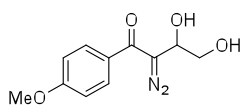
1-cycloheptyl-2-diazo-3,4-dihydroxybutan-1-one (S18): ^1H NMR (400 MHz, CDCl_3)
 δ ppm 4.75-4.78 (1H, m), 3.82-3.89 (1H, m), 3.72-3.79 (1H, m), 2.90-2.97 (1H, br), 2.67-2.75 (1H, m), 1.76-1.89 (5H, m), 1.63-1.72 (2H, m), 1.56-1.61 (4H, m), 1.43-1.51 (2H, m); ^{13}C NMR (100 MHz, CDCl_3) δ ppm 200.0, 66.9, 64.5, 48.1, 31.0, 28.6, 27.0; IR: 3401, 2924, 2857, 2086, 1615 cm^{-1}



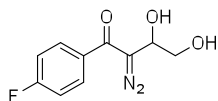
2-diazo-1-(furan-2-yl)-3,4-dihydroxybutan-1-one (S19): ^1H NMR (400 MHz, CDCl_3)
 δ ppm 7.50 (1H, dd, $J = 0.7, 1.7$ Hz), 7.17 (1H, d, $J = 0.7$ Hz), 6.55 (1H, dd, $J = 1.7, 3.6$ Hz), 4.96 (1H, br), 3.95-3.91 (1H, m), 3.86-3.81 (1H, m), 3.58-3.55 (1H, m) ^{13}C NMR (400 MHz, CDCl_3) δ ppm 174.3, 151.3, 144.2, 118.0, 111.9, 66.9, 63.8 IR: 3246, 2359, 2341, 2105, 1571, 1543 cm^{-1} Yield: 20% (over 2 steps)



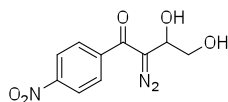
2-diazo-3,4-dihydroxy-1-phenylbutan-1-one (S20): ^1H NMR (400 MHz, CDCl_3) δ ppm 7.63-7.65 (2H, m), 7.54-7.56 (2H, m), 7.47-7.50 (1H, m), 4.97 (1H, br), 3.98-4.01 (2H, m); ^{13}C NMR (400 MHz, CDCl_3) δ ppm 190.3, 137.4, 132.5, 129.2, 127.7, 127.6, 67.8, 64.7 IR: 3400, 2925, 2360, 2341, 1597, 1570 cm^{-1} Yield: 18% (over 2 steps)



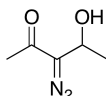
2-diazo-3,4-dihydroxy-1-(4-methoxyphenyl)butan-1-one (S21): ^1H NMR (400 MHz, CDCl_3) δ ppm 7.61-7.62 (2H, m), 6.92-6.96 (2H, m), 4.93 (1H, t, $J=4.8, 4.8$ Hz), 3.96 (1H, dd, $J=4.4, 11.6$ Hz), 3.88 (3H, s), 3.85-3.89 (1H, m); ^{13}C NMR (400 MHz, CDCl_3) δ ppm 189.1, 163.1, 129.9, 114.3, 69.4, 64.7, 55.9



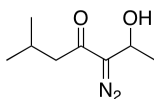
2-diazo-1-(4-fluorophenyl)-3,4-dihydroxybutan-1-one (S22): ^1H NMR (400 MHz, CDCl_3) δ ppm 7.61-7.64 (2H, m), 7.13-7.16 (2H, m), 4.93 (1H, t, $J=4.8, 4.4$ Hz), 3.96 (1H, dd, $J=4.4, 7.2$ Hz), 3.87 (1H, dd, $J=4.8, 11.2$ Hz) ^{13}C NMR (400 MHz, CDCl_3) δ ppm 188.6, 166.5, 163.9, 133.6, 130.2, 116.3, 67.7, 64.7; Yield: 9.5% (over 2 steps)



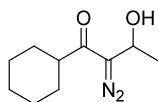
2-diazo-3,4-dihydroxy-1-(4-nitrophenyl)butan-1-one (S23): ^1H (400MHz, d_6 -Acetone) ppm δ 8.37–8.40 (2H, m), 7.94–7.96 (2H, m), 4.85 (1H, br s), 3.81 (2H, d, $J=4.8$ Hz); C^{13} (100MHz, d_6 -Acetone) ppm δ : 149.7, 128.9, 124.2, 78.7, 66.6, 64.5; Yield: 16% (over 2 steps)



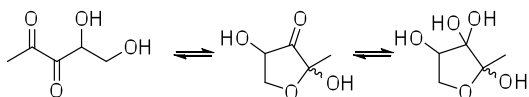
3-diazo-4-hydroxypentan-2-one (S24): ^1H NMR (CDCl_3 , 400 MHz) δ 5.04 (d, $J= 5.6$ Hz, 1H), 3.22 (br, 1H), 2.28 (s, 3H), 1.77 (br, 1H), 1.40 (d, $J= 6.4$ Hz, 3H); ^{13}C NMR (CDCl_3 , 100 MHz) δ 192.3, 62.4, 26.2, 19.5. IR: 3391, 2922, 2850, 2480, 2363, 2093, 1715, 1612 cm^{-1} Yield: 20% (over 2 steps)



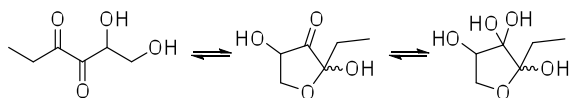
3-diazo-2-hydroxy-6-methylheptan-4-one (S25): ^1H NMR (CDCl_3 , 400 MHz) δ ppm 5.02 (d, $J= 6.0$ Hz, 1H), 3.53 (br, 1H), 2.35 (d, $J= 7.2$ Hz, 2H), 2.12–2.19 (m, 1H), 1.38 (d, $J= 6.4$ Hz, 3H), 0.95 (d, $J= 6.8$ Hz, 6H); ^{13}C NMR (CDCl_3 , 100 MHz) δ ppm 195.1, 72.9, 62.3, 47.6, 37.0, 26.2, 22.9, 19.6. IR: 3401, 2960, 2872, 2075, 1609 cm^{-1} Yield: 28% (over 2 steps)



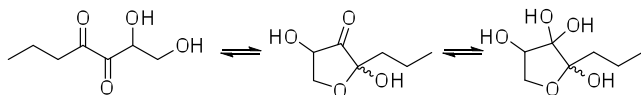
1-cyclohexyl-2-diazo-3-hydroxybutan-1-one (S26): ^1H NMR (CDCl_3 , 400 MHz) δ ppm 5.04 (1H, q, $J = 6.4, 6.8, 6.4$ Hz), 2.52-2.56 (1H, m), 1.76-1.79 (4H, m), 1.69-1.73 (2H, m), 1.39-1.54 (2H, m), 1.33 (3H, d, $J = 5.2$ Hz), 1.22-1.28 (2H, m); ^{13}C NMR (CDCl_3 , 100 MHz) δ ppm 198.9, 62.4, 46.7, 29.1, 26.2, 21.7, 19.6, 14.6. IR: 2931, 2856, 2361, 2340, 2076, 1616 cm^{-1}



DPD (4,5-dihydroxypentane-2,3-dione) and cyclic compounds (55): ^1H NMR (400 MHz, D_2O) δ ppm 4.24-4.28 (2H, m), 4.04-4.10 (6H, m), 3.93-3.95 (2H, m), 3.84-3.86 (2H, m), 3.67-3.72 (4H, m), 3.52-3.59 (3H, m), 3.44-3.48 (2H, m), 2.26 (3H, s), 1.30 (6H, s), 1.26 (6H, s). ^{13}C NMR (100 MHz, D_2O) δ ppm 103.9, 99.1, 74.3, 73.5, 71.2, 61.4, 24.8, 20.2, 19.6.

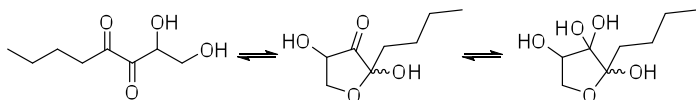


Ethyl-DPD (1,2-dihydroxyhexane-3,4-dione) and cyclic compounds (108): ^1H NMR (400 MHz, CDCl_3) δ ppm 4.94 (1H, t, $J = 3.1$), 3.99-4.07 (2H, m), 2.91-3.01 (1H, m), 2.75-2.85 (1H, m), 1.80-1.88 (2H, m), 1.15 (3H, t, $J = 7.2$ Hz). ^{13}C NMR (100 MHz, CDCl_3) δ ppm 200.2, 198.8, 75.2, 64.2, 30.9, 18.9, 6.9.

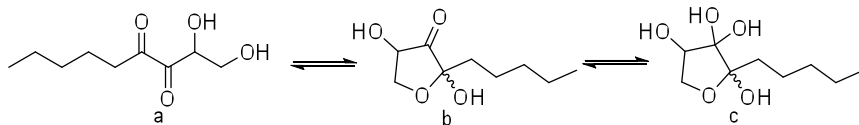


Propyl-DPD (1,2-dihydroxyheptane-3,4-dione) and cyclic compounds (109): ^1H NMR (400 MHz, CDCl_3) δ ppm 4.91 (1H, t, $J = 3.1$ Hz), 3.96-4.04 (2H, m), 2.81-2.89

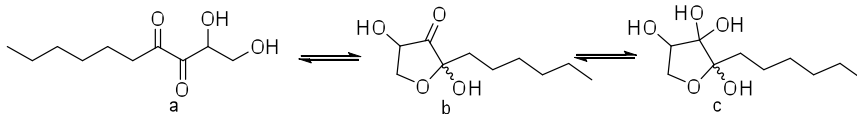
(1H, m), 2.70-2.78 (1H, m), 1.61-1.70 (3H, m), 0.88-0.99 (6H, m). ^{13}C NMR (100 MHz, CDCl_3) δ 199.3, 198.4, 74.7, 63.7, 38.7, 16.2, 13.5.



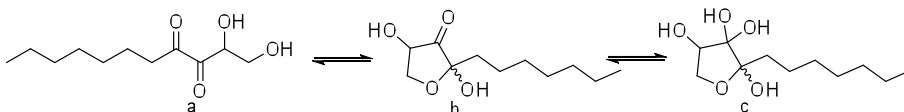
Butyl-DPD (1,2-dihydroxyoctane-3,4-dione) and cyclic compounds (110): ^1H NMR (400 MHz, CDCl_3) δ ppm 4.94, (1H, t, $J = 3.2$ Hz), 3.98-4.06 (2H, m), 2.86-2.94 (1H, m), 2.74-2.83 (1H, m), 1.59-1.67 (2H, m), 1.34-1.43 (2H, m), 0.95 (3H, t, $J = 7.3$ Hz). ^{13}C NMR (400 MHz, CDCl_3) δ ppm 199.2, 198.2, 74.5, 63.5, 36.4, 24.4, 21.9, 13.5.



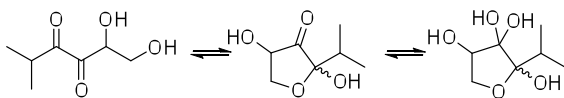
Pentyl-DPD (1,2-dihydroxynonane-3,4-dione) and cyclic compounds (111): ^1H NMR (D_2O , 400 MHz) **a:** δ 3.85-3.87 (1H, m), 3.60-3.64 (1H, m), 3.48-3.43 (1H, m), 2.62-2.67 (2H, m), 1.51-1.61 (2H, m), 1.13-1.17 (2H, m), 0.70-0.73 (3H, m); **b:** δ 3.97-4.01 (1H, m), 3.73-3.80 (1H, m), 3.60-3.64 (1H, m), 1.40-1.43 (2H, m), 1.13-1.17 (6H, m), 0.70-0.73 (3H, m); **c:** δ 3.75-3.80 (1H, m), 3.38-3.48 (1H, m), 3.34-3.38 (1H, m), 1.40-1.43 (2H, m), 1.13-1.17 (6H, m), 0.70-0.73 (3H, m); ^{13}C NMR (CDCl_3 , 125 MHz) δ 212.9, 97.3, 74.6, 62.0, 37.3, 33.7, 32.3, 31.3, 23.3, 22.6, 14.2.



Hexyl-DPD (1,2-dihydroxydecane-3,4-dione) and cyclic compounds (112): ^1H NMR (D_2O , 600 MHz) **a:** δ 4.01-4.05 (1H, m), 3.64-3.68 (1H, m), 3.48-3.52 (1H, m), 2.59-2.70 (2H, m), 1.57-1.62 (2H, m), 1.16-1.18 (6H, m) 0.74-0.75 (3H, m); **b:** δ 4.25-4.27 (1H, m), 3.82-3.84 (1H, m), 3.64-3.68 (1H, m), 1.43-1.46 (2H, m), 1.16-1.18 (8H, m), 0.74-0.75 (3H, m); **c:** δ 3.91-3.92 (1H, m), 3.48-3.52 (1H, m), 3.39-3.42 (1H, m), 1.43-1.46 (2H, m), 1.16-1.18 (8H, m), 0.74-0.75 (3H, m); ^{13}C NMR (CDCl_3 , 150 MHz) δ 73.7, 61.1, 36.5, 30.7, 28.8, 27.8, 22.6, 21.7, 13.2.

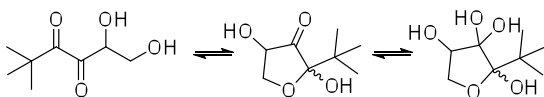


Heptyl-DPD (1,2-dihydroxyundecane-3,4-dione) and cyclic compounds (113): ^1H NMR (D_2O , 400 MHz) **a:** δ 4.04-4.05 (1H, m), 3.65-3.71 (1H, m), 3.49-3.54 (1H, m), 2.64-2.69 (2H, m), 1.58-1.63 (2H, m), 1.18-1.20 (8H, m), 0.74-0.76 (3H, m); **b:** δ 4.25-4.27 (1H, m), 3.83-3.86 (1H, m), 3.65-3.71 (1H, m), 1.46-1.48 (2H, m), 1.18-1.20 (8H, m), 0.74-0.76 (3H, m); **c:** δ 3.91-3.94 (1H, m), 3.49-3.54 (1H, m), 3.40-3.44 (1H, m), 1.46-1.48 (2H, m), 1.18-1.20 (8H, m), 0.74-0.76 (3H, m); ^{13}C NMR (CDCl_3 , 125 MHz) δ 216.5, 74.8, 69.5, 62.5, 37.5, 31.8, 29.0, 22.8, 14.2.



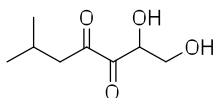
Isopropyl-DPD (1,2-dihydroxy-5-methylhexane-3,4-dione) and cyclic compounds

(114): ^1H NMR (400 MHz, CDCl_3) δ ppm 4.92 (1H, t, $J = 3.2$ Hz), 3.98 (2H, d, $J = 3.3$ Hz), 3.72 (1H, q, $J = 7.0$ Hz), 3.34-3.41 (1H, m), 1.23-1.29 (3H, m), 1.19 (1H, dd, $J = 6.9, 1.4$ Hz) 1.15 (6H, dd, $J = 6.9, 6.3$ Hz), 1.03 (3H, dd, $J = 6.9, 1.5$ Hz), 0.92 (1H, d, $J = 6.9$ Hz); ^{13}C NMR (100 MHz, CDCl_3) δ ppm 203.1, 199.5, 75.3, 63.9, 35.3, 34.1, 30.1, 17.7, 17.3.



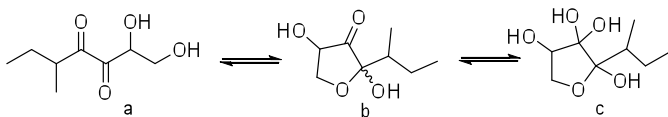
Tertbutyl-DPD (1,2-dihydroxy-5,5-dimethylhexane-3,4-dione) and cyclic compounds

(115): ^1H NMR (400 MHz, CDCl_3) δ ppm 4.78 (1H, t, $J = 3.5$ Hz), 4.37-4.45 (2H, m), 3.91 (2H, d, $J = 3.5$ Hz), 3.69-3.74 (1H, m), 1.27 (9H, s), 1.23 (3H, s), 1.09 (1H, s), 1.06 (1H, s), 1.01 (6H, s). ^{13}C NMR (100 MHz, CDCl_3) δ ppm 213.8, 207.4, 201.4, 101.7, 75.5, 73.1, 66.8, 63.2, 42.9, 37.1, 26.6, 26.1, 24.6, 24.1.



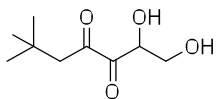
Isobutyl-DPD (1,2-dihydroxy-6-methylheptane-3,4-dione) (116):

^1H NMR (D_2O , 400 MHz) δ 3.85 (1H, dd, $J = 11.2, 3.6$ Hz), 3.68 (1H, dd, $J = 15.6, 3.6$ Hz), 3.52 (1H, dd, $J = 19.2, 7.6$ Hz), 2.54-2.59 (2H, m), 1.97-2.02 (1H, m), 0.83-0.85 (6H, m); ^{13}C NMR (CDCl_3 , 100 MHz) δ 211.7, 96.8, 73.9, 61.6, 45.7, 41.9, 23.8, 22.0.

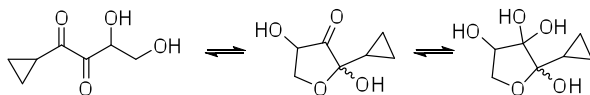


Secbutyl-DPD (1,2-dihydroxy-5-methylheptane-3,4-dione) and cyclic compounds

(117): ^1H NMR (D_2O , 400 MHz) **a:** δ 3.63-3.66 (1H, m), 3.46-3.51 (1H, m), 2.95-2.98 (1H, m), 1.46-1.58 (2H, m), 0.79-0.84 (3H, m), 0.68-0.77 (3H, m); **b:** δ 3.81-3.83 (1H, m), 3.70-3.74 (1H, m), 1.46-1.58 (2H, m), 1.19-1.28 (1H, m), 0.89-0.94 (3H, m), 0.68-0.77 (3H, m); **c:** δ 3.81-3.83 (1H, m), 3.70-3.74 (1H, m), 1.46-1.58 (2H, m), 1.19-1.28 (1H, m), 0.89-0.94 (3H, m), 0.68-0.77 (3H, m); ^{13}C NMR (CDCl_3 , 125 MHz) δ 217.2, 97.8, 75.2, 74.2, 72.4, 63.5, 62.3, 42.1, 40.9, 27.3, 26.9, 25.4, 24.2, 17.3, 16.9, 14.8, 12.1, 11.6, 11.3.



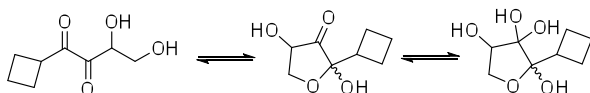
Neopentyl-DPD (1,2-dihydroxy-6,6-dimethylheptane-3,4-dione) (118): ^1H NMR (D_2O , 400 MHz) δ 3.81-3.85 (1H, m), 3.65-3.69 (1H, m), 3.48-3.53 (1H, m), 2.60 (2H, dd, $J=$ 44.0, 13.2 Hz), 0.91 (9H, s); ^{13}C NMR (CDCl_3 , 100 MHz) δ 210.8, 202.1, 96.8, 74.3, 74.0, 63.2, 51.7, 48.3, 48.2, 31.2, 30.1, 29.3, 29.1.



Cyclopropyl-DPD (1-cyclopropyl-3,4-dihydroxybutane-1,2-dione) and cyclic compounds

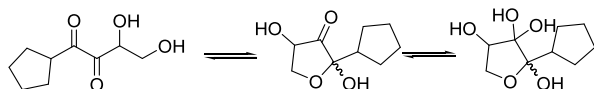
(119): ^1H NMR (400 MHz, CDCl_3) δ ppm 4.90 (1H, t, $J =$ 3.2 Hz), 4.00

(2H, d, $J=3.2$ Hz), 2.71-2.75 (1H, m), 1.09-1.24 (12H, m), 0.83-0.89 (4H, m). ^{13}C NMR (100 MHz, CDCl_3) δ ppm 74.7, 63.7, 29.7, 16.3, 14.3.



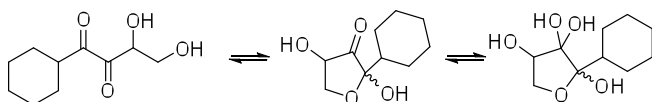
Cyclobutyl-DPD (1-cyclobutyl-3,4-dihydroxybutane-1,2-dione) and cyclic

compounds (120): ^1H NMR (400 MHz, D_2O) δ ppm 4.78-4.81 (1H, m), 4.51-4.61 (1H, m), 4.39-4.42 (1H, m), 4.20-4.29 (2H, m), 4.11-4.16 (1H, m), 4.00-4.06 (1H, m), 3.87-3.90 (1H, m), 3.75-3.79 (2H, m), 3.61-3.69 (2H, m), 3.42-3.49 (1H, m), 2.56-2.78 (2H, m), 2.81-2.89 (1H, m), 2.43-2.55 (2H, m), 1.97-2.13 (18H, m), 1.72-1.96 (24H, m); ^{13}C NMR (100 MHz, D_2O) 104.6, 75.5, 73.9, 71.7, 70.9, 69.4, 61.4, 54.2, 38.1, 30.6, 25.6, 25.5, 25.4, 23.0, 22.9, 22.5, 18.2, 17.8

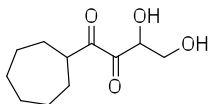


Cyclopentyl-DPD (1-cyclopentyl-3,4-dihydroxybutane-1,2-dione) and cyclic

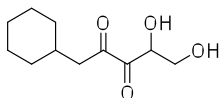
compounds (121): ^1H NMR (400 MHz, D_2O) δ ppm 4.03-4.06 (1H, m), 3.88-3.90 (1H, m), 3.77-3.81 (1H, m), 3.65-3.69 (1H, m), 3.49-3.54 (1H, m), 3.31-3.35 (1H, m), 2.17-2.26 (1H, m), 1.80-1.83 (2H, m), 1.39-1.67 (18H, m); ^{13}C NMR (100 MHz, D_2O) 218.1, 99.7, 76.4, 74.2, 69.4, 64.2, 47.9, 47.3, 34.5, 34.1



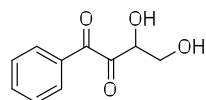
Cyclohexyl-DPD (1-cyclohexyl-3,4-dihydroxybutane-1,2-dione) and cyclic compounds (122): ^1H NMR (400 MHz, CDCl_3) δ ppm 4.93 (1H, br), 4.00 (2H, d, $J = 2.8$ Hz), 3.14-3.20 (1H, m), 1.71-1.92 (18 H, m), 1.23-1.48 (16H, m). ^{13}C NMR (100 MHz, CDCl_3) δ ppm 202.4, 199.6, 75.2, 63.9, 44.6, 28.1, 27.6, 26.1, 26.0, 25.9, 25.5.



Cycloheptyl-DPD (1-cycloheptyl-3,4-dihydroxybutane-1,2-dione) (123): ^1H NMR (400 MHz, D_2O) δ ppm 3.78-3.82 (1H, m), 3.73-3.75 (1H, m), 3.64-3.66 (1H, m), 3.61-3.63 (1H, m), 1.61-1.80 (5H,m), 1.50-1.60 (2H,m), 1.24-1.47 (4H,m)

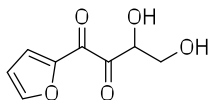


CH_2 -Cyclohexyl-DPD (1-cyclohexyl-4,5-dihydroxypentane-2,3-dione) (124): ^1H NMR (400 MHz, D_2O) δ ppm 3.65-3.69 (2H, m), 2.60-2.62 (1H, m), 1.79-1.83 (2H, m), 1.54-1.60 (3H, m), 1.04-1.23 (6H, m), 0.82-0.94 (4H, m) ^{13}C NMR (100 MHz, D_2O) 199.5, 198.3, 75.2, 64.1, 44.7, 35.2, 33.6, 33.5, 33.4, 26.5, 26.4, 26.3

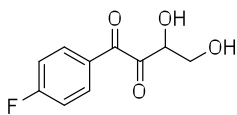


Phenyl-DPD (3,4-dihydroxy-1-phenylbutane-1,2-dione) (125): ^1H NMR (400 MHz, D_2O) δ ppm 8.06-8.09 (1H, m), 7.85-7.86 (1H, m), 7.66-7.71 (1H, m), 7.46-7.48 (8H, m),

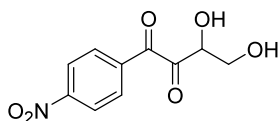
7.32-7.34 (9H, m), 4.93-4.95 (1H, m), 4.46-4.49 (2H, m), 4.30-4.34 (3H, m), 4.23-4.27 (3H, m), 4.08-4.09 (1H, m), 3.98-4.00 (4H, m), 3.89-3.95 (4H, m), 3.66-3.74 (4H, m) ¹³C NMR (100 MHz, D₂O) 137.8, 130.4, 129.6, 129.4, 129.1, 128.5, 128.4, 127.7, 127.4, 127.3, 100.5, 74.6, 73.7, 71.8, 69.1



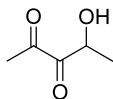
Furanoyl-DPD (1-(furan-2-yl)-3,4-dihydroxybutane-1,2-dione) (126): ¹H NMR (400 MHz, D₂O) δ ppm 7.80 (1H, d, *J*= 0.5), 7.65 (1H, dd, *J*= 0.5, 3.7 Hz), 6.64 (1H, dd, *J*= 1.7, 3.7 Hz), 4.01 (1H, dd, *J*= 3.7, 7.6 Hz), 3.73 (1H, dd, *J*= 3.7, 11.8 Hz), 3.53 (1H, dd, *J*= 7.6, 11.8 Hz), 2.59-2.56 (1H, m); ¹³C NMR (100 MHz, D₂O) 187.9, 149.9, 149.4, 125.2, 120.0, 113.5, 97.2, 75.6, 61.6



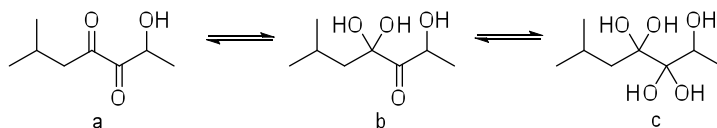
Fluorophenyl-DPD (1-(4-fluorophenyl)-3,4-dihydroxybutane-1,2-dione) (128): ¹H NMR (400 MHz, D₂O) δ ppm 8.13-8.16 (1H, m) 7.91-7.94 (2H, m), 7.70-7.74 (2H, m), 7.42-7.46 (4H, m), 7.13-7.19 (6H, m), 7.00-7.08 (4H, m), 4.55-4.58 (1H, m), 4.42-4.46 (1H, m), 4.27-4.30 (1H, m), 4.19-4.24 (1H, m), 4.00-4.03 (1H, m), 3.95-3.07 (1H, m), 3.87-3.91 (1H, m), 3.62-3.69 (2H, m)



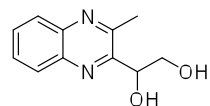
Nitrophenyl-DPD (3,4-Dihydroxy-1-(4-nitro-phenyl)-butane-1,2-dione) (129): ^1H NMR (D_2O , 400 MHz) 8.17 (2H, dd, $J = 0.8, 8.4$ Hz), 7.68 (2H, dd, $J = 2, 6.8$ Hz), 4.47 (1H, t, $J = 6.8, 7.2$ Hz), 4.34-4.38 (1H, m), 4.25-4.28 (1H, m), 4.00-4.02 (1H, m), 3.95-3.98 (1H, m)



Deoxy-Methyl DPD (4-hydroxypentane-2,3-dione) (134a): ^1H NMR (D_2O , 400 MHz) δ 3.94 (1H, q, $J = 6.5$ Hz), 2.25 (3H, s), 1.08 (3H, d, $J = 10.0$ Hz); ^{13}C NMR (CDCl_3 , 150 MHz) δ 211.3, 97.7, 69.8, 24.8, 15.4.

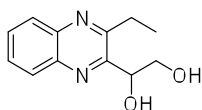


Deoxy-Isobutyl DPD (134b): ^1H NMR (D_2O , 400 MHz) **b:** δ 4.23 (1H, q, $J = 6.8, 6.8, 6.8$ Hz), 2.82-2.86 (2H, m), 2.28 (2H, s), 1.36-1.38 (3H, m), 1.07-1.11 (6H, m); **c:** δ 3.84 (1H, q, $J = 6.8, 6.8, 6.8$ Hz), 2.76 (2H, d, $J = 6.8$ Hz), 2.41 (2H, s), 1.36-1.38 (3H, m), 1.07-1.11 (6H, m) ^{13}C NMR (CDCl_3 , 125 MHz) δ 217.2, 97.8, 75.2, 74.2, 72.4, 63.5, 62.3, 42.1, 40.9, 27.3, 26.9, 25.4, 24.2, 17.3, 16.9, 14.8, 12.1, 11.6, 11.3.

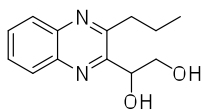


1-(3-methylquinoxalin-2-yl)ethane-1,2-diol (S27): ^1H NMR (500 MHz, CDCl_3) δ ppm 8.03-8.06 (2H, m), 7.72-7.78 (2H, m), 5.11-5.16 (1H, m, br), 4.55 (1H, d, $J = 7.6$ Hz),

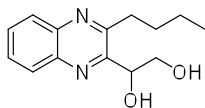
4.03-4.08 (1H, m), 3.86 (1H, dd, $J = 11.4, 5.5$ Hz), 2.83 (3H, s). ^{13}C NMR (125 MHz, CDCl_3) δ ppm 153.1, 152.2, 142.1, 139.6, 130.3, 129.8, 128.8, 128.6, 71.2, 66.2, 29.9, 22.2. HRMS (ESI+): Found 205.0978 Calc'd 205.0977 (M+H).



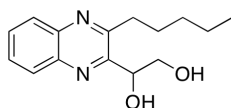
1-(3-ethylquinoxalin-2-yl)ethane-1,2-diol (S28): ^1H NMR (500 MHz, CDCl_3) δ ppm 8.10 (1H, dd, $J = 8.4, 1.8$ Hz), 8.02 (1H, d, $J = 8.0$ Hz), 7.71-7.78 (2H, m), 5.17 (1H, s, br), 4.56 (1H, d, $J = 7.0$ Hz), 4.01-4.06 (1H, m), 3.83 (1H, dd, $J = 11.6, 5.7$ Hz), 3.02-3.16 (2H, m), 1.46 (3H, t, $J = 7.5$ Hz). ^{13}C NMR (125 MHz, CDCl_3) δ ppm 156.4, 152.7, 142.3, 139.5, 130.2, 129.7, 128.9, 128.6, 70.9, 66.7, 29.6, 12.8. HRMS (ESI+): Found 219.1131 Calc'd 219.1134 (M+H).



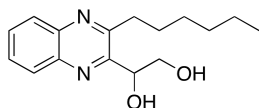
1-(3-propylquinoxalin-2-yl)ethane-1,2-diol (S29): ^1H NMR (500 MHz, CDCl_3) δ ppm 8.06 (1H, dd, $J = 8.3, 1.7$ Hz), 8.02 (1H, d, $J = 8.0$ Hz), 7.70-7.77 (2H, m), 5.17 (1H, s, br), 4.56 (1H, d, $J = 7.0$ Hz), 4.06-4.01 (1H, m), 3.83 (1H, dd, $J = 11.7, 5.7$ Hz), 3.02-3.16 (2H, m), 1.46 (3H, t, $J = 7.5$ Hz). ^{13}C NMR (125 MHz, CDCl_3) δ ppm 156.4, 152.7, 142.3, 139.5, 130.2, 129.7, 128.9, 128.6, 70.9, 66.7, 29.6, 12.8. HRMS (ESI+): Found 233.1331 Calc'd 233.1290 (M+H).



1-(3-butylquinoxalin-2-yl)ethane-1,2-diol (S30): ^1H NMR (500 MHz, CDCl_3) δ ppm 8.07 (1H, d, $J = 8.0$ Hz), 8.03 (1H, d, $J = 7.5$ Hz), 7.71-7.77 (2H, m), 5.17 (1H, s, br), 4.57 (1H, s, br), 4.04 (1H, dd, $J = 11.6, 3.2$ Hz), 3.81 (1H, dd, $J = 11.6, 5.9$ Hz), 2.99-3.10 (2H, m), 1.79-1.94 (2H, m), 1.47-1.55 (2H, m), 1.00 (3H, t, $J = 7.4$ Hz). ^{13}C NMR (125 MHz, CDCl_3) δ ppm 155.8, 152.8, 142.3, 139.4, 130.2, 129.7, 128.9, 128.6, 70.9, 66.8, 34.3, 31.2, 23.1, 14.2. HRMS (ESI+): Found 247.1459 Calc'd 247.1447 (M+H).

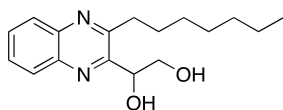


1-(3-pentylquinoxalin-2-yl) ethane-1,2-diol (S31): ^1H NMR (500 MHz, CDCl_3) δ 8.02-8.08 (2H, m), 7.72-7.76 (2H, m), 5.16-5.18 (1H, m), 4.02-4.05 (1H, m) 3.80-3.83 (1H, m), 3.01-3.06 (2H, m), 1.87-1.91 (2H, m), 1.44-1.46 (6H, m), 0.94 (3H, t, $J = 7.0, 7.0$ Hz); ^{13}C NMR (125 MHz, CDCl_3) δ 155.8, 152.8, 142.3, 139.4, 130.2, 129.7, 128.9, 128.6, 70.9, 66.8, 34.5, 32.1, 29.9, 28.7, 22.8, 14.2. HRMS (m/z): Found, 261.1612 Calc'd. 261.1603 (M+H).

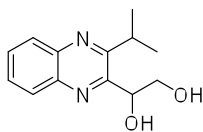


1-(3-hexylquinoxalin-2-yl) ethane-1,2-diol (S32): ^1H NMR (600 MHz, CDCl_3) δ 8.03-8.08 (2H, m), 7.73-7.77 (2H, m), 5.17 (1H, br), 4.56-4.57 (1H, m), 3.06 (1H, br), 3.81 (1H, m), 3.01-3.06 (2H, m), 1.86-1.89 (2H, m), 1.47-1.48 (2H, m), 1.35-1.37 (4H, m),

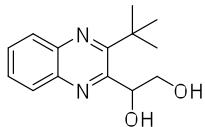
0.90-0.92 (3H, m); ^{13}C NMR (150 MHz, CDCl_3) δ 155.8, 152.8, 142.3, 139.5, 130.2, 129.7, 128.9, 128.6, 70.9, 66.8, 34.6, 31.9, 29.6, 29.0, 22.8, 14.3. HRMS (m/z): Found, 275.1753 Calc'd. 275.1760 (M+H).



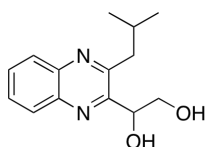
1-(3-heptylquinoxalin-2-yl) ethane-1,2-diol (S33): ^1H NMR (500 MHz, CDCl_3) δ 8.02-8.08 (2H, m), 7.72-7.76 (2H, m), 5.14 (1H, br), 4.55 (1H, br), 4.02-4.07 (1H, m), 3.79-3.82 (1H, m), 3.01-3.06 (2H, m), 1.87-1.89 (2H, m), 1.46-1.49 (2H, m), 1.30-1.32 (4H, m), 0.90 (3H, t, $J = 7.0$ Hz); ^{13}C NMR (125 MHz, CDCl_3) δ 155.8, 152.8, 142.2, 139.4, 130.2, 129.7, 128.9, 128.6, 70.9, 66.8, 34.6, 31.9, 29.9, 29.4, 29.1, 22.8, 14.3. HRMS (m/z): Found, 289.1908 Calc'd. 289.1916 (M+H).



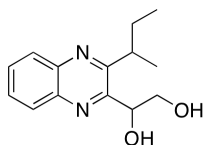
1-(3-isopropylquinoxalin-2-yl)ethane-1,2-diol (S34): ^1H NMR (600 MHz, CDCl_3) δ ppm 8.08 (1H, d, $J = 7.8$ Hz), 8.03 (1H, d, $J = 7.8$ Hz), 7.71-7.77 (2H, m), 5.22 (1H, s), 4.69 (1H, s), 4.03 (1H, dd, $J = 11.4, 2.5$ Hz), 3.77 (1H, dd, $J = 11.6, 6.0$ Hz), 3.43-3.47 (1H, m), 1.45 (3H, d, $J = 6.7$ Hz), 1.39 (3H, d, $J = 6.7$ Hz). ^{13}C NMR (150 MHz, CDCl_3) δ ppm 160.4, 151.9, 142.5, 139.4, 130.0, 129.7, 129.1, 128.5, 70.7, 67.2, 31.2, 29.9, 22.9, 21.8. MS (ESI+): Found 233.13 Calc'd 233.12 (M+H).



1-(3-tert-butylquinoxalin-2-yl)ethane-1,2-diol (S35): ^1H NMR (600 MHz, CDCl_3) δ ppm 8.06 (1H, d, $J = 8.4$ Hz), 7.99 (1H, d, $J = 7.8$ Hz), 7.71-7.76 (2H, m), 5.42-5.44 (1H, m), 3.97 (1H, dd, $J = 11.6, 2.9$ Hz), 3.83 (1H, dd, $J = 11.6, 6.3$ Hz), 1.59 (9H, s). ^{13}C NMR (100 MHz, CDCl_3) δ ppm 161.1, 154.7, 141.1, 139.3, 130.2, 129.8, 129.5, 128.2, 71.6, 68.1, 39.1, 30.6. HRMS (ESI⁺): Found 247.1455 Calc'd 247.1447 (M+H).

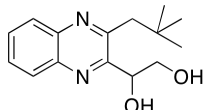


1-(3-isobutylquinoxalin-2-yl) ethane-1,2-diol (S36): ^1H NMR (400 MHz, CDCl_3) δ 8.05-8.11 (2H, m), 7.76-7.81 (2H, m), 5.21 (1H, t, $J = 3.2, 3.2$ Hz), 4.05 (1H, dd, $J = 11.6, 3.2$ Hz), 3.79 (1H, dd, $J = 11.6, 5.6$ Hz), 2.95 (2H, d, $J = 7.2$ Hz), 2.44-2.47 (1H, m), 1.07 (3H, d, $J = 4.0$ Hz), 1.06 (3H, d, $J = 3.6$ Hz); ^{13}C NMR (100 MHz, CDCl_3) δ 155.3, 153.2, 142.4, 139.5, 130.4, 129.9, 129.2, 128.8, 71.0, 66.9, 43.2, 28.9, 23.2, 22.8. HRMS (m/z): Found, 247.1444 Calc'd. 247.1447 (M+H).

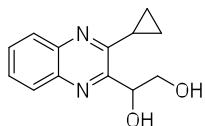


1-(3-sec-butylquinoxalin-2-yl) ethane-1,2-diol (S37): ^1H NMR (400 MHz, CDCl_3) δ 8.04-8.11 (2H, m), 7.73-7.79 (2H, m), 5.20-5.26 (1H, m), 4.03-4.08 (1H, m), 3.71-3.82

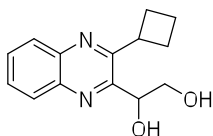
(1H, m), 3.18-3.22 (1H, m), 1.93-1.21 (1H, m), 1.75-1.85 (1H, m), 1.40 (3H, dd, $J= 29.5, 6.5$ Hz), 0.90 (3H, dt, $J= 20.5, 7.5, 7.5$ Hz); ^{13}C NMR (100 MHz, CDCl_3) δ 130.2, 129.9, 129.3, 128.7, 70.9, 67.3, 38.6, 38.3, 21.2, 20.2, 12.8, 12.6. HRMS (m/z): Found, 247.1446 Calc'd. 247.1447 (M+H).



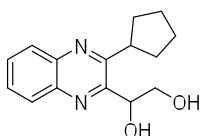
1-(3-neopentylquinoxalin-2-yl) ethane-1,2-diol (S38): ^1H NMR (400 MHz, CDCl_3) δ 8.05-8.13 (2H, m), 7.76-7.79 (2H, m), 5.29-5.33 (1H, m), 4.01 (1H, dd, $J= 4.5, 3.2$ Hz), 3.73 (1H, dd, $J= 6.0, 5.6$ Hz), 3.02 (2H, q, $J= 24.8, 13.6, 13.6$ Hz), 1.11 (9H, s); ^{13}C NMR (100 MHz, CDCl_3) δ 154.3, 153.7, 142.1, 130.4, 130.1, 129.4, 128.7, 71.4, 67.2, 46.2, 34.1, 30.3. HRMS (m/z): Found, 261.1604 Calc'd. 261.1603 (M+H).



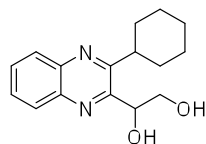
1-(3-cyclopropylquinoxalin-2-yl)ethane-1,2-diol (S39): ^1H NMR (500 MHz, CDCl_3) δ ppm 8.01 (1H, dd, $J = 8.0, 1.2$ Hz), 7.96 (1H, dd, $J = 8.3, 1.2$ Hz), 7.65-7.72 (2H, m), 5.36-5.39 (1H, m), 4.85 (1H, d, $J = 6.0\text{Hz}$), 4.17 (1H, d, $J = 11.2\text{Hz}$), 3.84 (1H, dd, $J = 6.0, 11.6\text{Hz}$), 2.78 (1H, s, br), 2.27-2.32 (1H, m), 1.48-1.52 (1H, m), 1.23-1.27 (1H, m), 1.15-1.21 (2H, m). ^{13}C NMR (125 MHz, CDCl_3) δ ppm 156.2, 152.3, 142.3, 138.9, 129.9, 129.1, 128.8, 128.5, 71.1, 66.6, 13.8, 11.9, 10.6. HRMS (ESI+): Found 231.1133 Calc'd 231.1134 (M+H).



1-(3-cyclobutylquinoxalin-2-yl)ethane-1,2-diol (S40): ^1H NMR (400 MHz, CDCl_3) δ ppm 8.19-8.25 (2H, m), 7.80-7.90 (2H, m), 5.21-5.22 (1H, br), 4.04-4.11 (1H, m), 3.80-3.83 (1H, m), 2.60-2.70 (2H, m), 2.33-2.47 (2H), 2.15-2.22 (2H, m), 1.93-2.07 (2H, m) ^{13}C NMR (100 MHz, CDCl_3) δ ppm 131.1, 131.0, 129.4, 126.9, 71.1, 66.7, 38.5, 28.1, 25.5, 18.4 MS (ESI+): Found 245.20 Calc'd 245.12 (M+H).

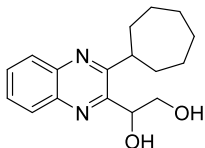


1-(3-cyclopentylquinoxalin-2-yl)ethane-1,2-diol (S41): ^1H NMR (400 MHz, CDCl_3) δ ppm 8.05-8.10 (2H, m), 7.73-7.77 (2H, m), 5.81 (1H, t, $J=3.2\text{Hz}$), 4.07 (1H, dd, $J=3.2, 11.6\text{Hz}$), 3.78 (1H, dd, $J=6.0, 11.6\text{Hz}$), 3.53-3.56 (1H, m), 2.15-2.17 (2H, m), 1.97-2.00 (4H, m), 1.78-1.81 (2H, m); ^{13}C NMR (100 MHz, CDCl_3) δ ppm 159.5, 152.4, 142.7, 139.3, 130.2, 129.8, 129.3, 128.5, 71.1, 67.4, 42.9, 34.7, 33.7, 26.6, 26.5 HRMS (ESI+): Found 259.2224 Calc'd 259.1368 (M+H).

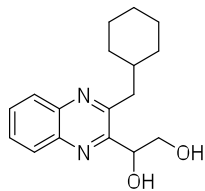


1-(3-cyclohexylquinoxalin-2-yl)ethane-1,2-diol (S42): ^1H NMR (500 MHz, CDCl_3) δ ppm 8.09 (1H, d, $J=8.0\text{Hz}$), 8.02 (1H, d, $J=8.0\text{Hz}$), 7.70-7.76 (2H, m), 5.21 (1H, s,

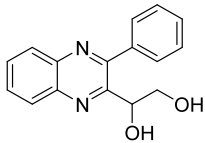
br), 4.66 (1H, s, br), 4.01-4.04 (1H, m), 3.75 (1H, dd, $J = 11.5, 6.1$ Hz), 3.01-3.07 (1H, m), 1.76-1.98 (6H, m), 1.44-1.49 (4H, m). ^{13}C NMR (125 MHz, CDCl_3) δ ppm 159.6, 152.0, 142.5, 139.4, 130.0, 129.6, 129.1, 128.5, 70.7, 67.3, 41.7, 33.2, 32.0, 26.8, 26.1. HRMS (ESI+): Found 273.1618 Calc'd 273.1603 (M+H).



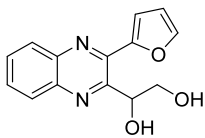
1-(3-cycloheptylquinoxaline-2-yl) ethane-1,2-diol (S43): ^1H NMR (400 MHz, CDCl_3) δ ppm 8.03-8.12 (2H, m), 7.72-7.78 (2H, m), 5.20-5.27 (1H, m), 4.01-4.11 (1H, m), 3.73-3.79 (1H, m), 3.19-3.28 (1H, m), 2.83-2.86 (1H, m), 2.14-2.22 (1H, m), 1.96-2.04 (4H, m), 1.75-1.83 (4H, m), 1.59-1.64 (4H, m) ^{13}C NMR (100 MHz, CDCl_3) δ 151.7, 130.2, 129.7, 129.3, 128.7, 70.9, 67.3, 35.6, 34.3, 28.5, 28.3, 27.6, 27.5. MS (ESI+): Found 287.27 Calc'd 287.17 (M+H).



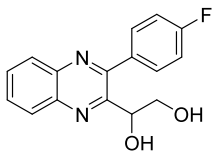
1-(3-(cyclohexylmethyl)quinoxalin-2-yl)ethane-1,2-diol (S44): ^1H NMR (500 MHz, CDCl_3) 8.03-8.12 (2H, m), 7.75-7.79 (2H, m), 5.18-5.21 (1H, m), 4.03 (1H, dd, $J = 3.3, 3.4$ Hz), 3.73-3.79 (1H, m), 2.94 (2H, d, $J = 7.0$ Hz), 2.32-2.35 (1H, m), 1.12-1.17 (4H, m), 0.85-0.92 (6H, m) ^{13}C NMR (100 MHz, CDCl_3) δ 155.5, 153.6, 130.7, 130.3, 129.6, 129.1, 71.4, 67.4, 42.4, 38.9, 34.3, 33.9, 27.1, 26.9 MS (ESI+): Found 287.19 Calc'd 287.17 (M+H).



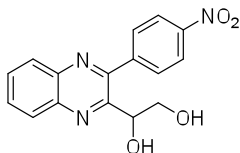
1-(3-phenylquinoxalin-2-yl)ethane-1,2-diol (S45): ^1H NMR (400 MHz, CDCl_3) δ ppm 8.08-8.16 (2H, m), 7.78-7.82 (2H, m), 7.75 (1H, dd, $J= 0.8, 2.4$ Hz), 7.44 (1H, dd, $J= 0.8, 2.8$ Hz), 6.69-6.70 (1H, m), 5.74-5.76 (1H, m), 4.12 (1H, dd, $J= 3.2, 11.6$ Hz), 3.72 (1H, dd, $J= 5.2, 11.6$ Hz); ^{13}C NMR (100 MHz, CDCl_3) δ ppm 145.4, 131.0, 130.6, 129.5, 128.7, 114.6, 113.0, 71.6, 66.9. HRMS (ESI+): Found 257.1679 Calc'd 257.0848 (M+H).



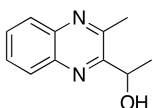
1-(3-(furan-2-yl)quinoxalin-2-yl)ethane-1,2-diol (S46): ^1H NMR (400 MHz, CDCl_3) δ ppm 8.08-8.16 (2H, m), 7.78-7.82 (2H, m), 7.75 (1H, dd, $J= 0.8, 2.4$ Hz), 7.44 (1H, dd, $J= 0.8, 2.8$ Hz), 6.69-6.70 (1H, m), 5.74-5.76 (1H, m), 4.12 (1H, dd, $J= 3.2, 11.6$ Hz), 3.72 (1H, dd, $J= 5.2, 11.6$ Hz); ^{13}C NMR (100 MHz, CDCl_3) δ ppm 145.4, 131.0, 130.6, 129.5, 128.7, 114.6, 113.0, 71.6, 66.9. HRMS (ESI+): Found 257.1679 Calc'd 257.0848 (M+H).



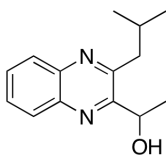
1-(3-fluorophenyl-quinoxalin-2-yl)-ethane-1,2-diol (S47): ^1H NMR (400 MHz, CDCl_3) δ 8.51-8.59 (1H, m), 8.32-8.33 (1H, m), 7.98-8.00 (2H, m), 7.86-7.89 (2H, m), 7.74-7.78 (2H, m), 5.43 (1H, t, $J= 4, 3.6$ Hz), 4.02 (1H, dd, $J= 3.2, 9.2$ Hz), 3.71 (1H, dd, $J= 4.4, 12$ Hz) MS (m/z): Found 285.13 Calc'd. 285.15 (M+H).



1-(3-(4-nitrophenyl)quinoxalin-2-yl)ethane-1,2-diol (S48): ^1H NMR (400 MHz, CDCl_3) δ 8.44-8.47 (2H, m), 8.17-8.22 (2H, m), 7.99-8.01 (2H, m), 7.89-7.92 (2H, m), 5.19 (1H, t, $J= 4.0, 4.4$ Hz), 3.83 (1H, dd, $J= 3.6, 8.0$ Hz), 3.76 (1H, dd, $J= 4.8, 6.8$ Hz) MS (m/z): Found 312.12 Calc'd. 312.09 (M+H).

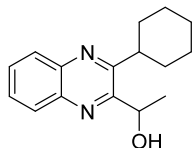


1-(3-methylquinoxalin-2-yl) ethanol (S49): ^1H NMR (400 MHz, CDCl_3) δ 8.03-8.06 (2H, m), 7.72-7.76 (2H, m), 5.19 (1H, q, $J= 6.4$ Hz), 2.77 (3H, s), 1.55 (3H, d, $J= 6.4$ Hz). ^{13}C NMR (100 MHz, CDCl_3) δ 157.4, 151.5, 142.0, 139.9, 130.1, 129.8, 128.8, 128.7, 67.0, 23.9, 22.3. HRMS (m/z): Found 189.1039 Calc'd. 189.1028 (M+H).



1-(3-isobutylquinoxalin-2-yl) ethanol (S50): ^1H NMR (500 MHz, CDCl_3) δ 8.06-8.10 (2H, m), 7.73-7.79 (2H, m), 5.25-5.30 (1H, m), 4.71 (1H, d, $J= 7.6$ Hz), 2.88 (2H, d, $J=$

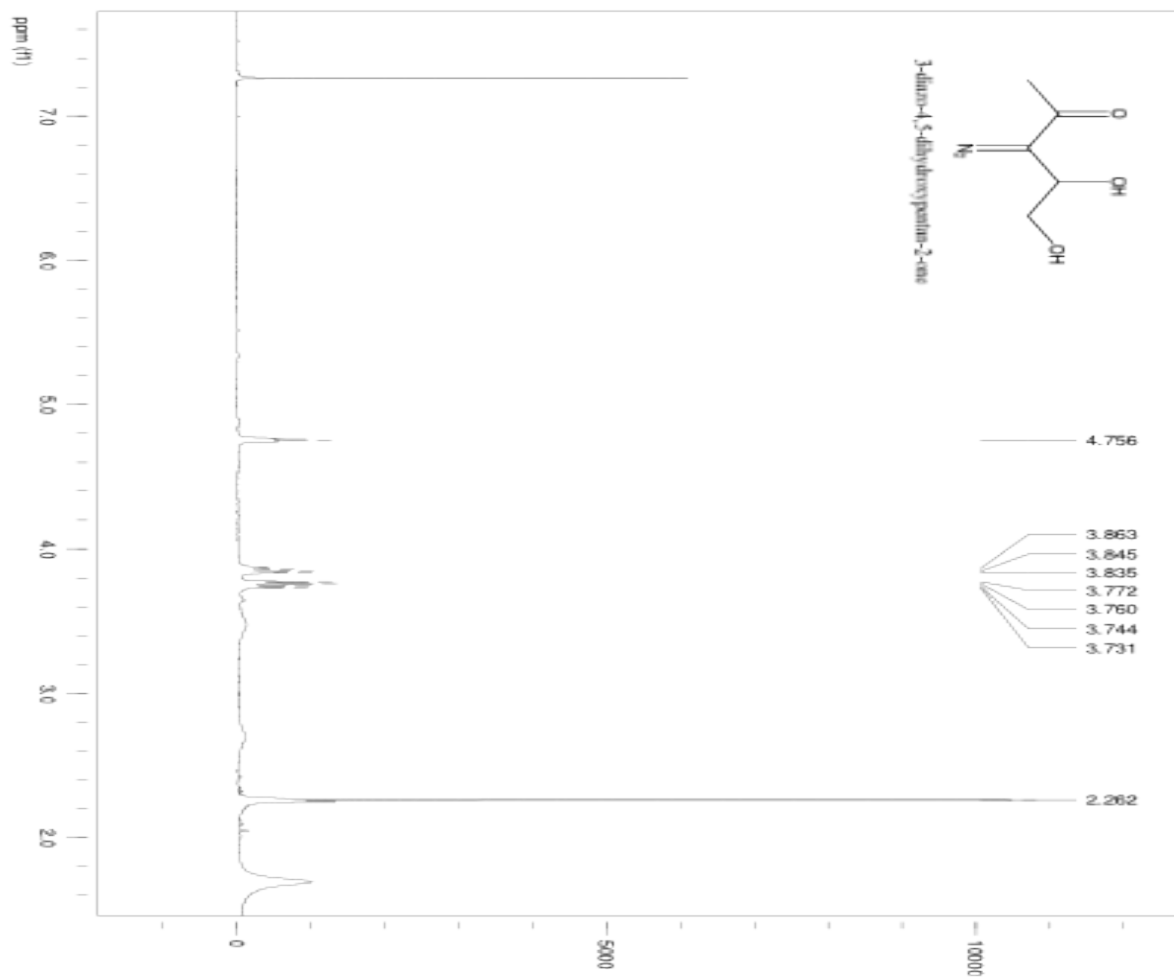
7.2 Hz), 2.42-2.49 (1H, m), 1.56 (3H, d, $J=6.4$ Hz), 1.08 (3H, d, $J=6.8$ Hz), 1.00 (3H, d, $J=7.6$ Hz); ^{13}C NMR (125 MHz, CDCl_3) δ 158.2, 155.2, 142.8, 140.4, 130.2, 130.0, 129.5, 129.1, 67.4, 43.8, 29.3, 25.4, 23.5, 23.2. HRMS (m/z): Found 231.1505 Calc'd. 231.1497 (M+H).

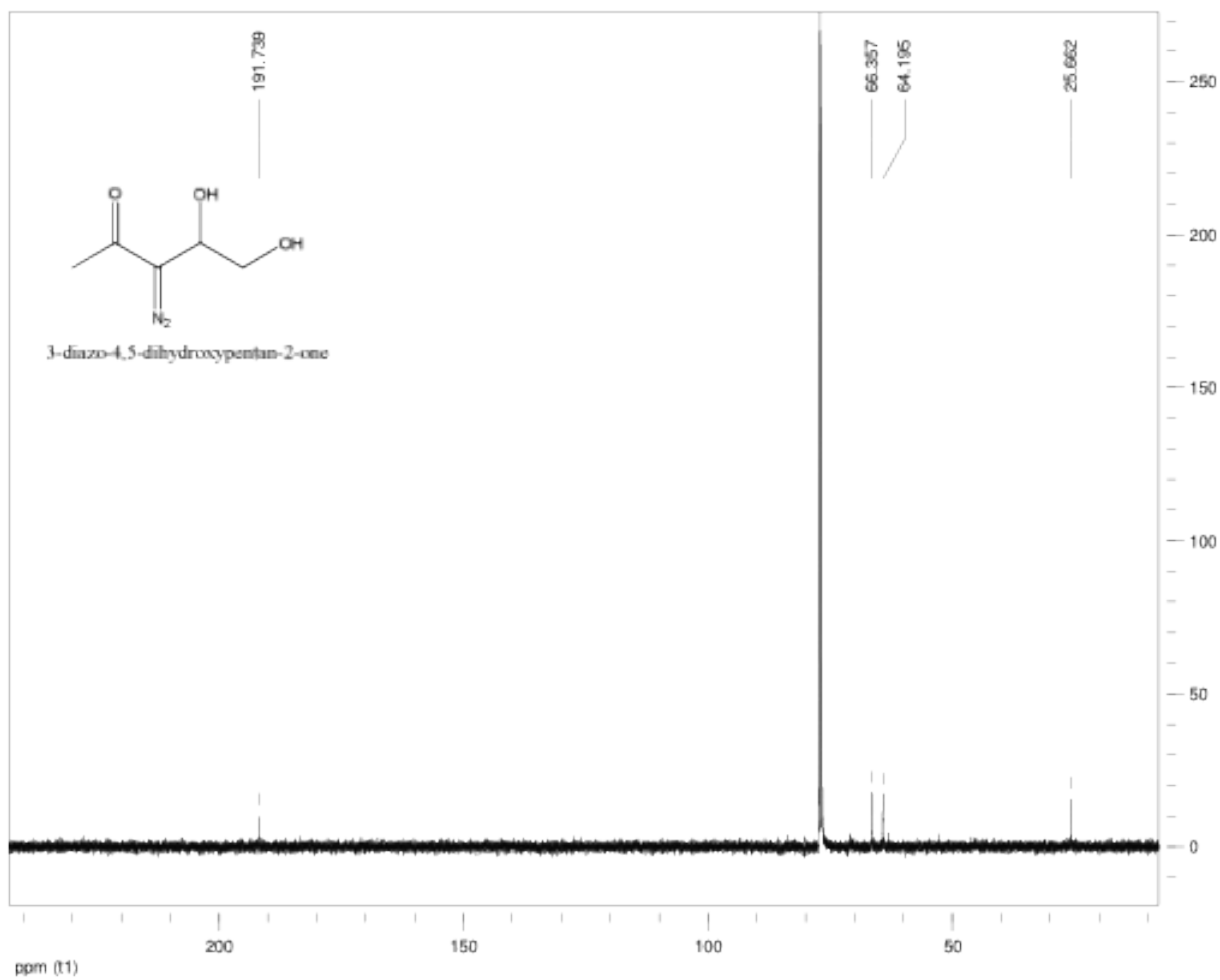


1-(3-cyclohexylquinoxalin-2-yl) ethanol (S51): ^1H NMR (400 MHz, CDCl_3) δ 8.04-8.10 (2H, m), 7.72-7.76 (2H, m), 5.29-5.31 (1H, m), 4.85 (1H, d, $J=7.6$ Hz). 2.92-3.01 (1H, m), 1.86-2.02 (6H, m), 1.61-1.63 (1H, m), 1.56 (3H, d, $J=6.4$ Hz), 1.44-1.57 (3H, m); ^{13}C NMR (100 MHz, CDCl_3) δ 159.0, 156.4, 142.5, 139.7, 129.7, 129.6, 129.2, 128.7, 66.5, 41.8, 33.5, 31.8, 27.0, 26.8, 26.2, 25.4. MS (m/z): Found 257.24 Calc'd. 257.16 (M+H).

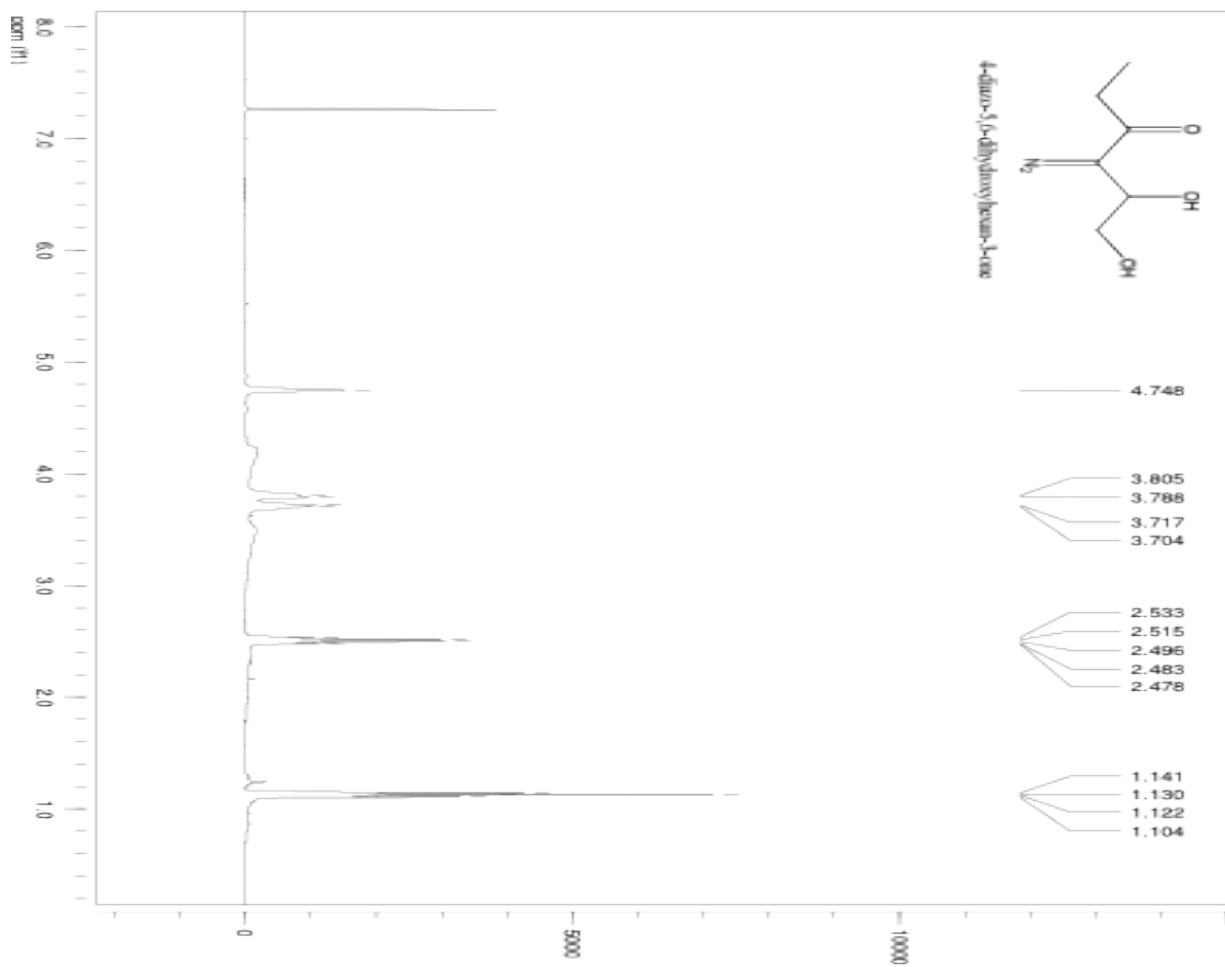
5.5. Spectra of AI-2 analogs

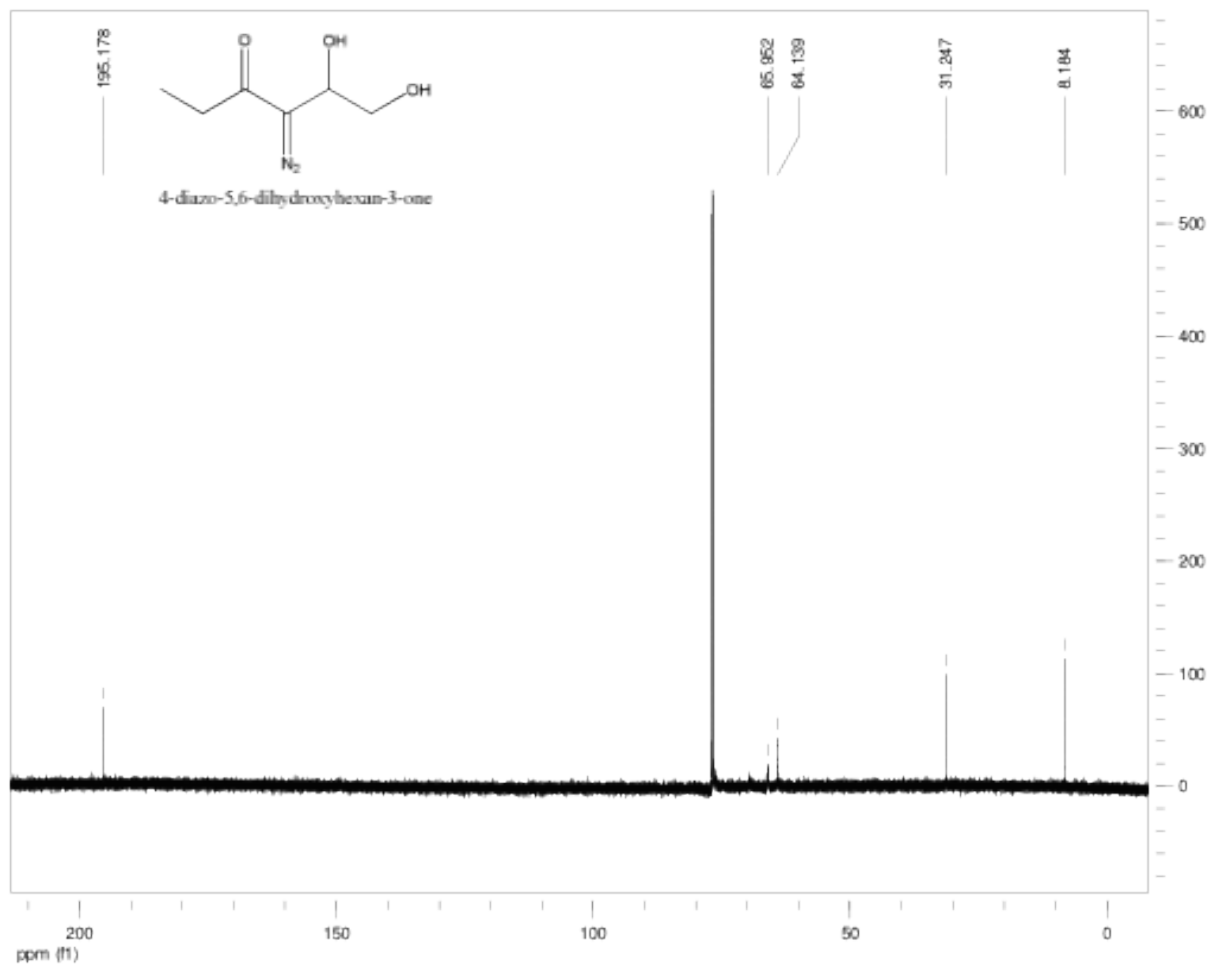
3-diazo-4, 5-dihydroxypentan-2-one (S1):



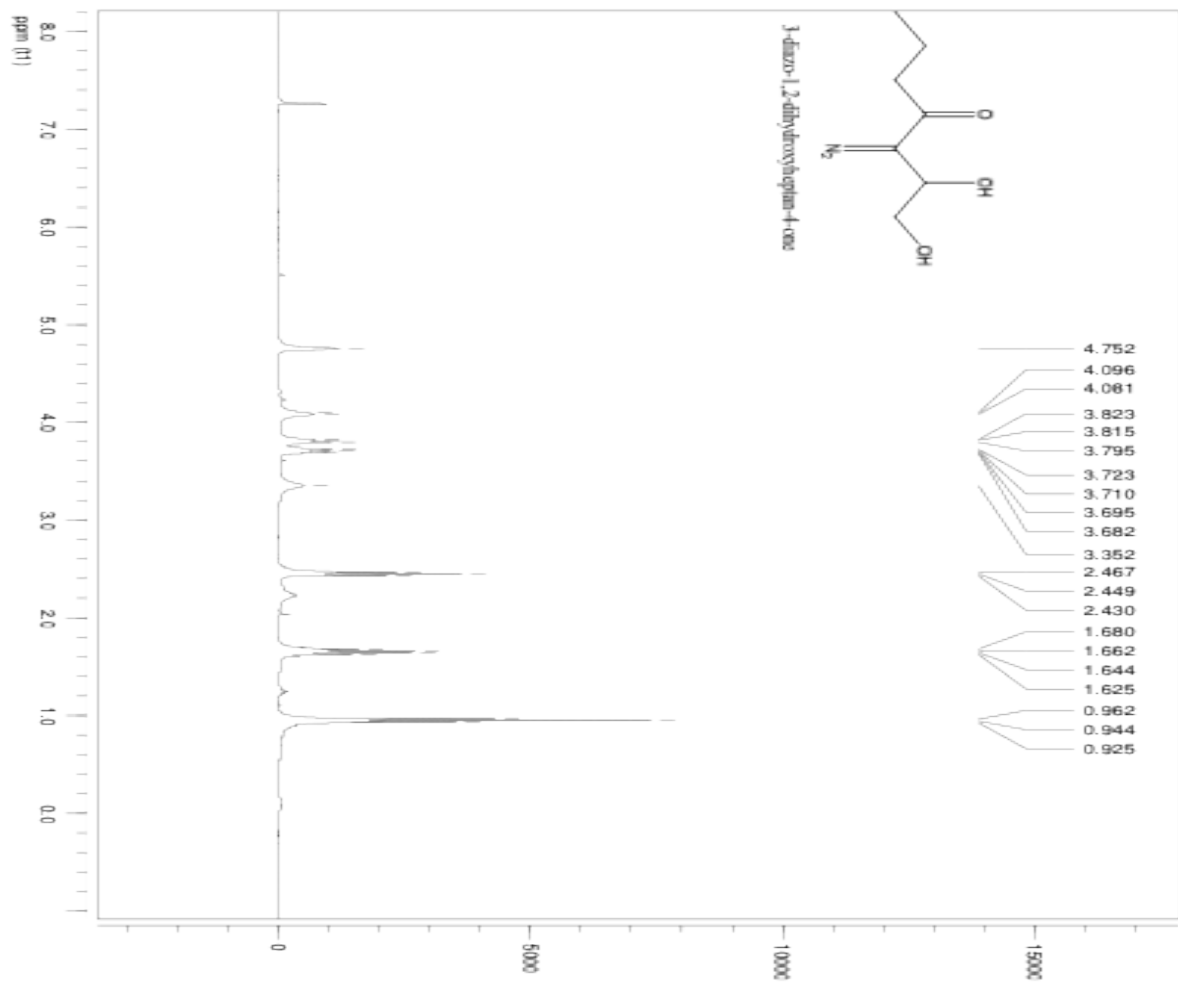


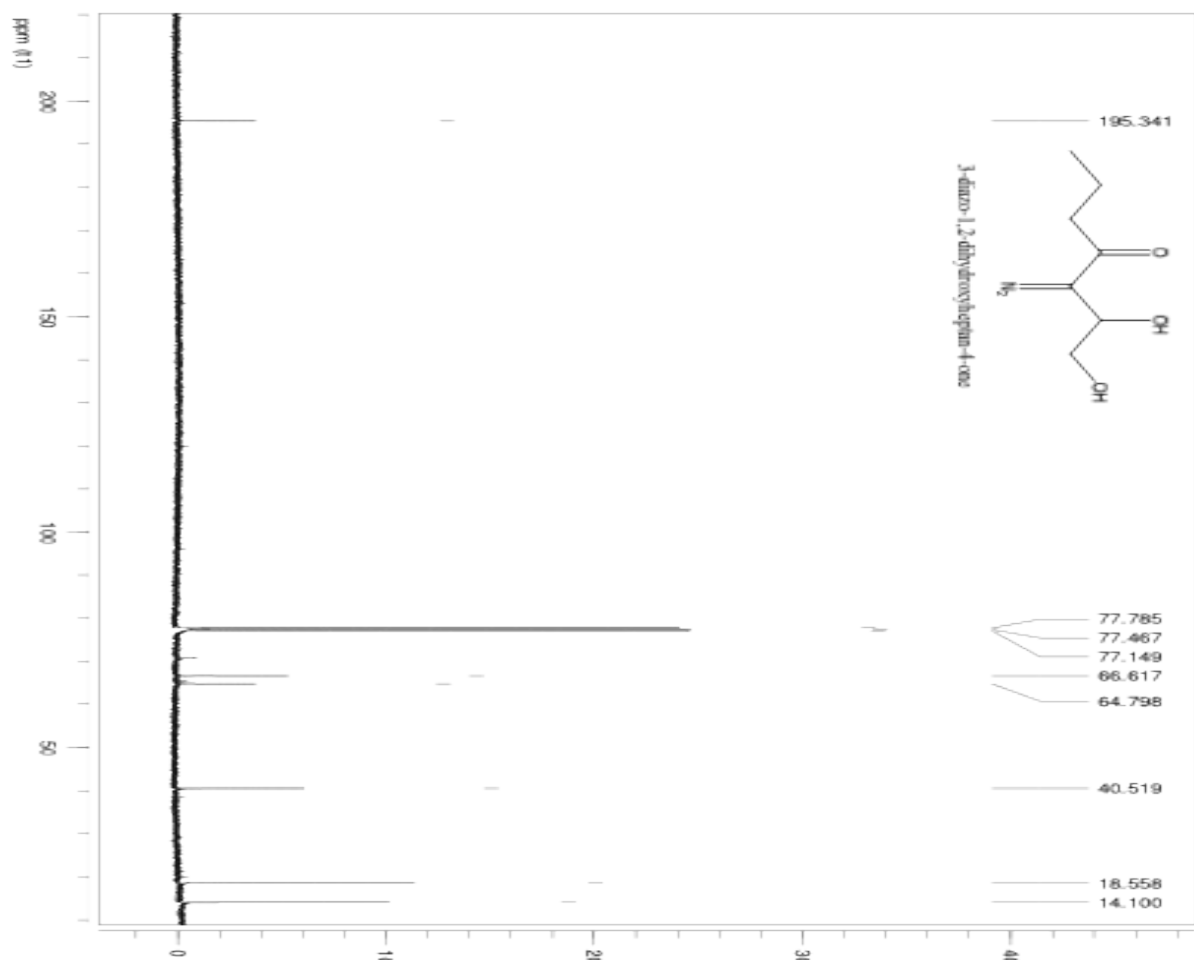
4-diazo-5,6-dihydroxyhexan-3-one (S2):



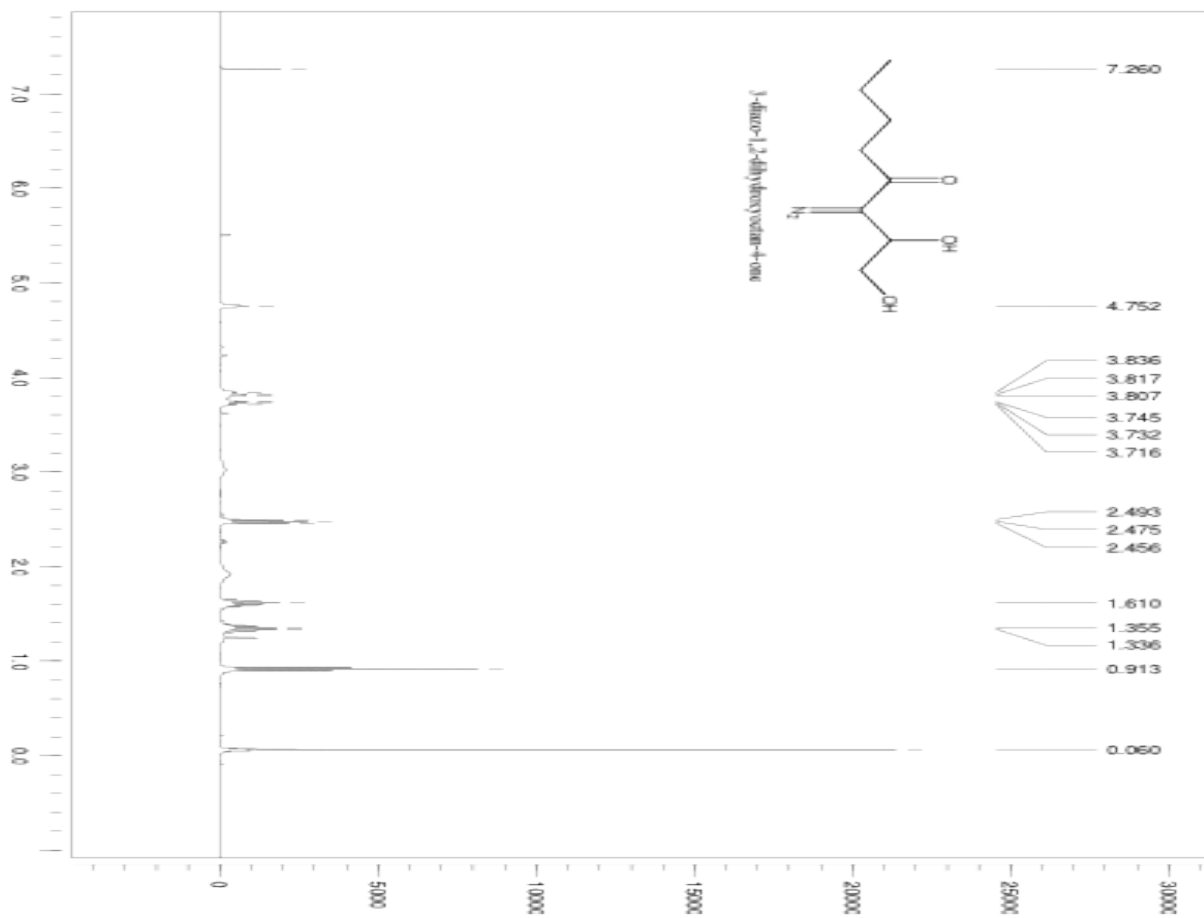


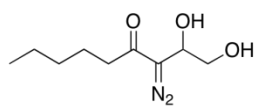
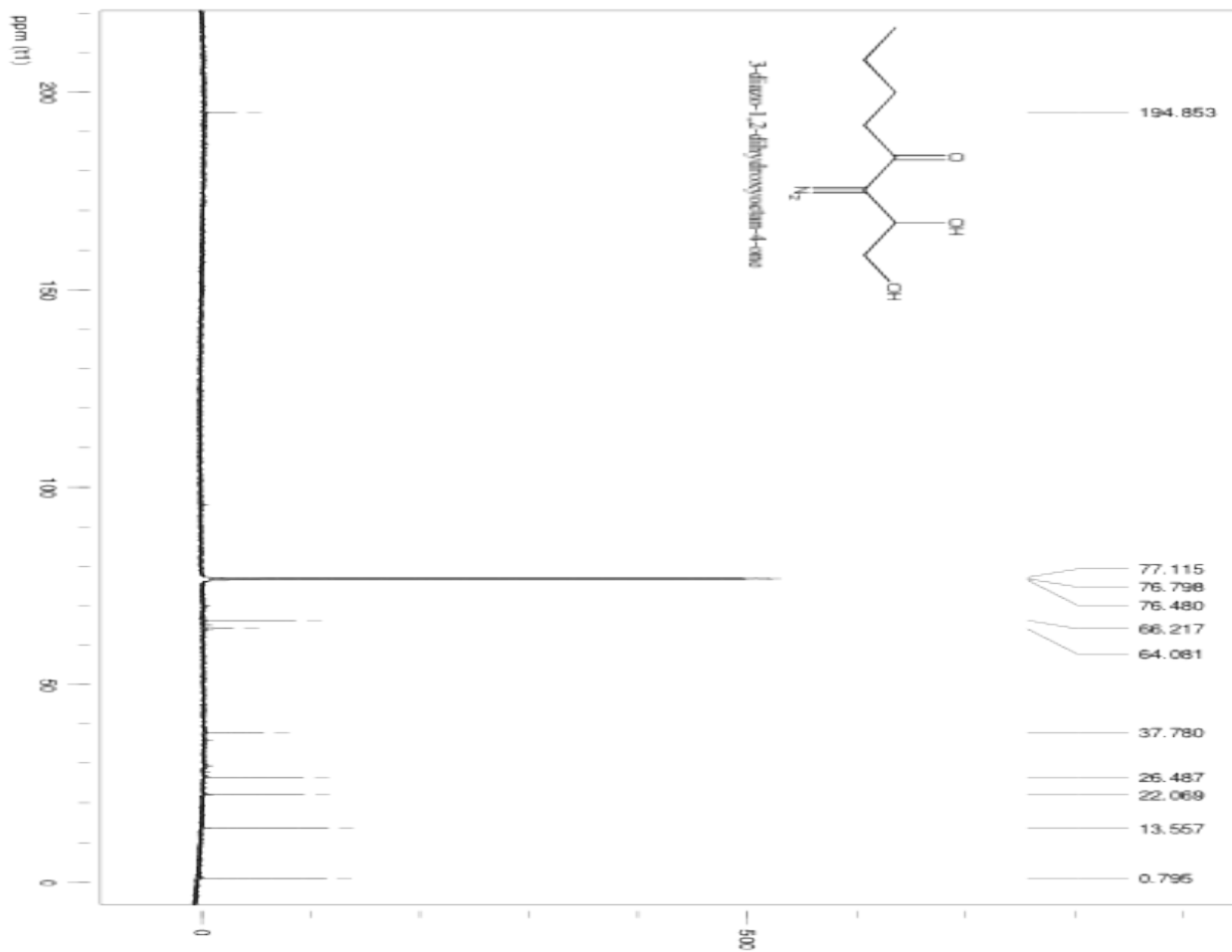
3-diazo-1,2-dihydroxyheptan-4-one (S3):





3-diazo-1,2-dihydroxyoctan-4-one (S4):





3-diazo-1,2-dihydroxynonan-4-one (S5):

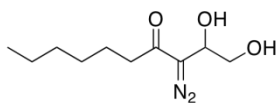
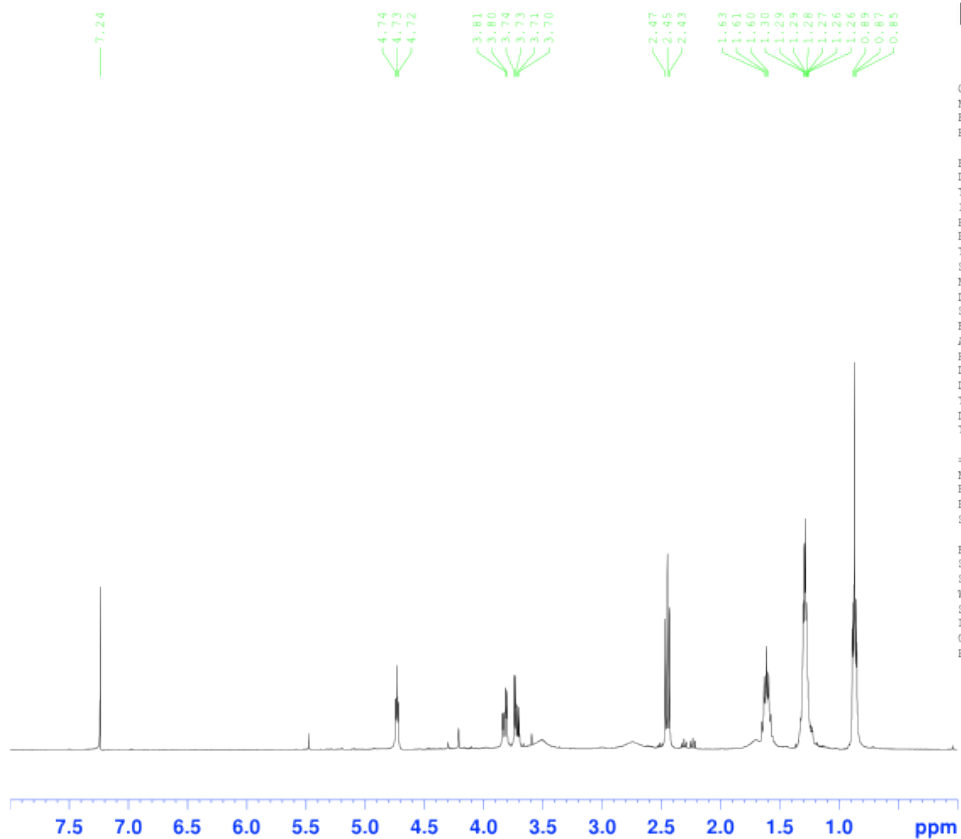


Current Data Parameters
NAME pentyl_diol
EXPNO 1
PROCNO 1

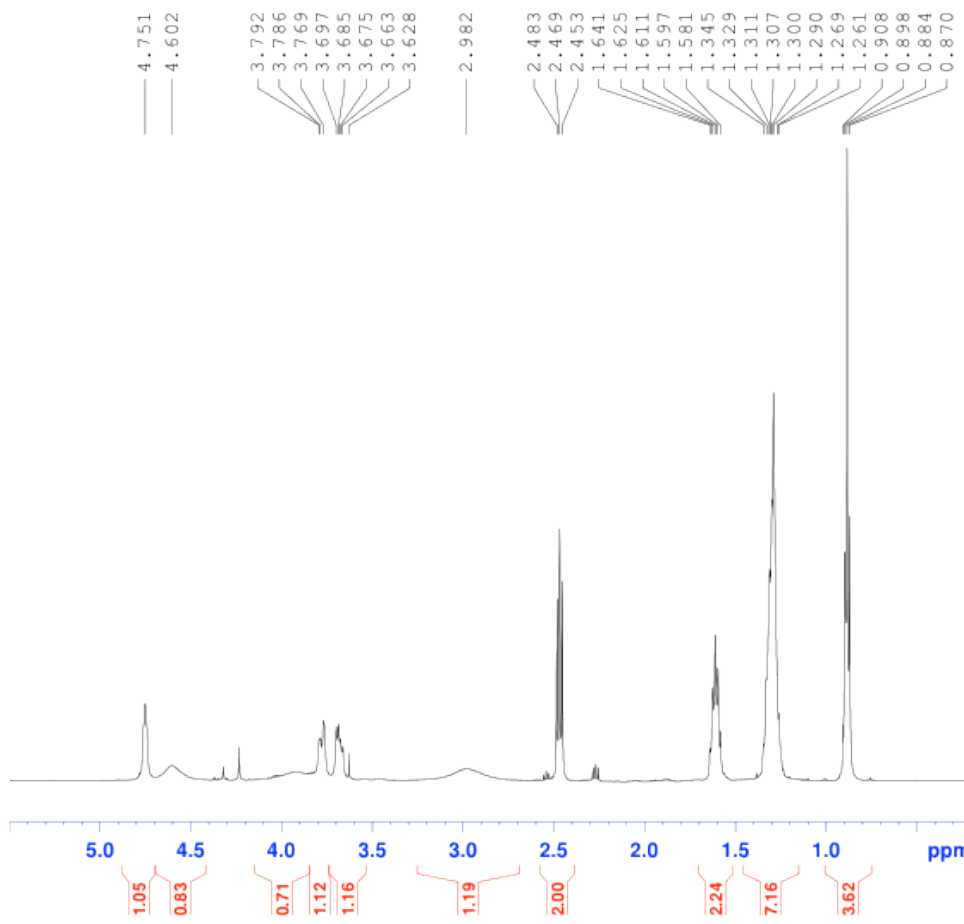
F2 - Acquisition Parameters
Date_ 20091205
Time 10.45
INSTRUM spect
PROBHD 5 mm QNP 1H/1
PULPROG zg30
TD 30720
SOLVENT CDCl3
NS 16
DS 2
SWH 6510.417 Hz
FIDRES 0.211928 Hz
AQ 2.3594227 sec
RG 256
DM 76.800 usec
DE 20.00 usec
TE 305.0 K
D1 2.00000000 sec
TD0 1

===== CHANNEL f1 =====
NUC1 1H
P1 10.35 usec
PL1 -2.00 dB
SFO1 400.1324008 MHz

F2 - Processing parameters
SI 16384
SF 400.1300179 MHz
MDW EM
SSB 0
LB 0.40 Hz
GB 0
PC 1.00



3-diazo-1,2-dihydroxydecan-4-one (S6):



```

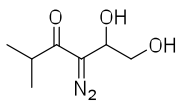
Current Data Parameters
NAME      C6H13_diazo_diol
EXPNO    1
PROCNO   1

F2 - Acquisition Parameters
Date_    20090814
Time     10.12
INSTRUM  spect
PROBHD   5 mm BBO2 new
PULPROG  zg
TD       65536
SOLVENT  CDCl3
NS       16
DS       2
SWH      6510.417 Hz
FIDRES   0.099341 Hz
AQ       5.0332146 sec
RG       22.6
DM       76.800 usec
DE       9.00 usec
TE       296.1 K
D1       4.00000000 sec
TD0      1

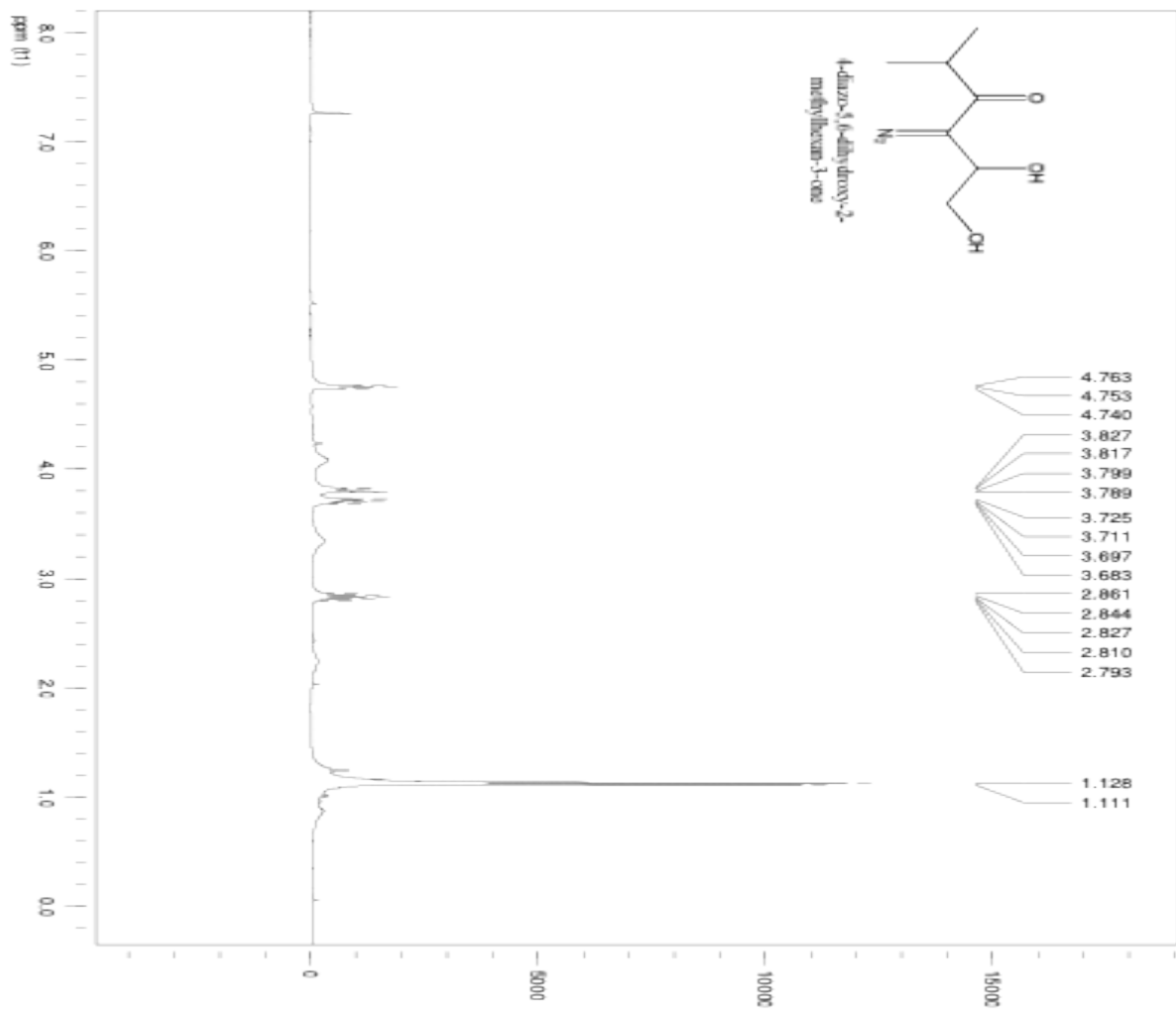
===== CHANNEL f1 =====
NUC1     1H
P1       11.10 usec
PL1      0.00 dB
SFO1     500.1330008 MHz

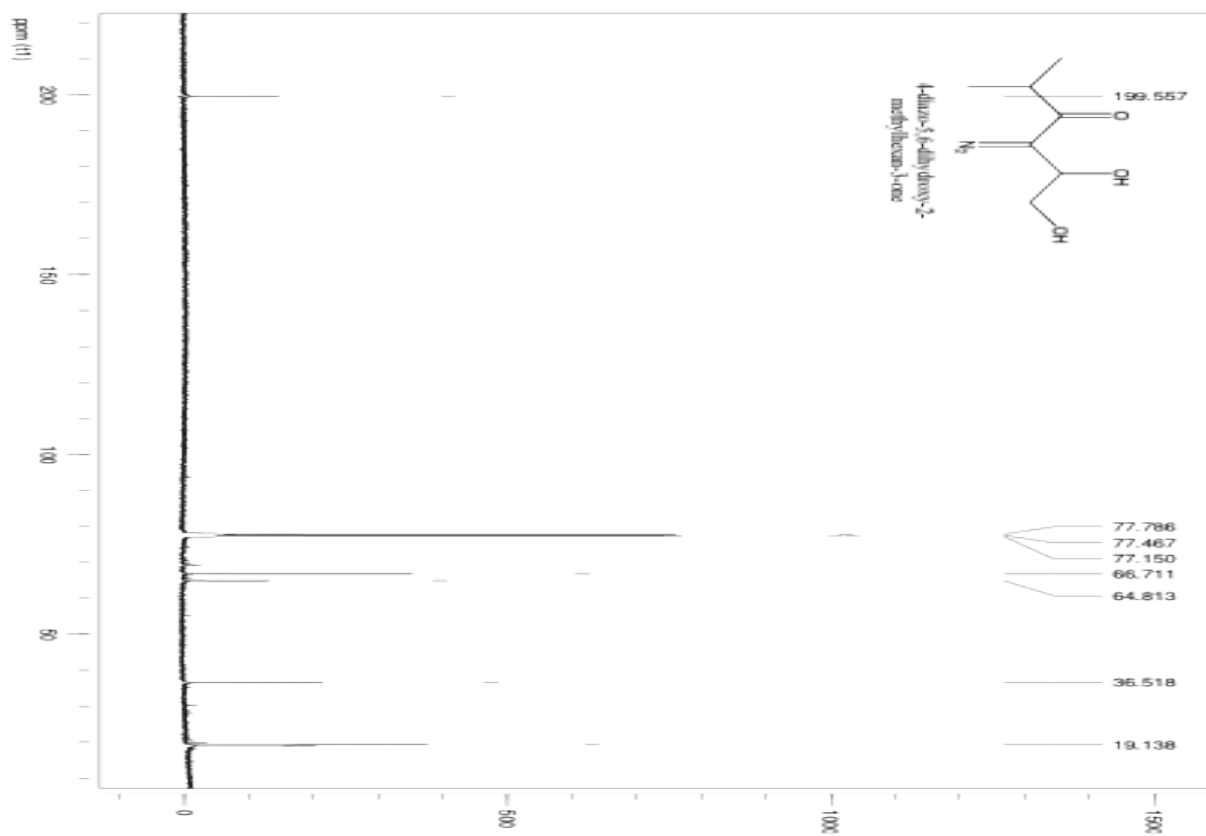
F2 - Processing parameters
SI       32768
SF       500.1300000 MHz
WDW      EM
SSB      0
LB       0.30 Hz
GB       0
PC       1.00

```

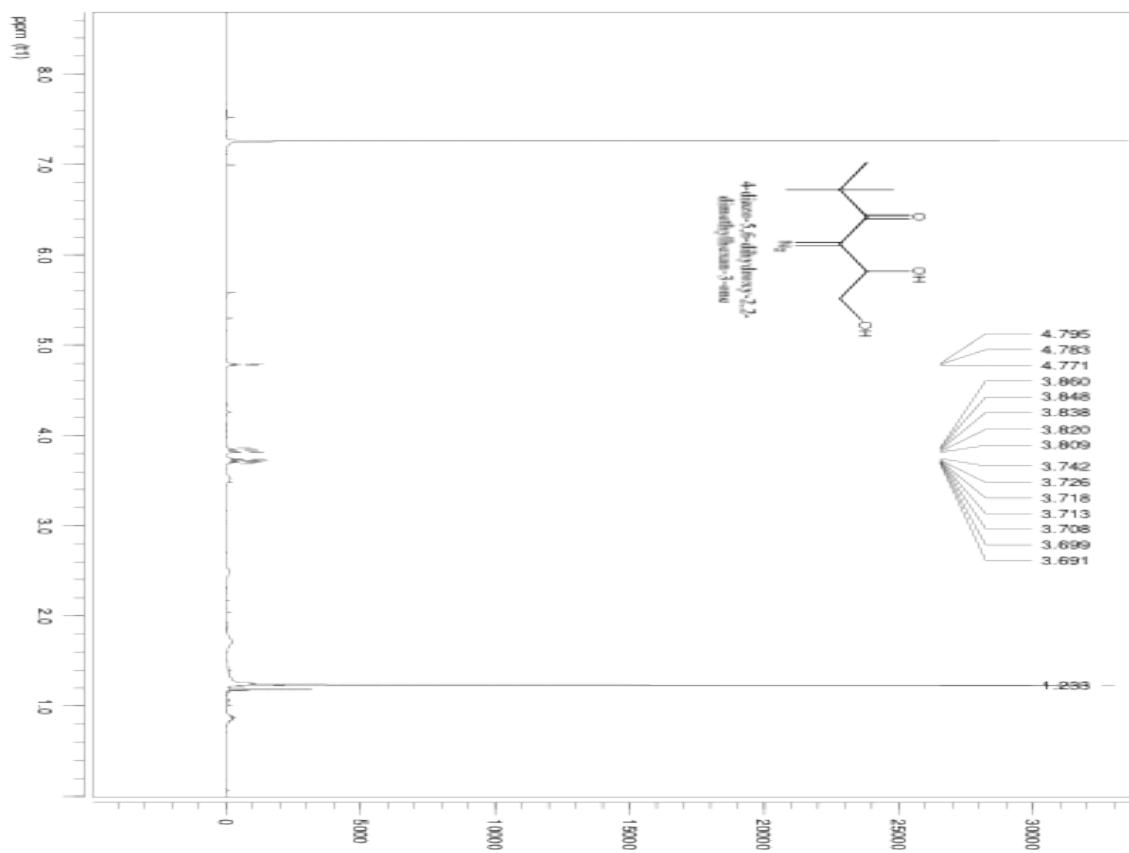


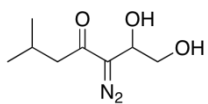
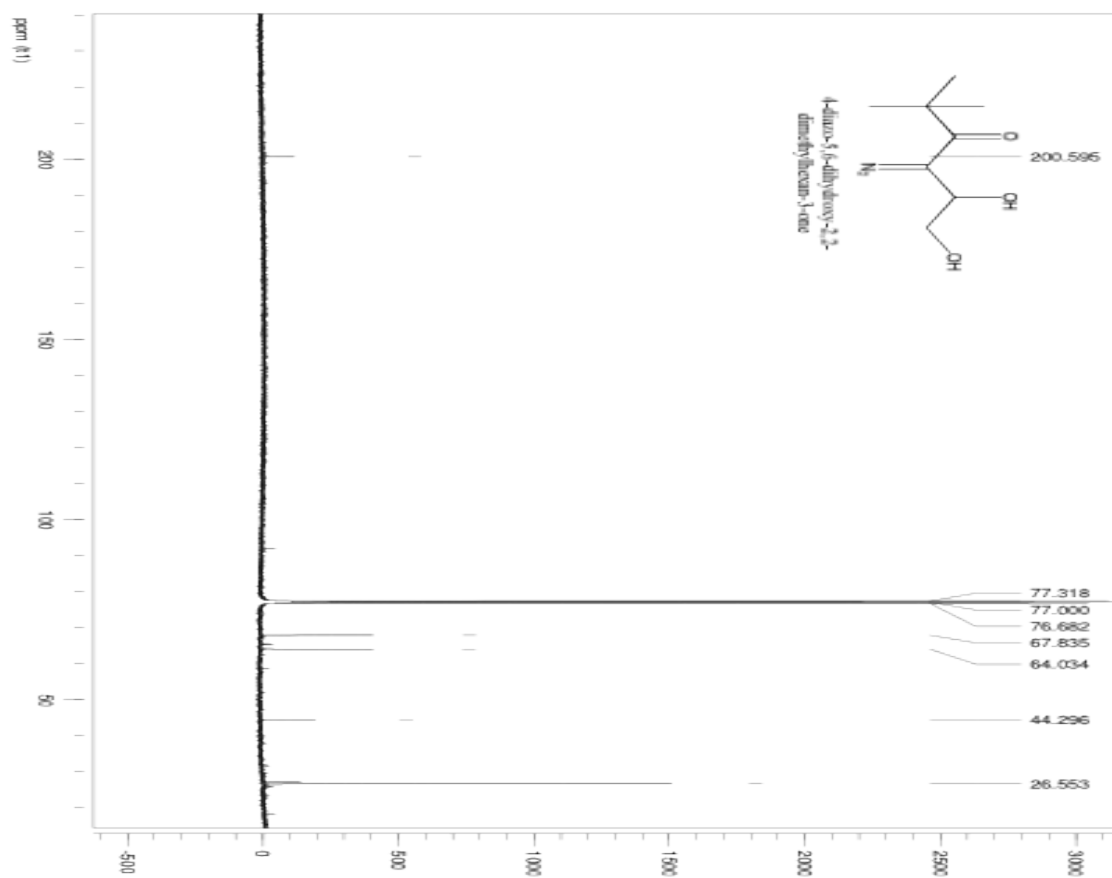
4-diazo-5,6-dihydroxy-2-methylhexan-3-one (S8):





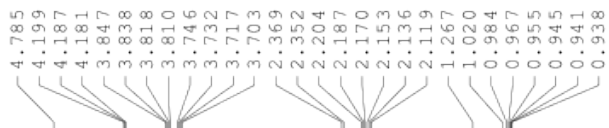
4-diazo-5,6-dihydroxy-2,2-dimethylhexan-3-one (S9):





3-diazo-1,2-dihydroxy-6-methylheptan-4-one (S10):

User Name smith
 Group sintim
 Sample Label isobutyl_diol

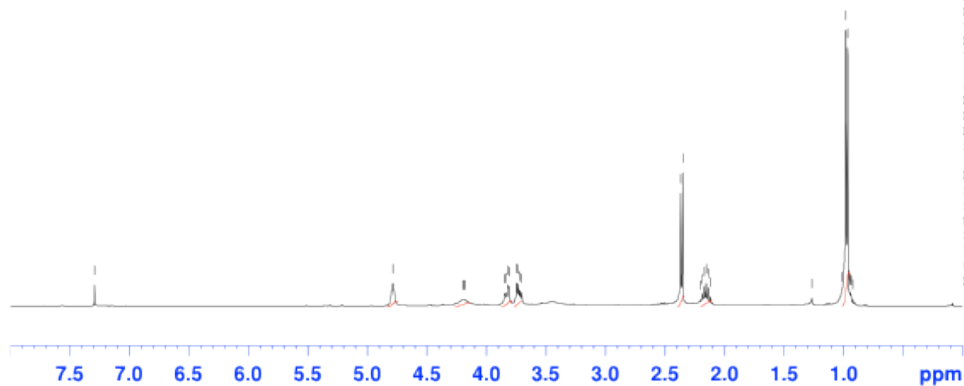


Current Data Parameters
 NAME 9-smith-0813
 EXPNO 10
 PROCNO 1

F2 - Acquisition Parameters
 Date_ 20090813
 Time 15.37
 INSTRUM spect
 PROBHD 5 mm QNP 1H/1
 PULPROG zg30
 TD 65536
 SOLVENT CDCl3
 NS 16
 DS 4
 SWH 8223.685 Hz
 FIDRES 0.125483 Hz
 AQ 3.9846387 sec
 RG 90.5
 DW 60.800 usec
 DE 6.00 usec
 TE 294.9 K
 D1 1.00000000 sec
 TD0 1

===== CHANNEL f1 =====
 NUC1 1H
 P1 10.00 usec
 PL1 -4.00 dB
 SFO1 399.7324685 MHz

F2 - Processing parameters
 SI 32768
 SF 399.7300000 MHz
 WDW EM
 SSB 0
 LB 0.30 Hz
 GB 0
 PC 2.00



1.00
 0.78
 1.16
 1.10
 2.22
 1.22
 6.93

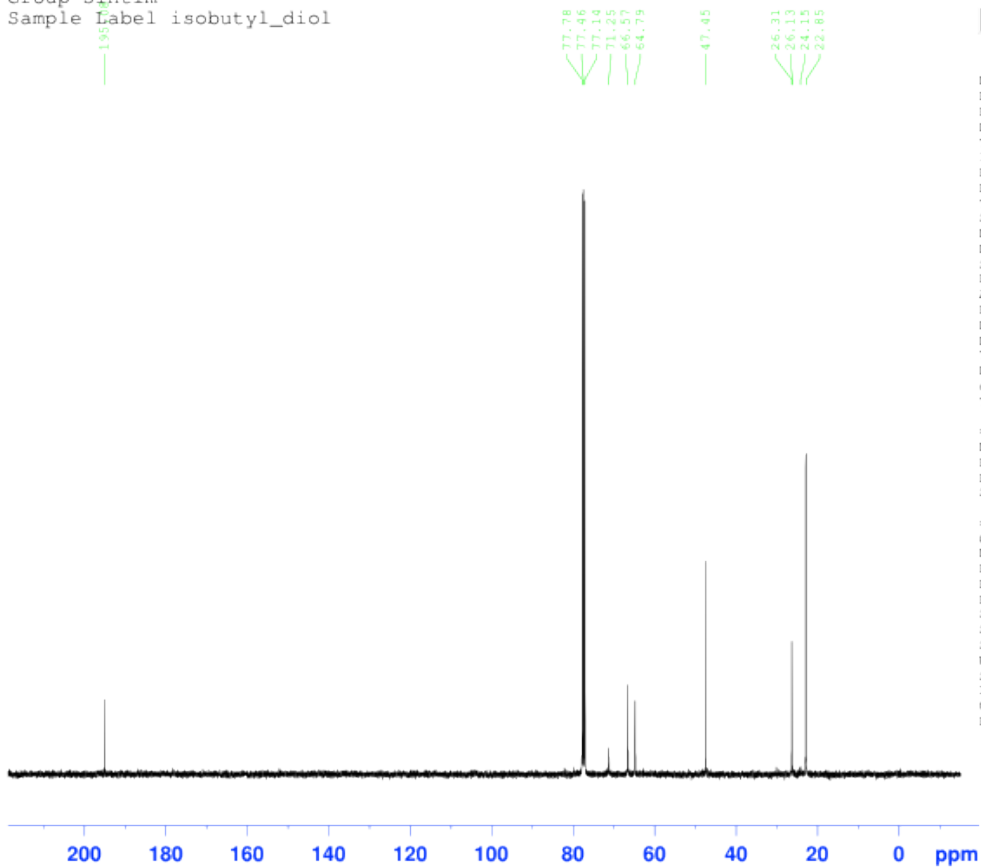
User Name smith
Group sintim
Sample Label isobutyl_diol

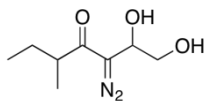


NAME 9-smith-0813
EXPNO 11
PROCNO 1
Date_ 20090813
Time 16.55
INSTRUM spect
PROBHD 5 mm QNP 1H/1
PULPROG zgdc30
TD 65536
SOLVENT CDCl3
NS 1300
DS 32
SWH 27173.912 Hz
FIDRES 0.414641 Hz
AQ 1.2059124 sec
RG 287.4
DW 18.400 usec
DE 6.00 usec
TE 295.6 K
D1 1.50000000 sec
d11 0.03000000 sec
TDO 1

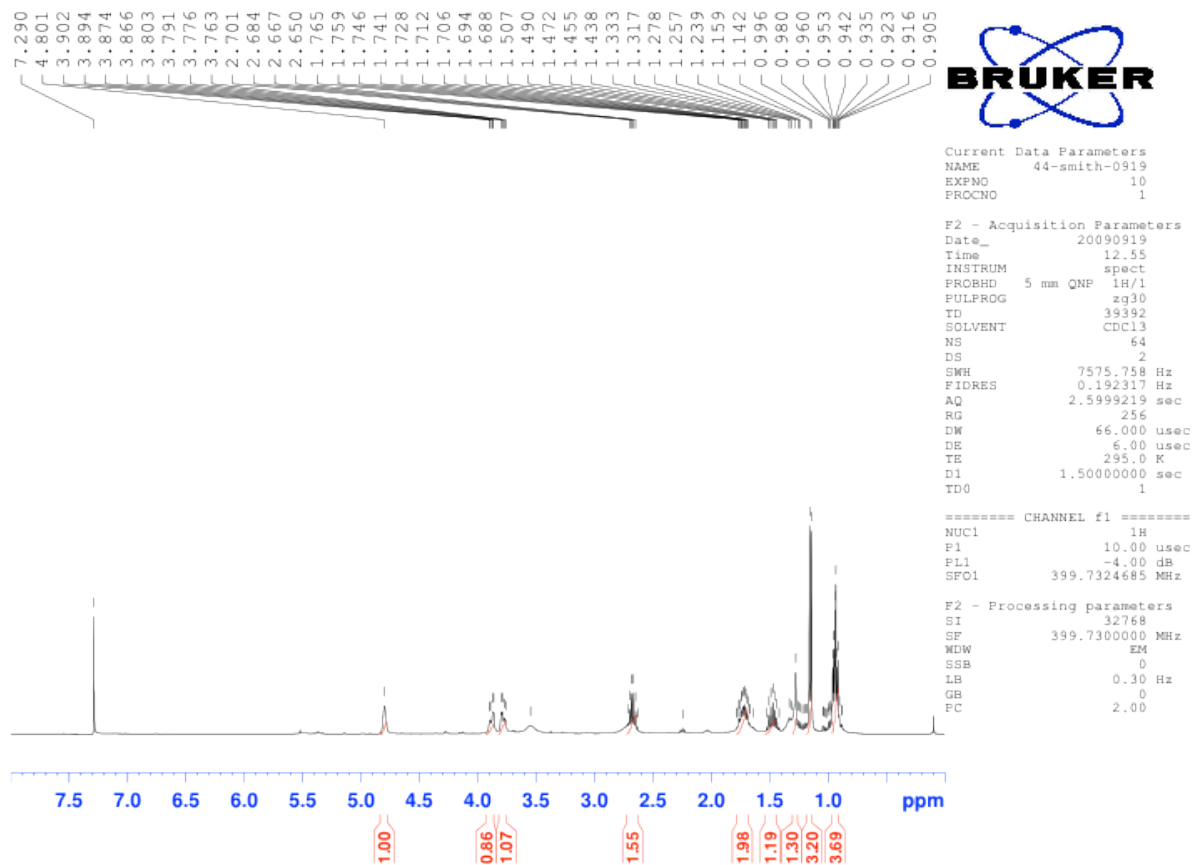
===== CHANNEL f1 =====
NUC1 13C
P1 4.50 usec
PL1 0.00 dB
SFO1 100.5242095 MHz

===== CHANNEL f2 =====
CPDPRG2 waltz16
NUC2 1H
PCPD2 89.00 usec
PL2 -4.00 dB
PL12 17.37 dB
SFO2 399.7315989 MHz
SI 32768
SF 100.5121480 MHz
WDW EM
SSB 0
LB 1.00 Hz
GB 0
PC 1.40

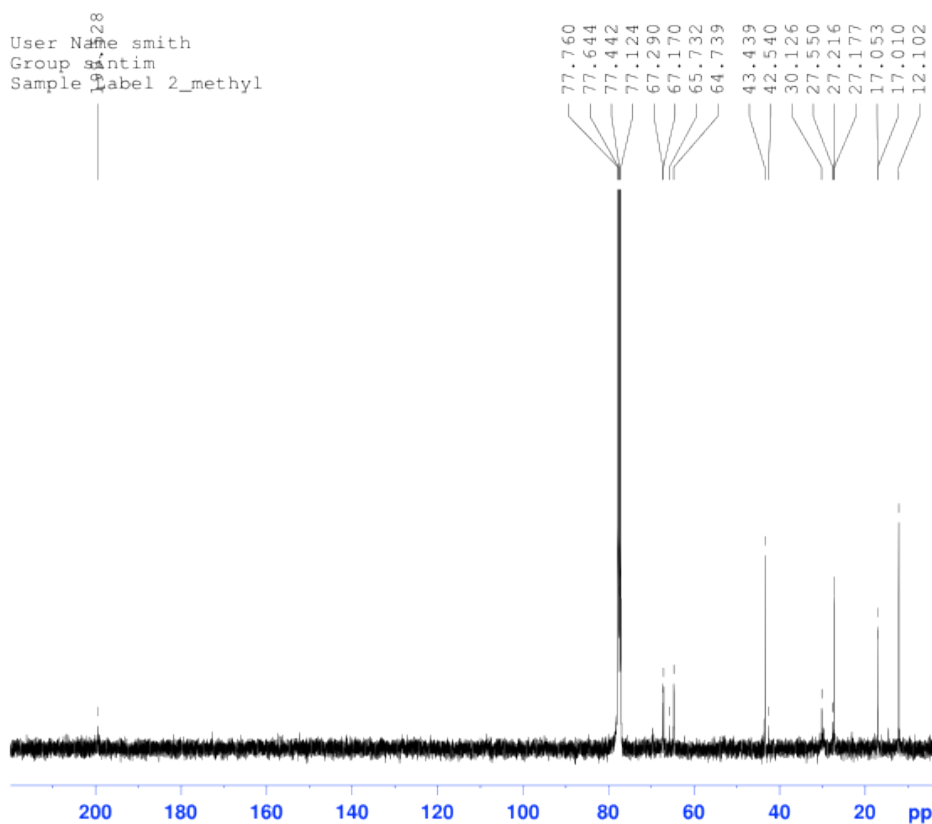




3-diazo-1,2-dihydroxy-5-methylheptan-4-one (S11):



User Name: smith
Group: Santim
Sample Label: 2_methyl



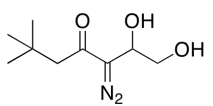
Current Data Parameters
NAME: 44-smith-0919
EXPNO: 21
PROCNO: 1

F2 - Acquisition Parameters
Date_: 20090921
Time: 20.10
INSTRUM: spect
PROBHD: 5 mm QNP 1H/1
FULPROG: zgpg30
TD: 85536
SOLVENT: CDCl3
NS: 3800
DS: 16
SWH: 27173.912 Hz
FIDRES: 0.414641 Hz
AQ: 1.2059124 sec
RG: 456.1
DW: 18.400 usec
DE: 6.00 usec
TE: 295.7 K
D1: 1.50000000 sec
d11: 0.03000000 sec
TDO: 1

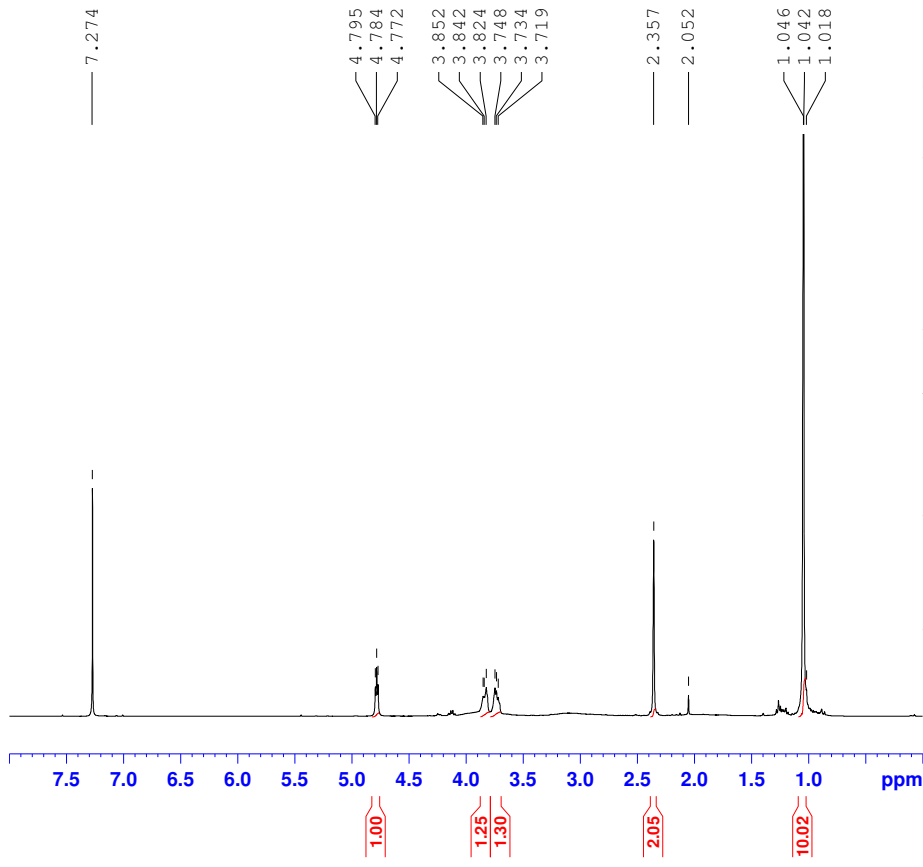
==== CHANNEL f1 =====
NUC1: 13C
P1: 4.50 usec
PL1: 0.00 dB
SFO1: 100.5242095 MHz

==== CHANNEL f2 =====
CFDPRG2: waltz16
NUC2: 1H
PCPD2: 89.00 usec
PL2: -4.00 dB
PL12: 17.37 dB
SFO2: 399.7315989 MHz

F2 - Processing parameters
SI: 32768
SF: 100.5121480 MHz
WDM: EM
SSB: 0
LB: 1.00 Hz
GB: 0
PC: 1.40



3-diazo-1,2-dihydroxy-6,6-dimethylheptan-4-one



```

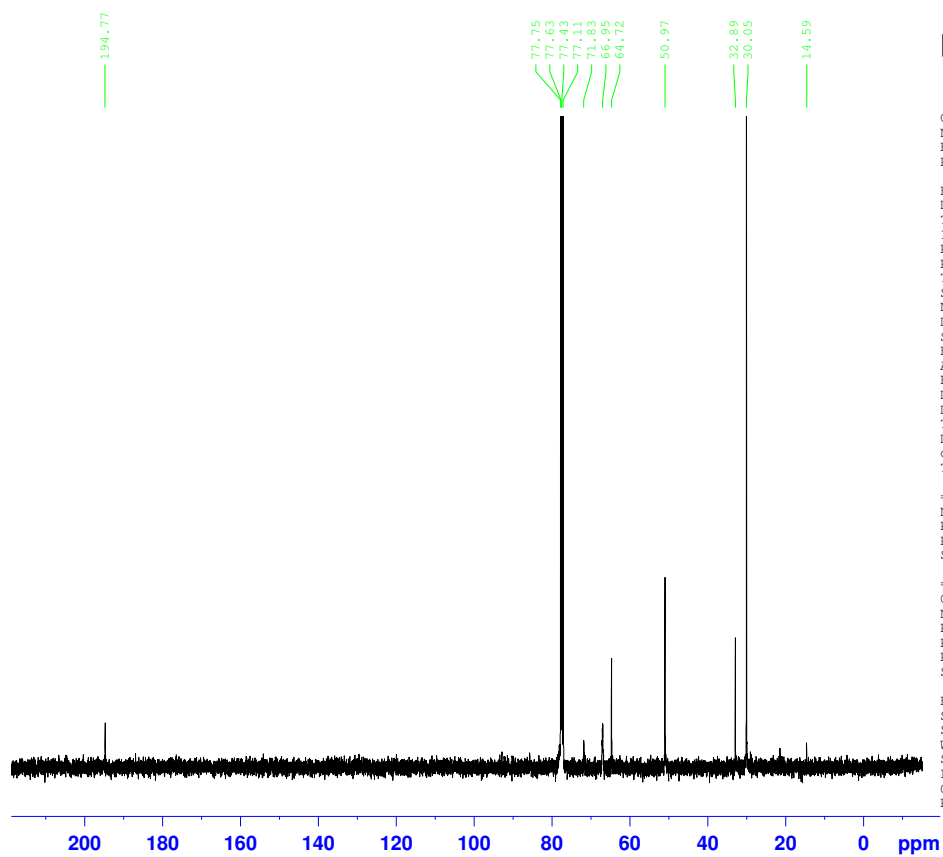
Current Data Parameters
NAME      33-smith-1021
EXPNO     10
PROCNO    1

F2 - Acquisition Parameters
Date_     20091021
Time      14.57
INSTRUM   spect
PROBHD    5 mm QNP 1H/1
PULPROG   zg30
TD         39392
SOLVENT   CDCl3
NS         64
DS         2
SWH        7575.758 Hz
FIDRES     0.192317 Hz
AQ         2.5999219 sec
RG         128
DW         66.000 usec
DE         6.00 usec
TE         295.4 K
D1         1.50000000 sec
TD0        1

===== CHANNEL f1 =====
NUC1       1H
P1         10.00 usec
PL1        -4.00 dB
SFO1       399.7324685 MHz

F2 - Processing parameters
SI         32768
SF         399.7300000 MHz
WDW        EM
SSB        0
LB         0.30 Hz
GB         0
PC         2.00

```

```

Current Data Parameters
NAME      33-smith-1021
EXPNO    20
PROCNO   1

F2 - Acquisition Parameters
Date_    20091021
Time     17.50
INSTRUM  spect
PROBHD   5 mm QNP 1H/1
PULPROG  zgpg30
TD       65536
SOLVENT  CDCl3
NS       1300
DS       32
SWH      27173.912 Hz
FIDRES   0.414641 Hz
AQ       1.2059124 sec
RG       362
DW       18.400 usec
DE       6.00 usec
TE       296.1 K
D1       1.50000000 sec
d11      0.03000000 sec
TD0      1

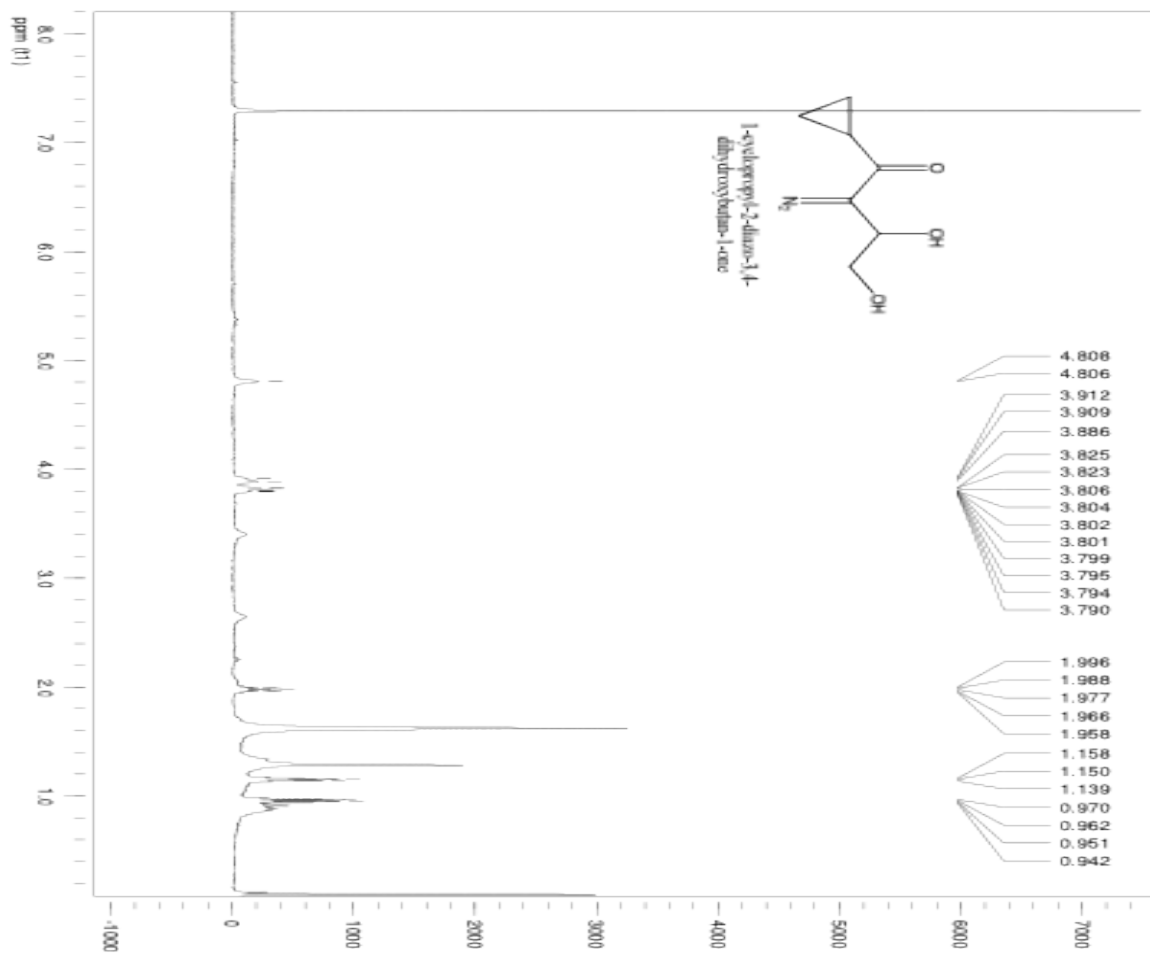
===== CHANNEL f1 =====
NUC1     13C
P1       4.50 usec
PL1      0.00 dB
SFO1     100.5242095 MHz

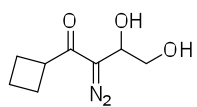
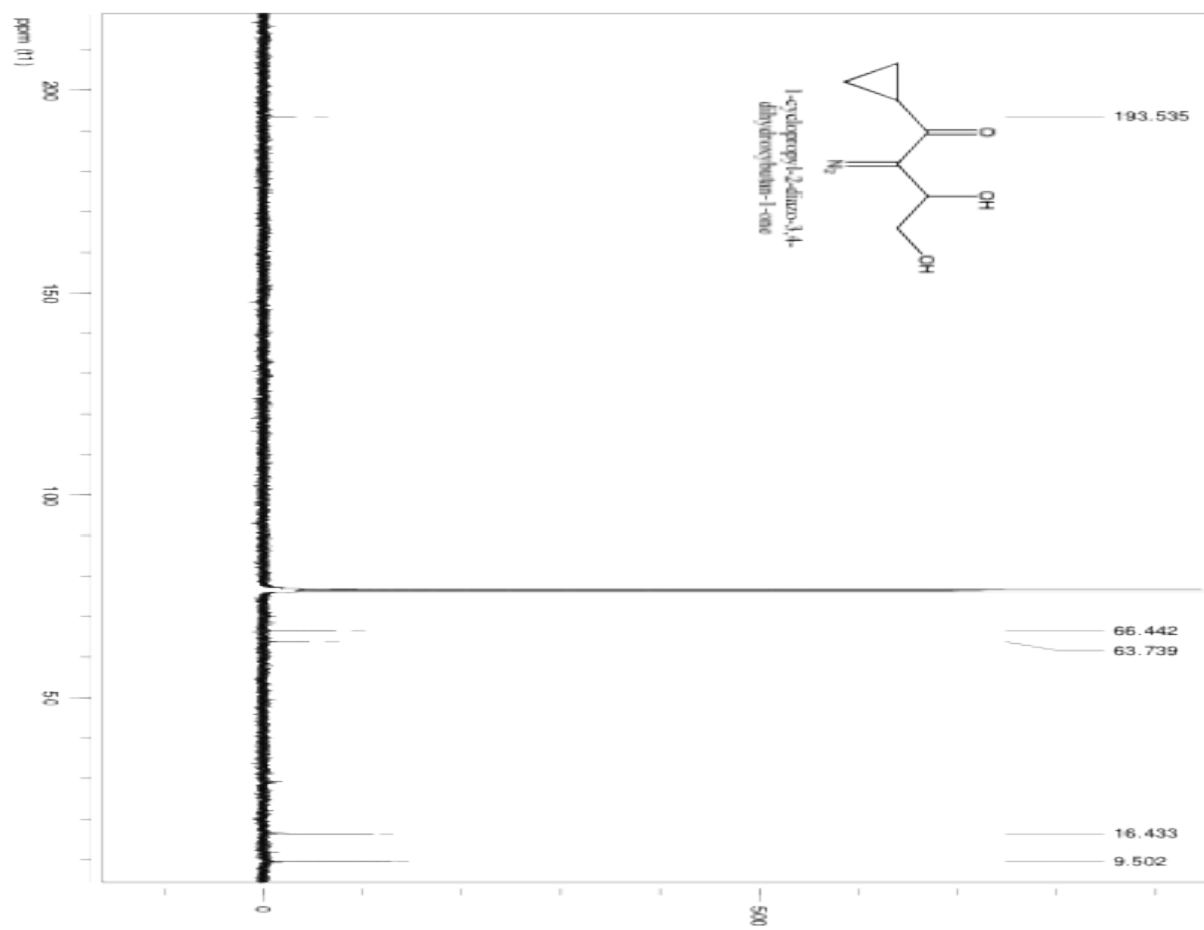
===== CHANNEL f2 =====
CPDPRG2  waltz16
NUC2     1H
PCPD2    89.00 usec
PL2      -4.00 dB
PL12     17.37 dB
SFO2     399.7315989 MHz

F2 - Processing parameters
SI       32768
SF       100.5121480 MHz
WDW      EM
SSB      0
LB       1.00 Hz
GB       0
PC       1.40

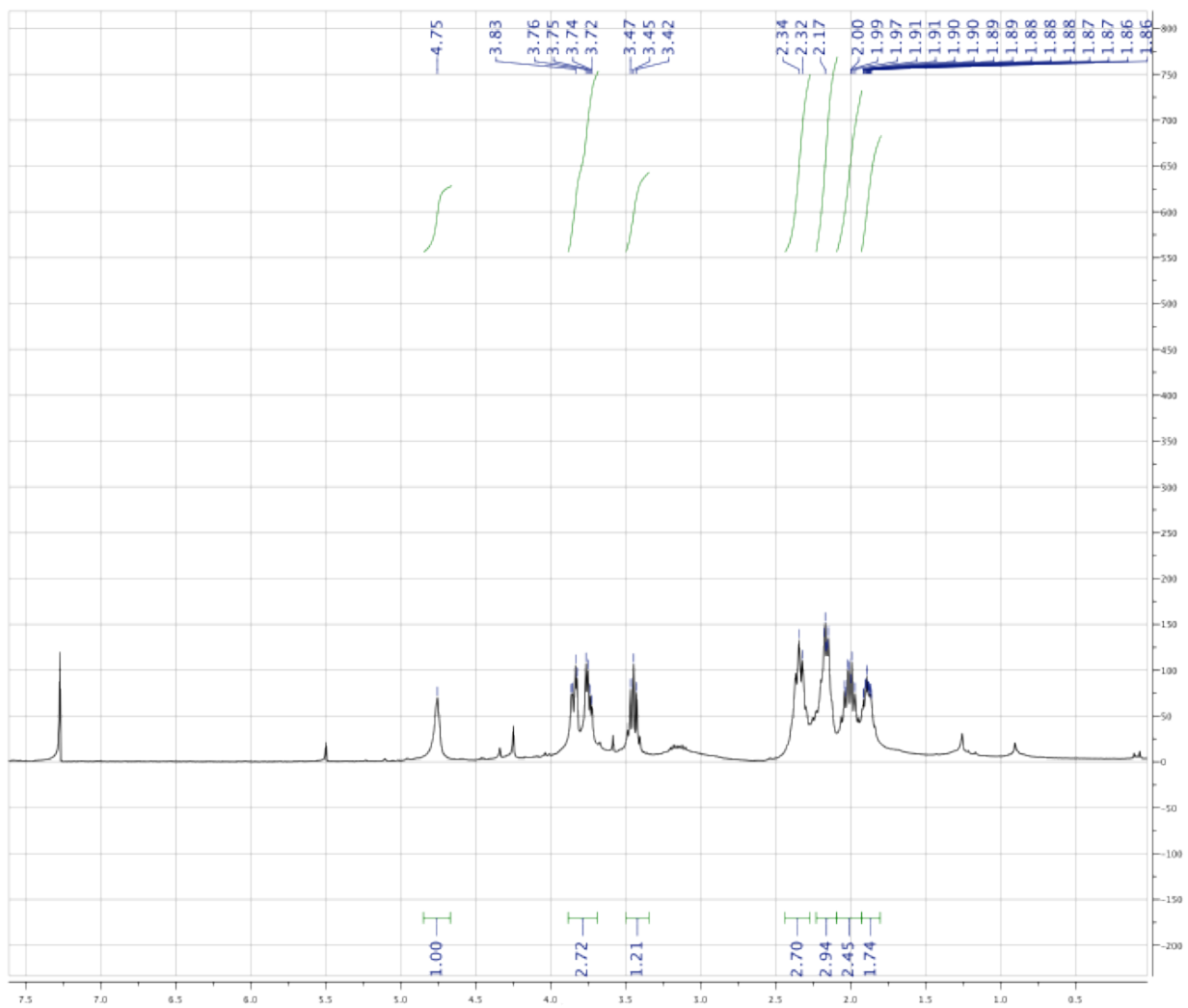
```

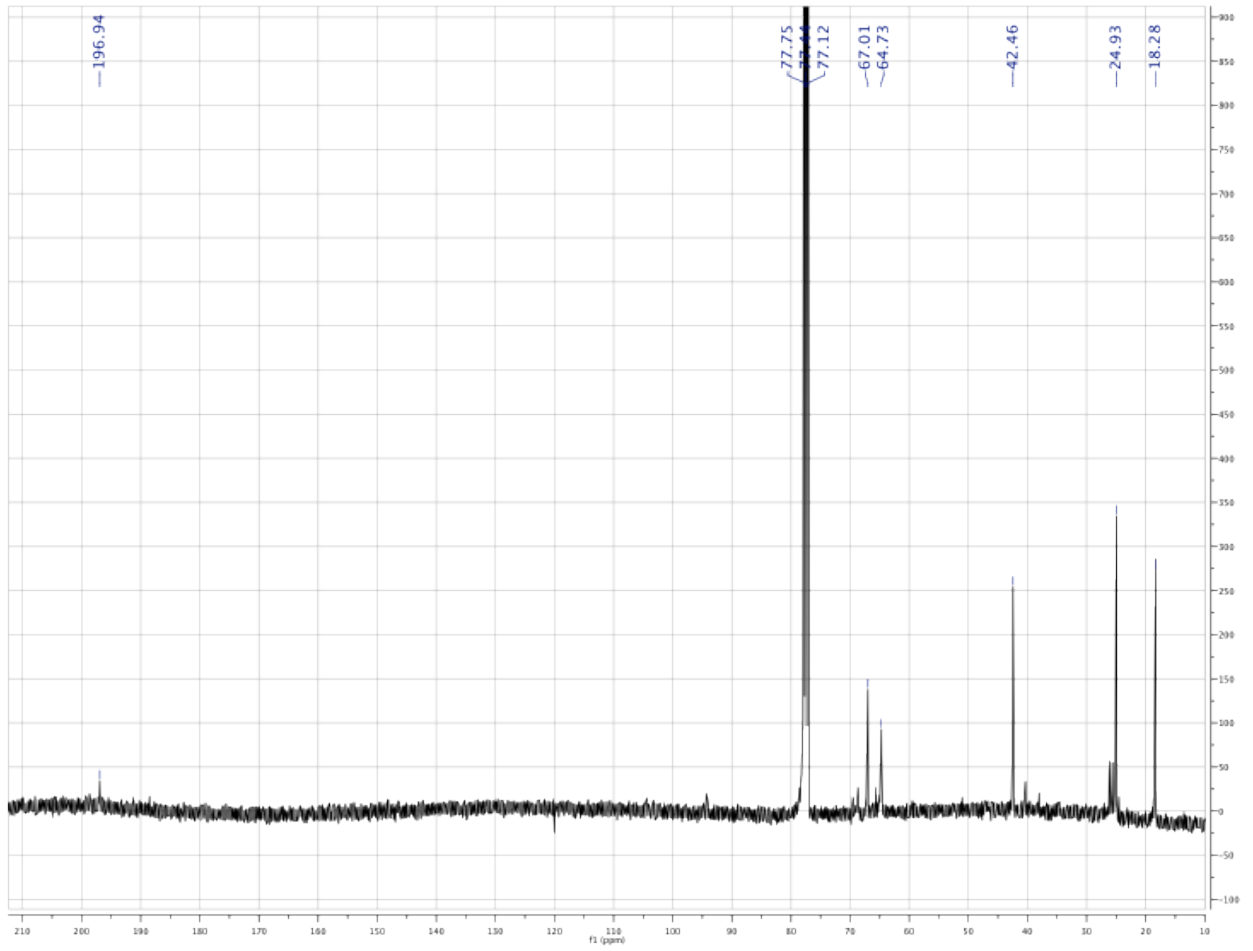
1-cyclopropyl-2-diazo-3,4-dihydroxybutan-1-one (S13):

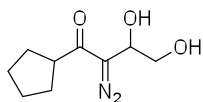




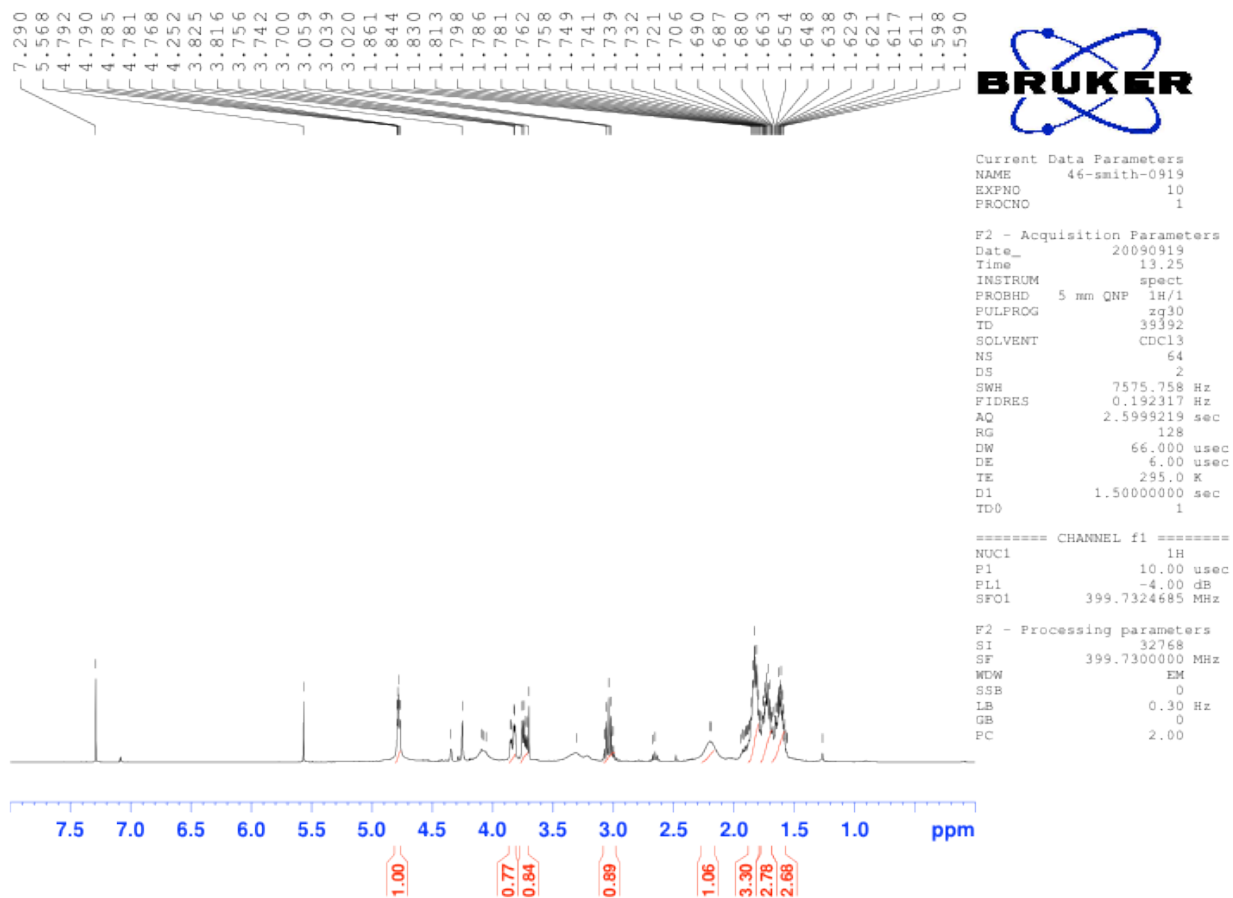
1-cyclobutyl-2-diazo-3,4-dihydroxybutan-1-one (S14):







1-cyclopentyl-2-diazo-3,4-dihydroxybutan-1-one (S15):



198.621

94.862
77.778
77.662
77.460
77.142
69.455
66.826
65.552
64.766
53.006
52.549
47.159
46.309
31.899
31.070
29.916
28.894
26.558
26.312
25.410



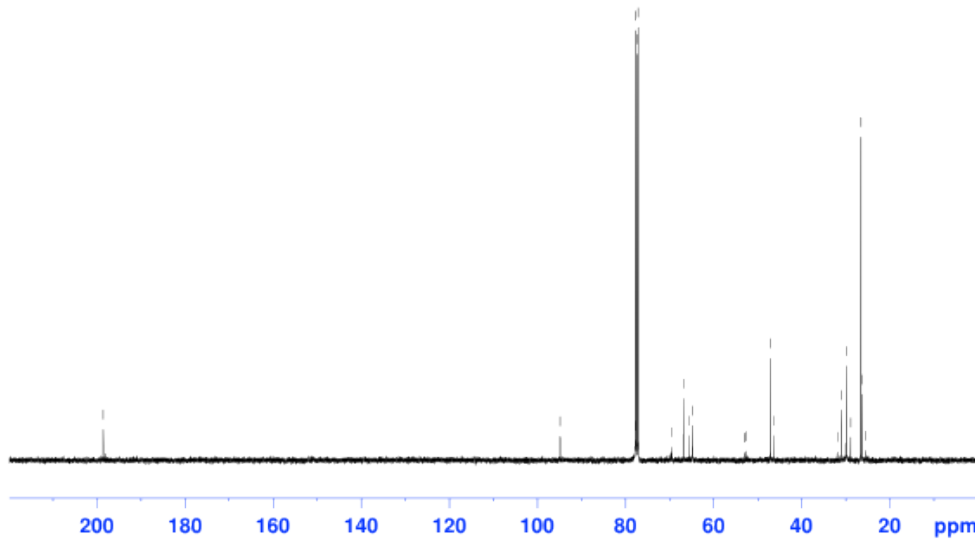
Current Data Parameters
NAME 46-smith-0919
EXPNO 11
PROCNO 1

F2 - Acquisition Parameters
Date_ 20090919
Time 14.00
INSTRUM spect
PROBHD 5 mm QNP 1H/1
PULPROG zgdc30
TD 65536
SOLVENT CDCl3
NS 900
DS 4
SWH 27173.912 Hz
FIDRES 0.414641 Hz
AQ 1.2059124 sec
RG 128
DW 18.400 usec
DE 6.00 usec
TE 295.7 K
D1 1.00000000 sec
d11 0.03000000 sec
TD0 1

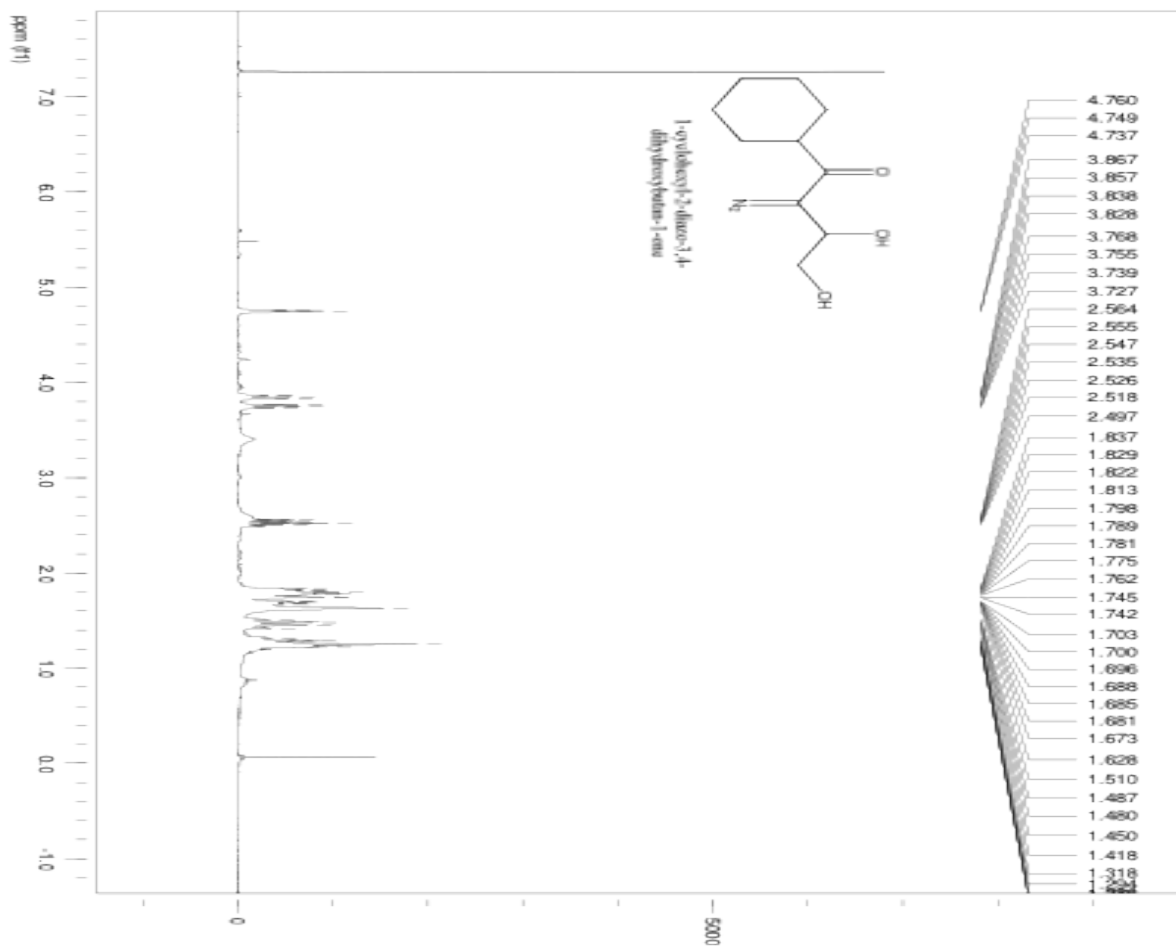
===== CHANNEL f1 =====
NUC1 13C
P1 4.50 usec
PL1 0.00 dB
SFO1 100.5242095 MHz

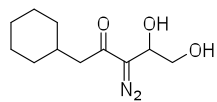
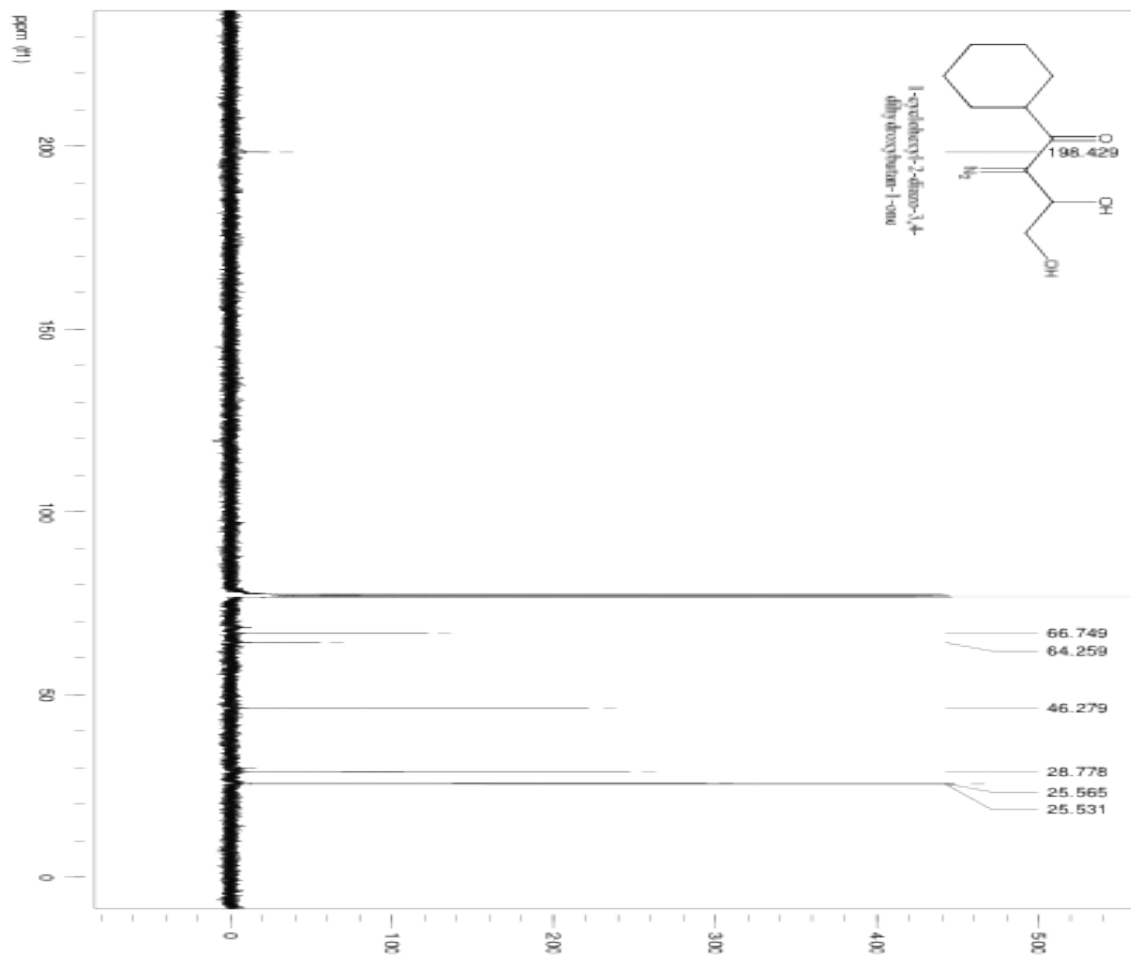
===== CHANNEL f2 =====
CPDPRG2 waltz16
NUC2 1H
PCPD2 89.00 usec
PL2 -4.00 dB
PL12 17.37 dB
SFO2 399.7315989 MHz

F2 - Processing parameters
SI 32768
SF 100.5121480 MHz
WDW EM
SSB 0
LB 1.00 Hz
GB 0
PC 1.40

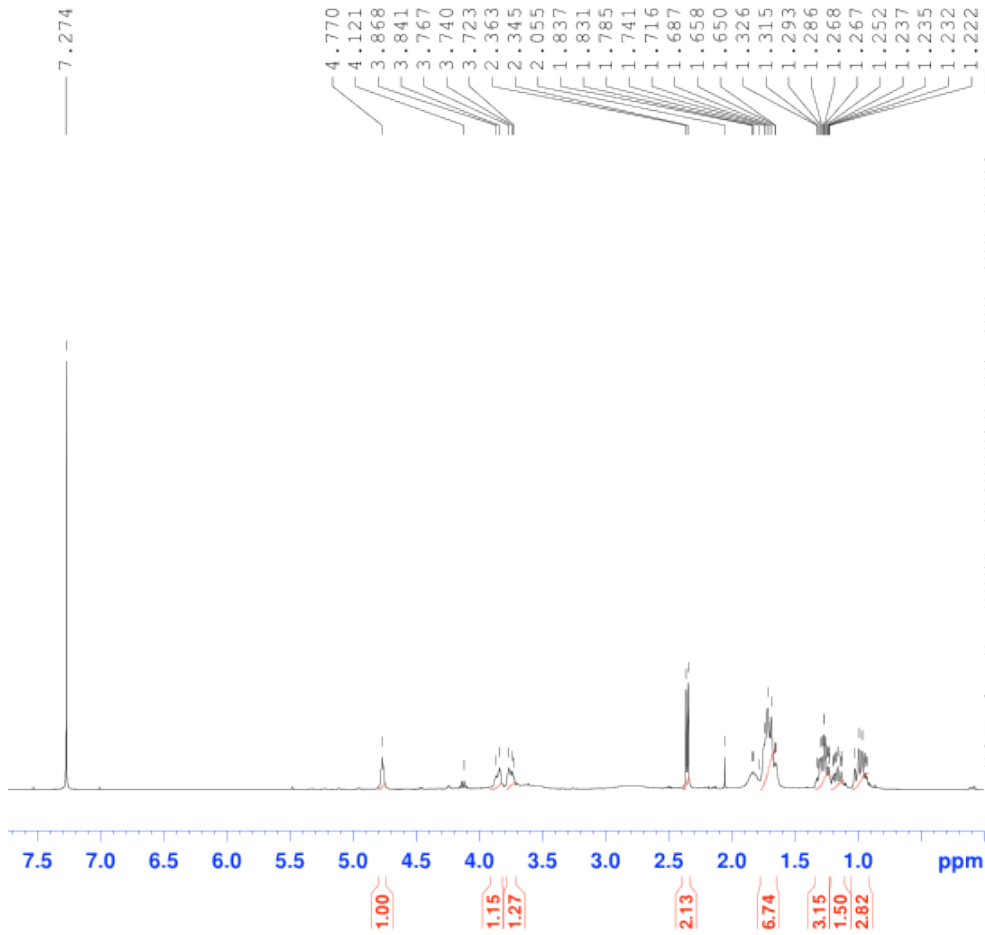


1-cyclohexyl-2-diazo-3,4-dihydroxybutan-1-one (S16):





1-cyclohexyl-3-diazo-4,5-dihydroxypentan-2-one (S17):

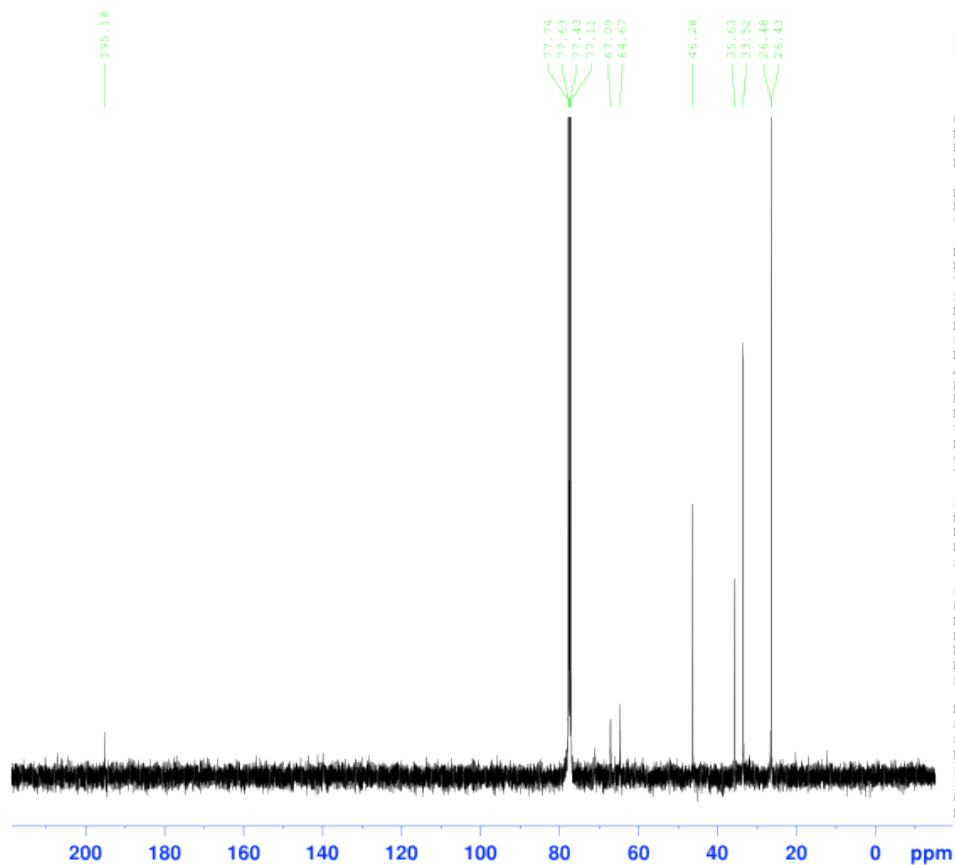


Current Data Parameters
 NAME 24-smith-1021
 EXPNO 10
 PROCNO 1

F2 - Acquisition Parameters
 Date_ 20091022
 Time 7.56
 INSTRUM spect
 PROBHD 5 mm QNP 1H/1
 PULPROG zg30
 TD 39392
 SOLVENT CDCl3
 NS 64
 DS 2
 SMH 7575.758 Hz
 FIDRES 0.192317 Hz
 AQ 2.5999219 sec
 RG 181
 DW 66.000 usec
 DE 6.00 usec
 TE 295.4 K
 D1 1.50000000 sec
 TD0 1

===== CHANNEL f1 =====
 NUC1 1H
 P1 10.00 usec
 PL1 -4.00 dB
 SFO1 399.7324685 MHz

F2 - Processing parameters
 SI 32768
 SF 399.7300000 MHz
 WDW EM
 SSB 0
 LB 0.30 Hz
 GB 0
 PC 2.00



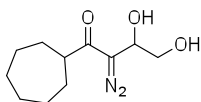
Current Data Parameters
NAME 24-smith-1021
EXPNO 11
PROCNO 1

F2 - Acquisition Parameters
Date_ 20091022
Time 8.59
INSTRUM spect
PROBHD 5 mm QNP 1H/1
PULPROG zgpg30
TD 65536
SOLVENT CDCl3
NS 1300
DS 32
SWH 27173.912 Hz
FIDRES 0.414641 Hz
AQ 1.2059124 sec
RG 645.1
DW 18.400 usec
DE 6.00 usec
TE 295.9 K
D1 1.5000000 sec
d11 0.0300000 sec
TD0 1

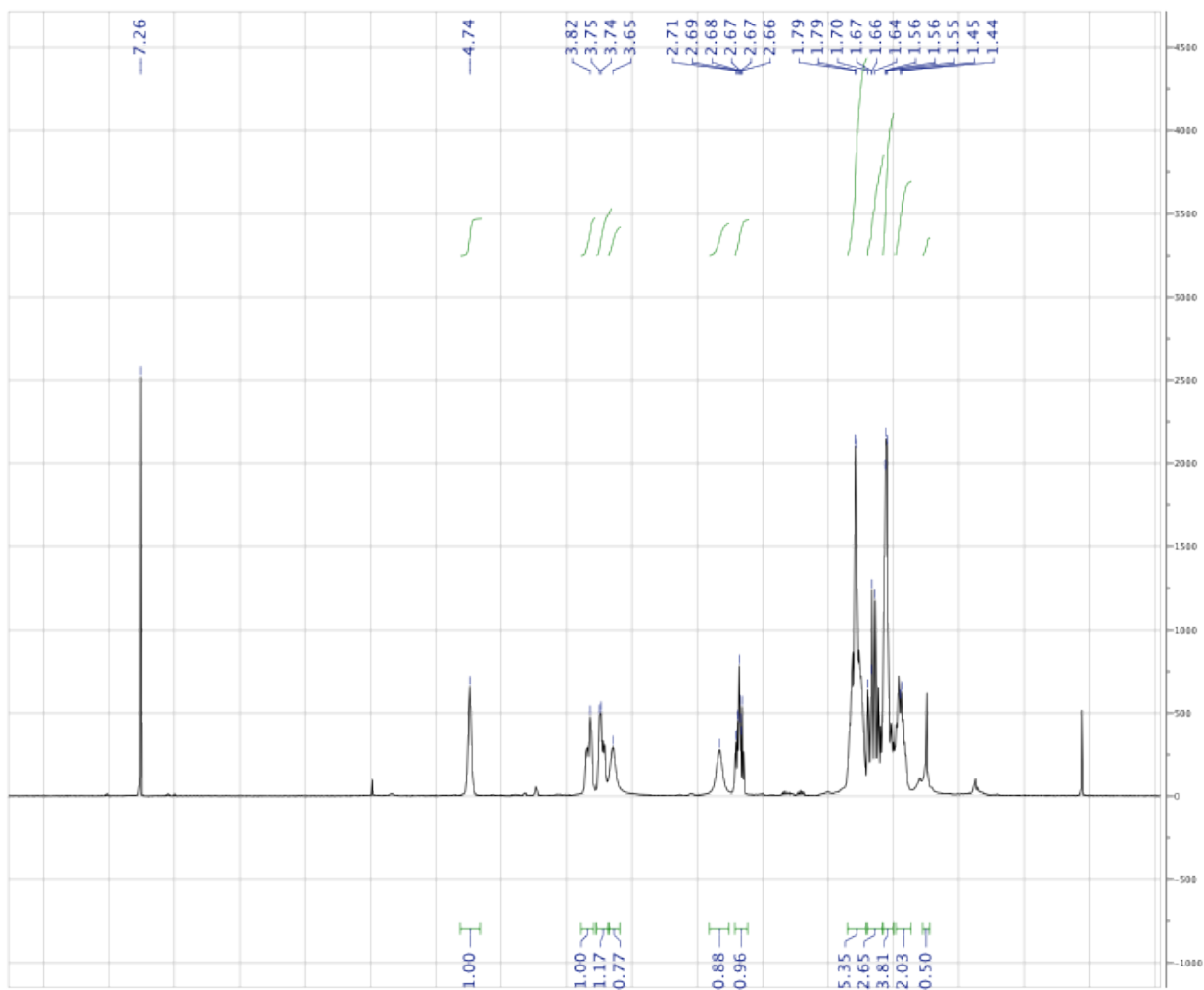
==== CHANNEL f1 =====
NUC1 13C
P1 4.50 usec
PL1 0.00 dB
SFO1 100.5242095 MHz

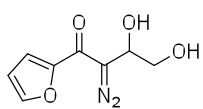
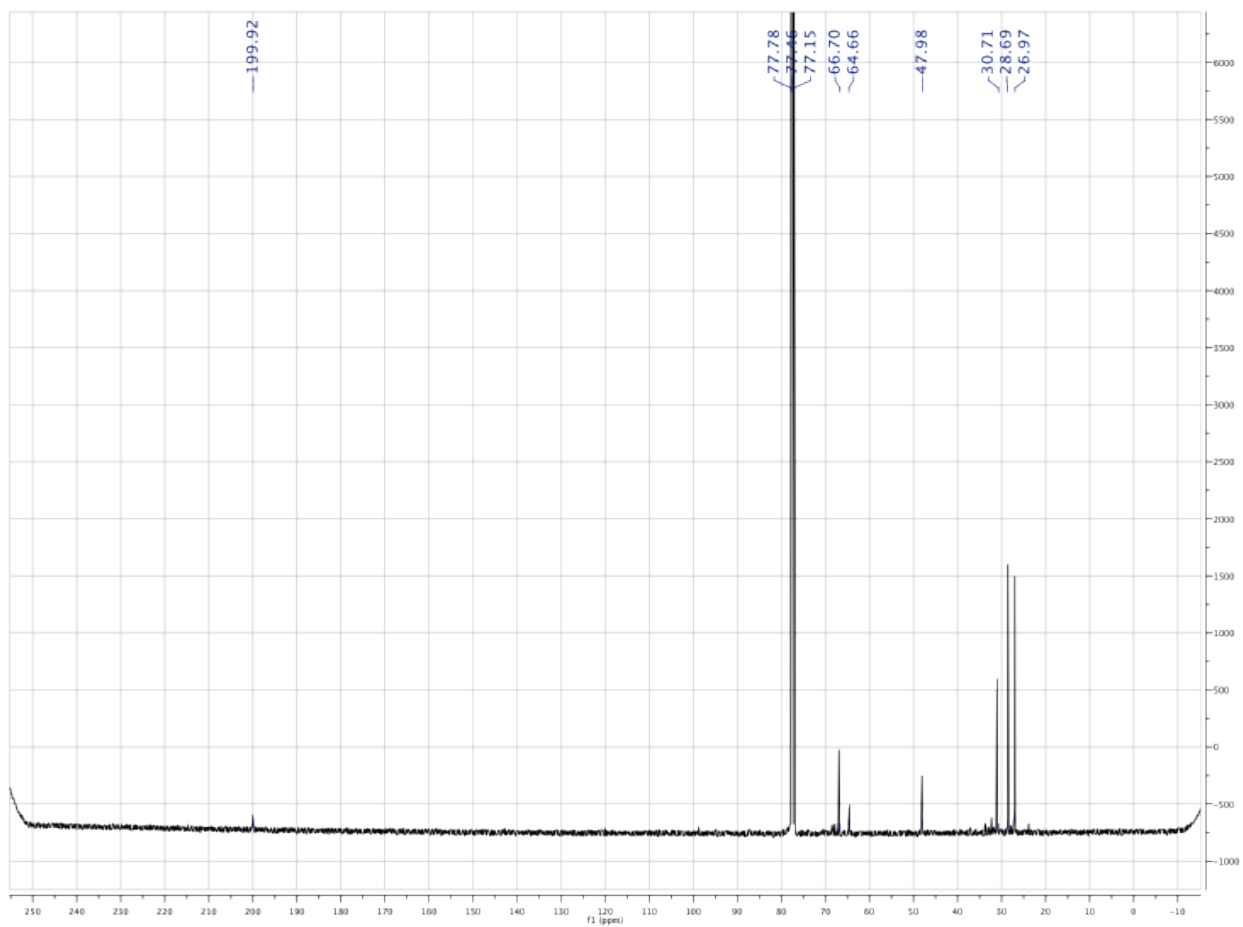
==== CHANNEL f2 =====
CPDPRG2 waltz16
NUC2 1H
PCPD2 89.00 usec
PL2 -4.00 dB
PL12 17.37 dB
SFO2 399.7315989 MHz

F2 - Processing parameters
SI 32768
SF 100.5121480 MHz
WDW EM
SSB 0
LB 1.00 Hz
GB 0
PC 1.40

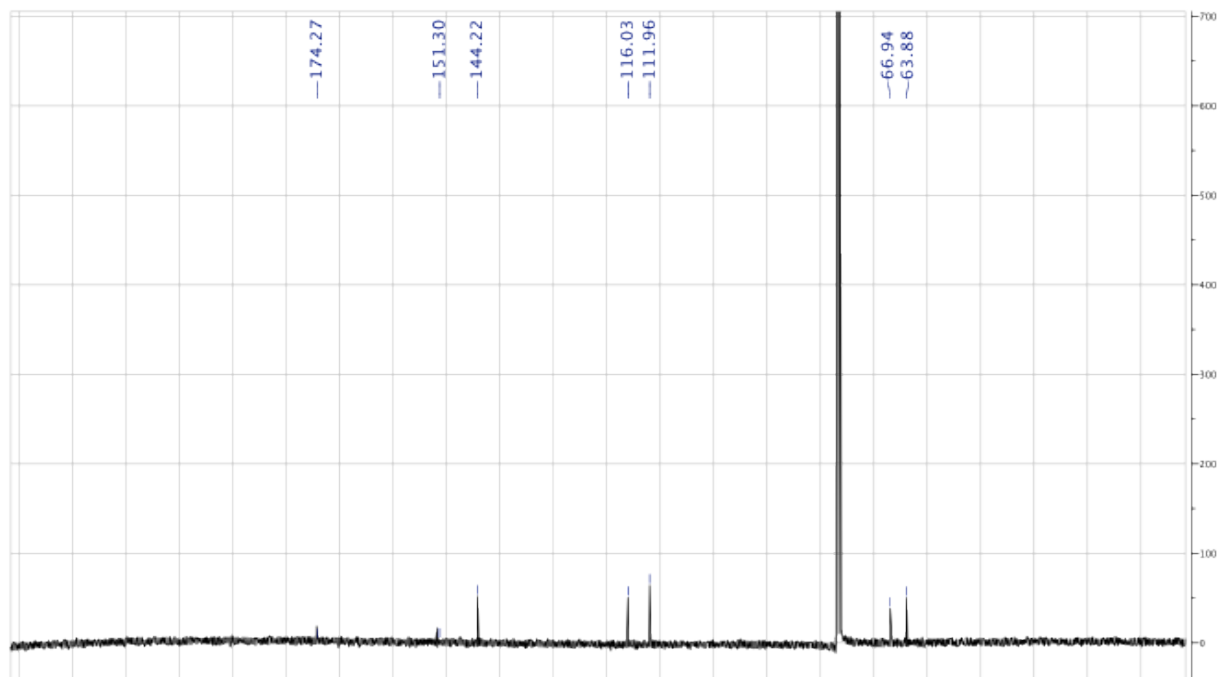
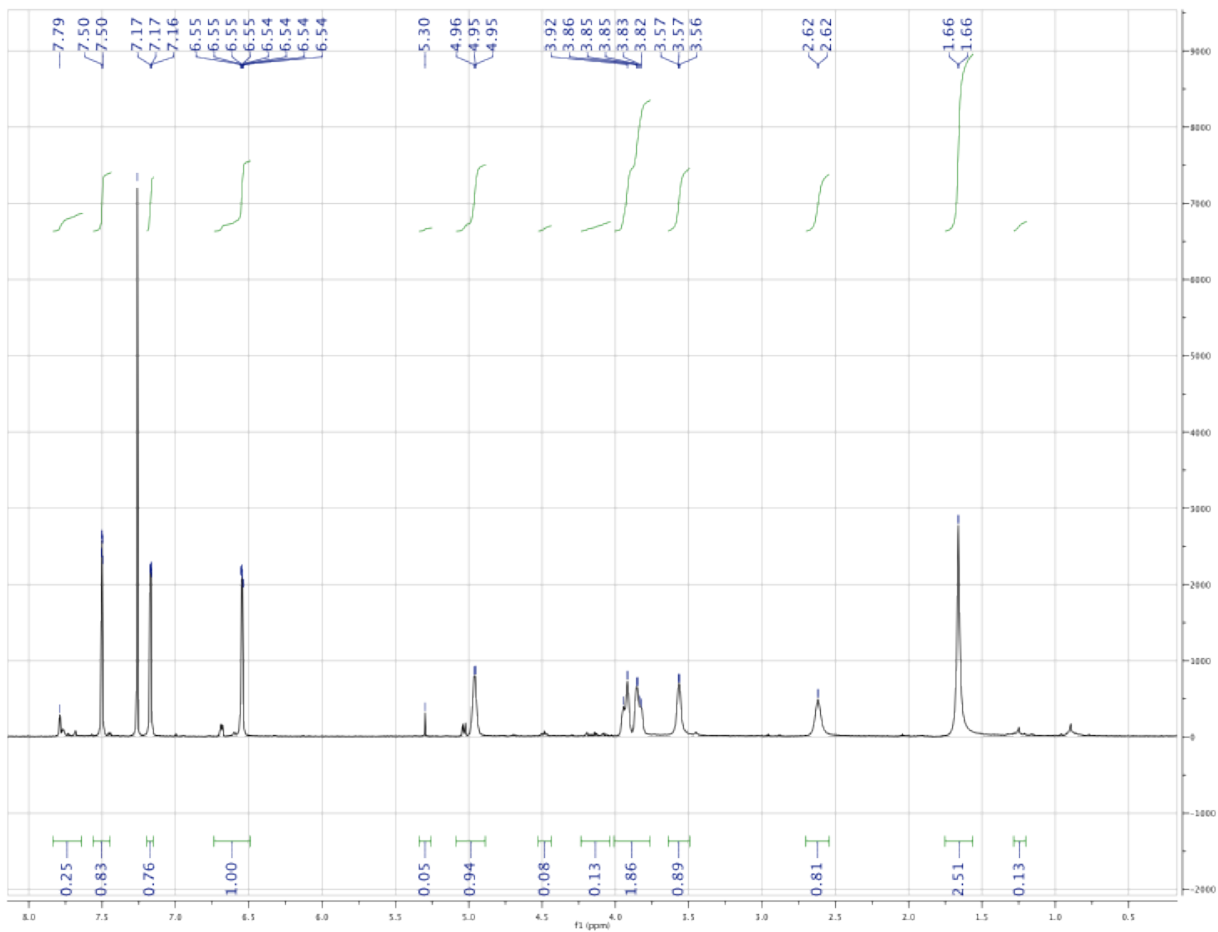


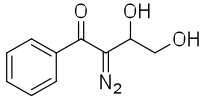
1-cycloheptyl-2-diazo-3,4-dihydroxybutan-1-one (S18):



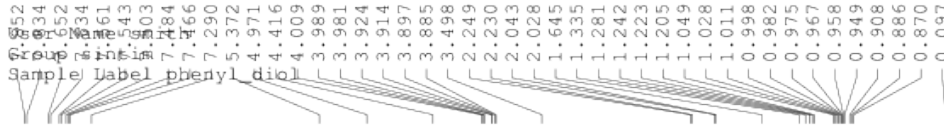


2-diazo-1-(furan-2-yl)-3,4-dihydroxybutan-1-one (S19):





2-diazo-3,4-dihydroxy-1-phenylbutan-1-one (S20):



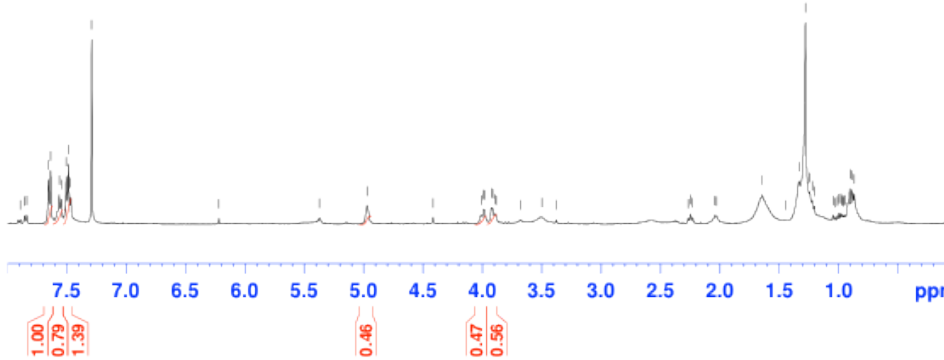
```

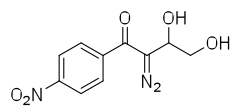
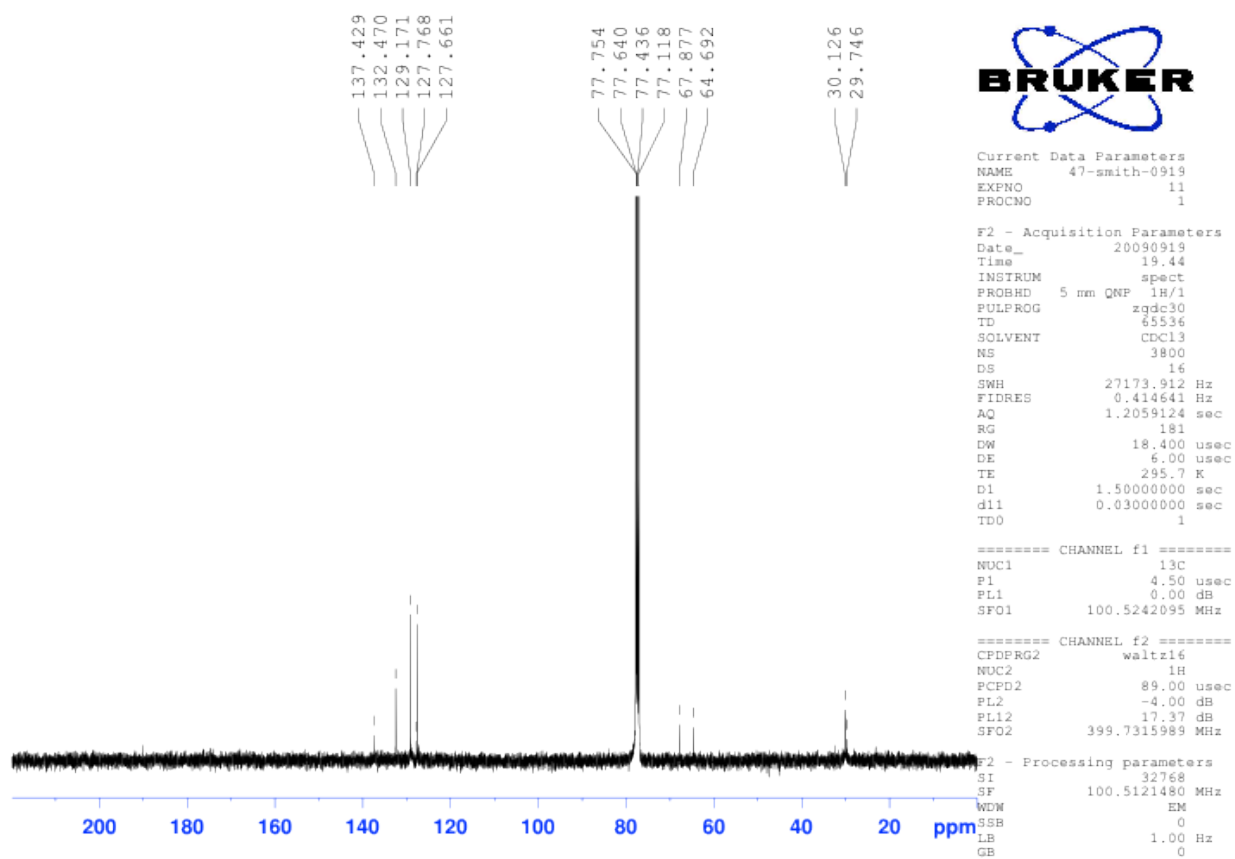
Current Data Parameters
NAME      47-smith-0919
EXPNO     10
PROCNO    1

F2 - Acquisition Parameters
Date_     20090919
Time      16.47
INSTRUM   spect
PROBHD    5 mm QNP 1H/1
PULPROG   zg30
TD         39392
SOLVENT   CDCl3
NS         64
DS         2
SWH        7575.758 Hz
FIDRES     0.192317 Hz
AQ         2.5999219 sec
RG         362
DW         66.000 usec
DE         6.00 usec
TE         295.2 K
D1         1.5000000 sec
TD0        1

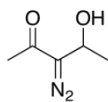
===== CHANNEL f1 =====
NUC1       1H
P1         10.00 usec
PL1        -4.00 dB
SFO1       399.7324685 MHz

F2 - Processing parameters
SI         32768
SF         399.7300000 MHz
WDW        EM
SSB        0
LB         0.30 Hz
GB         0
PC         2.00
  
```

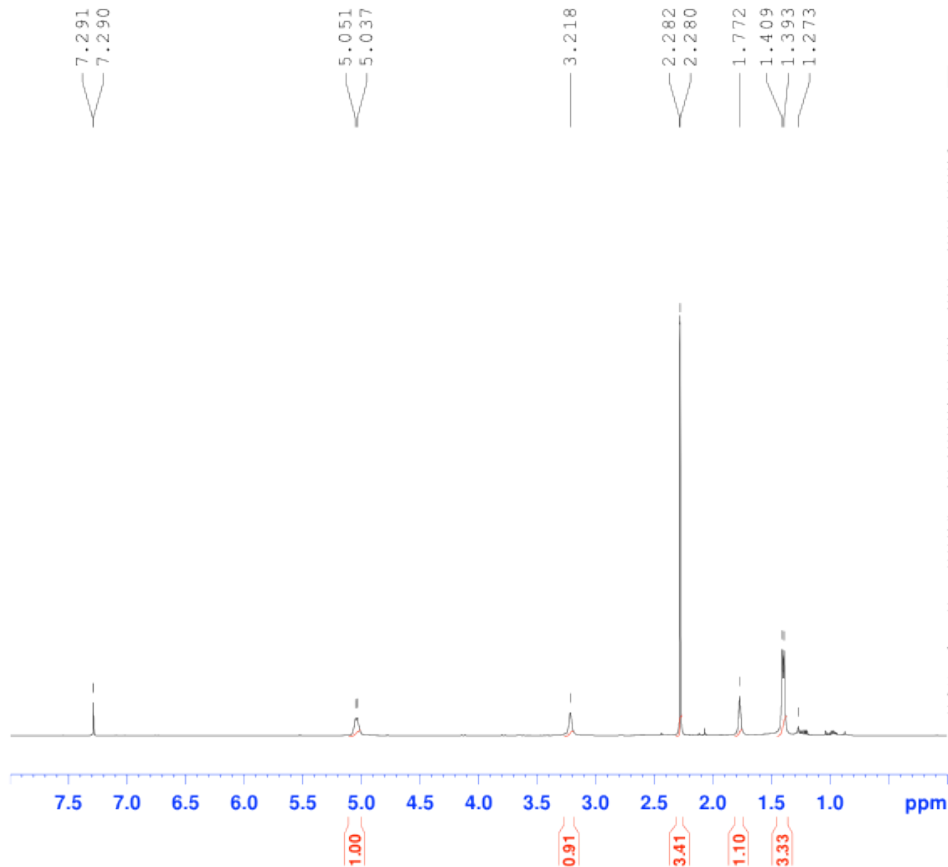




2-diazo-3,4-dihydroxy-1-(4-nitrophenyl)butan-1-one (S23):



3-diazo-4-hydroxypentan-2-one (S24):



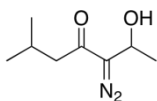
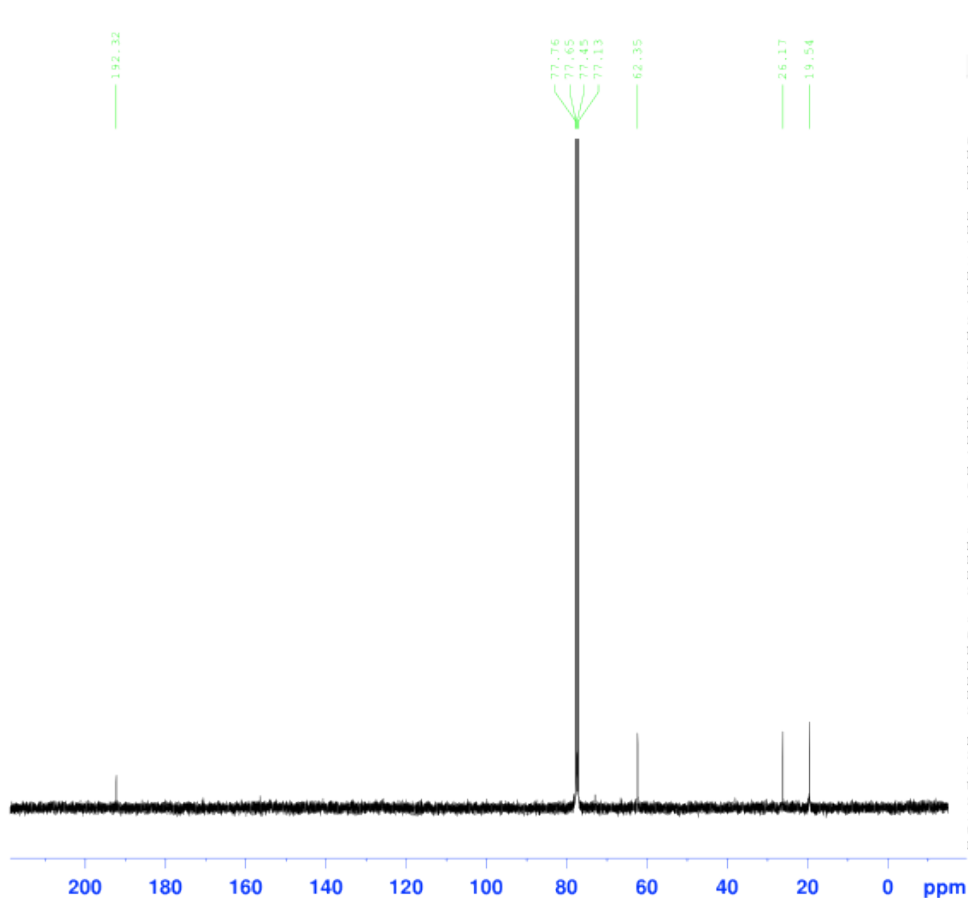
```

Current Data Parameters
NAME      13-smith-0915
EXPNO     10
PROCNO    1

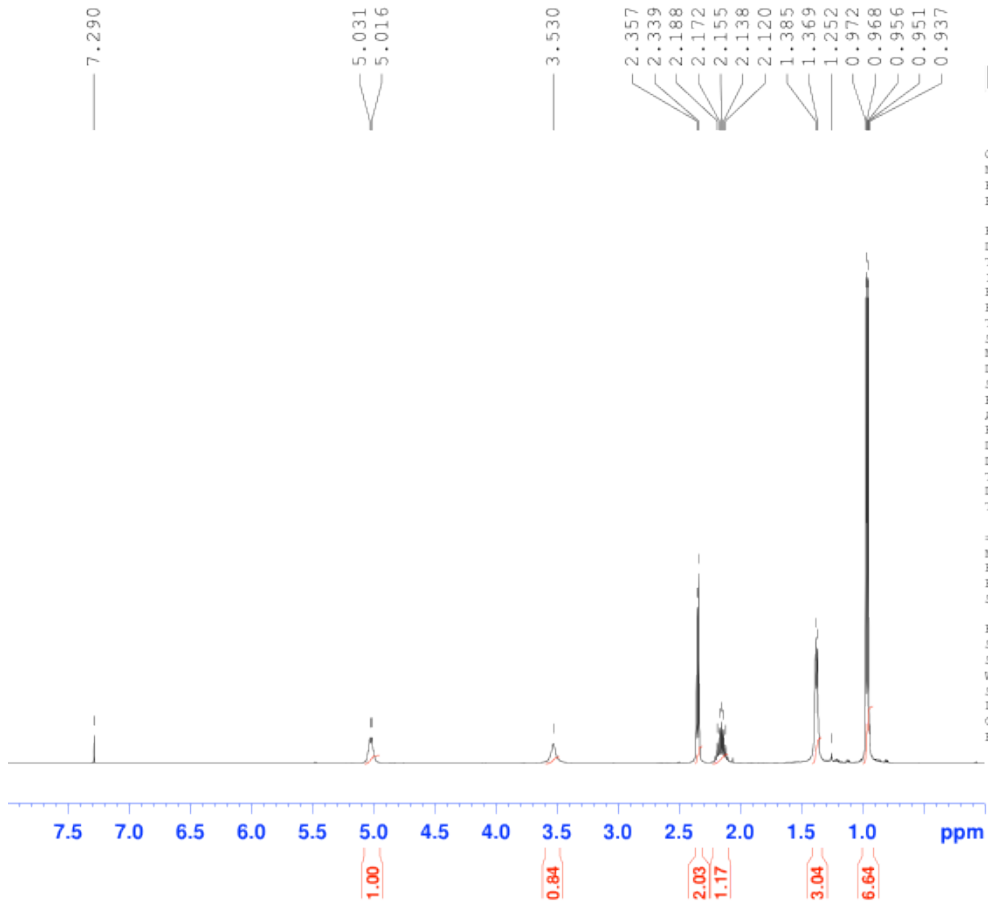
F2 - Acquisition Parameters
Date_     20090915
Time      19.24
INSTRUM   spect
PROBHD    5 mm QNP 1H/1
PULPROG   zg30
TD         39392
SOLVENT   CDCl3
NS         64
DS         2
SWH        7575.758 Hz
FIDRES     0.192317 Hz
AQ         2.5999219 sec
RG         228.1
DW         66.000 usec
DE         6.000 usec
TE         295.1 K
D1         1.50000000 sec
TD0        1

===== CHANNEL f1 =====
NUC1       1H
P1         10.00 usec
PL1        -4.00 dB
SFO1       399.7324685 MHz

F2 - Processing parameters
SI         32768
SF         399.7300000 MHz
WDW        EM
SSB        0
LB         0.30 Hz
GB         0
PC         2.00
  
```



3-diazo-2-hydroxy-6-methylheptan-4-one (S25):

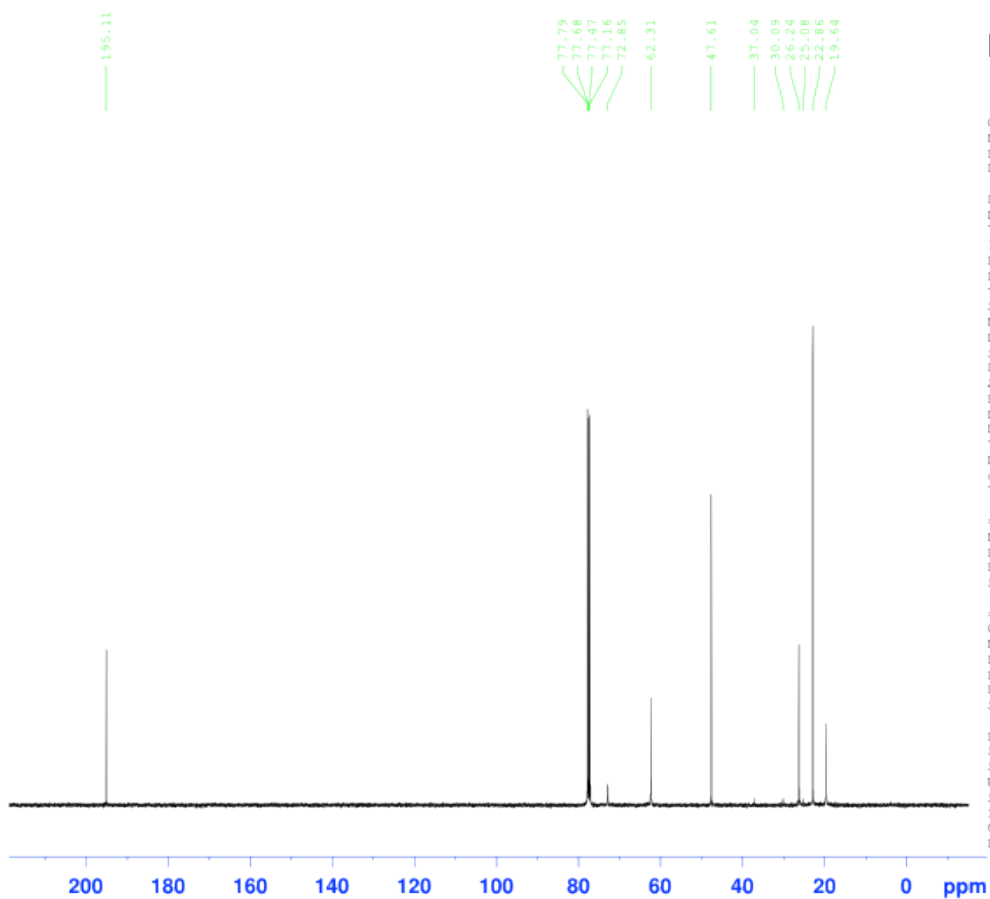


Current Data Parameters
 NAME 51-smith-1009
 EXPNO 10
 PROCNO 1

F2 - Acquisition Parameters
 Date_ 20091009
 Time 17.51
 INSTRUM spect
 PROBHD 5 mm QNP
 PULPROG zg30
 TD 39392
 SOLVENT CDCl3
 NS 64
 DS 2
 SMH 7575.758 Hz
 FIDRES 0.192317 Hz
 AQ 2.5999219 sec
 RG 40.3
 DW 66.000 usec
 DE 6.00 usec
 TE 295.2 K
 D1 1.50000000 sec
 TD0 1

===== CHANNEL f1 =====
 NUC1 1H
 P1 10.00 usec
 PL1 -4.00 dB
 SFO1 399.7324685 MHz

F2 - Processing parameters
 SI 32768
 SF 399.7300000 MHz
 WDW EM
 SSB 0
 LB 0.30 Hz
 GB 0
 PC 2.00



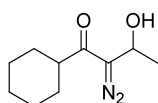
Current Data Parameters
 NAME 51-smith-1009
 EXPNO 11
 PROCNO 1

F2 - Acquisition Parameters
 Date_ 20091009
 Time 18.53
 INSTRUM spect
 PROBHD 5 mm QNP 1H/1
 FULPROG zgpg30
 TD 6536
 SOLVENT CDCl3
 NS 1300
 DS 32
 SMH 27173.912 Hz
 FIDRES 0.414641 Hz
 AQ 1.2059124 sec
 RG 322.5
 DW 18.400 usec
 DE 6.00 usec
 TE 295.7 K
 D1 1.50000000 sec
 d11 0.03000000 sec
 TDO 1

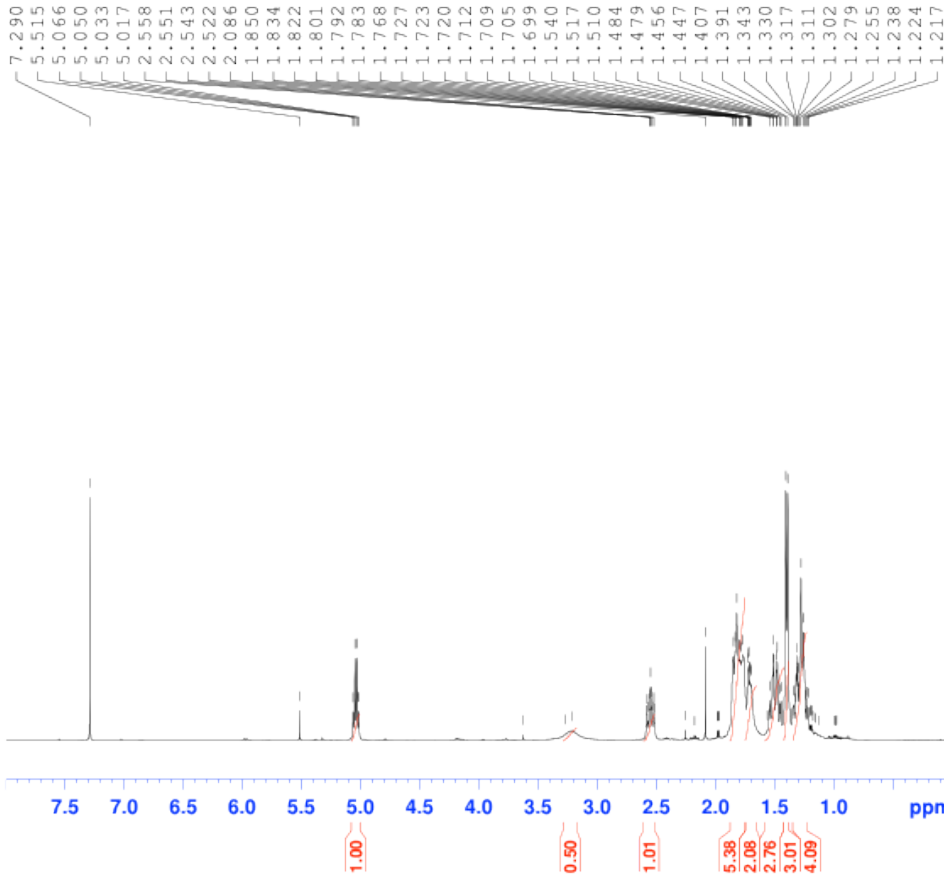
===== CHANNEL f1 =====
 NUC1 13C
 P1 4.50 usec
 PL1 0.00 dB
 SFO1 100.5242095 MHz

===== CHANNEL f2 =====
 CPDPRG2 waltz16
 NUC2 1H
 FCFD2 89.00 usec
 PL2 -4.00 dB
 PL12 17.37 dB
 SFO2 399.7315989 MHz

F2 - Processing parameters
 SI 32768
 SF 100.5121480 MHz
 WDW EM
 SSB 0
 LB 1.00 Hz
 GB 0
 PC 1.40



1-cyclohexyl-2-diazo-3-hydroxybutan-1-one (S26):



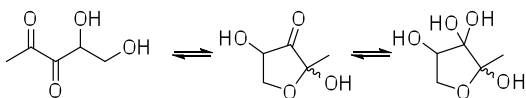
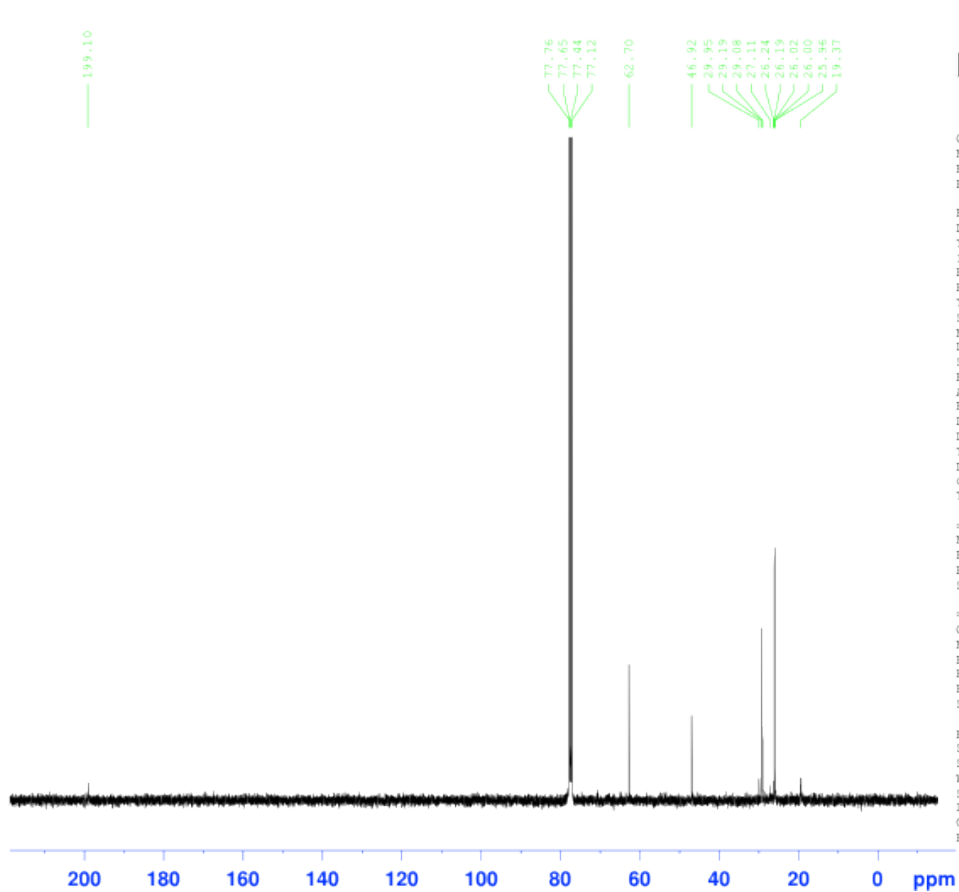
```

Current Data Parameters
NAME      27-smith-0918
EXPNO     10
PROCNO    1

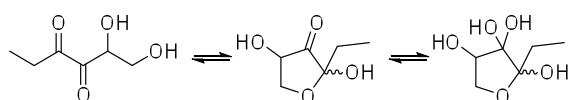
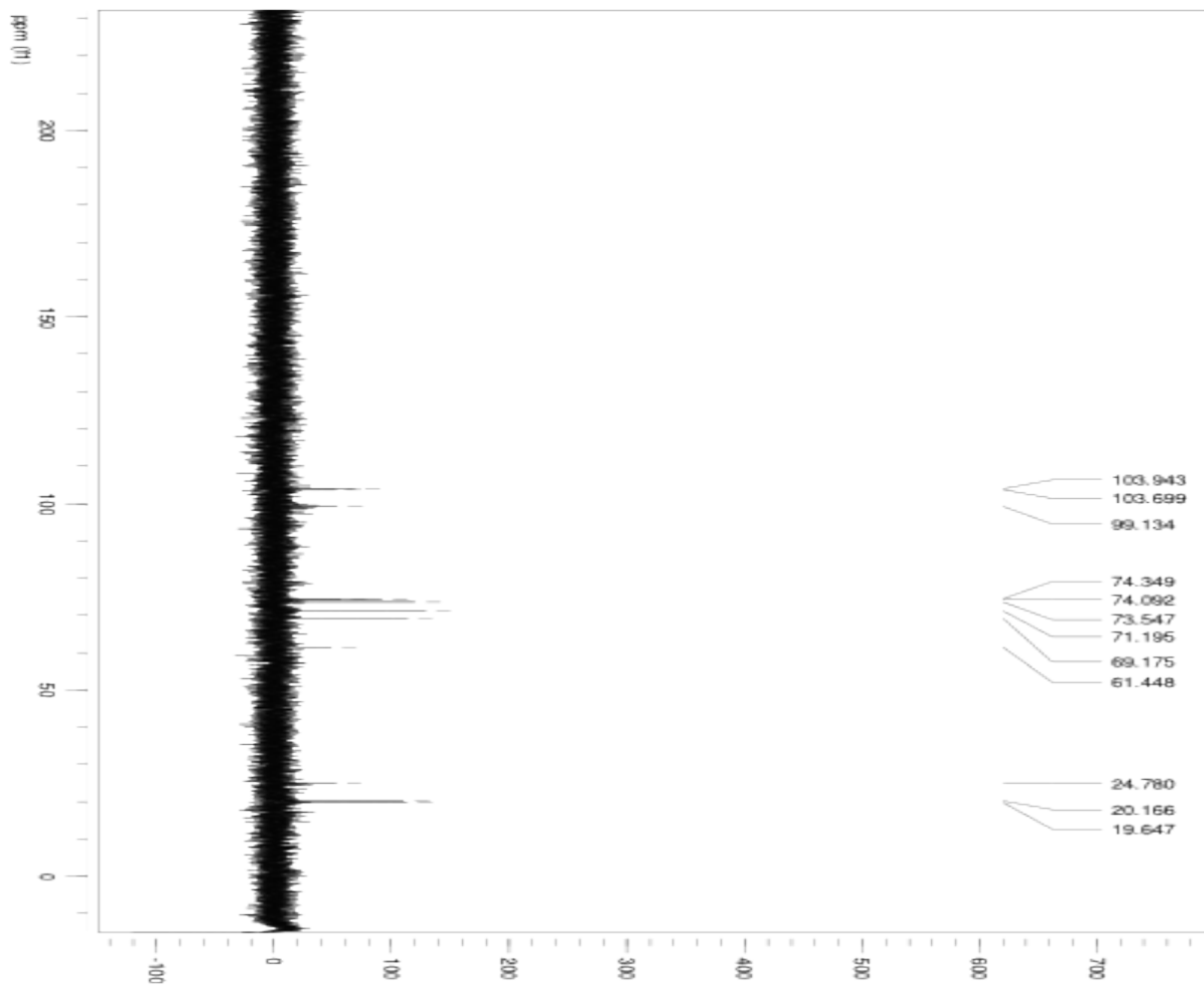
F2 - Acquisition Parameters
Date_     20090918
Time      16.33
INSTRUM   spect
PROBHD    5 mm QNP 1H/1
PULPROG   zg30
TD         39392
SOLVENT   CDCl3
NS         64
DS         2
SWH        7575.758 Hz
FIDRES     0.192317 Hz
AQ         2.5999219 sec
RG         181
DM         66.000 usec
DE         6.000 usec
TE         295.1 K
D1         1.50000000 sec
TD0        1

===== CHANNEL f1 =====
NUC1       1H
P1         10.00 usec
PL1        -4.00 dB
SFO1       399.7324685 MHz

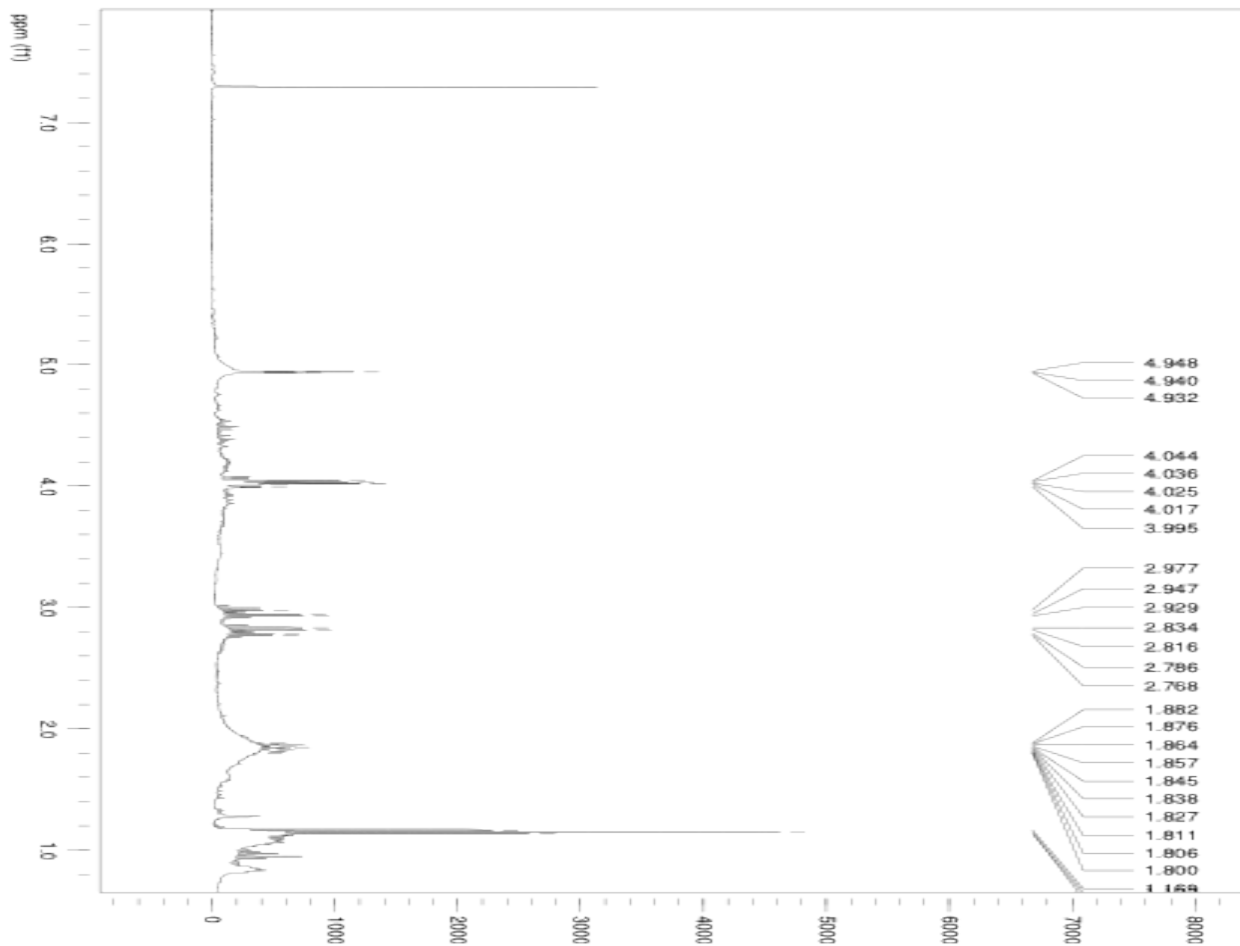
F2 - Processing parameters
SI         32768
SF         399.7300000 MHz
MDW        EM
SSB        0
LB         0.30 Hz
GB         0
PC         2.00
  
```

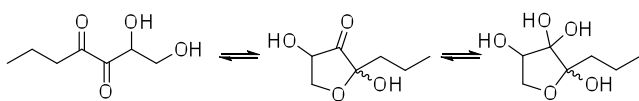
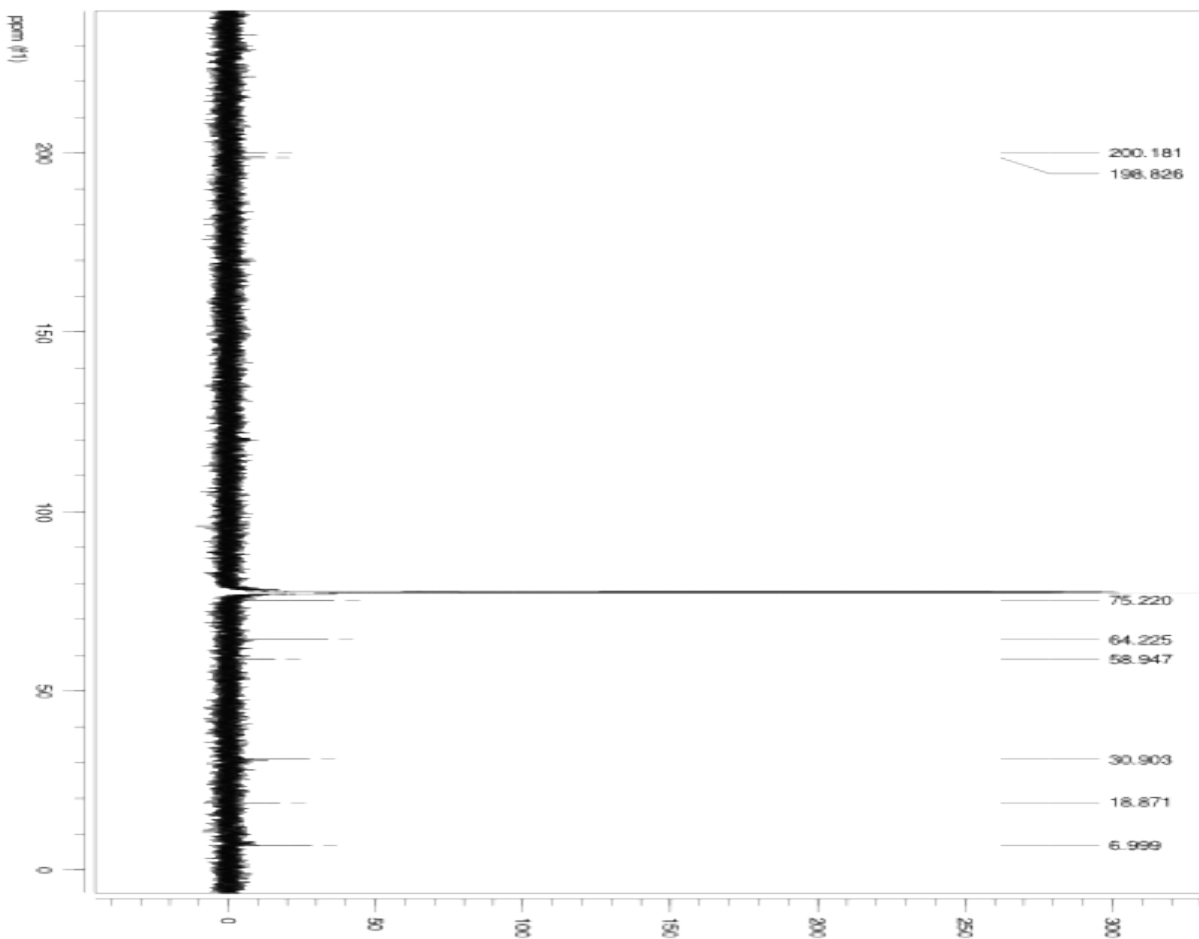


DPD (4,5-dihydroxypentane-2,3-dione) and cyclic compounds (55):

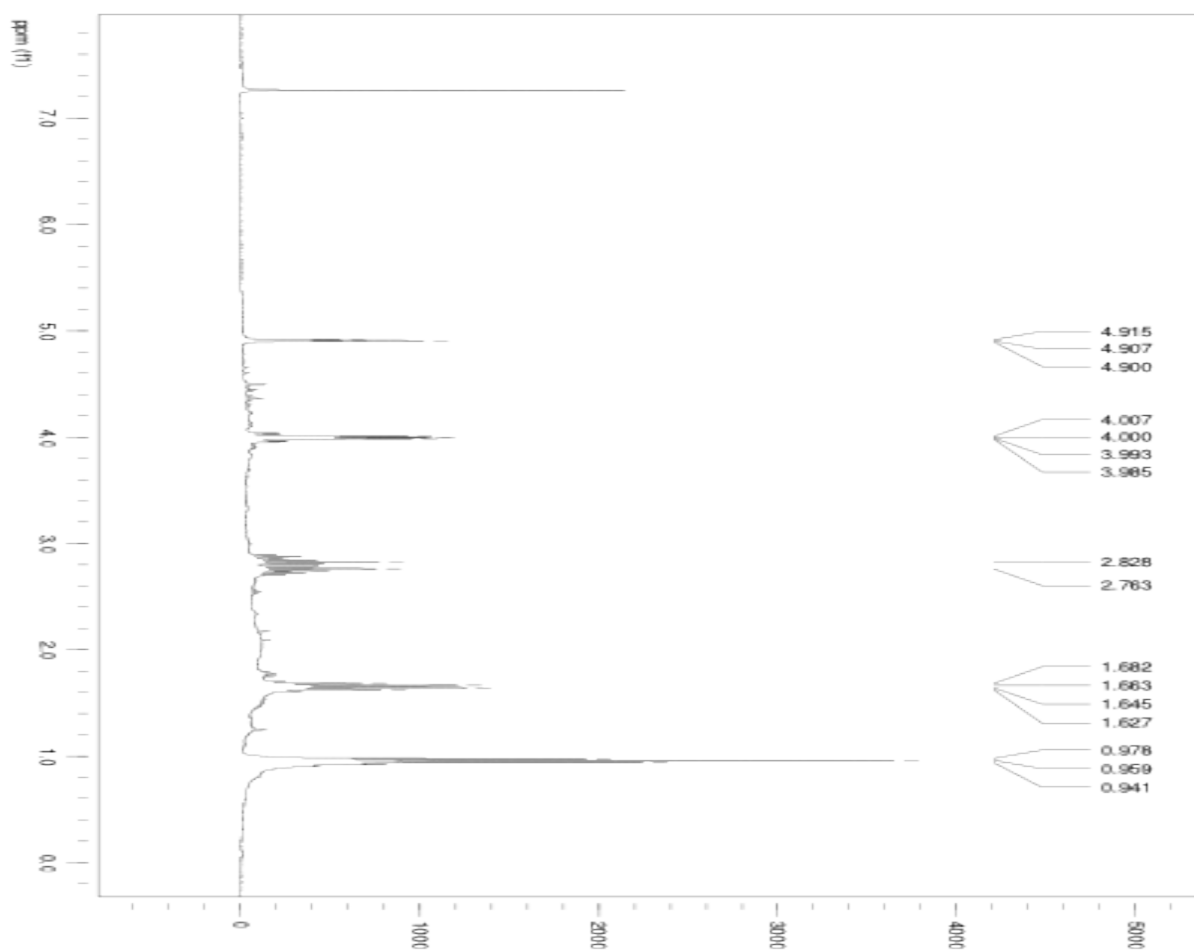


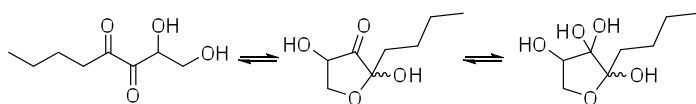
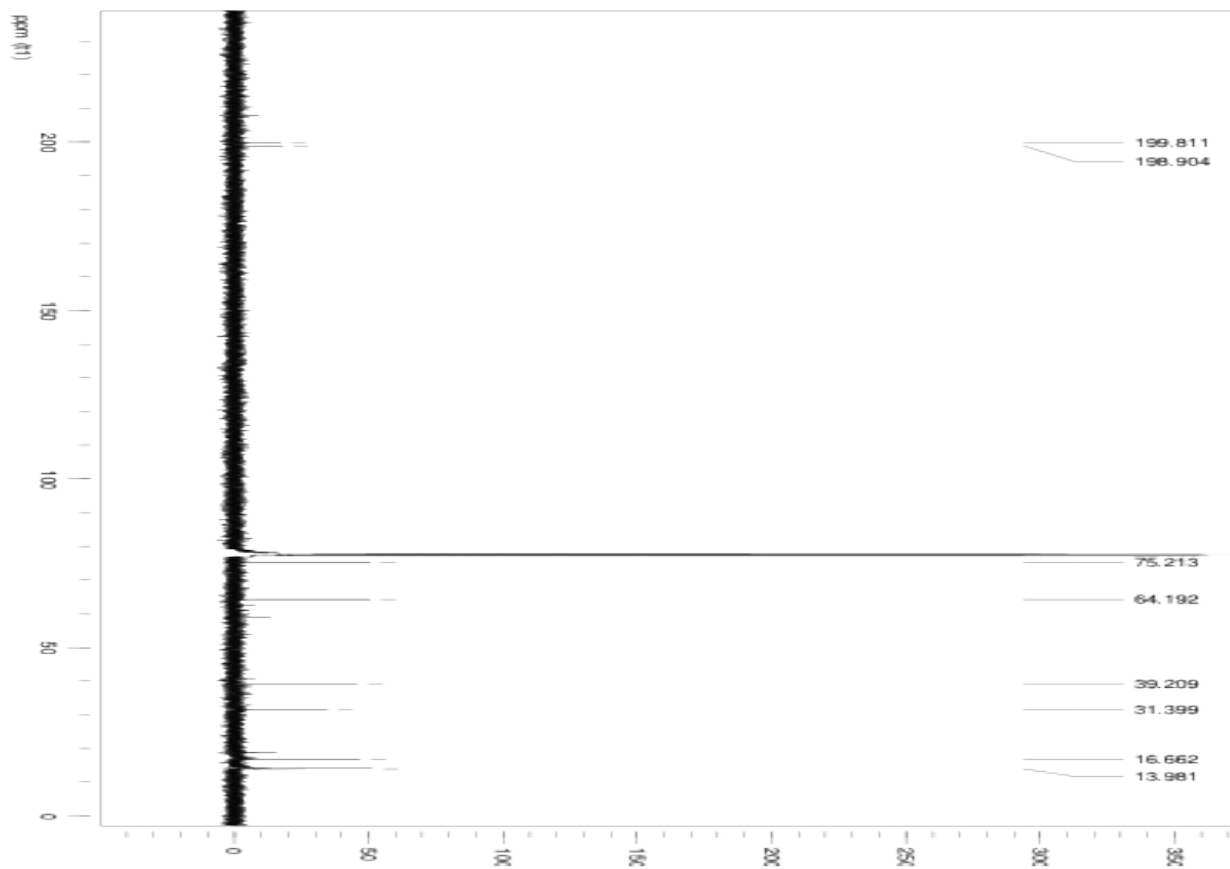
Ethyl-DPD (1,2-dihydroxyhexane-3,4-dione) and cyclic compounds (108):



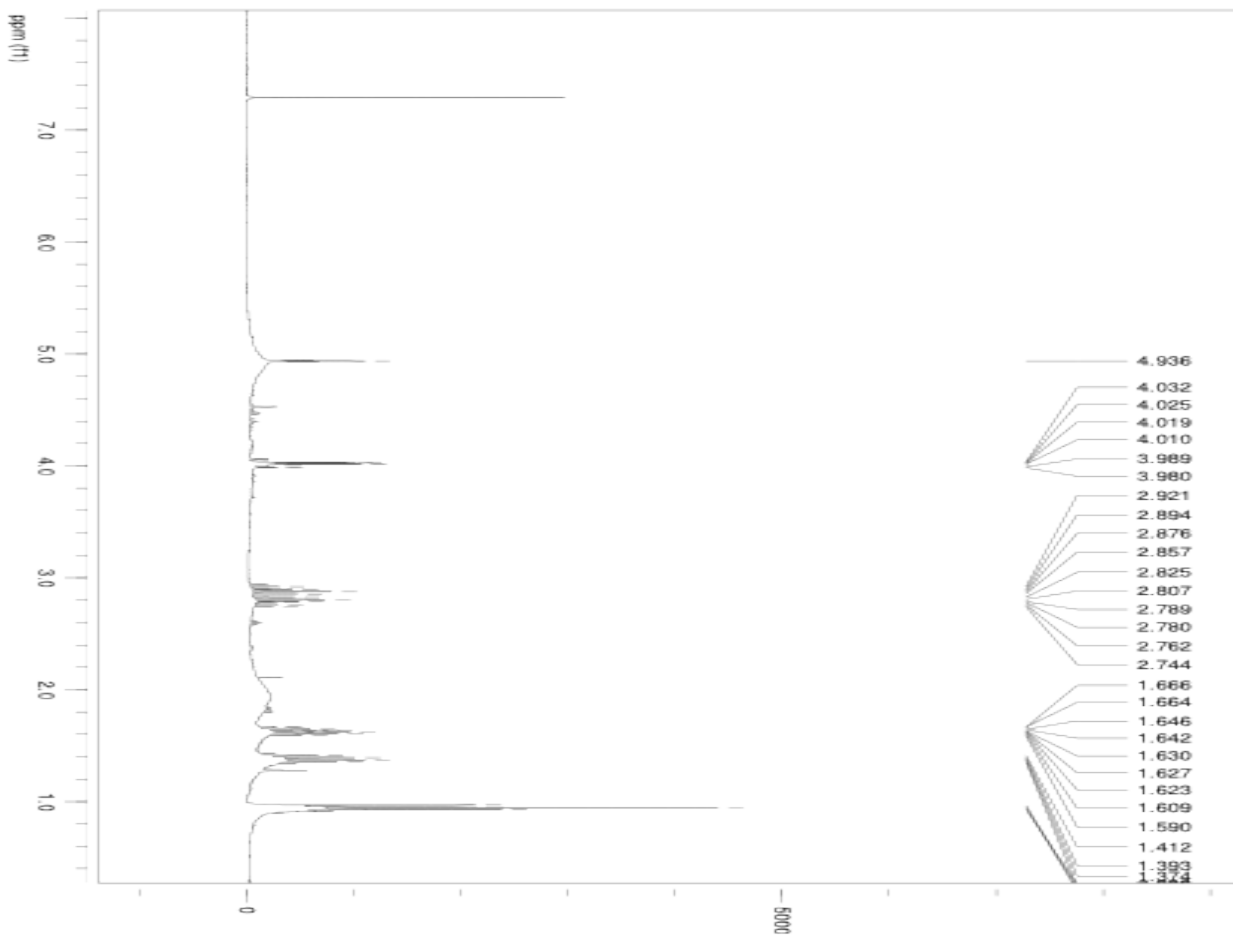


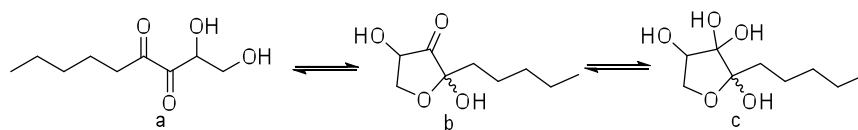
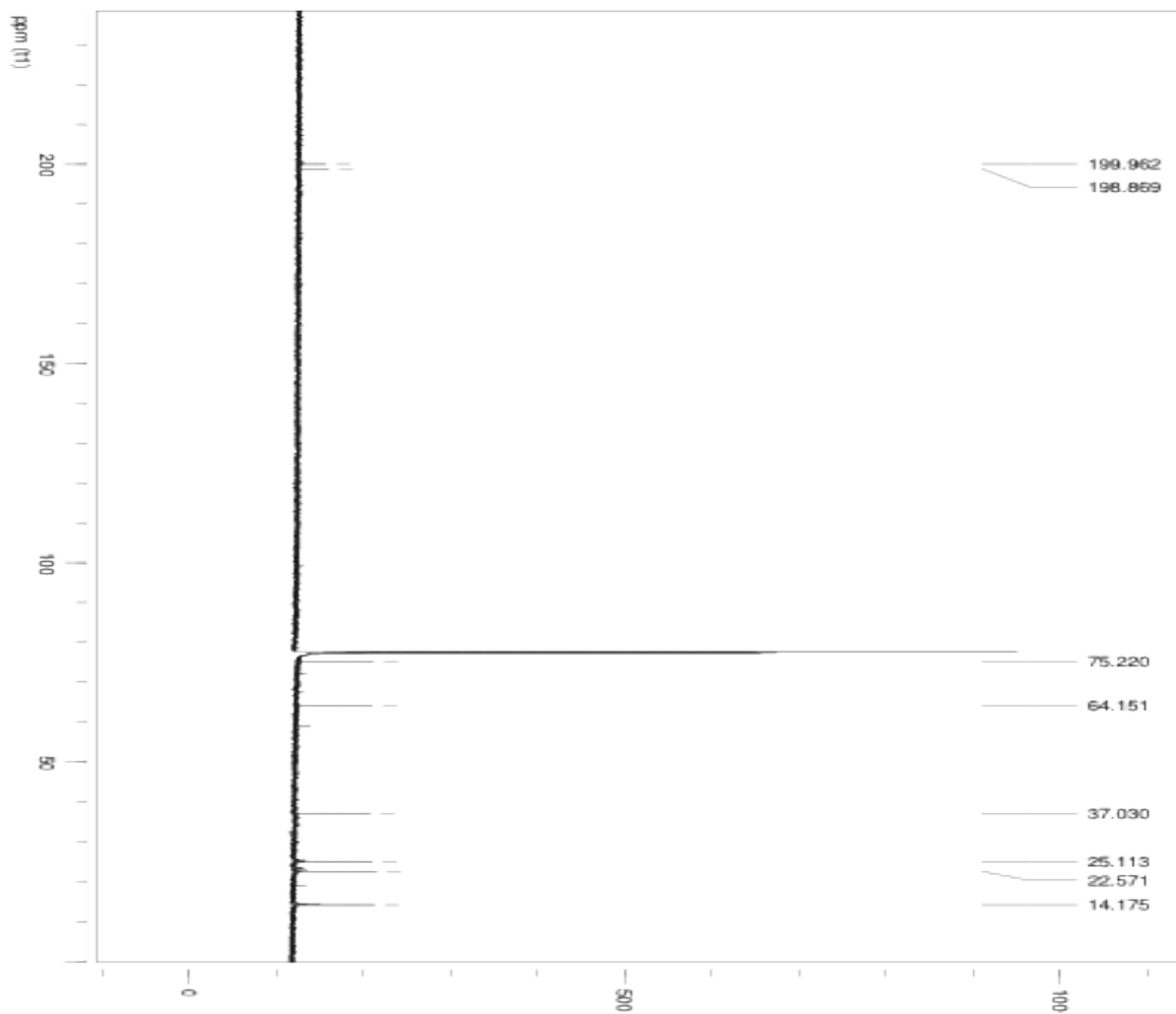
Propyl-DPD (1,2-dihydroxyheptane-3,4-dione) and cyclic compounds (109):



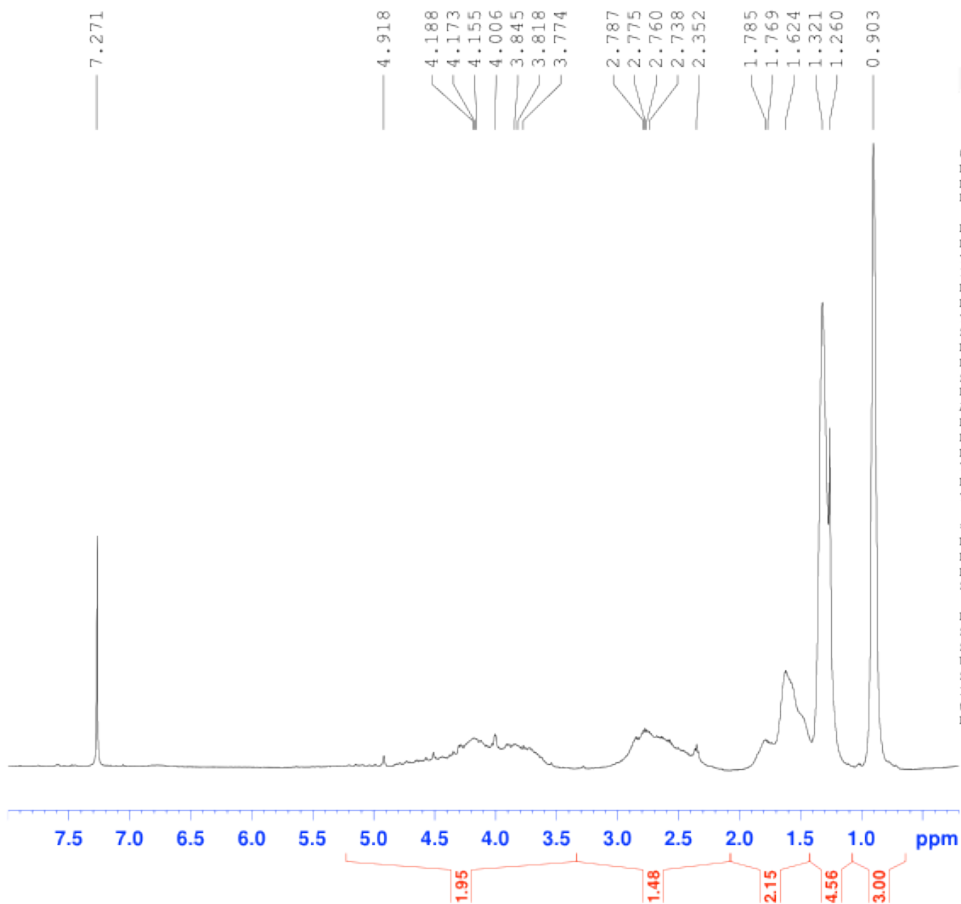


Butyl-DPD (1,2-dihydroxyoctane-3,4-dione) and cyclic compounds (110):





Pentyl-DPD (1,2-dihydroxynonane-3,4-dione) and cyclic compounds (111):

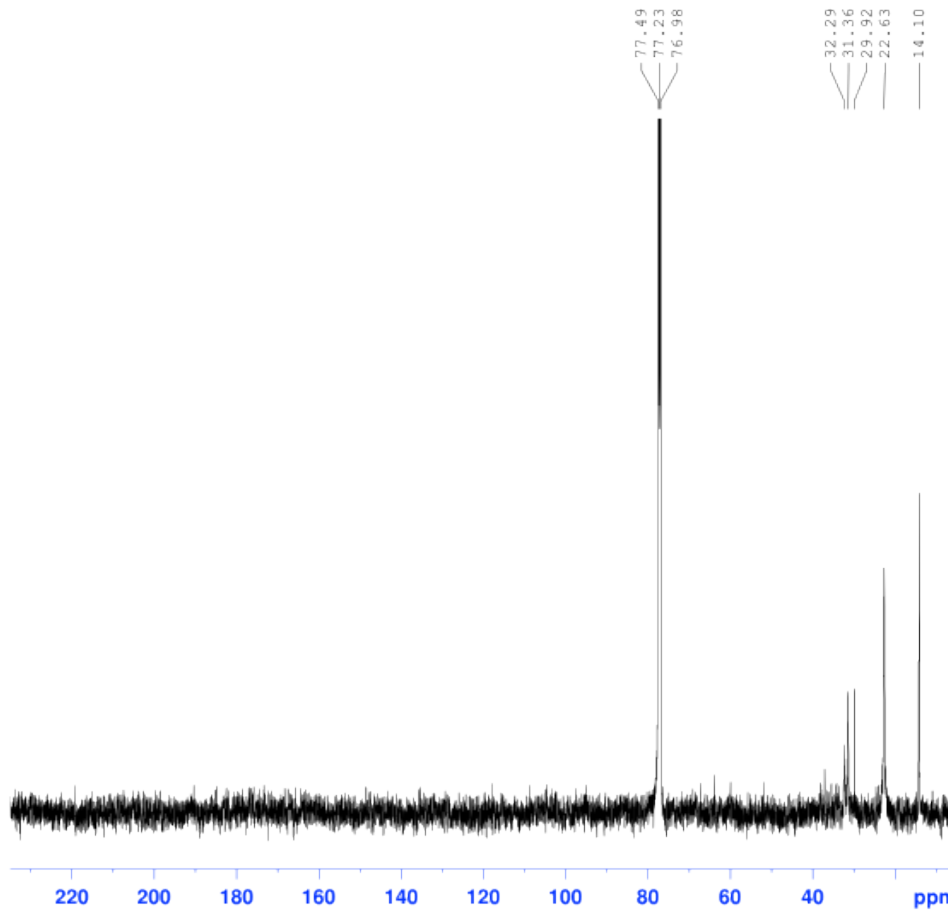


Current Data Parameters
NAME c5_dpd
EXPNO 1
PROCNO 1

F2 - Acquisition Parameters
Date_ 20090804
Time 21.25
INSTRUM spect
PROBHD 5 mm BBO2 new
PULPROG zg
TD 65536
SOLVENT CDCl3
NS 16
DS 2
SWH 6510.417 Hz
FIDRES 0.099341 Hz
AQ 5.0332146 sec
RG 80.6
DW 76.800 usec
DE 9.00 usec
TE 296.5 K
D1 5.00000000 sec
TD0 1

==== CHANNEL f1 =====
NUC1 1H
P1 11.10 usec
PL1 0.00 dB
SFO1 500.1330008 MHz

F2 - Processing parameters
SI 32768
SF 500.1300080 MHz
WDW EM
SSB 0
LB 0.30 Hz
GB 0
PC 1.00



```

Current Data Parameters
NAME          C5_DPD
EXPNO         2
PROCNO        1

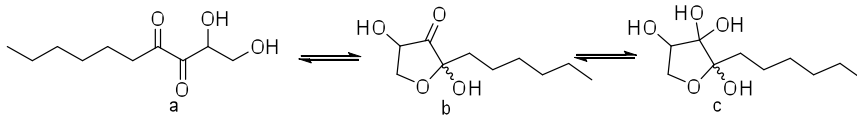
F2 - Acquisition Parameters
Date_         20090804
Time          22.33
INSTRUM       spect
PROBHD        5 mm BBO2 new
PULPROG       zgpg30
TD            65536
SOLVENT       C6D6
NS            3416
DS            8
SMH           30120.482 Hz
FIDRES        0.459602 Hz
AQ            1.0879476 sec
RG            9195.2
DM            16.600 usec
DE            6.50 usec
TE            299.1 K
D1            1.00000000 sec
d11           0.03000000 sec
DELTA         0.899999998 sec
TD0           1

===== CHANNEL f1 =====
NUC1          13C
F1            13.10 usec
PL1           3.00 dB
SFO1          125.7728299 MHz

===== CHANNEL f2 =====
CPDPRG2       waltz16
NUC2          1H
PCPD2         60.00 usec
PL2           0.00 dB
PL12          17.80 dB
PL13          20.00 dB
SFO2          500.1325007 MHz

F2 - Processing parameters
SI            32768
SF            125.7577619 MHz
WDW           EM
SSB           0
LB            3.00 Hz
GB            0
PC            1.40

```



Hexyl-DPD (1,2-dihydroxydecane-3,4-dione)

User Name smith
 Group sintim
 Sample Label hexyl_dpd

4.936
 4.035
 4.027
 4.023
 4.015
 2.874
 2.801
 2.783
 2.203
 2.120
 1.902
 1.881
 1.874
 1.844
 1.836
 1.821
 1.803
 1.796
 1.677
 1.658
 1.640
 1.621
 1.603
 1.586
 1.567
 1.541
 1.528

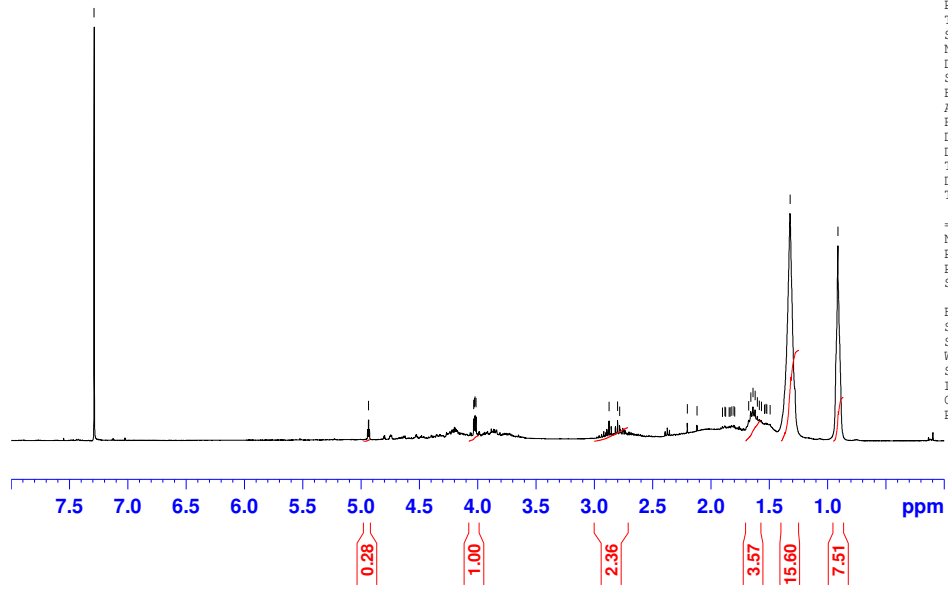


Current Data Parameters
 NAME 10-smith-0817
 EXPNO 10
 PROCNO 1

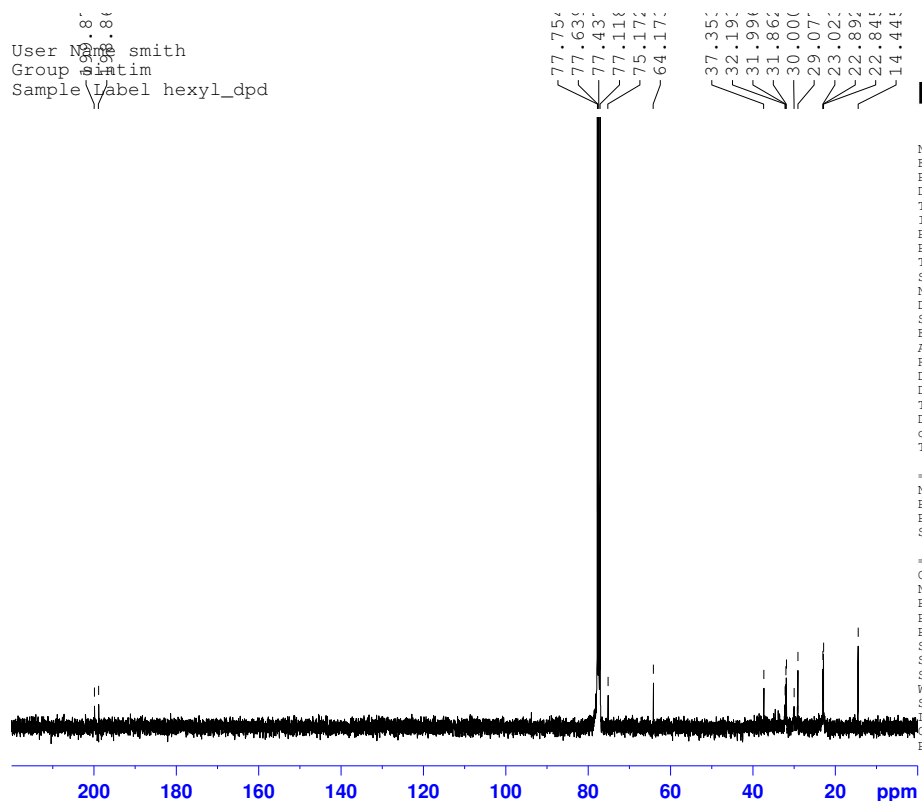
F2 - Acquisition Parameters
 Date_ 20090817
 Time_ 13.00
 INSTRUM spect
 PROBHD 5 mm QNP 1H/1
 PULPROG zg30
 TD 39392
 SOLVENT CDC13
 NS 64
 DS 2
 SWH 7575.758 Hz
 FIDRES 0.192317 Hz
 AQ 2.5999219 sec
 RG 256
 DW 66.000 usec
 DE 6.00 usec
 TE 294.9 K
 D1 1.50000000 sec
 TDO 1

==== CHANNEL f1 =====
 NUC1 1H
 P1 10.00 usec
 PL1 -4.00 dB
 SF01 399.7324685 MHz

F2 - Processing parameters
 SI 32768
 SF 399.7300000 MHz
 WDW EM
 SSB 0
 LB 0.30 Hz
 GB 0
 PC 2.00



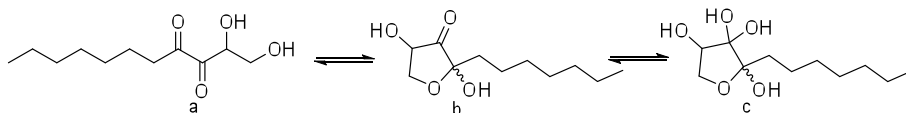
User Name smith
 Group satim
 Sample Label hexyl_dpd



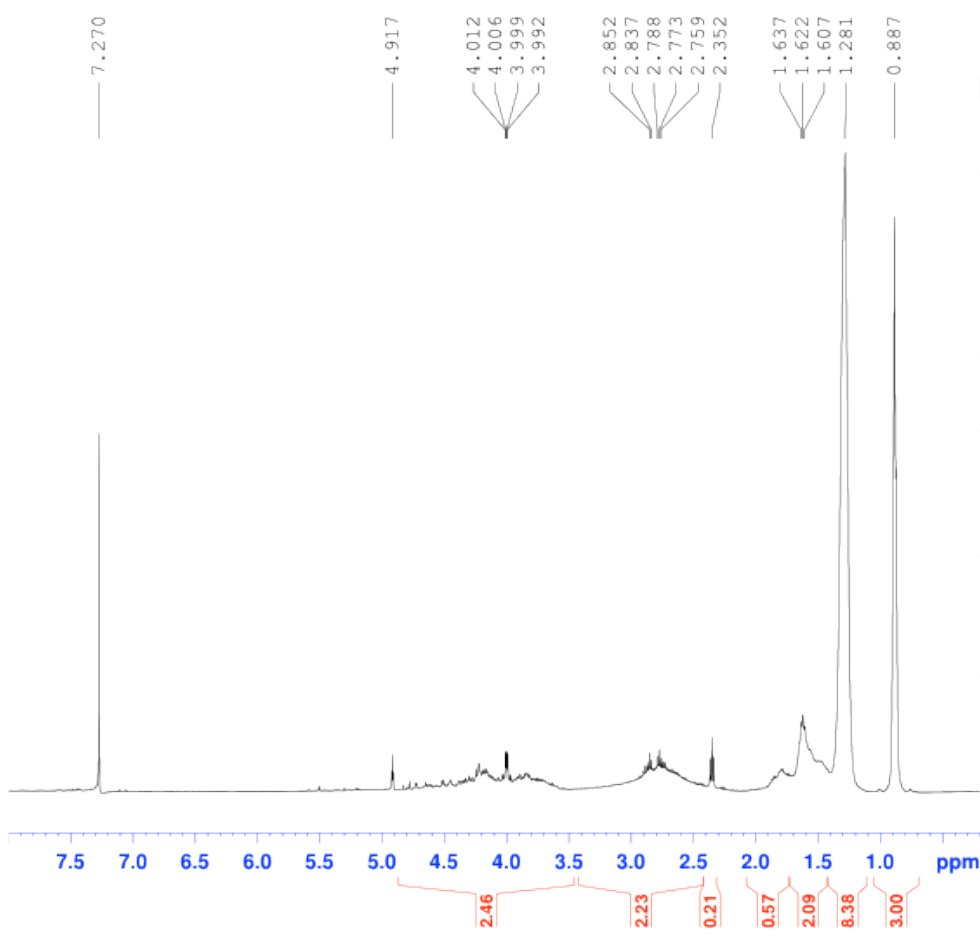
NAME 10-smith-0817
 EXPNO 11
 PROCNO 1
 Date_ 20090817
 Time 23.08
 INSTRUM spect
 PROBHD 5 mm QNP 1H/1
 PULPROG zgdc30
 TD 65536
 SOLVENT cdc13
 NS 3800
 DS 16
 SWH 27173.912 Hz
 FIDRES 0.414641 Hz
 AQ 1.2059124 sec
 RG 181
 DW 18.400 usec
 DE 6.00 usec
 TE 295.6 K
 D1 1.5000000 sec
 d11 0.0300000 sec
 TD0 1

===== CHANNEL f1 =====
 NUC1 13C
 P1 4.50 usec
 PL1 0.00 dB
 SFO1 100.5242095 MHz

===== CHANNEL f2 =====
 CPDPRG2 waltz16
 NUC2 1H
 PCPD2 89.00 usec
 PL2 -4.00 dB
 PL12 17.37 dB
 SFO2 399.7315989 MHz
 SI 32768
 SF 100.5121480 MHz
 WDW EM
 SSB 0
 LB 1.00 Hz
 GB 0
 PC 1.40



Heptyl-DPD (1,2-dihydroxyundecane-3,4-dione) and cyclic compounds (113):



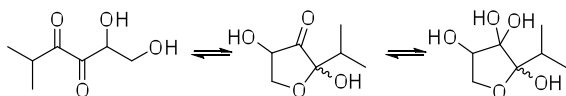
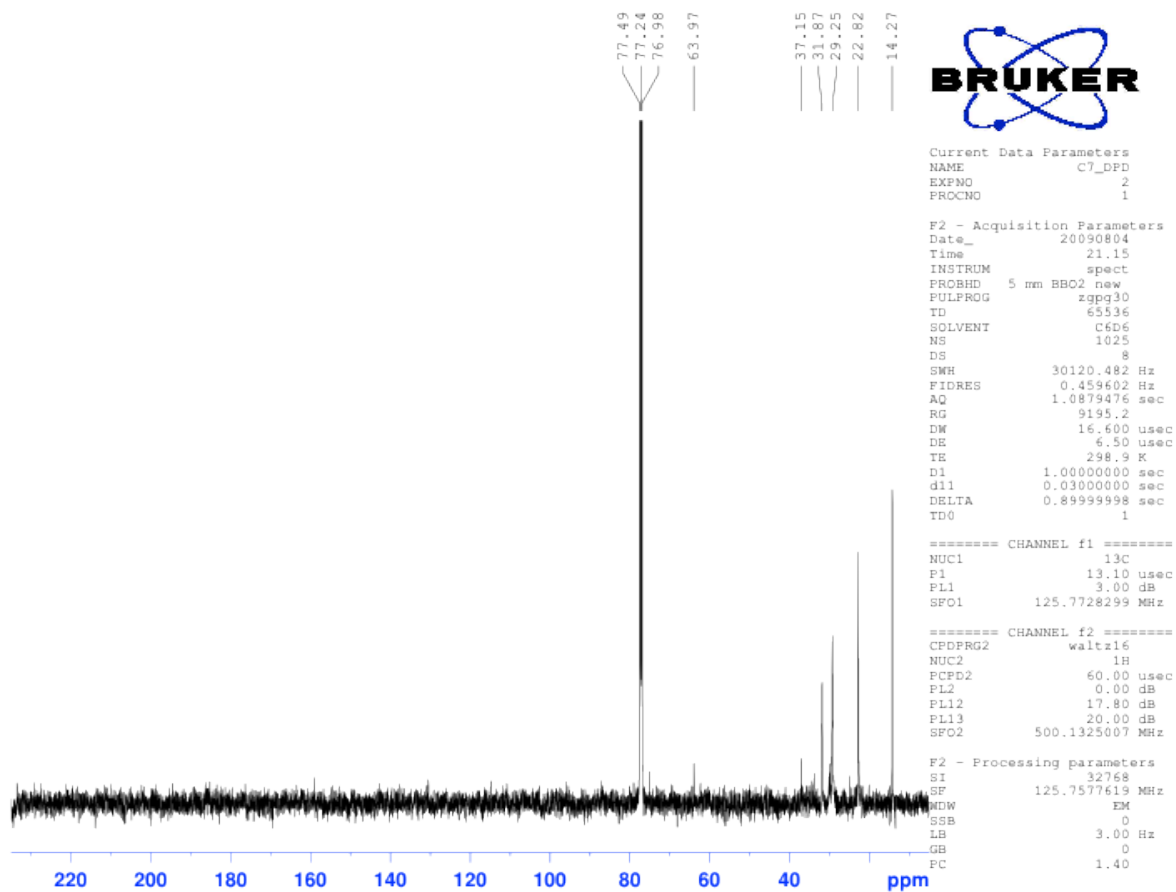
```

Current Data Parameters
NAME      C7_DPD
EXPNO     1
PROCNO    1

F2 - Acquisition Parameters
Date_     20090804
Time      20.40
INSTRUM   spect
PROBHD    5 mm BBO2 new
PULPROG   zg
TD         65536
SOLVENT   CDCl3
NS         16
DS         2
SWH        6510.417 Hz
FIDRES     0.099341 Hz
AQ         5.0332146 sec
RG         80.6
DW         76.800 usec
DE         9.00 usec
TE         296.1 K
D1         10.00000000 sec
TD0        1

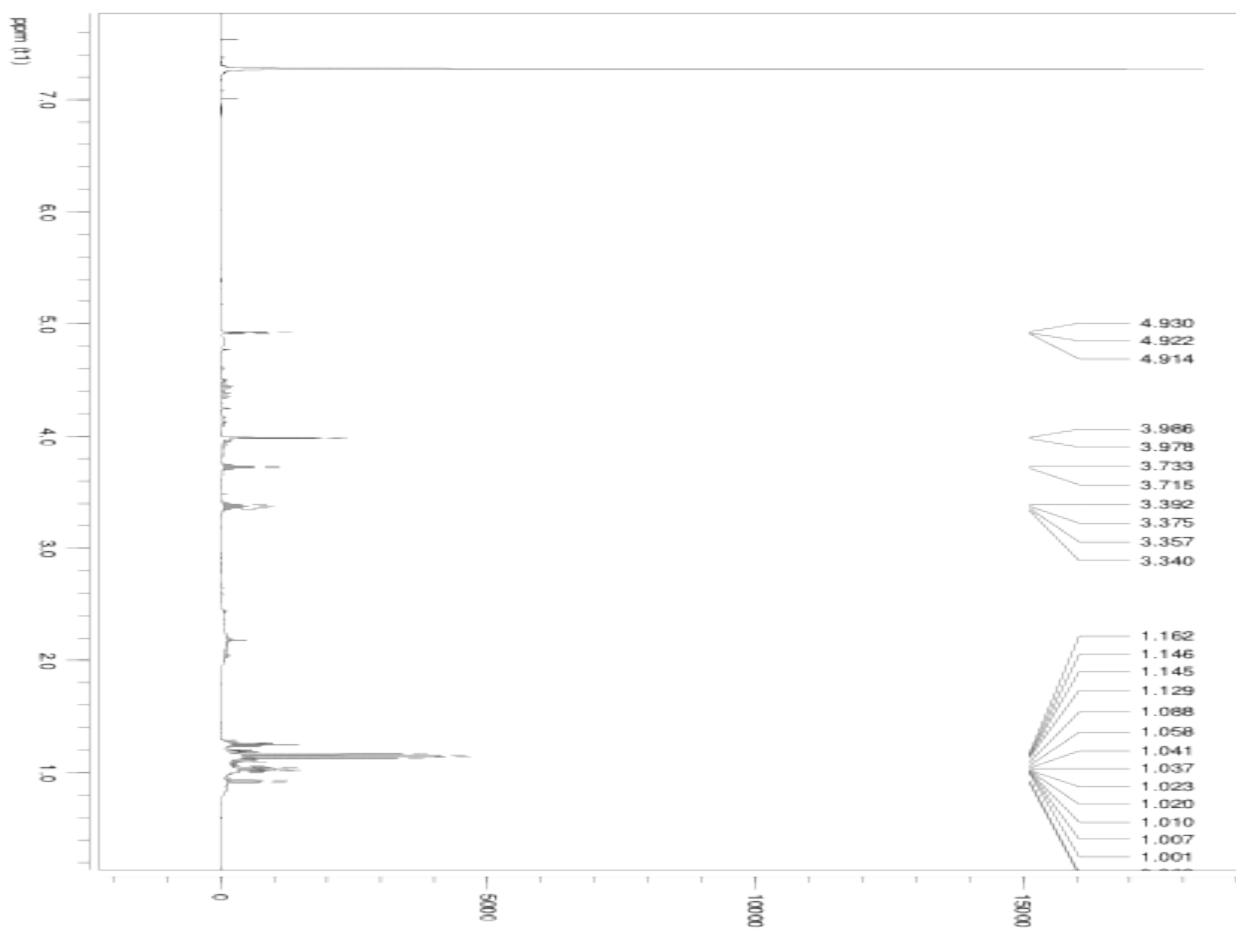
===== CHANNEL f1 =====
NUC1       1H
P1         11.10 usec
PL1        0.00 dB
SFO1       500.1330008 MHz

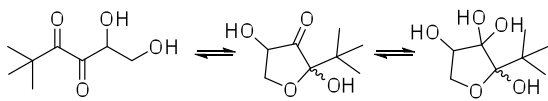
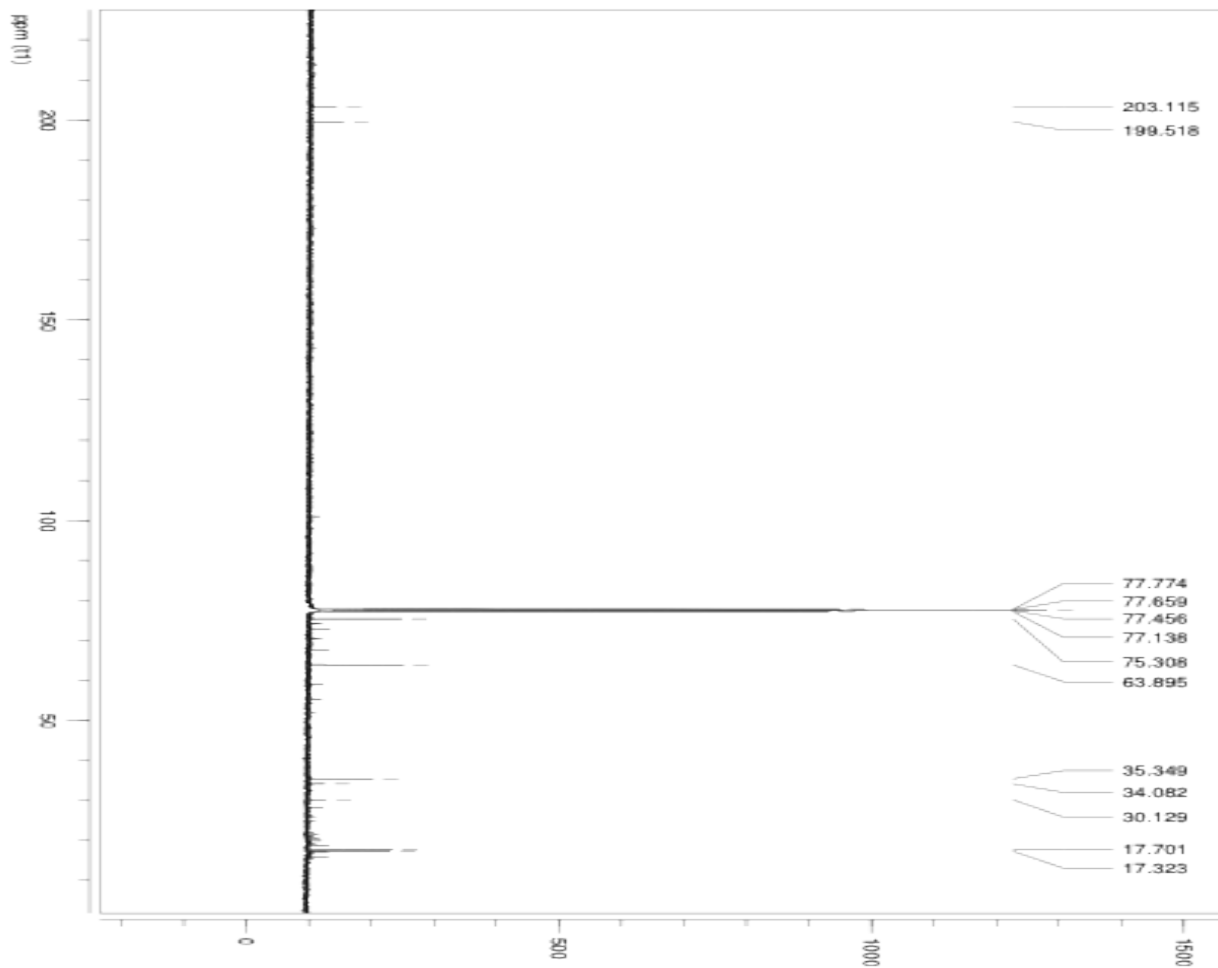
F2 - Processing parameters
SI         32768
SF         500.1300083 MHz
WDW        EM
SSB        0
LB         0.30 Hz
GB         0
PC         1.00
  
```



Isopropyl-DPD (1,2-dihydroxy-5-methylhexane-3,4-dione) and cyclic compounds

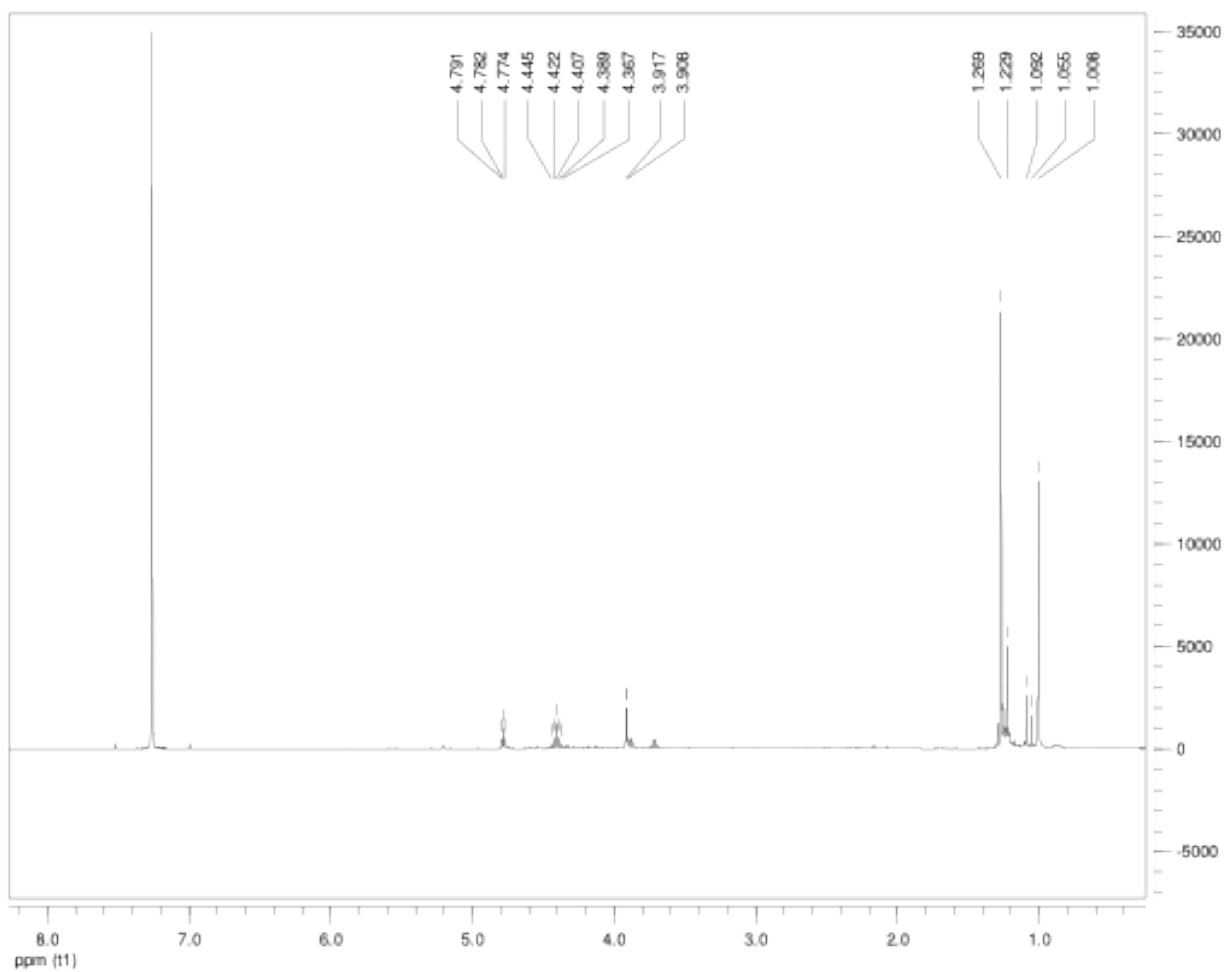
(114):

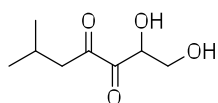
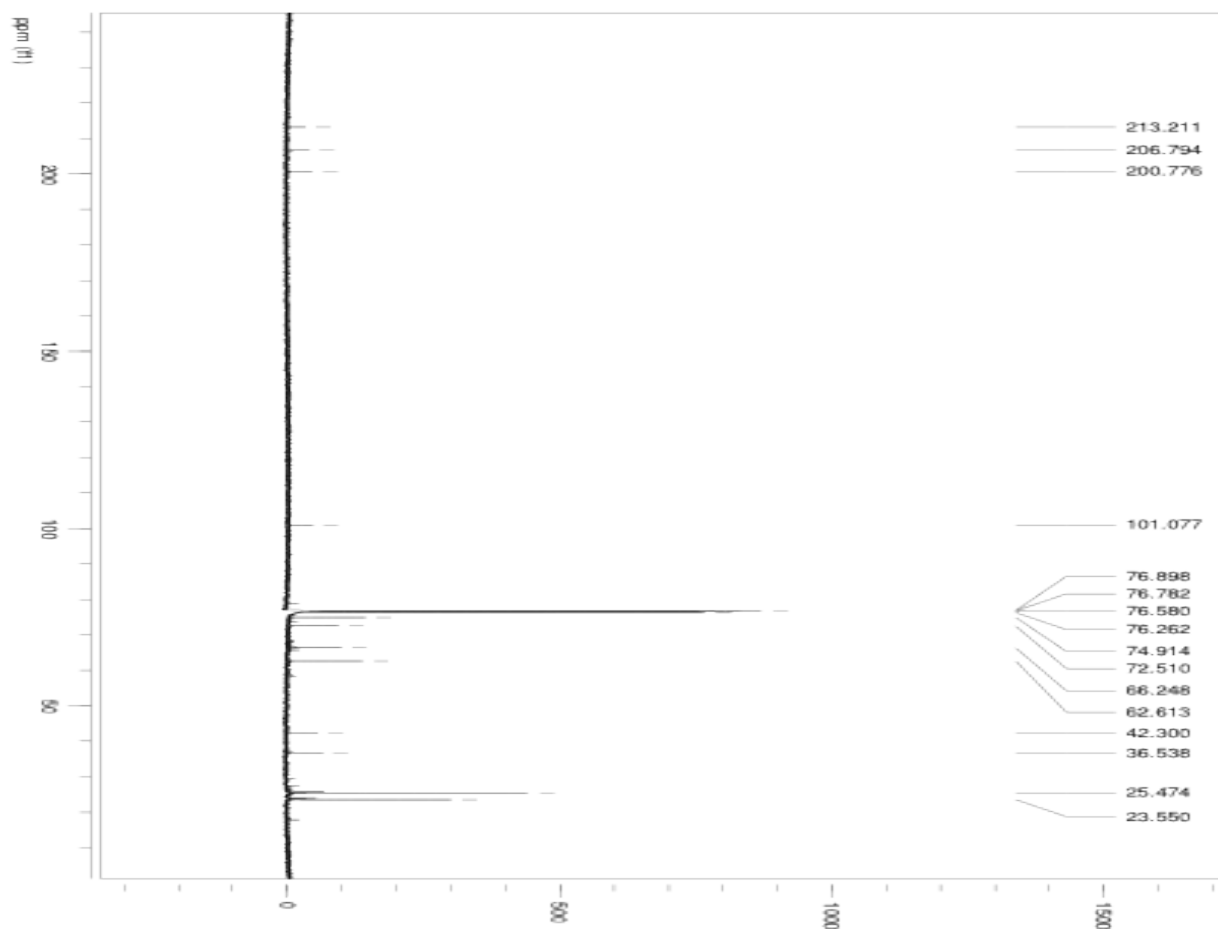




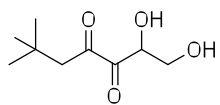
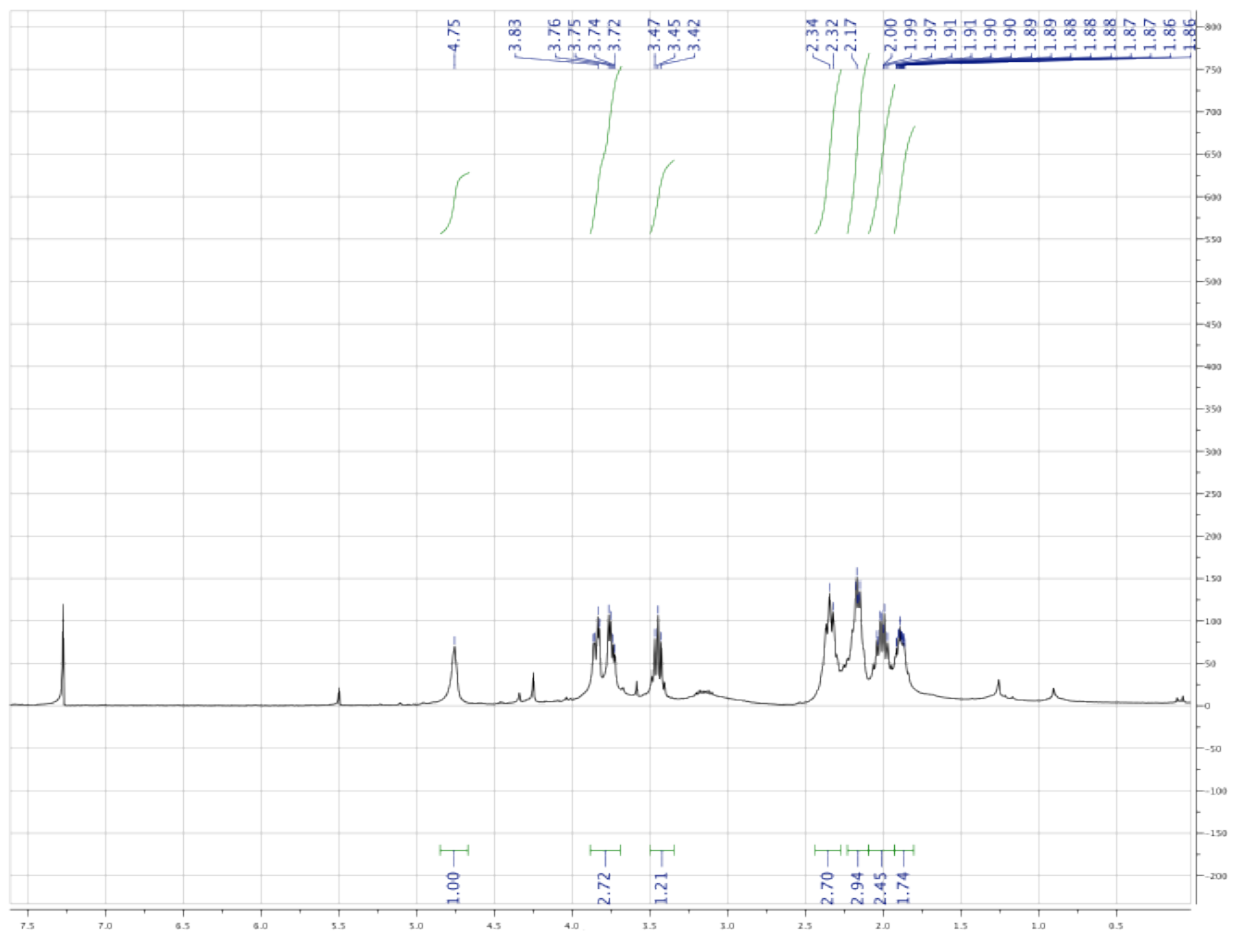
Tertbutyl-DPD (1,2-dihydroxy-5,5-dimethylhexane-3,4-dione) and cyclic compounds

(115):

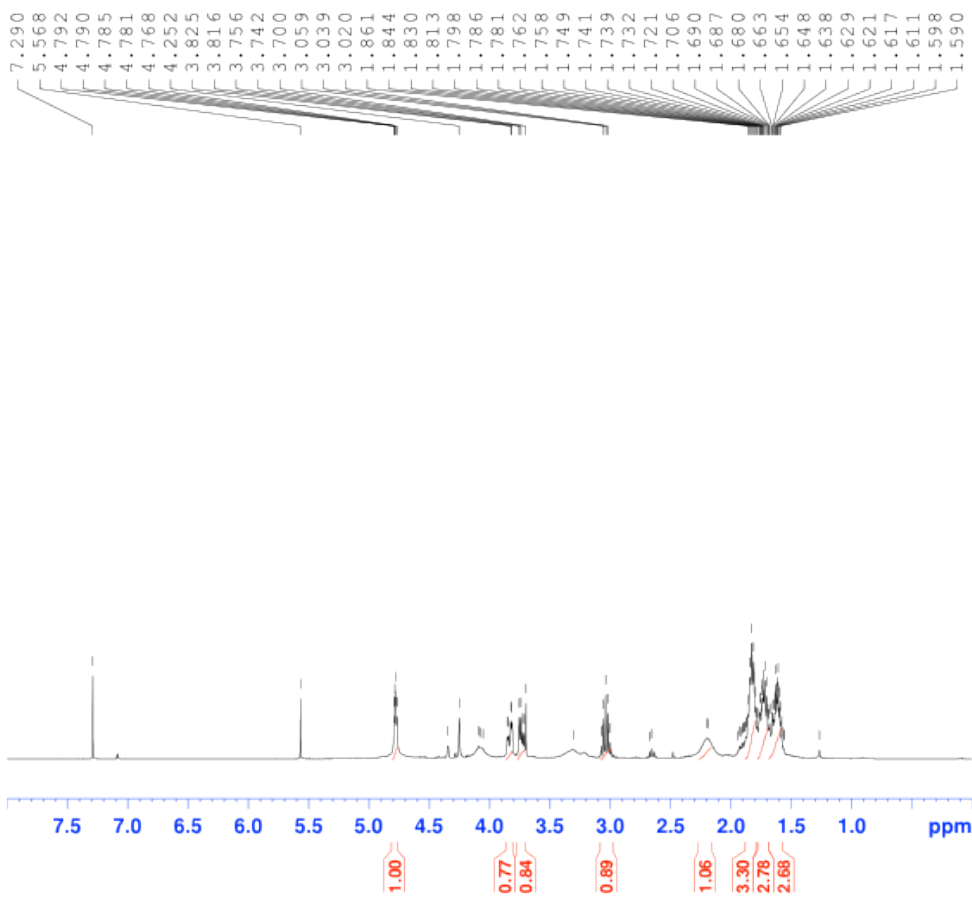




Isobutyl-DPD (1,2-dihydroxy-6-methylheptane-3,4-dione) (116):



Neopentyl-DPD (1,2-dihydroxy-6,6-dimethylheptane-3,4-dione) (118):



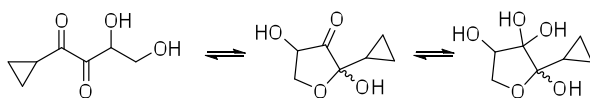
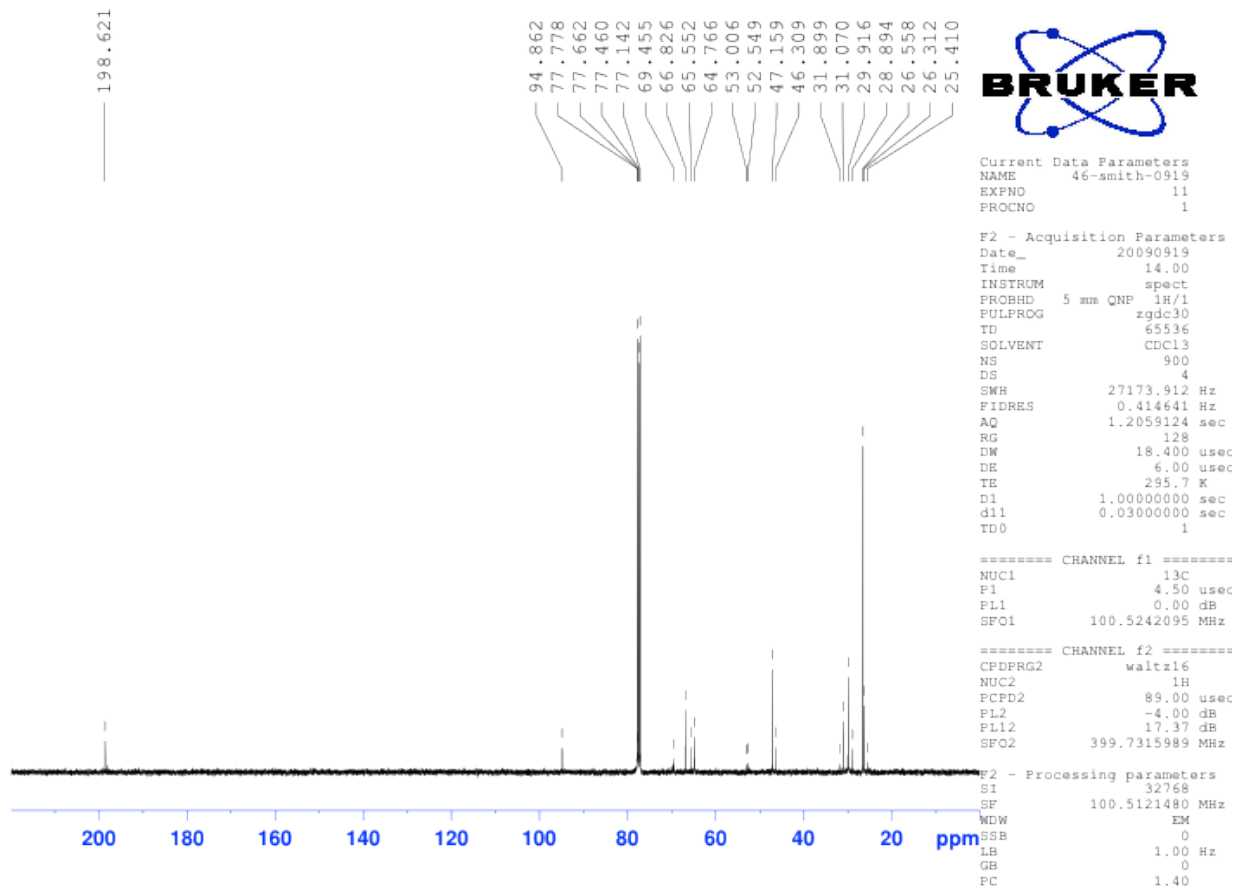
```

Current Data Parameters
NAME      46-smith-0919
EXPNO    10
PROCNO   1

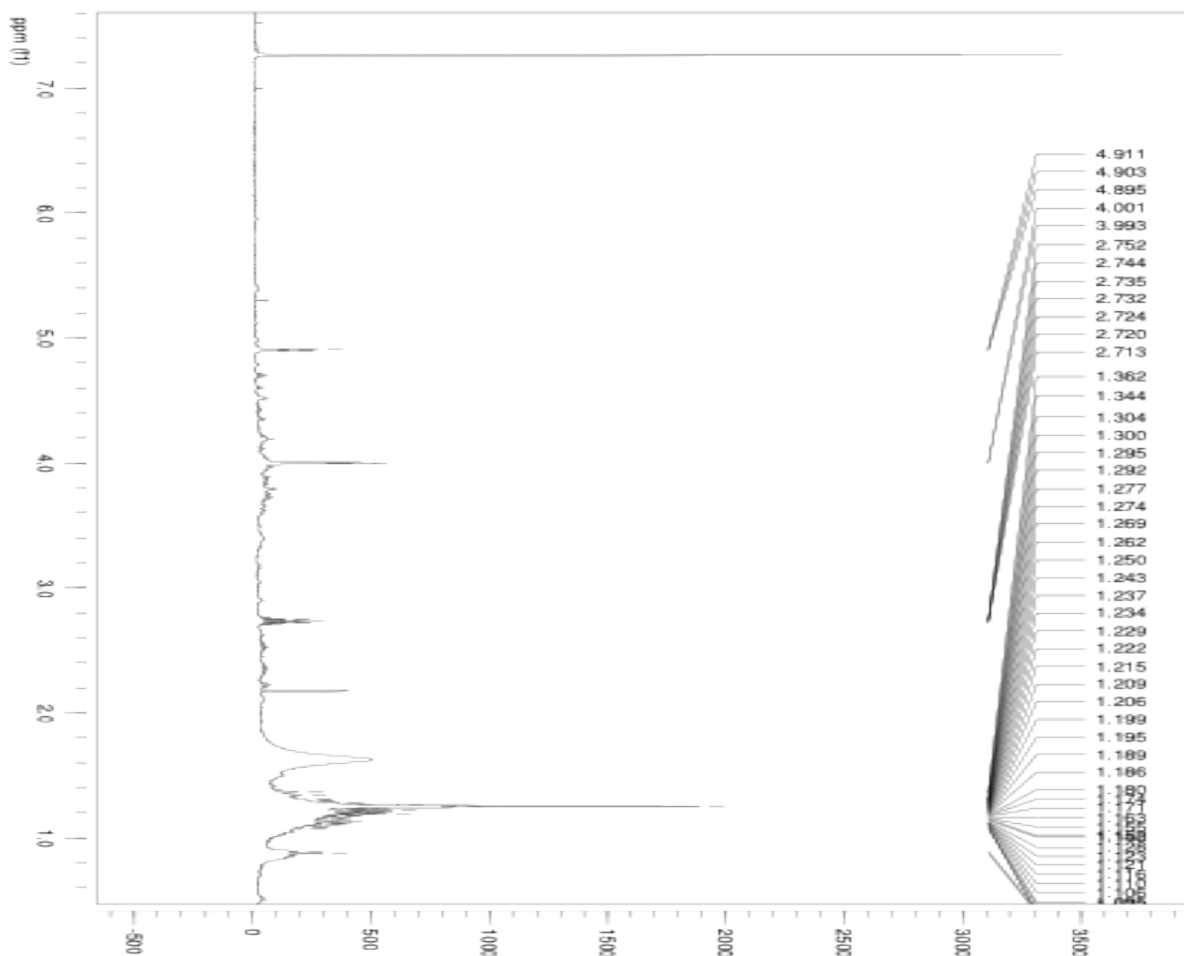
F2 - Acquisition Parameters
Date_    20090919
Time     13.25
INSTRUM  spect
PROBHD   5 mm QNP 1H/1
PULPROG  zg30
TD       39392
SOLVENT  CDCl3
NS       64
DS       2
SWH      7575.758 Hz
FIDRES   0.192317 Hz
AQ       2.5999219 sec
RG       128
DW       66.000 usec
DE       6.00 usec
TE       295.0 K
D1       1.50000000 sec
TD0      1

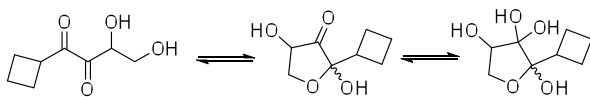
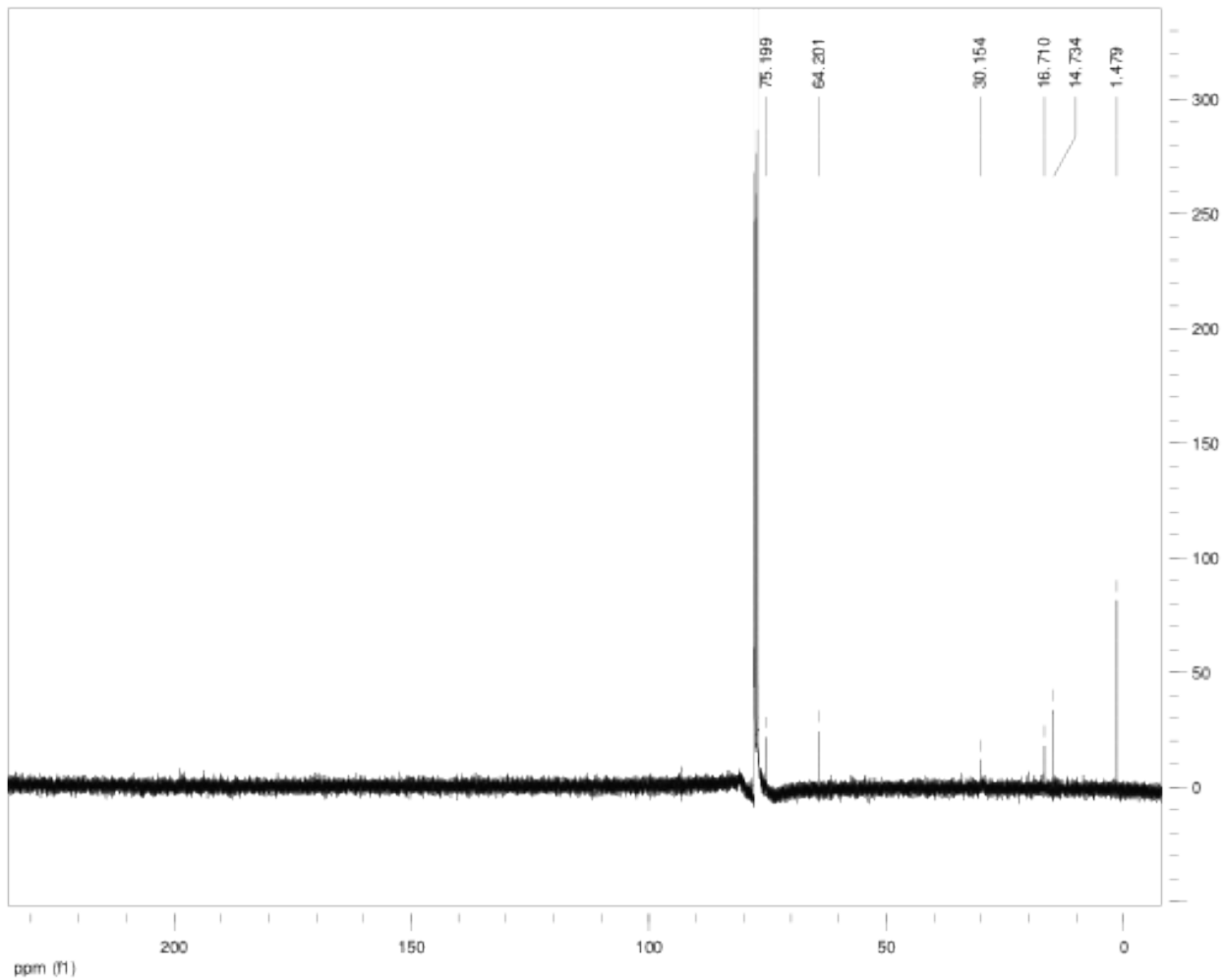
===== CHANNEL f1 =====
NUC1     1H
P1       10.00 usec
PL1      -4.00 dB
SFO1     399.7324685 MHz

F2 - Processing parameters
SI       32768
SF       399.7300000 MHz
WDW      EM
SSB      0
LB       0.30 Hz
GB       0
PC       2.00
  
```



Cyclopropyl-DPD (1-cyclopropyl-3,4-dihydroxybutane-1,2-dione) and cyclic compounds (119):





Cyclobutyl-DPD (1-cyclobutyl-3,4-dihydroxybutane-1,2-dione)

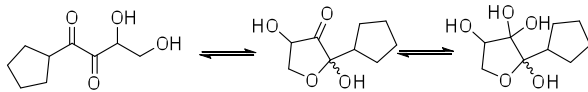


NAME cyclolobityl_cpd
EXPNO 2
PROCNO 1
Date_ 20091223
Time_ 9:38
INSTRUM spect
PROBHD 5 mm BBI
PULPROG zgpg30p2
TD 32768
SOLVENT D2O
NS 16
DS 4
SWH 8012.800 Hz
FIDRES 0.244532 Hz
AQ 2.0447731 sec
RG 812.7
DM 62.400 usec
DE 6.00 usec
TE 294.4 K
D1 7.0000000 sec
D12 0.0002000 sec
D16 0.0004000 sec
TDO 1

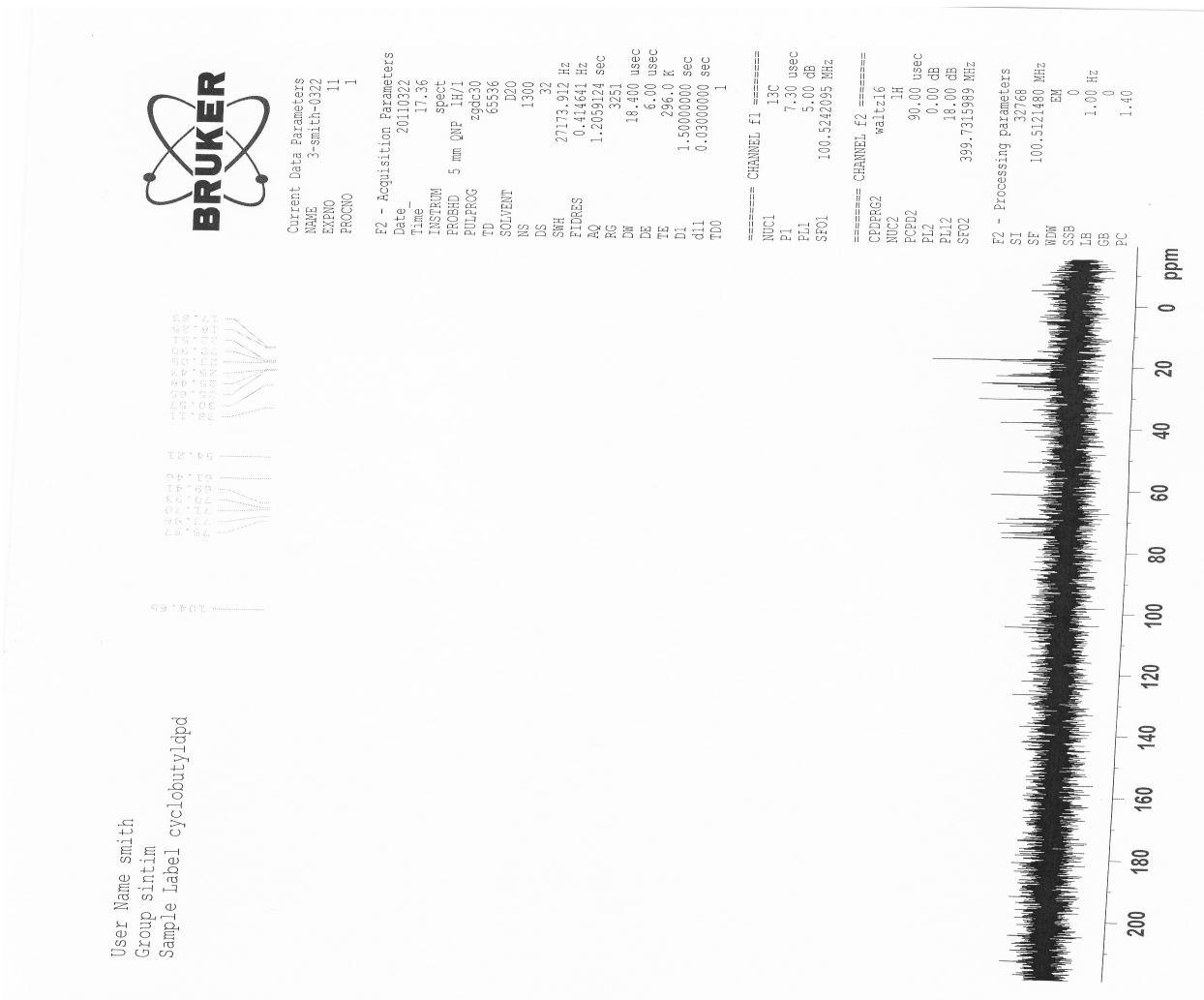
===== CHANNEL f1 =====
NUC1 1H
P1 7.30 usec
PL1 0.00 dB
PL2 45.00 dB
SFO1 400.1318627 MHz

===== GRADIENT CHANNEL =====
GPNM1 sine.100
GZG1 40.00 %
PLG 1000.00 usec
SL 32768
SF 400.1300174 MHz
WDW EM
SSB 0
LB 0.25 Hz
GB 0
PC 2.00





Cyclopentyl-DPD (1-cyclopentyl-3,4-dihydroxybutane-1,2-dione)





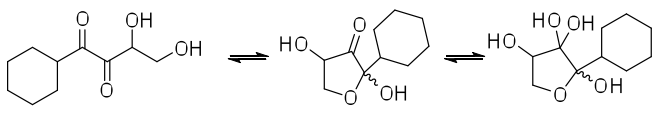
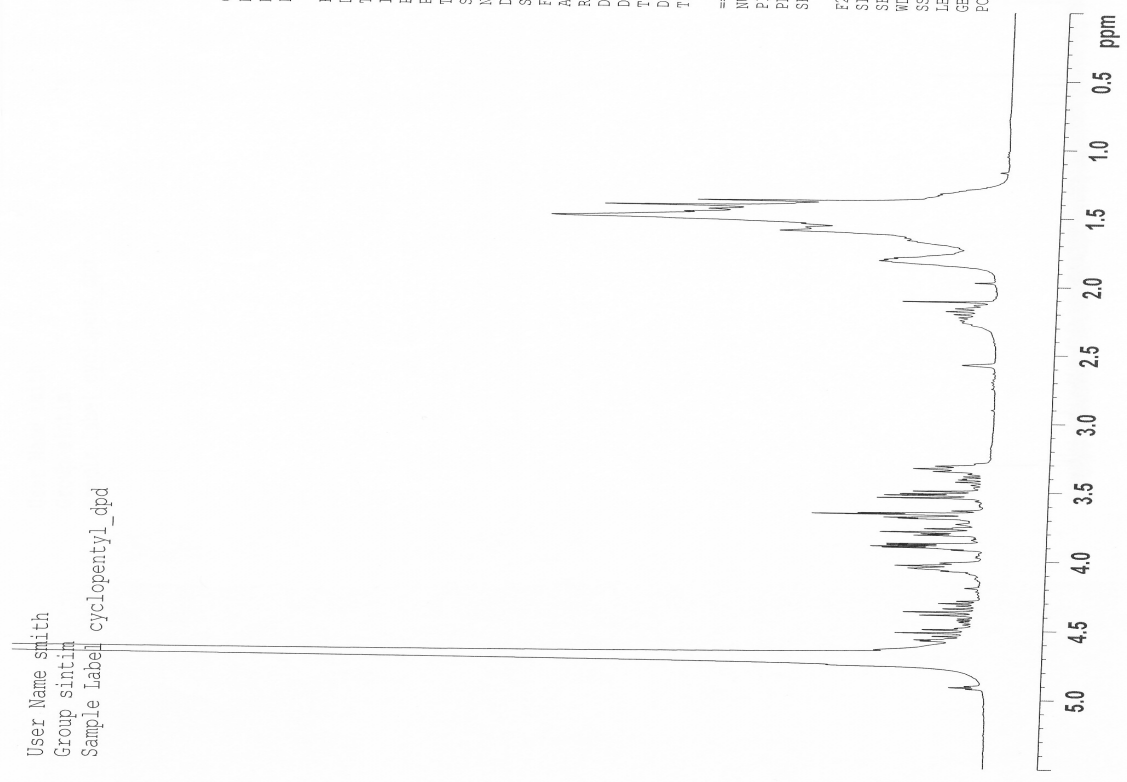
Current Data Parameters
NAME Z2-smith-0610
EXPNO 10
PROCNO 1

F2 - Acquisition Parameters
Date_ 20090610
Time_ 12.21
INSTRUM spect
PROBHD 5 mm QNP 1H/1
PULPROG zg30
TD 39392
SOLVENT D2O
NS 64
DS 2
SWH 7575.758 Hz
FIDRES 0.192317 Hz
AQ 2.5989219 sec
RG 40.3
DM 66.000 usec
DE 6.00 usec
TE 294.9 K
D1 1.50000000 sec
TDO 1

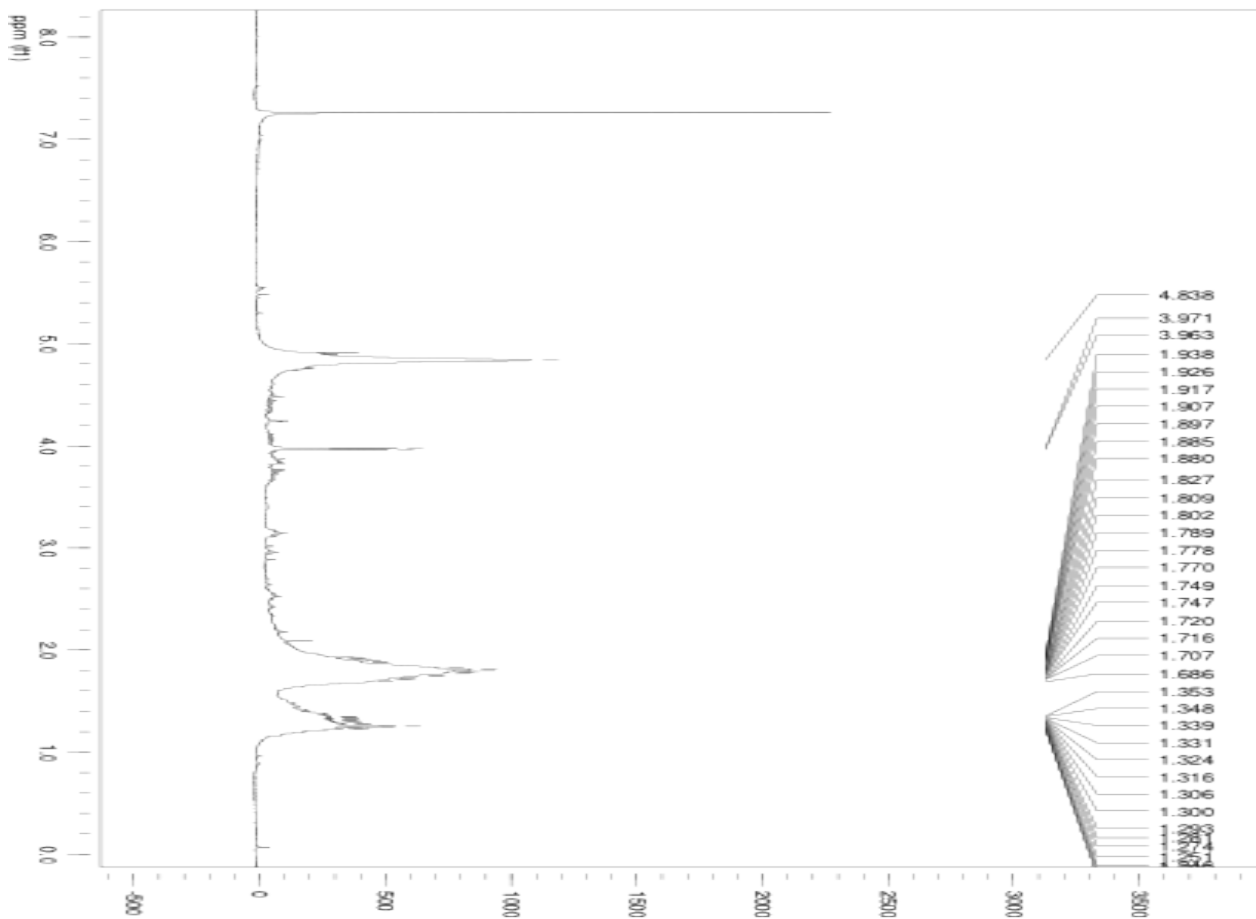
===== CHANNEL f1 =====
NUC1 1H
P1 10.00 usec
PL1 -4.00 dB
SFO1 399.7324685 MHz

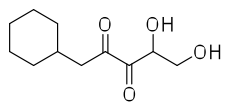
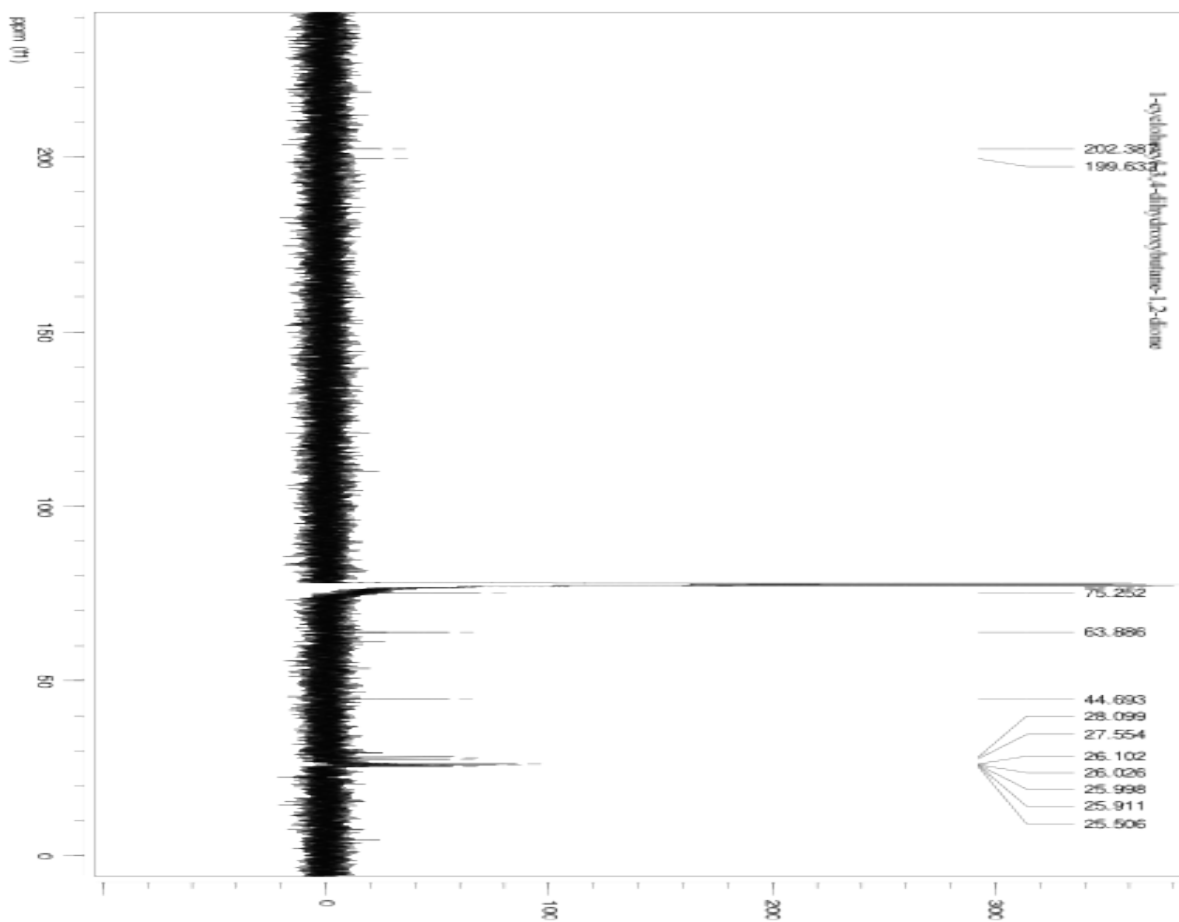
F2 - Processing parameters
SI 32768
SF 399.7300000 MHz
WDW EM
SSB 0
LB 0.30 Hz
GB 0
PC 2.00

User Name smith
Group sintim
Sample Label cyclopentyl_dpd

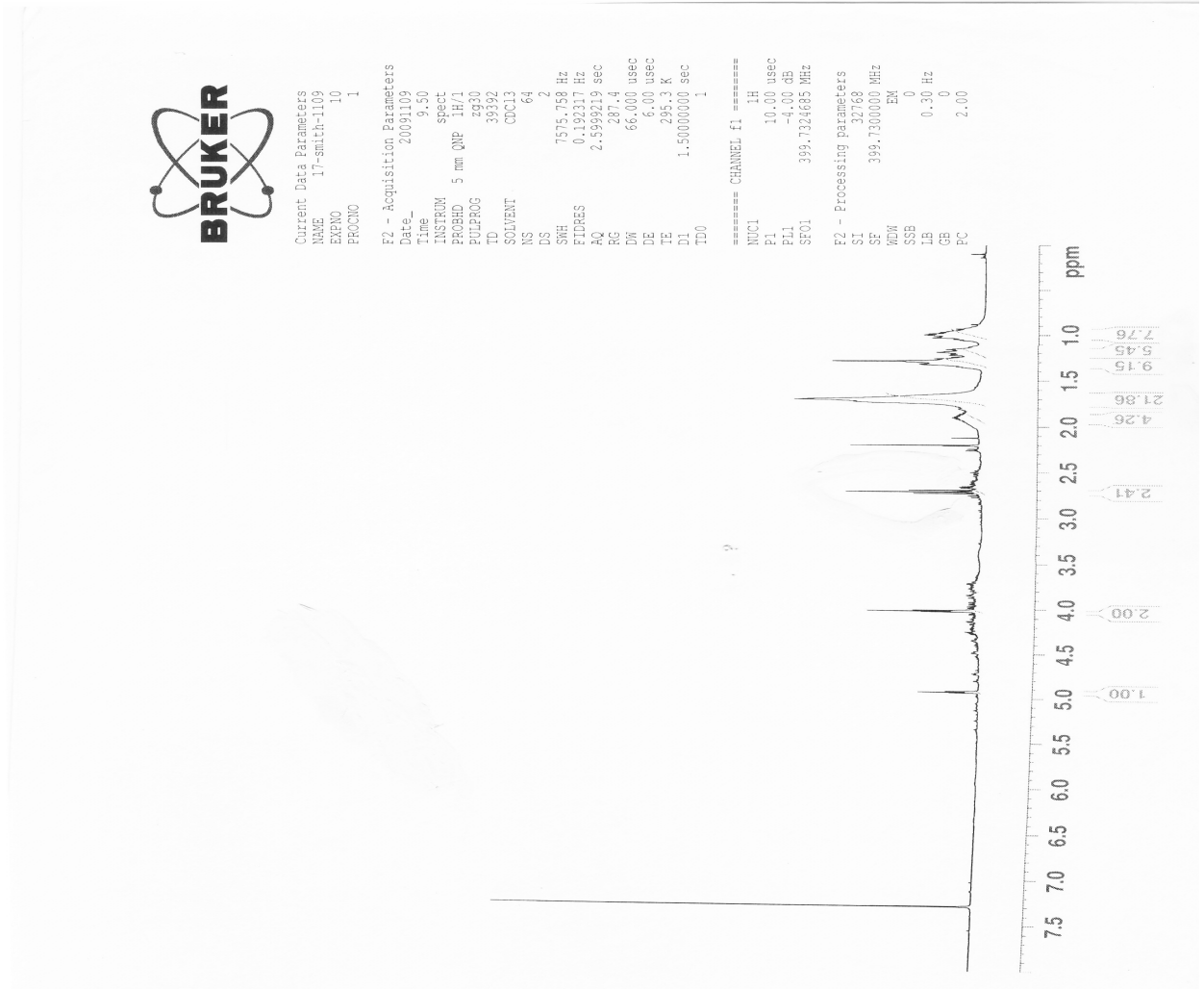


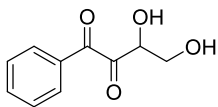
Cyclohexyl-DPD (1-cyclohexyl-3,4-dihydroxybutane-1,2-dione) and cyclic compounds (122):



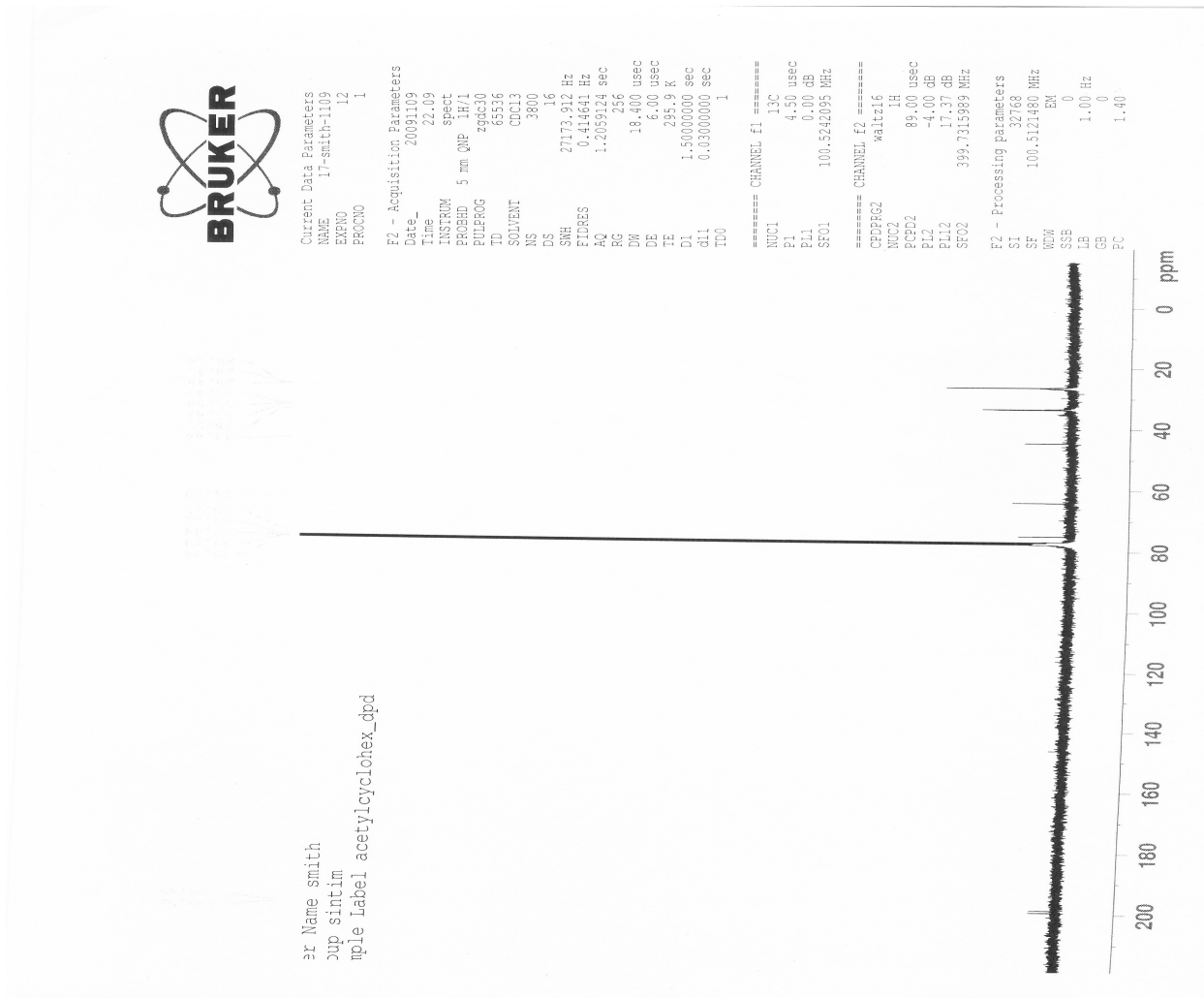


CH₂-Cyclohexyl-DPD(1-cyclohexyl-4,5-dihydroxypentane-2,3-dione):





Phenyl-DPD (3,4-dihydroxy-1-phenyl-butane-1,2-dione) (125):



User Name smith
Group sintim
Sample Label phenyl.dpd

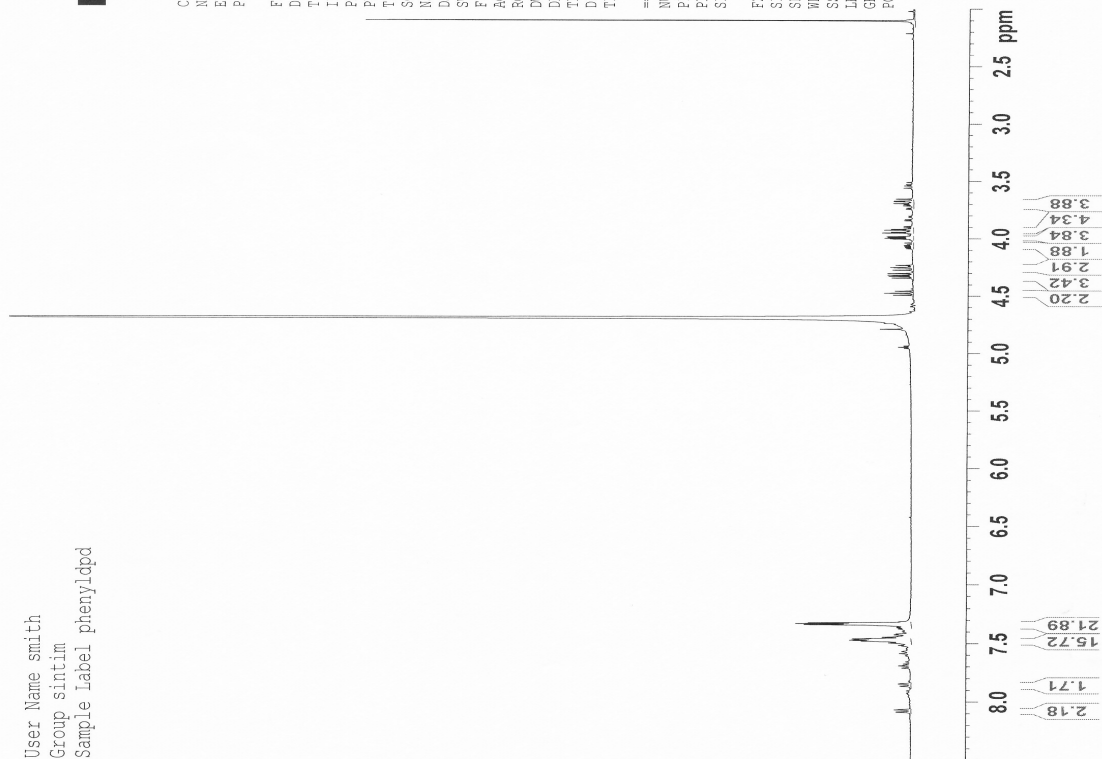


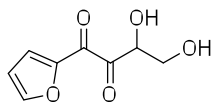
Current Data Parameters
NAME 4-smith-0322
EXPNO 10
PROCNO 1

F2 - Acquisition Parameters
Date_ 20110322
Time 15.34
INSTRUM spect
PROBHD 5 mm QNP 1H/1
PULPROG zg30
TD 39392
SOLVENT D2O
NS 64
DS 2
SWH 7575.758 Hz
FIDRES 0.192317 Hz
AQ 2.9399219 sec
RG 128
DM 66.000 usec
DE 6.00 usec
TE 295.5 K
D1 1.5000000 sec
TD0 1

==== CHANNEL f1 =====
NUC1 1H
P1 11.50 usec
PL1 0.00 dB
SFO1 399.7324685 MHz

F2 - Processing parameters
SI 32768
SF 399.7300000 MHz
WDW EM
SSB 0
LB 0.30 Hz
GB 0
PC 2.00





Furanoyl-DPD (1-(furan-2-yl)-3,4-dihydroxybutane-1,2-dione) (126):

User Name smith
 Group sintim
 Sample Label phenyl0pbd



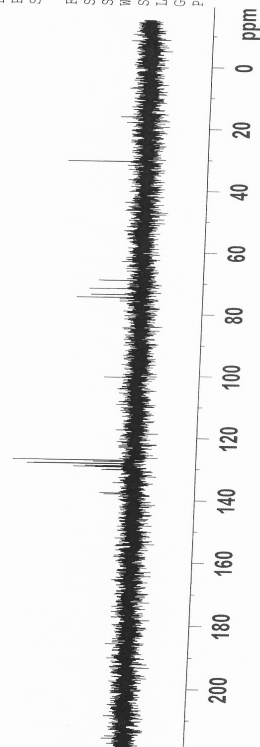
Current Data Parameters
 NAME 4-smith-0322
 EXPNO 11
 PROCNO 1

F2 - Acquisition Parameters
 Date_ 20110322
 Time 18:52
 INSTRUM spect
 PROBHD 5 mm QNP 1H/1
 TD 494030
 SOLVENT agdc30
 NS 6536
 DS 2
 SWH 27113.912 Hz
 FIDRES 0.414641 Hz
 AQ 1.2059124 sec
 RG 3649.1
 DW 18.400 usec
 DE 6.00 usec
 TE 295.9 K
 D1 1.50000000 sec
 d11 0.03000000 sec
 TDO 1

==== CHANNEL f1 =====
 NUC1 13C
 P1 7.30 usec
 PL1 5.00 dB
 SF01 100.5242095 MHz

==== CHANNEL f2 =====
 CPDPRG2 waltz16
 NUC2 1H
 PCPD2 90.00 usec
 PL2 0.00 dB
 PLL2 18.00 dB
 SF02 399.7315989 MHz

F2 - Processing parameters
 SI 32768
 SF 100.512180 MHz
 WDW EM
 SSB 0
 LB 1.00 Hz
 GB 0
 PC 1.40



8.52
 8.34
 8.16
 7.98
 7.80
 7.62
 7.44
 7.26
 7.08
 6.90
 6.72
 6.54
 6.36
 6.18
 6.00
 5.82
 5.64
 5.46
 5.28
 5.10
 4.92
 4.74
 4.56
 4.38
 4.20
 4.02
 3.84
 3.66
 3.48
 3.30
 3.12
 2.94
 2.76
 2.58
 2.40
 2.22
 2.04
 1.86
 1.68
 1.50
 1.32
 1.14
 0.96
 0.78
 0.60
 0.42
 0.24
 0.06

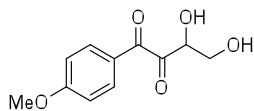
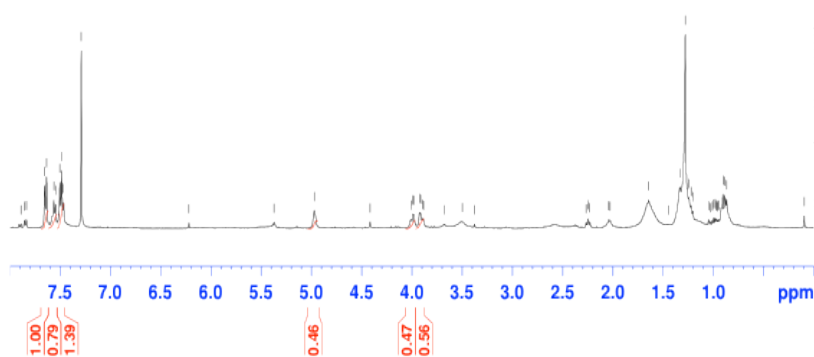


Current Data Parameters
 NAME 47-smith-0919
 EXPNO 10
 PROCNO 1

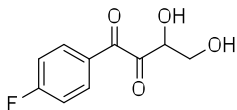
F2 - Acquisition Parameters
 Date_ 20090919
 Time 16.47
 INSTRUM spect
 PROBHD 5 mm QNP 1H/1
 PULPROG zg30
 TD 33392
 SOLVENT CDCl3
 NS 64
 DS 2
 SWH 7575.758 Hz
 FIDRES 0.192317 Hz
 AQ 2.5999219 sec
 RG 362
 DW 66.000 usec
 DE 6.00 usec
 TE 295.2 K
 D1 1.5000000 sec
 TD0 1

===== CHANNEL f1 =====
 NUC1 1H
 P1 10.00 usec
 PL1 -4.00 dB
 SF01 399.7324685 MHz

F2 - Processing parameters
 SI 32768
 SF 399.7300000 MHz
 MDW EM
 SSB 0
 LB 0.30 Hz
 GB 0
 PC 2.00



Methoxyphenyl-DPD (3,4-dihydroxy-1-(4-methoxyphenyl)butane-1,2-dione):



Fluorophenyl-DPD (1-(4-fluorophenyl)-3,4-dihydroxybutane-1,2-dione):

Ah1
 also named as Aproton
 Aug 8, 2009 yflam TOPspin1.8
 The application can be used for

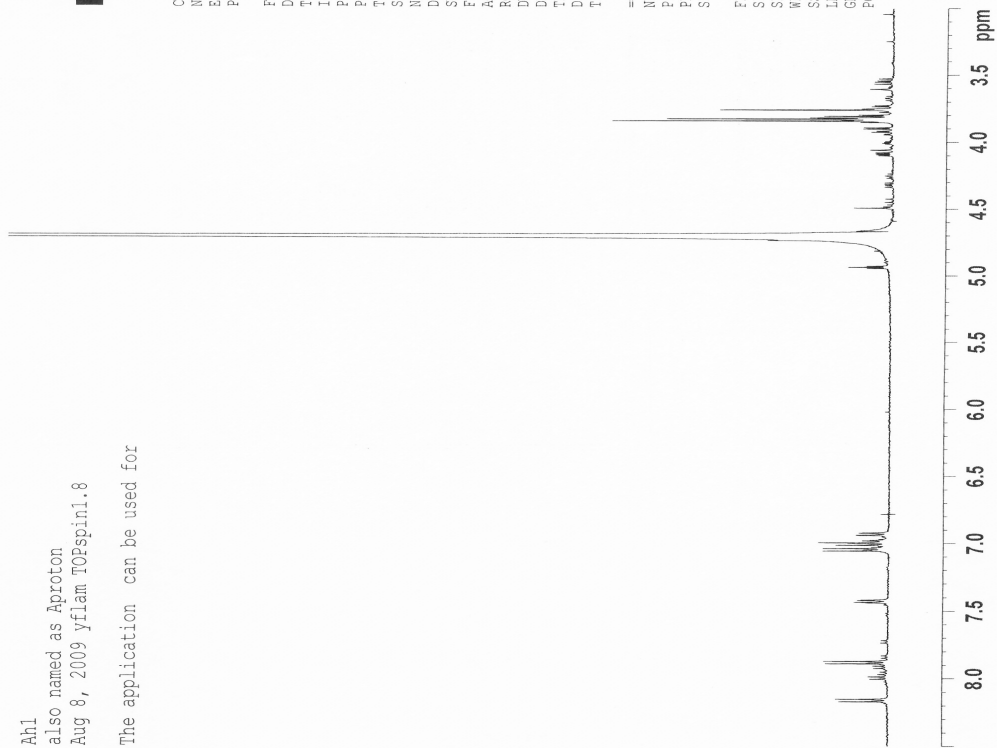


Current Data Parameters
 NAME methoxyphenyl_dpd
 EXPRNO 1
 PROCNO 1

F2 - Acquisition Parameters
 Date_ 20100301
 Time_ 9.43
 INSTRUM spect
 PROBRD 5 mm BBO2 new
 PULPROG zg30
 TD 66560
 SOLVENT D2O
 NS 16
 DS 2
 SWH 8012.820 Hz
 FIDRES 0.120385 Hz
 AQ 4.1533942 sec
 RG 80.6
 DW 62.400 usec
 DE 6.50 usec
 TE 296.0 K
 D1 1.0000000 sec
 TDO 1

===== CHANNEL f1 =====
 NUC1 1H
 P1 11.10 usec
 PL1 0.00 dB
 SFO1 500.1330018 MHz

F2 - Processing parameters
 SI 32768
 SF 500.1300000 MHz
 WDW EM
 SSB 0
 LB 0.30 Hz
 GB 0
 EC 1.00





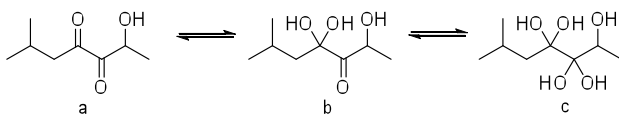
Current Data Parameters
NAME fluorophenyl_dpd
EXPNO 2
PROCNO 1

F2 - Acquisition Parameters
Date_ 20100301
Time 12.44
INSTRUM spect
PROBHD 5 mm BBO2 new
PULPROG zg30
TD 66560
SOLVENT CDCl3
NS 128
DS 2
SWH 8012.820 Hz
FIDRES 0.120385 Hz
AQ 4.1533942 sec
RG 161.3
DW 62.400 usec
DE 6.50 usec
TE 296.6 K
D1 1.00000000 sec
TD0 1

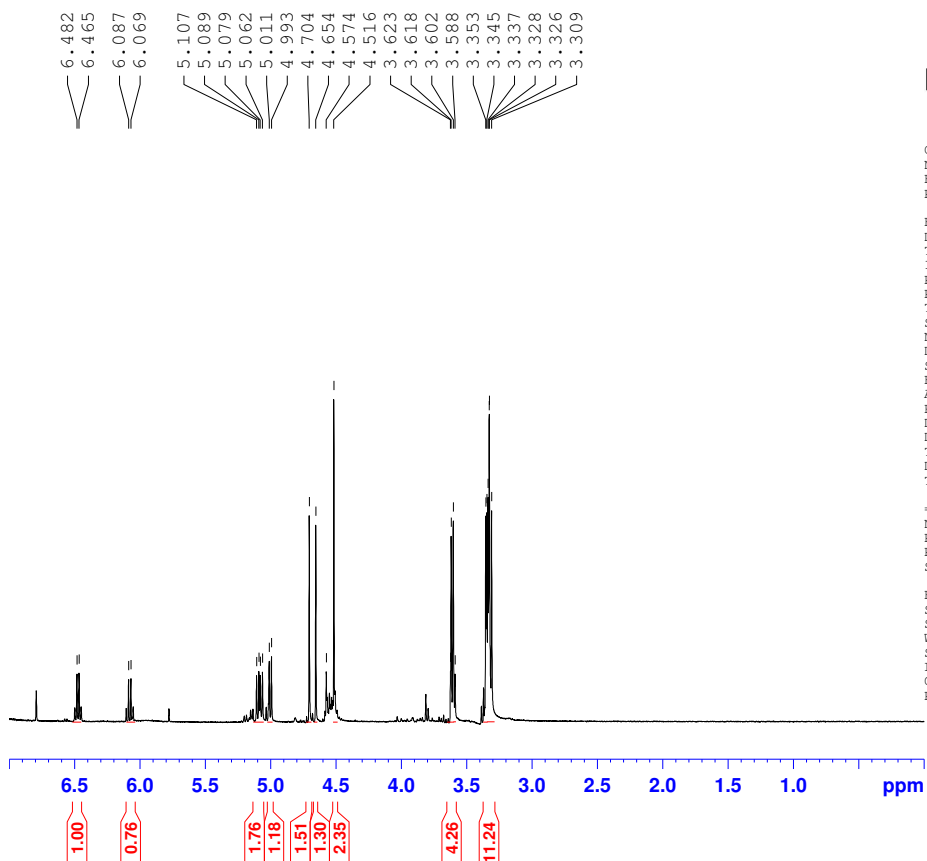
==== CHANNEL f1 =====
NUC1 1H
P1 11.10 usec
PL1 0.00 dB
SFO1 500.1330008 MHz

F2 - Processing parameters
SI 32768
SF 500.1300000 MHz
WDW EM
SSB 0
LB 0.30 Hz
GB 0
PC 1.00

Ah1
also named as Aproton
Aug 8, 2009 yflam TOPSpin1.8
The application can be used for



Deoxy-Isobutyl DPD (134b):

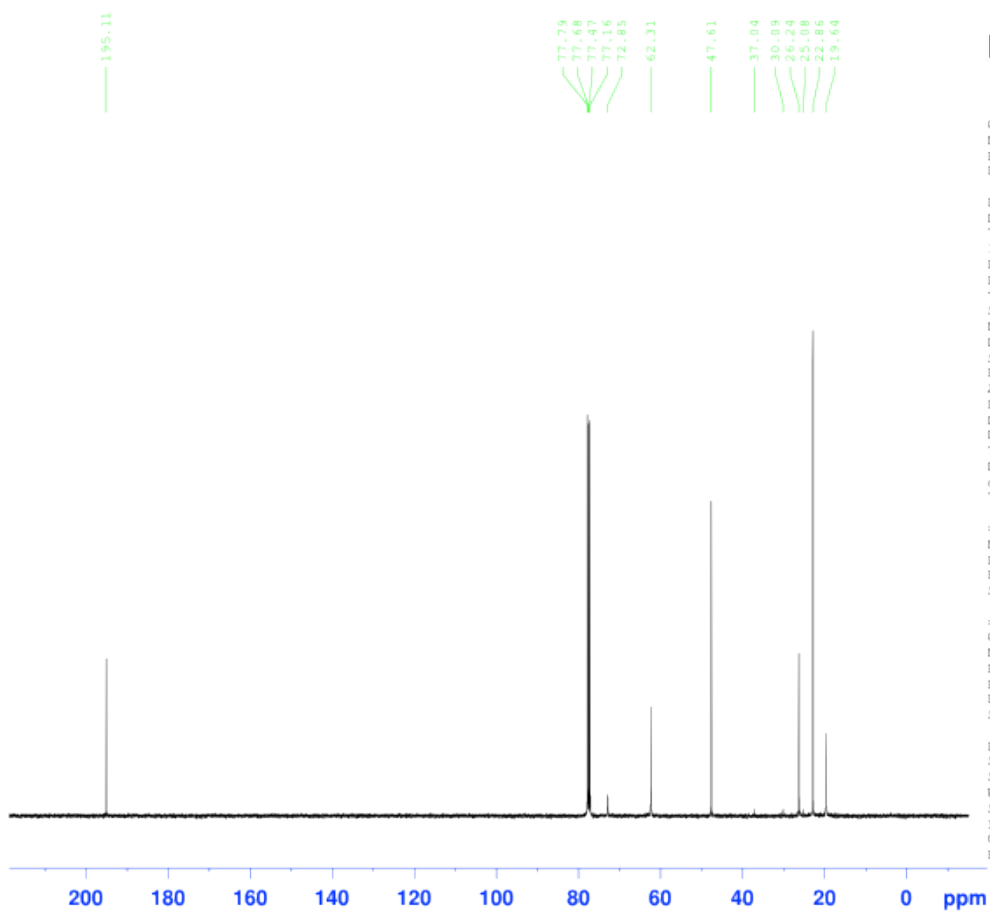


Current Data Parameters
 NAME 20-smith-1012
 EXPNO 11
 PROCNO 1

F2 - Acquisition Parameters
 Date_ 20091012
 Time_ 9.12
 INSTRUM spect
 PROBHD 5 mm QNP 1H/1
 PULPROG zg30
 TD 39392
 SOLVENT D2O
 NS 64
 DS 2
 SWH 7575.758 Hz
 FIDRES 0.192317 Hz
 AQ 2.5999219 sec
 RG 128
 DW 66.000 usec
 DE 6.00 usec
 TE 295.0 K
 D1 1.5000000 sec
 TD0 1

===== CHANNEL f1 =====
 NUC1 1H
 P1 10.00 usec
 PL1 -4.00 dB
 SF01 399.7324685 MHz

F2 - Processing parameters
 SI 32768
 SF 399.7300000 MHz
 WDW EM
 SSB 0
 LB 0.30 Hz
 GB 0
 PC 2.00



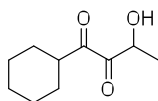
Current Data Parameters
 NAME 51-smith-1009
 EXPNO 11
 PROCNO 1

F2 - Acquisition Parameters
 Date_ 20091009
 Time 18.53
 INSTRUM spect
 PROBHD 5 mm QNP 1H/1
 PULPROG zgpg30
 TD 65536
 SOLVENT CDCl3
 NS 1300
 DS 32
 SWH 27173.912 Hz
 FIDRES 0.414641 Hz
 AQ 1.2059124 sec
 RG 322.5
 DW 18.400 usec
 DE 6.00 usec
 TE 295.7 K
 D1 1.50000000 sec
 d11 0.03000000 sec
 TDO 1

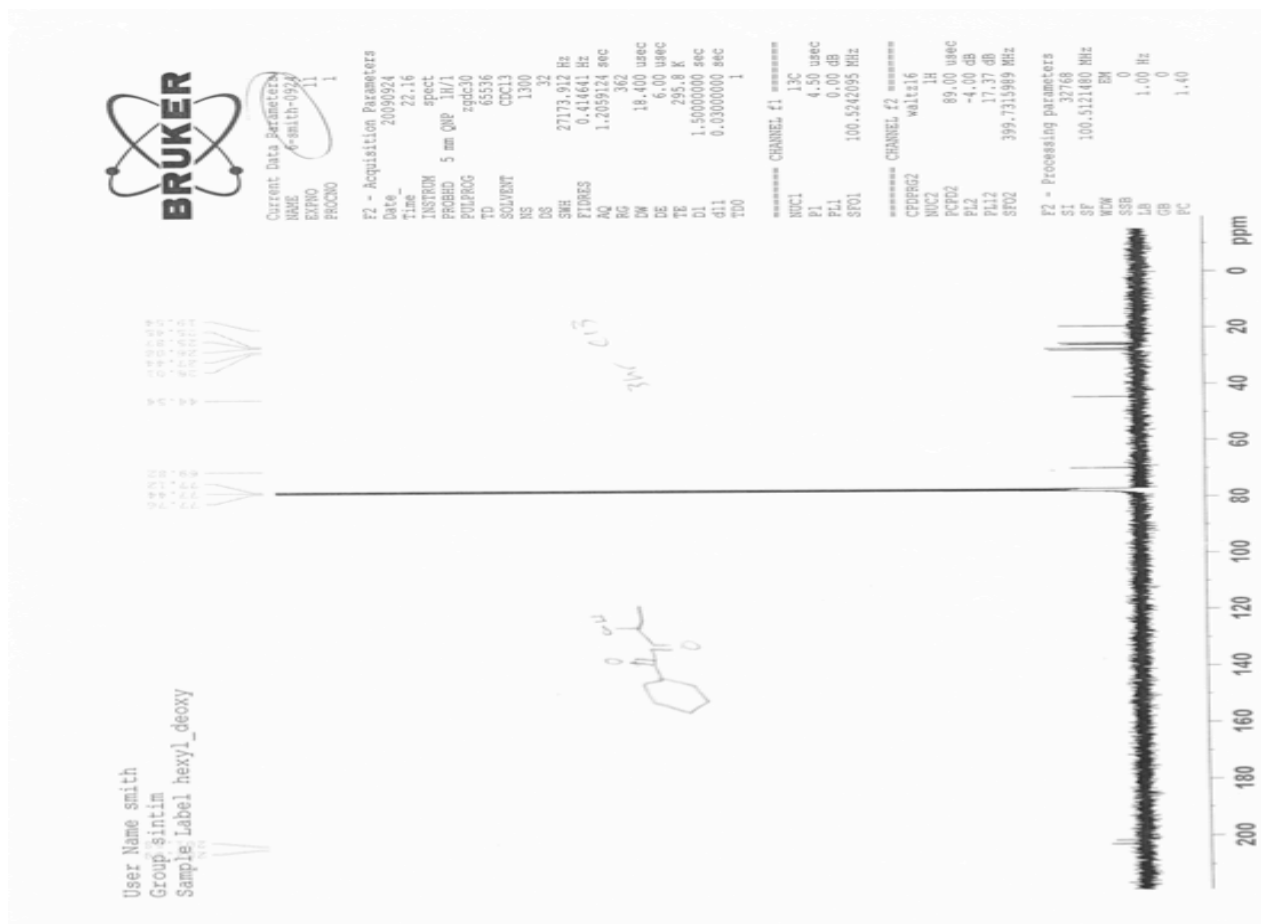
===== CHANNEL f1 =====
 NUC1 13C
 P1 4.50 usec
 PL1 0.00 dB
 SFO1 100.5242095 MHz

===== CHANNEL f2 =====
 CPDPRG2 waltz16
 NUC2 1H
 P1 89.00 usec
 PL2 -4.00 dB
 PL12 17.37 dB
 SFO2 399.7315989 MHz

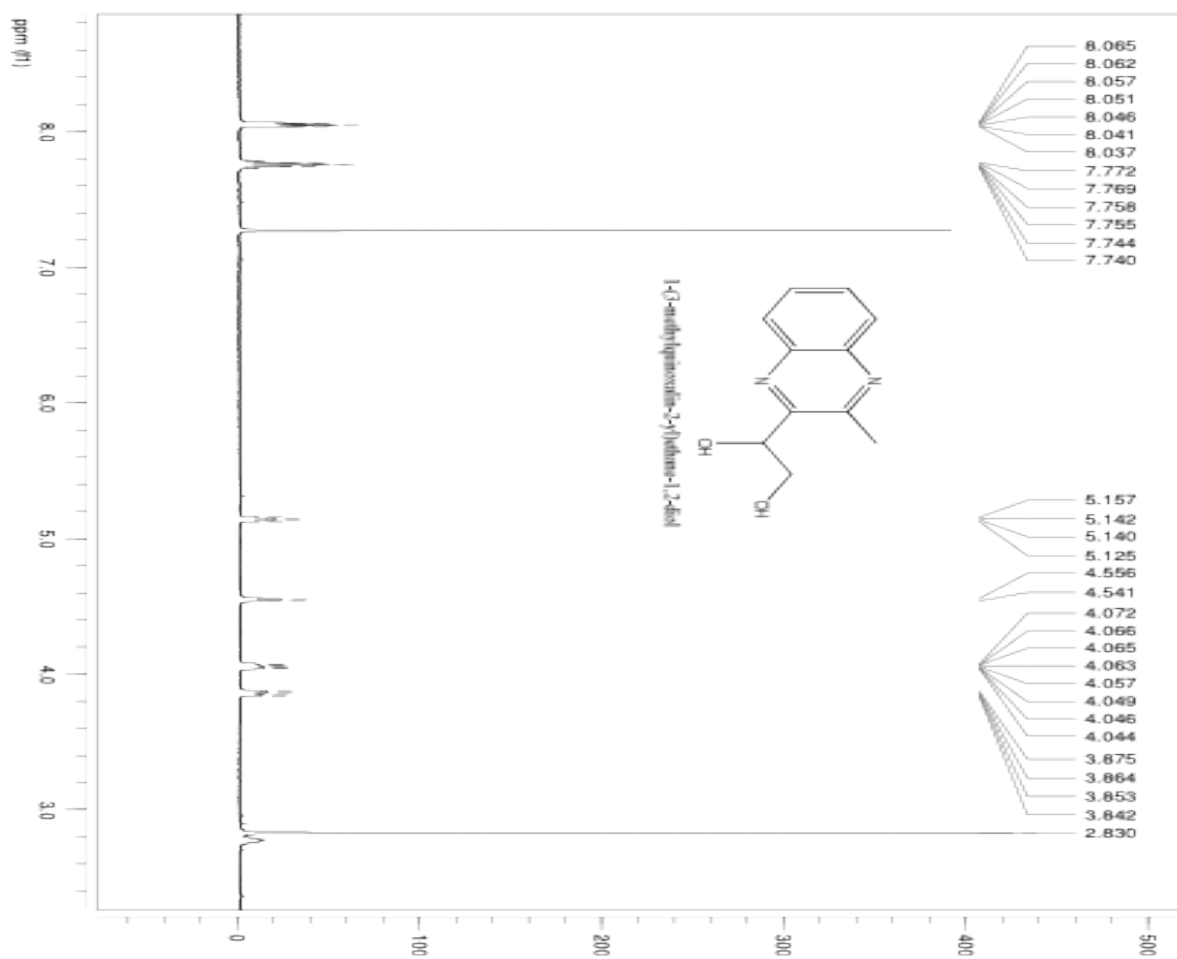
F2 - Processing parameters
 SI 32768
 SF 100.5121480 MHz
 WDW EM
 SSB 0
 LB 1.00 Hz
 GB 0
 PC 1.40

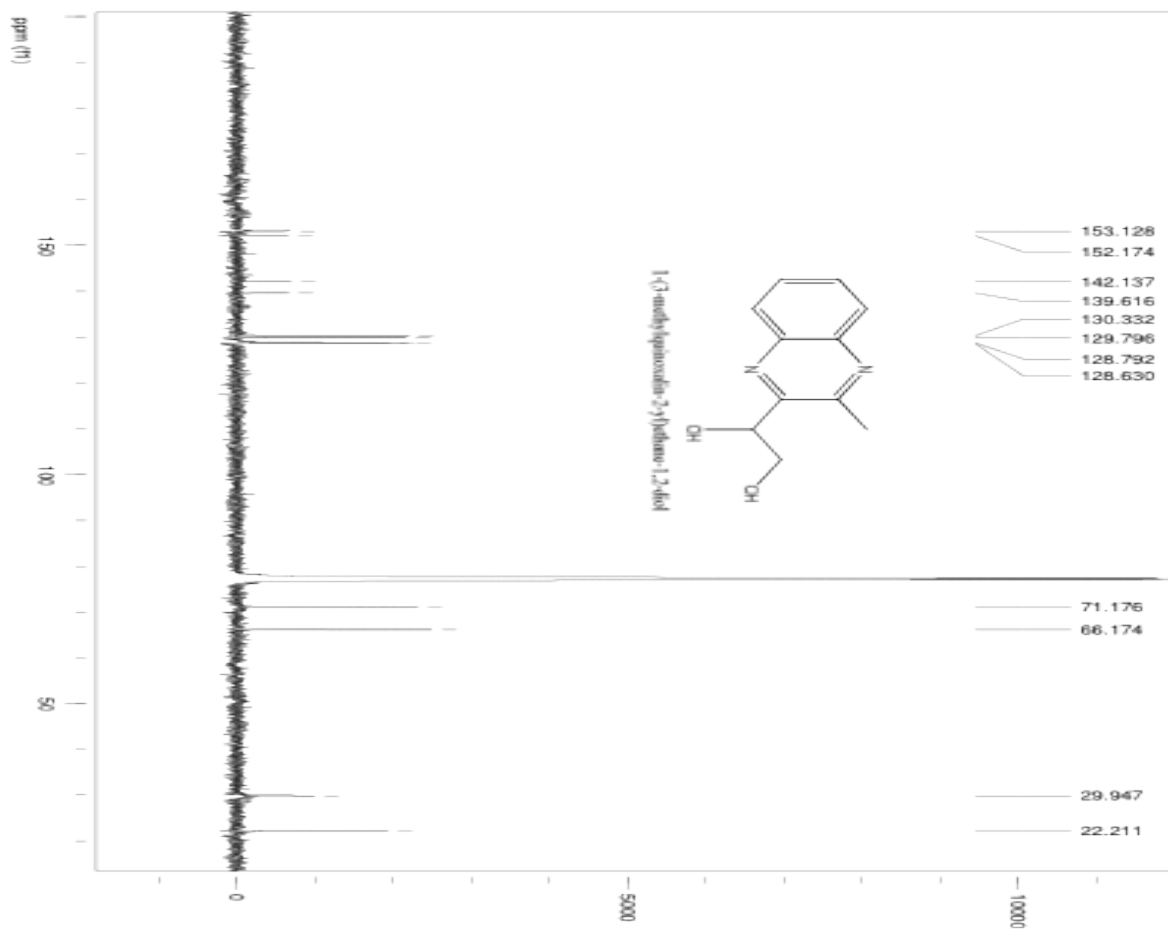


1-cyclohexyl-3-hydroxybutane-1,2-dione (134c):

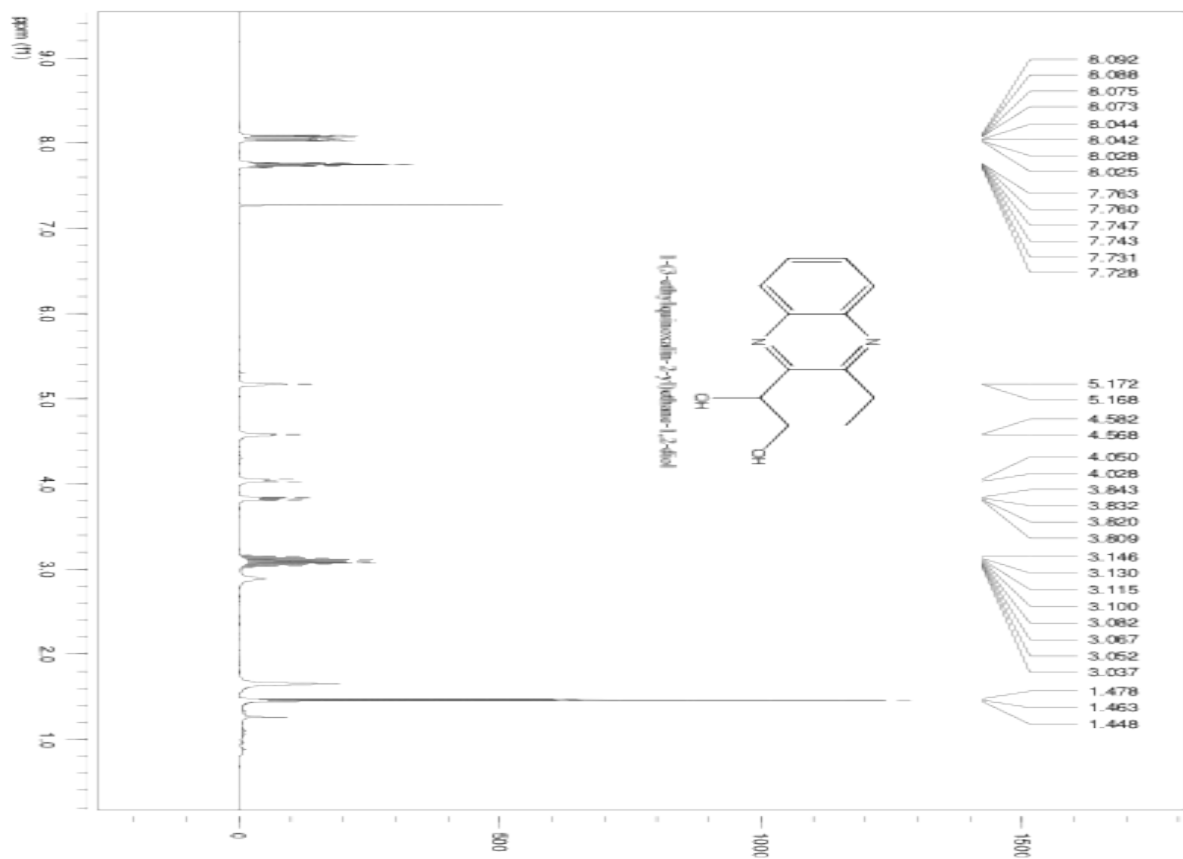


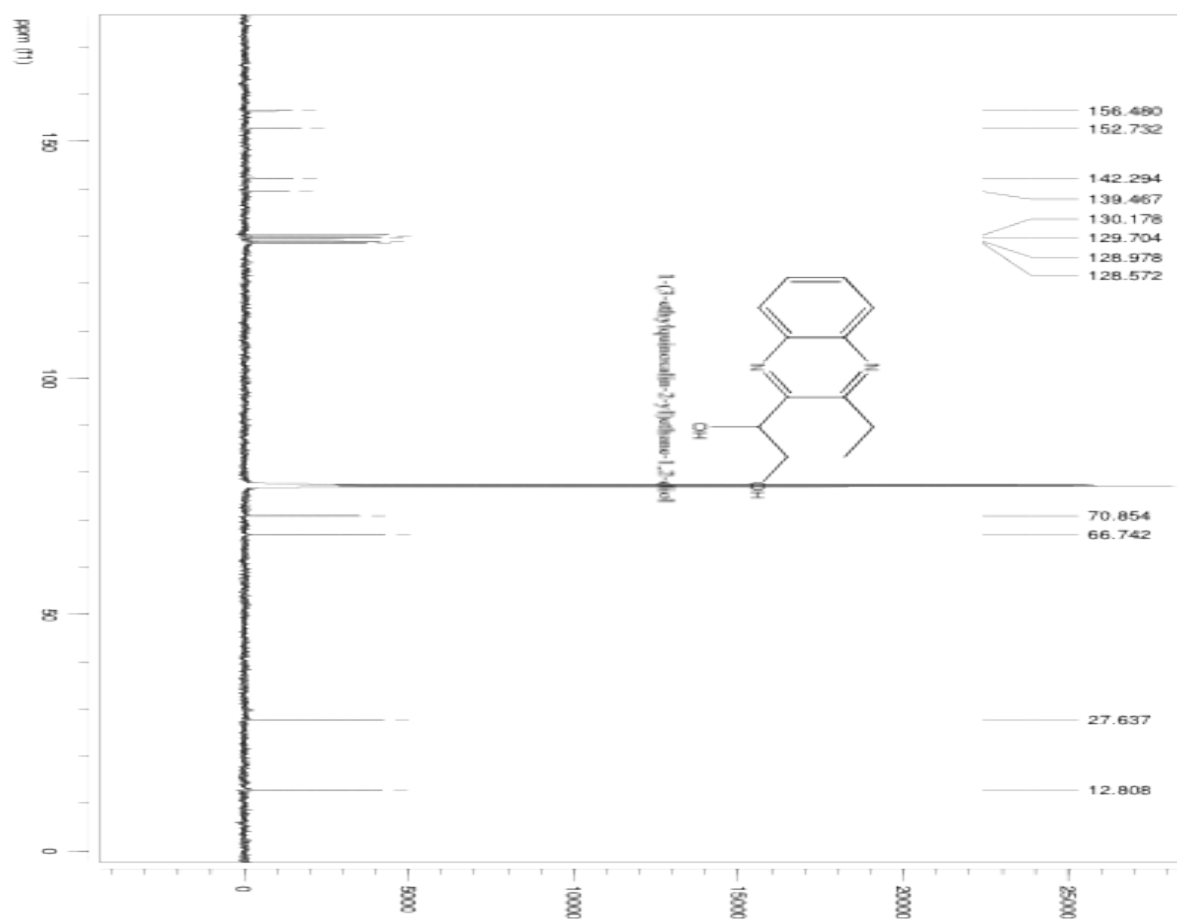
1-(3-methylquinoxalin-2-yl)ethane-1,2-diol (S27):



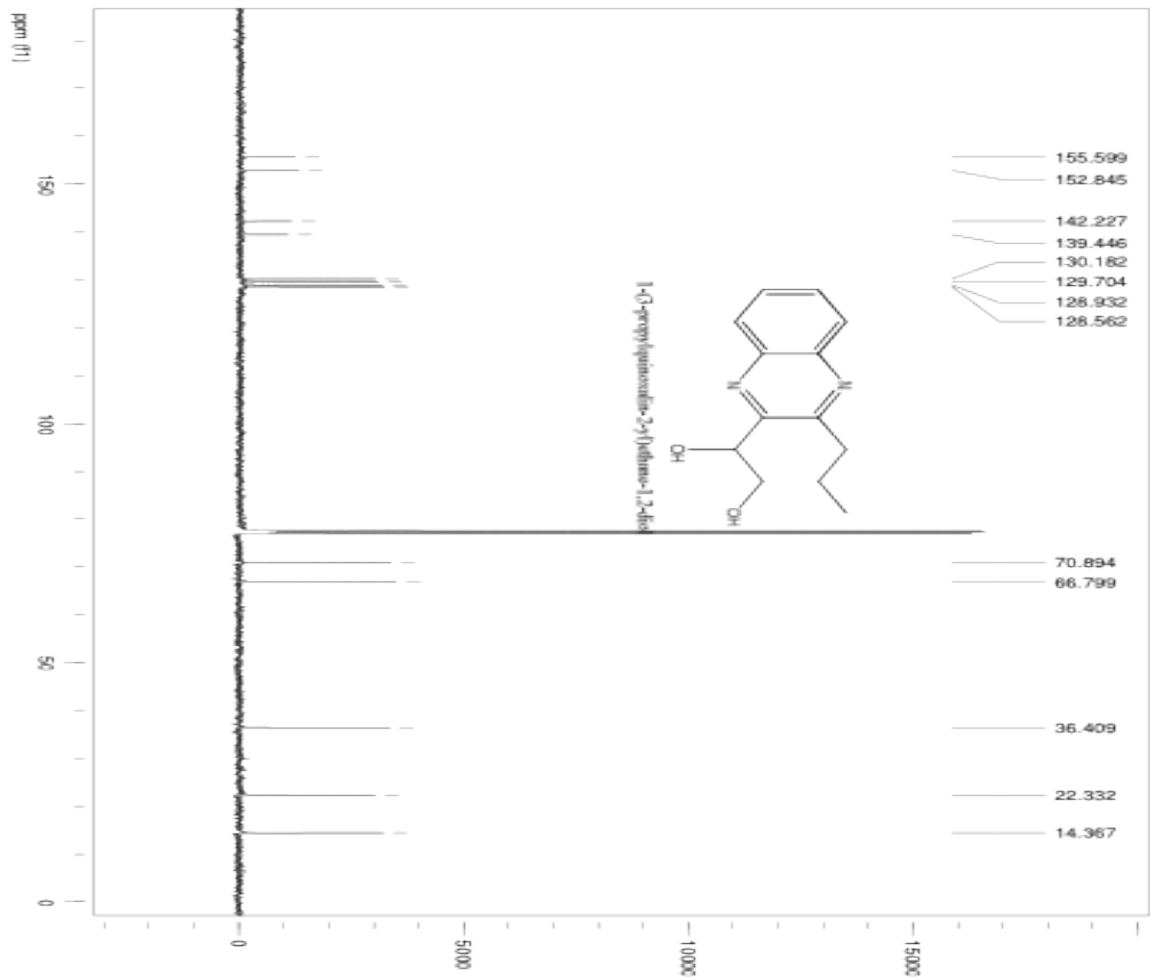


1-(3-ethylquinoxalin-2-yl)ethane-1,2-diol (S28):

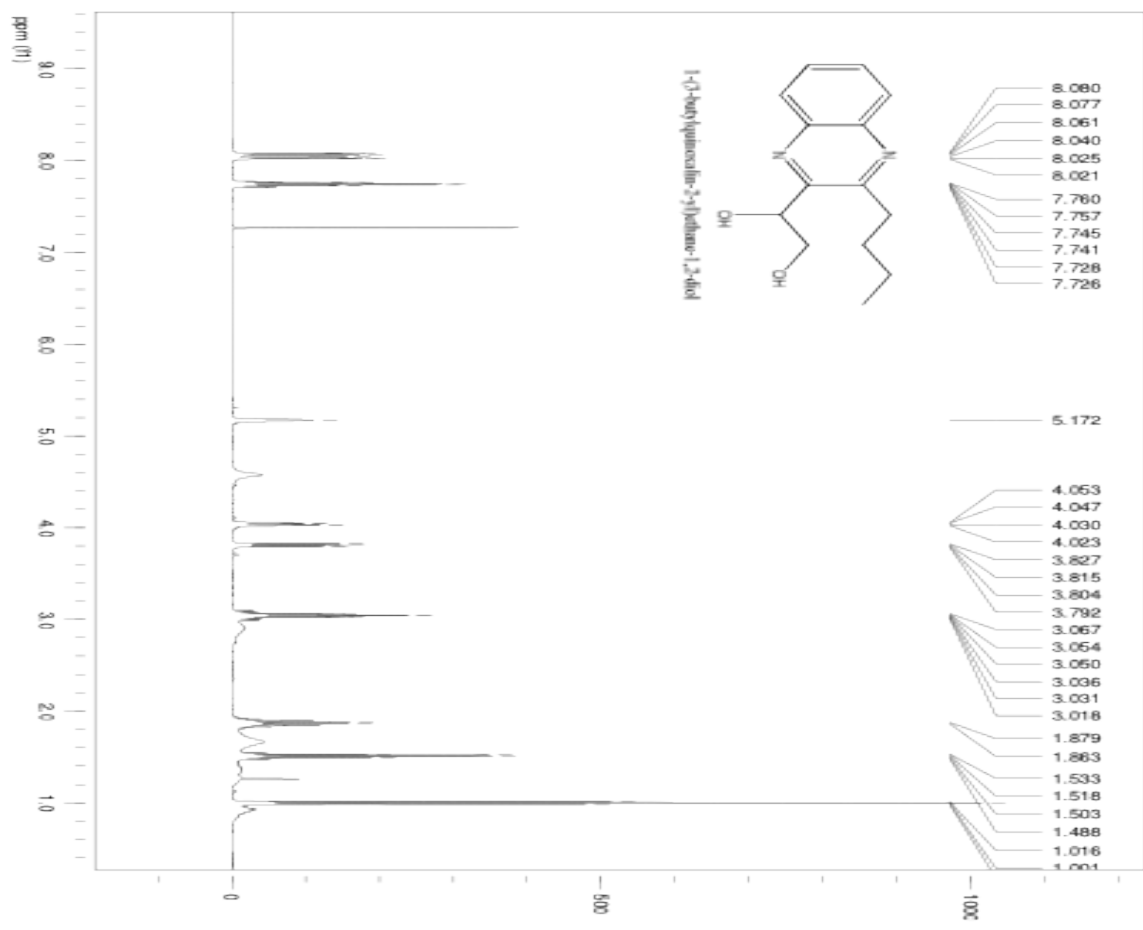


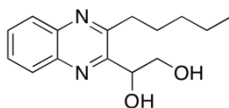
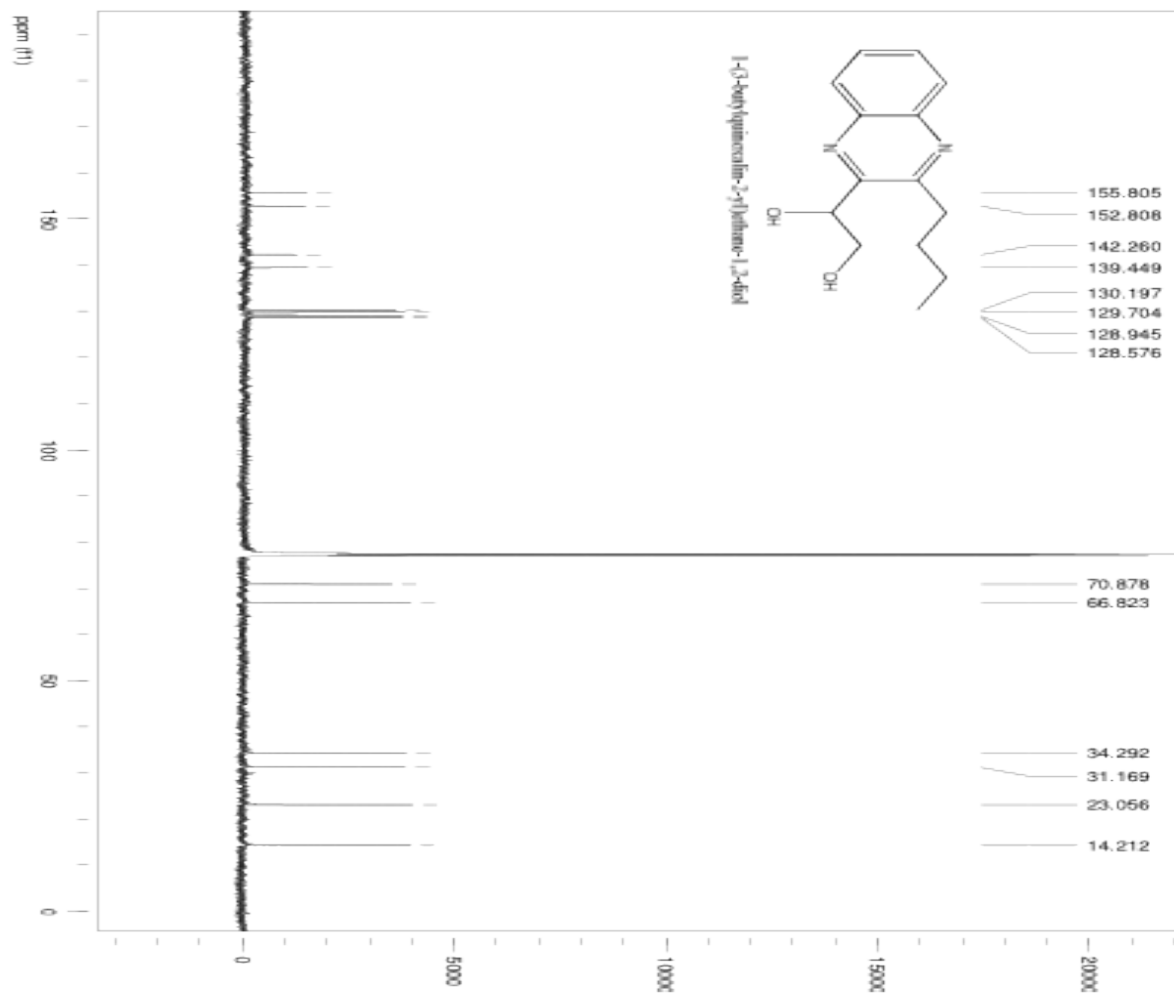


1-(3-propylquinoxalin-2-yl)ethane-1,2-diol (S29):



1-(3-butylquinoxalin-2-yl)ethane-1,2-diol (S30):





1-(3-pentylquinoxalin-2-yl) ethane-1,2-diol (S31):

8.081
8.078
8.064
8.062
8.039
8.037
8.024
8.020
7.759
7.756
7.744
7.739
7.727
7.724
7.270
5.181
5.175
5.170
5.163
4.053
4.047
4.030
4.024
3.826
3.814
3.803
3.058
3.045
3.041
3.027
3.022
3.009
1.913
1.897
1.895
1.881
1.865
1.464
1.450
1.427
1.413
0.949
0.935
0.921

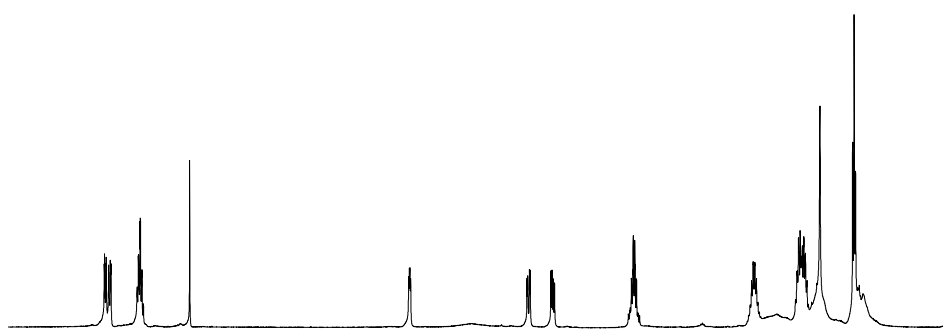


Current Data Parameters
NAME C5H11_quinoxaline
EXPNO 1
PROCNO 1

F2 - Acquisition Parameters
Date_ 20090810
Time 11.45
INSTRUM spect
PROBHD 5 mm BBO2 new
PULPROG zg
TD 65536
SOLVENT CDC13
NS 16
DS 2
SWH 6510.417 Hz
FIDRES 0.099341 Hz
AQ 5.0332146 sec
RG 181
DW 76.800 usec
DE 9.00 usec
TE 296.6 K
D1 4.0000000 sec
TDO 1

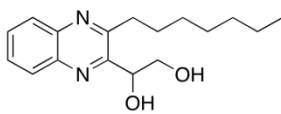
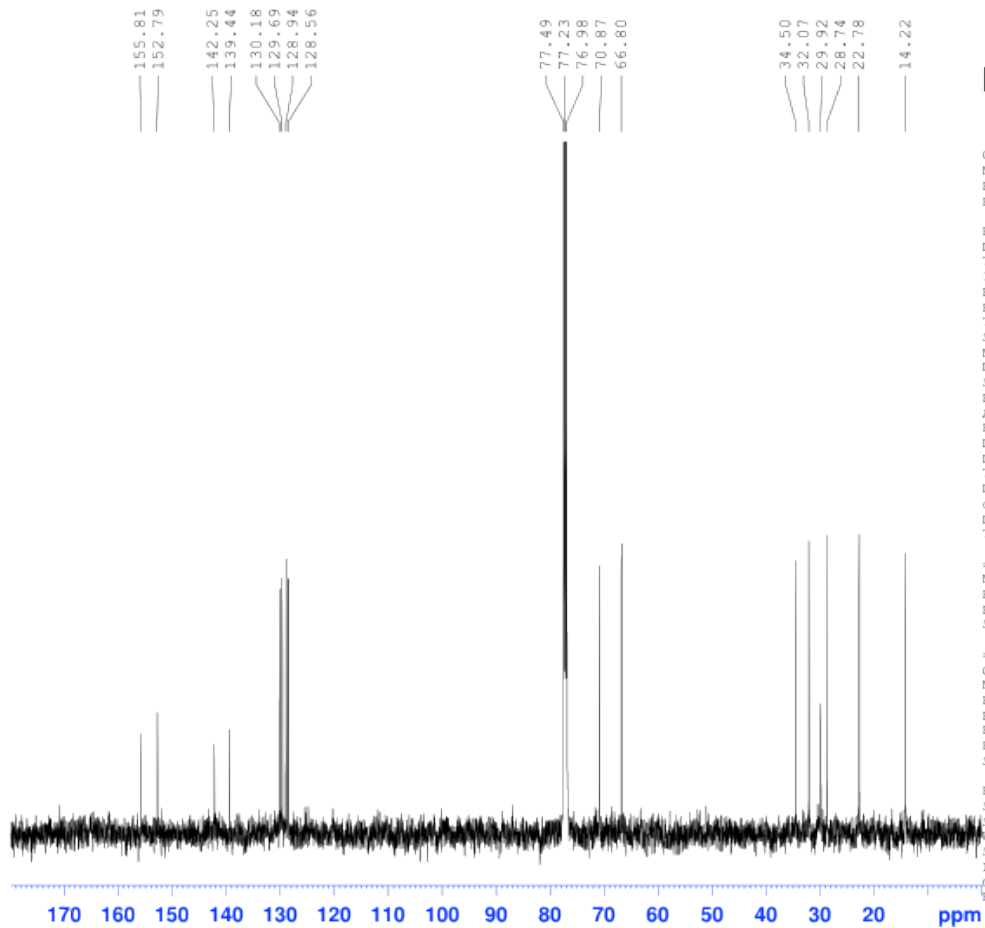
===== CHANNEL f1 =====
NUC1 1H
P1 11.10 usec
PL1 0.00 dB
SFO1 500.1330008 MHz

F2 - Processing parameters
SI 32768
SF 500.1300082 MHz
WDW EM
SSB 0
LB 0.30 Hz
GB 0
PC 1.00



8.5 8.0 7.5 7.0 6.5 6.0 5.5 5.0 4.5 4.0 3.5 3.0 2.5 2.0 1.5 1.0 ppm

2.07 2.12 0.97 0.98 0.95 2.00 2.31 4.68 3.33



1-(3-heptylquinoxalin-2-yl) ethane-1,2-diol (S33):

8.082
8.078
8.067
8.065
8.063
8.042
8.040
8.027
8.023
7.762
7.759
7.747
7.743
7.731
7.727
7.270
3.821
3.809
3.798
3.786
3.058
3.045
3.040
3.026
3.022
3.009
1.890
1.887
1.874
1.490
1.474
1.459
1.396
1.382
1.378
1.366
1.319
1.312
1.305
1.297
0.910
0.896
0.882

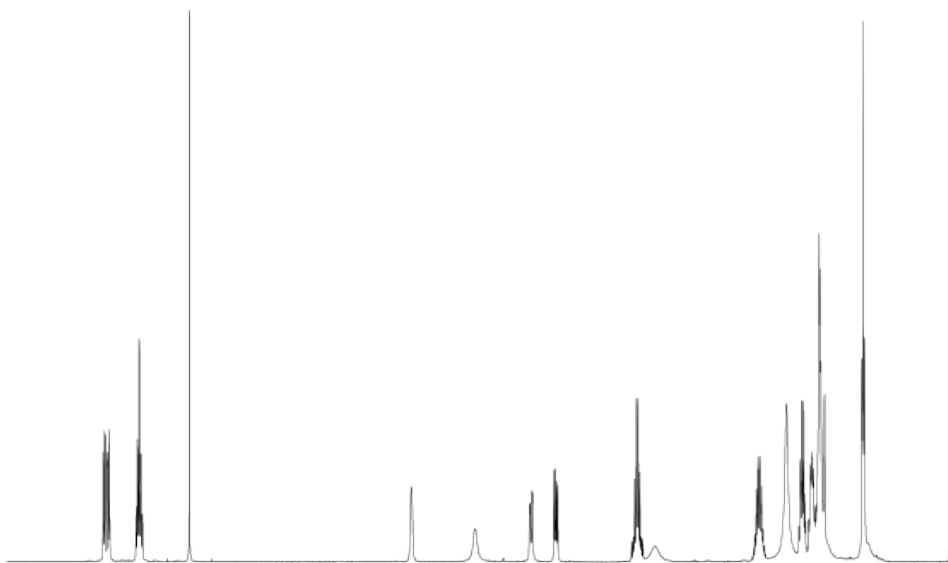


Current Data Parameters
NAME C7H15_quinoxaline
EXPNO 1
PROCNO 1

F2 - Acquisition Parameters
Date_ 20090810
Time 10.13
INSTRUM spect
PROBHD 5 mm BBO2 new
PULPROG zg
TD 65536
SOLVENT CDCl3
NS 16
DS 2
SWH 6510.417 Hz
FIDRES 0.099341 Hz
AQ 5.0332146 sec
RG 181
DW 76.800 usec
DE 9.00 usec
TE 295.8 K
D1 4.00000000 sec
TD0 1

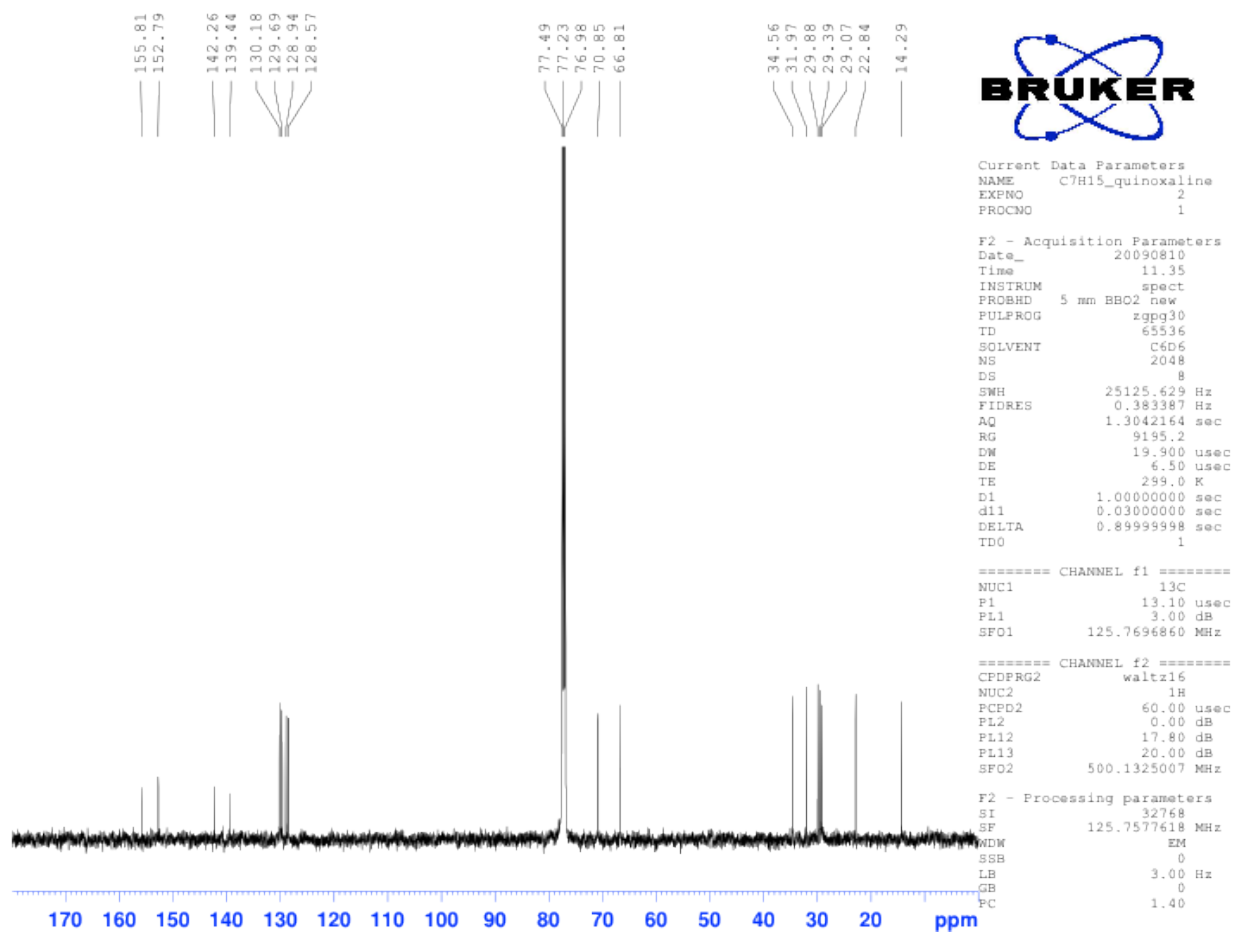
===== CHANNEL f1 =====
NUC1 1H
P1 11.10 usec
PL1 0.00 dB
SFO1 500.1330008 MHz

F2 - Processing parameters
SI 32768
SF 500.13300082 MHz
WDW EM
SSB 0
LB 0.30 Hz
GB 0
PC 1.00

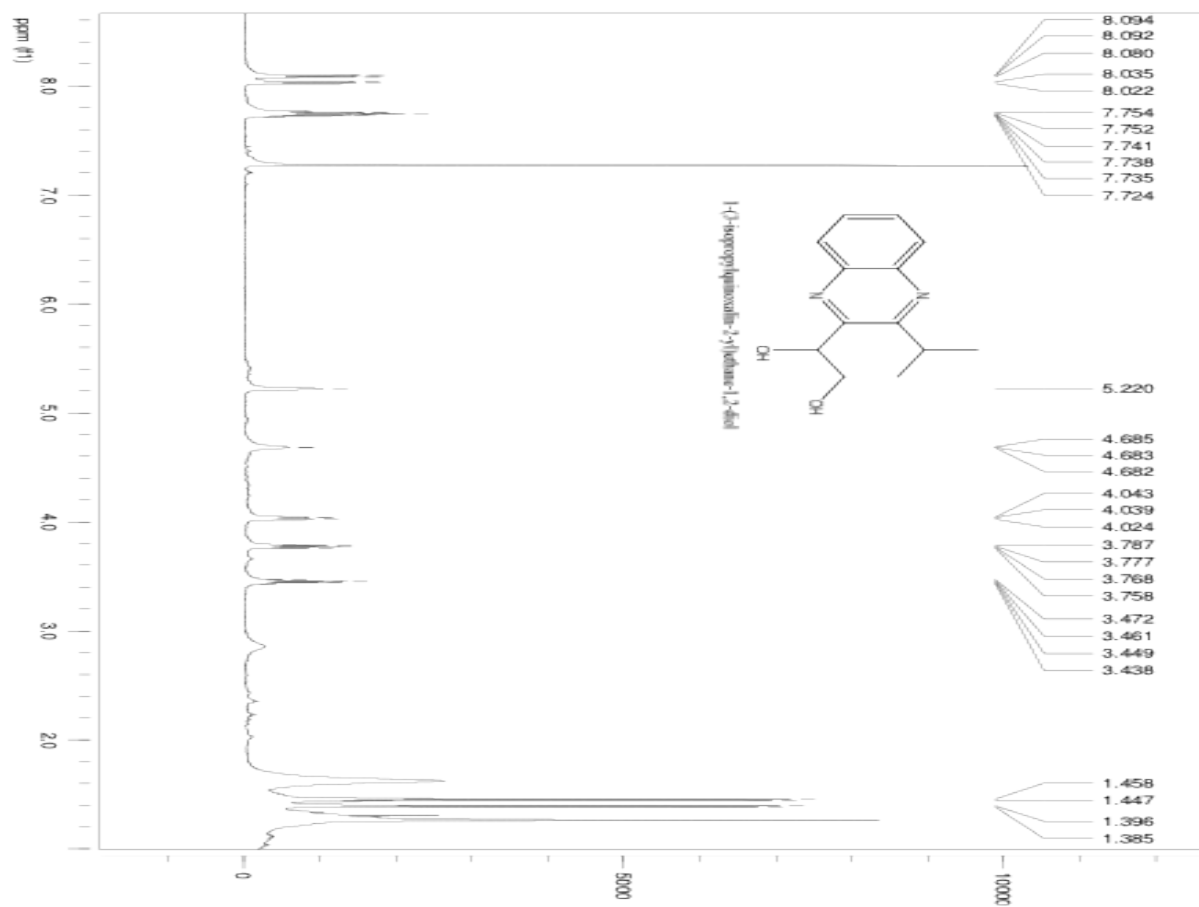


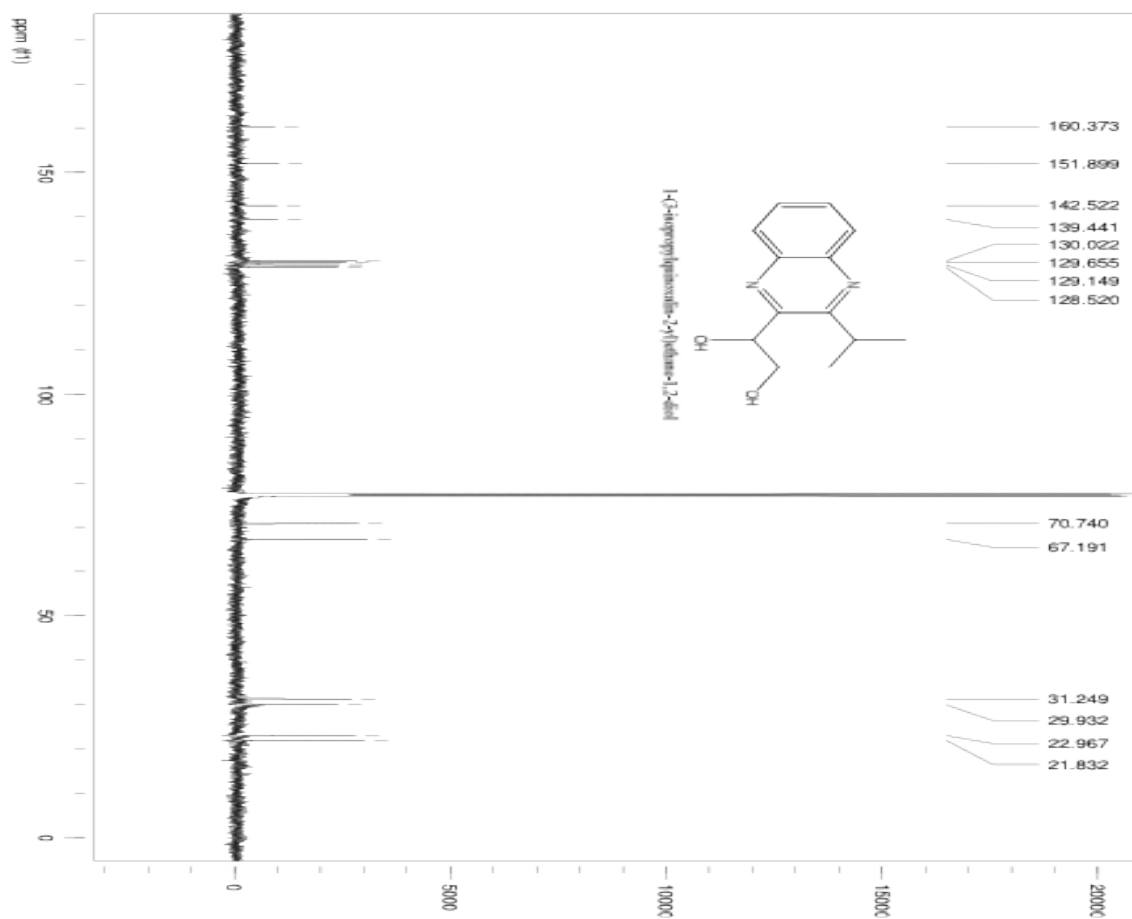
8.5 8.0 7.5 7.0 6.5 6.0 5.5 5.0 4.5 4.0 3.5 3.0 2.5 2.0 1.5 1.0 ppm

2.01
2.04
1.00
0.92
1.01
0.99
2.06
0.79
2.15
2.30
2.23
4.57
3.56

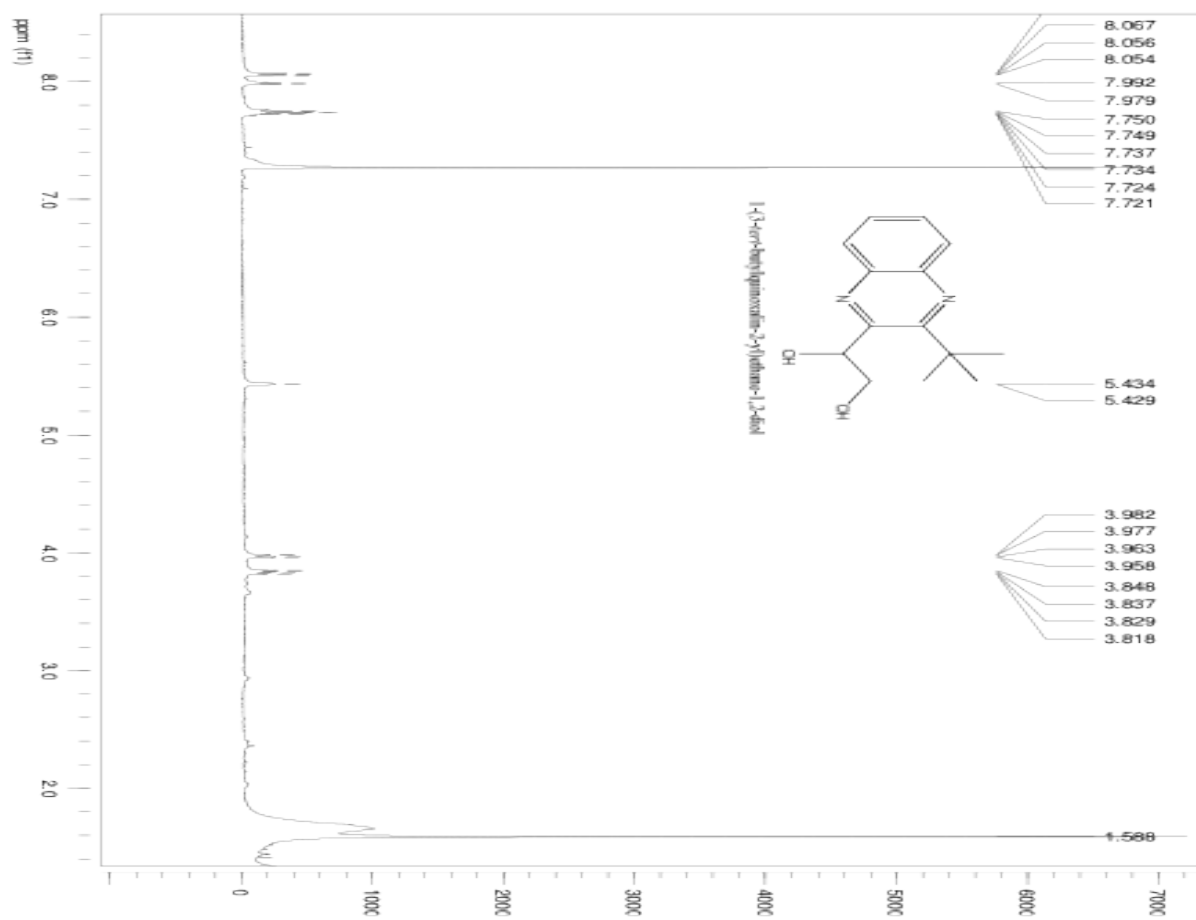


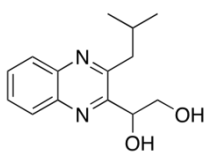
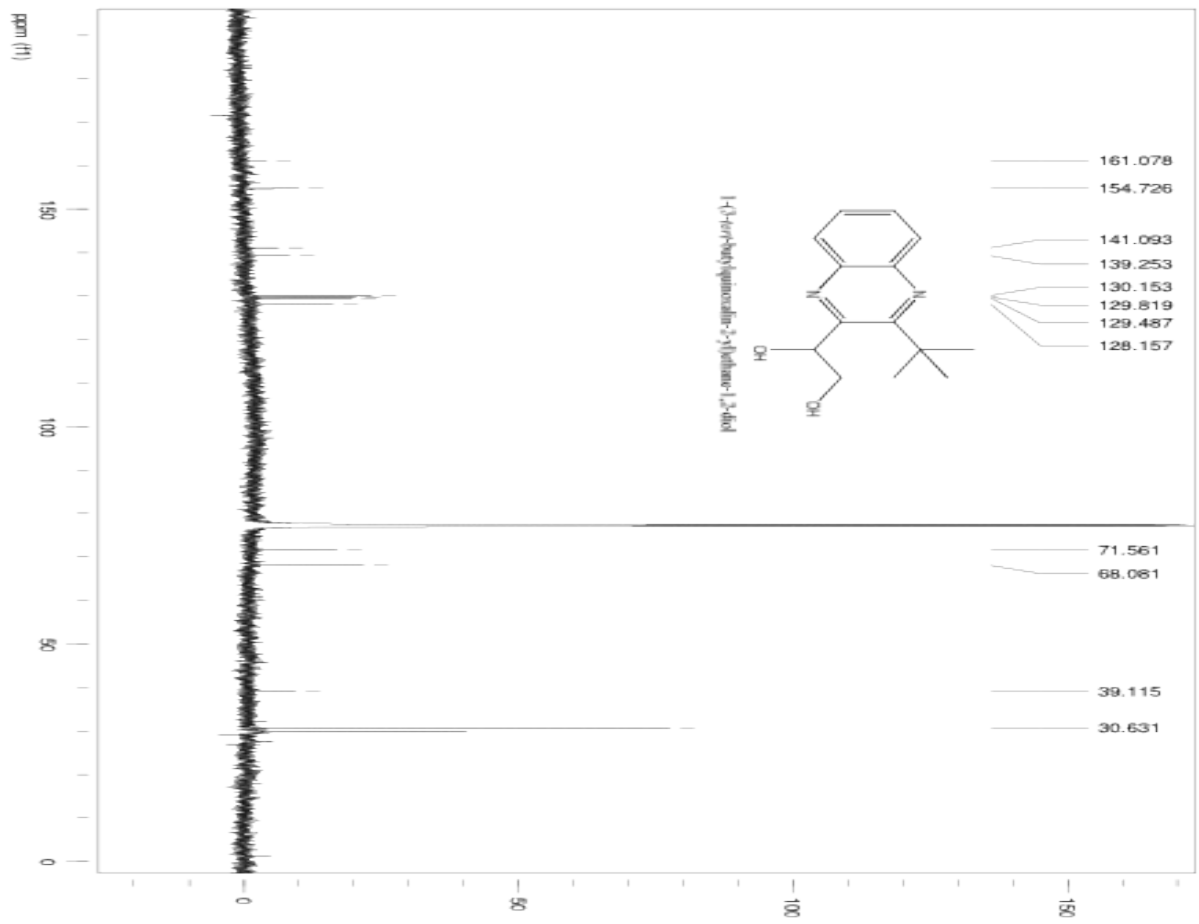
1-(3-isopropylquinoxalin-2-yl)ethane-1,2-diol (S34):



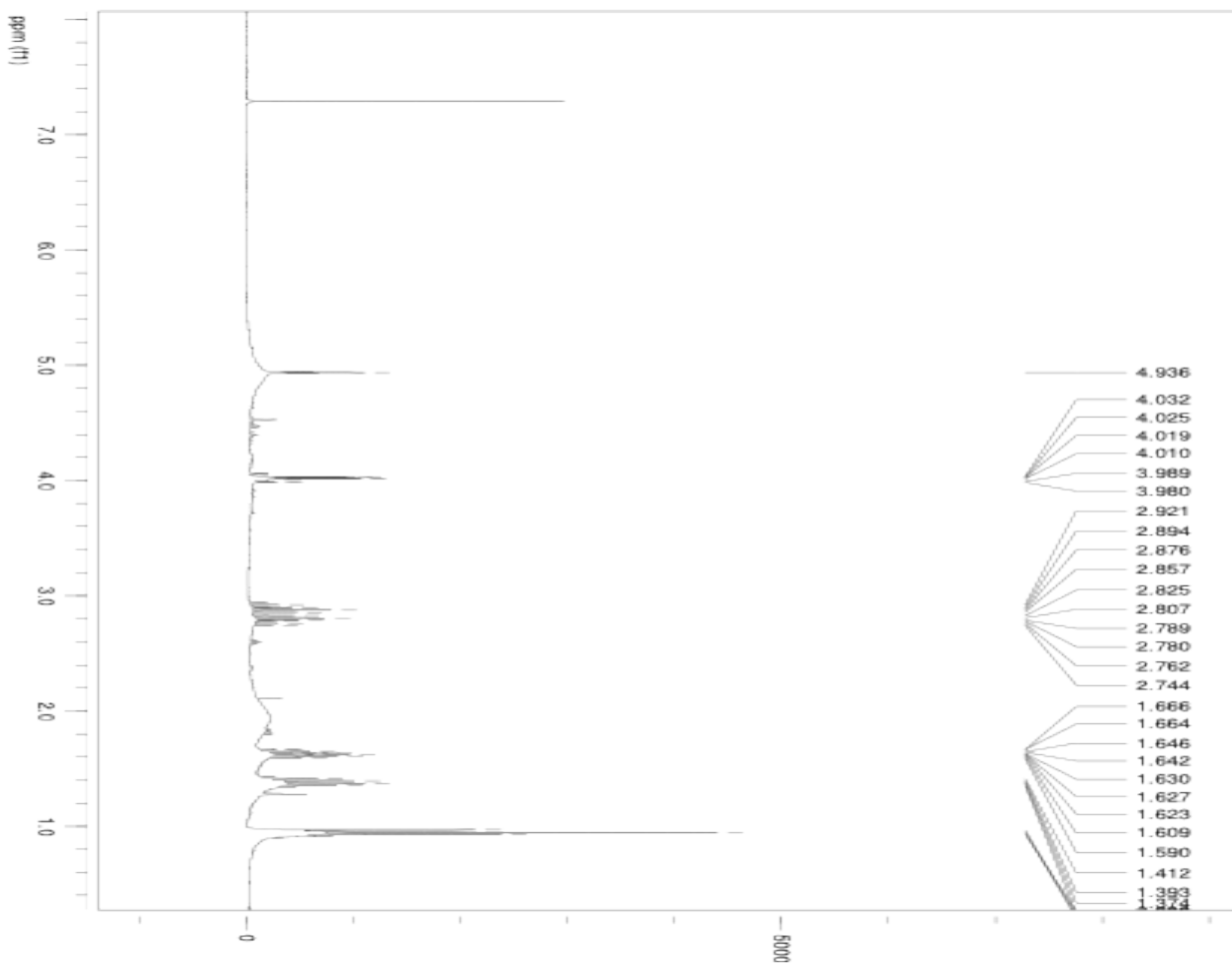


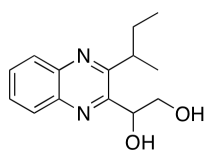
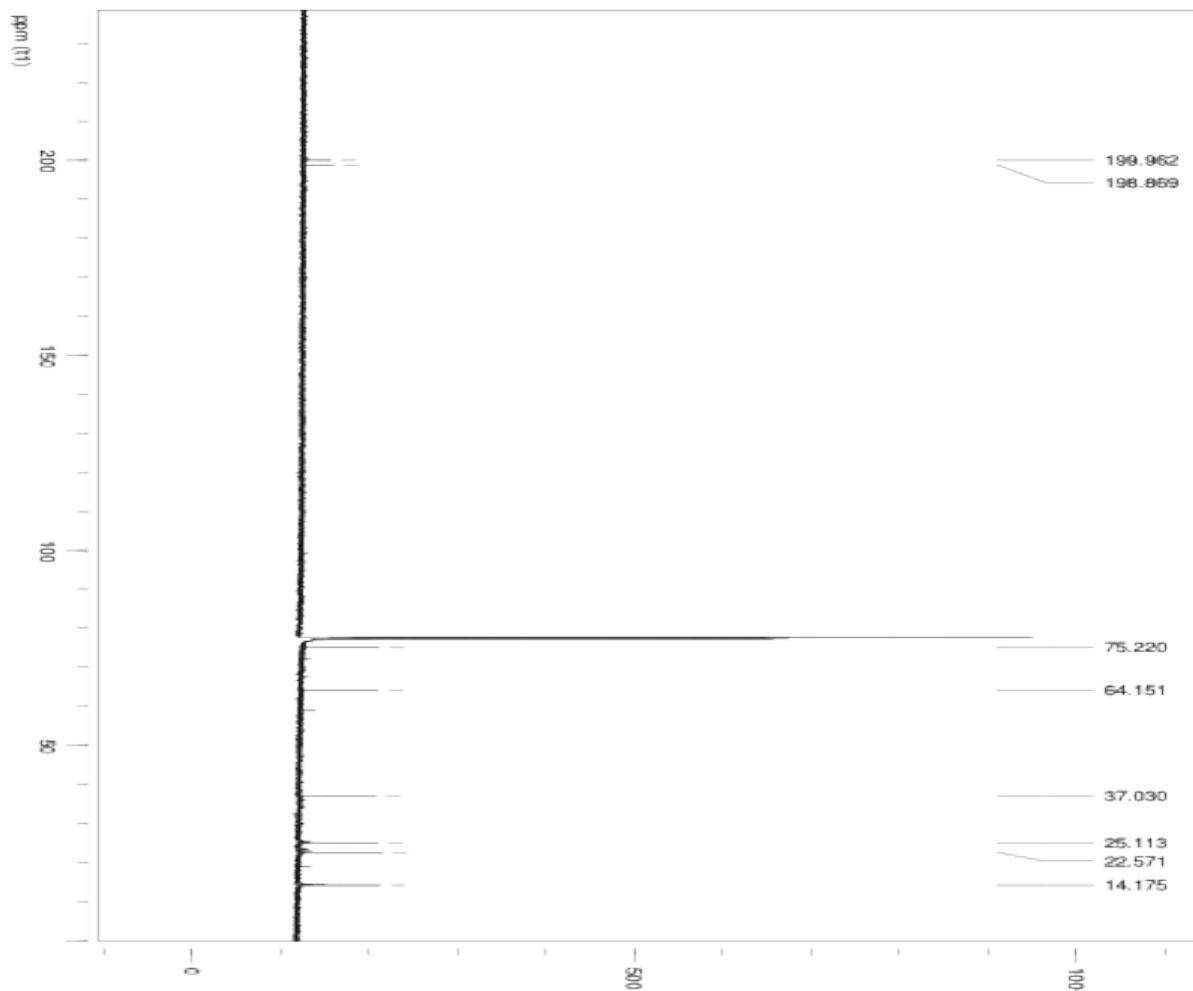
1-(3-tert-butylquinoxalin-2-yl)ethane-1,2-diol (S35):





1-(3-isobutylquinoxalin-2-yl) ethane-1,2-diol (S36):





1-(3-*sec*-butylquinoxalin-2-yl) ethane-1,2-diol:

User Name smith
Group sintim
Sample Label 2methyl_quin

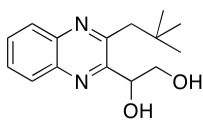
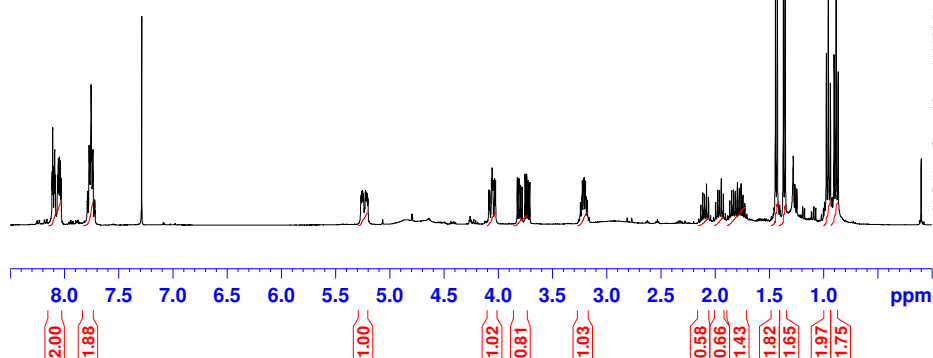


Current Data Parameters
NAME 9-smith-1214
EXPNO 10
PROCNO 1

F2 - Acquisition Parameters
Date_ 20091214
Time 10.34
INSTRUM spect
PROBHD 5 mm QNP 1H/1
PULPROG zg30
TD 39392
SOLVENT cdcl3
NS 64
DS 2
SWH 7575.758 Hz
FIDRES 0.192317 Hz
AQ 2.5999219 sec
RG 128
DW 66.000 usec
DE 6.00 usec
TE 295.0 K
D1 1.5000000 sec
TD0 1

===== CHANNEL f1 =====
NUC1 1H
P1 10.00 usec
PL1 -4.00 dB
SFO1 399.7324685 MHz

F2 - Processing parameters
SI 32768
SF 399.7300000 MHz
WDW EM
SSB 0
LB 0.30 Hz
GB 0
PC 2.00



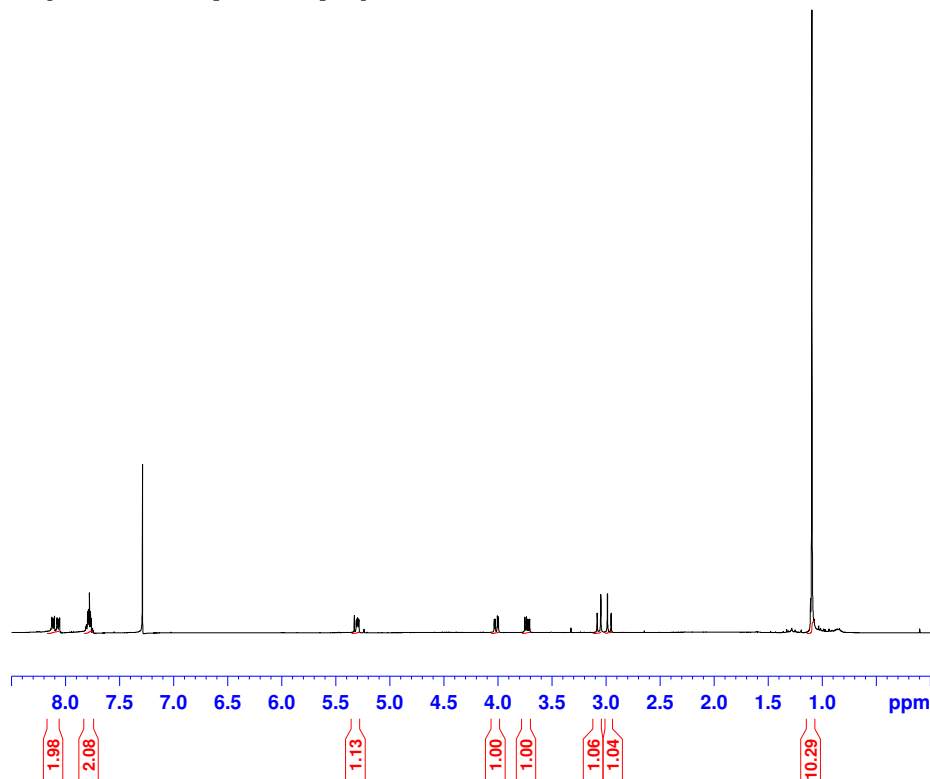
1-(3-neopentylquinoxalin-2-yl) ethane-1,2-diol:

User Name smith
Group sintim
Sample Label acetyltertbutyl_quinox

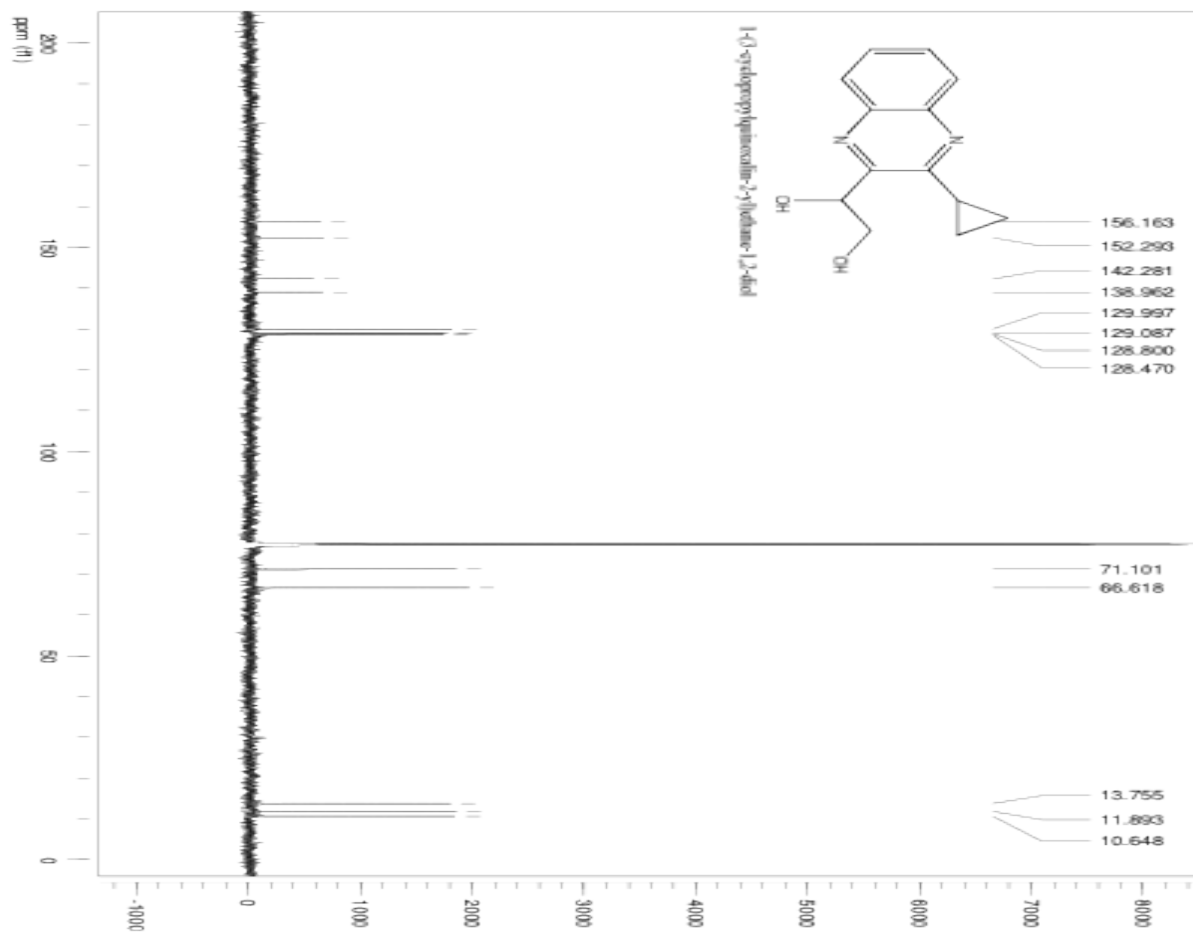


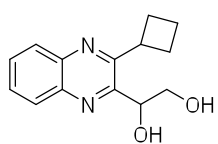
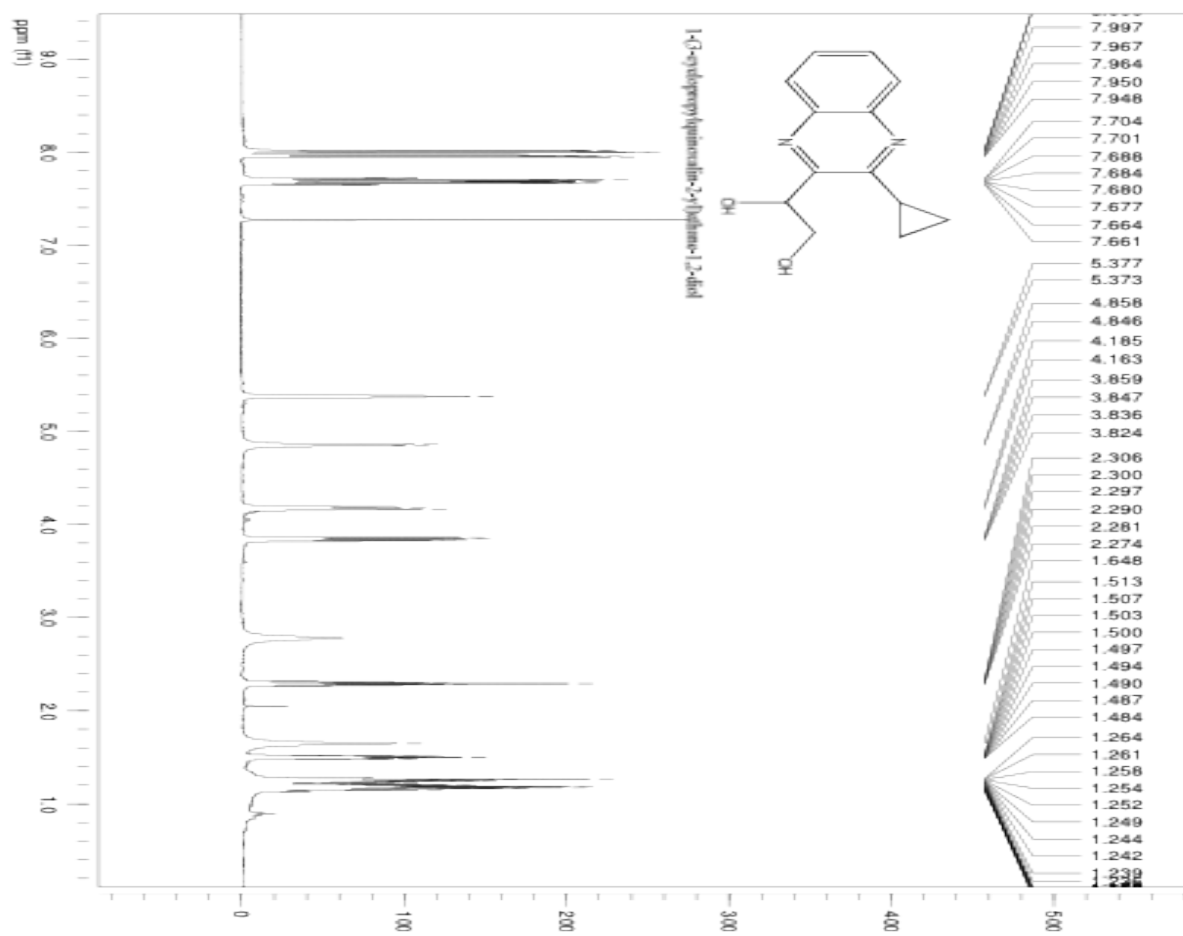
Current Data Parameters
NAME 26-smith-1110
EXPNO 10
PROCNO 1

F2 - Acquisition Parameters
Date_ 20091110
Time 19.28
INSTRUM spect
PROBHD 5 mm QNP 1H/1
PULPROG zg30
TD 39392
SOLVENT CDCl3
NS 64
DS 2
SWH 7575.758 Hz
FIDRES 0.192317 Hz
AQ 2.5999219 sec
RG 456.1
DW 66.000 usec
DE 6.00 usec
TE 295.2 K
D1 1.5000000 sec
TD0 1

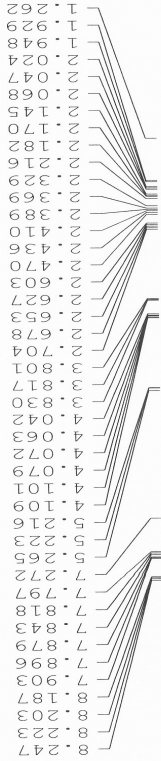


1-(3-cyclopropylquinoxalin-2-yl)ethane-1,2-diol (S39):





1-(3-cyclobutylquinoxalin-2-yl)ethane-1,2-diol:



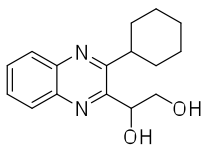
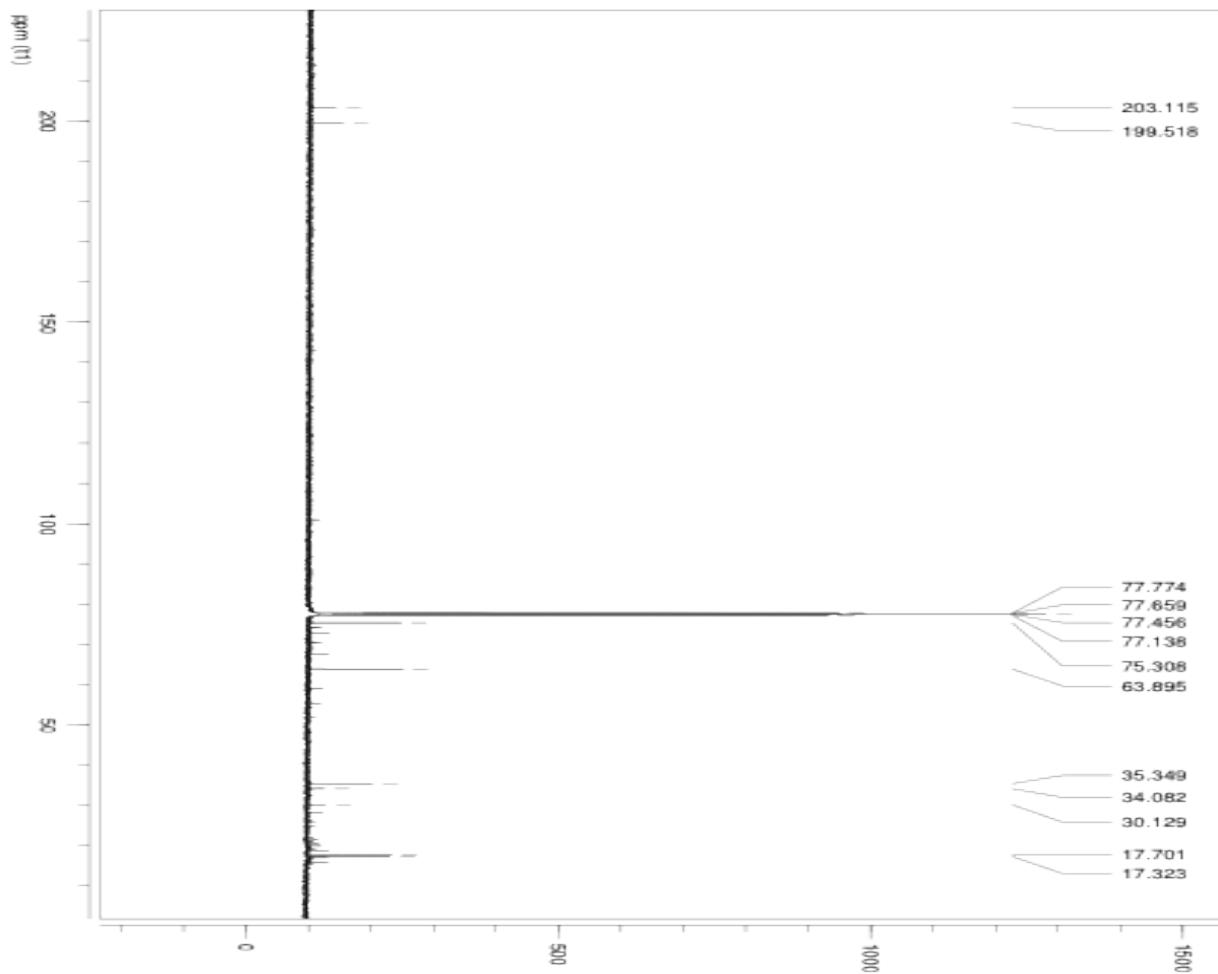
User Name smith
Group sintim
Sample Label cyclobutyl_quinox

Current Data Parameters
NAME 13-smith-0323
EXPNO 10
PROCNO 1

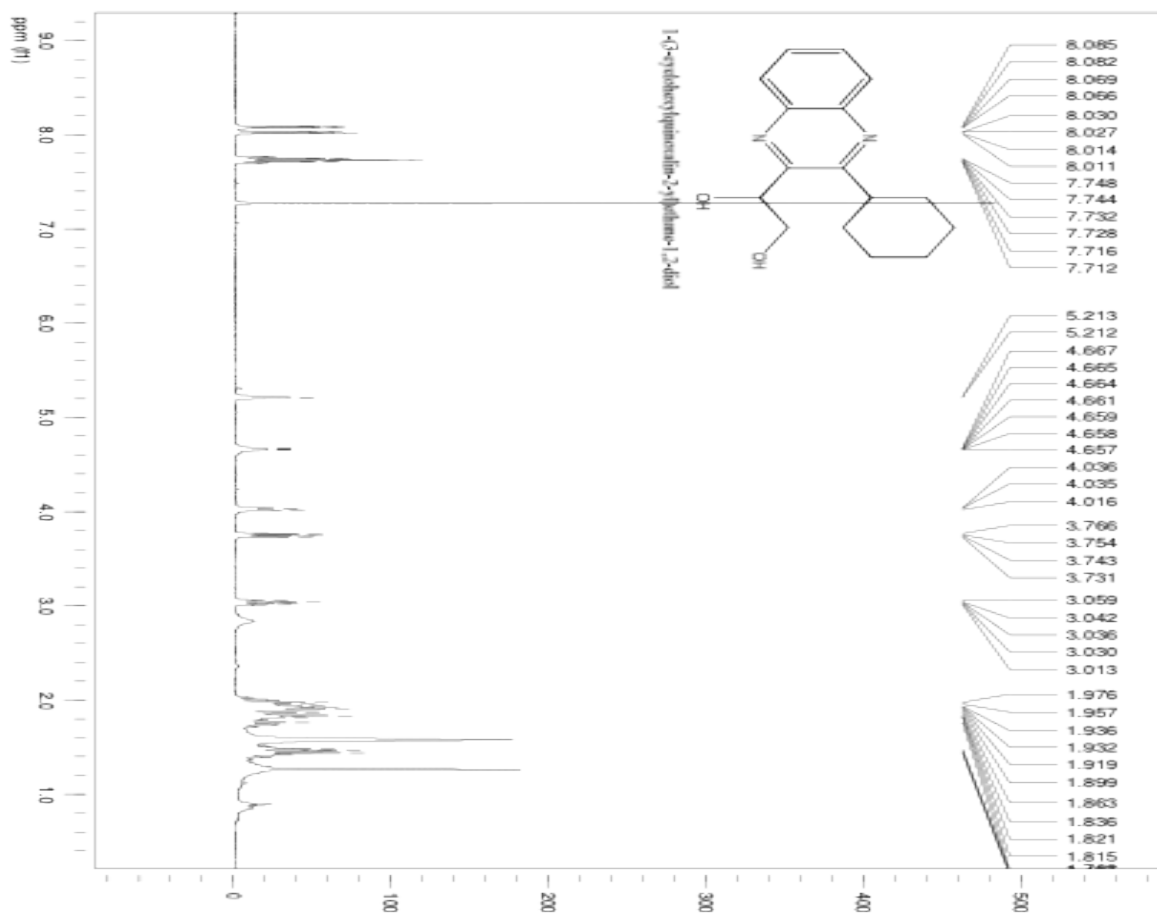
F2 - Acquisition Parameters
Date 20110323
Time 15.04
INSTRUM spect
PROBHD 5 mm QNP 1H/1
PULPROG zg30
TD 65536
SOLVENT CDCl3
NS 16
DS 4
SWH 8223.685 Hz
FIDRES 0.125483 Hz
AQ 3.9646387 sec
RG 436.1
DM 60.800 usec
DE 6.00 usec
TE 285.4 K
D1 1.00000000 sec
TD0 1

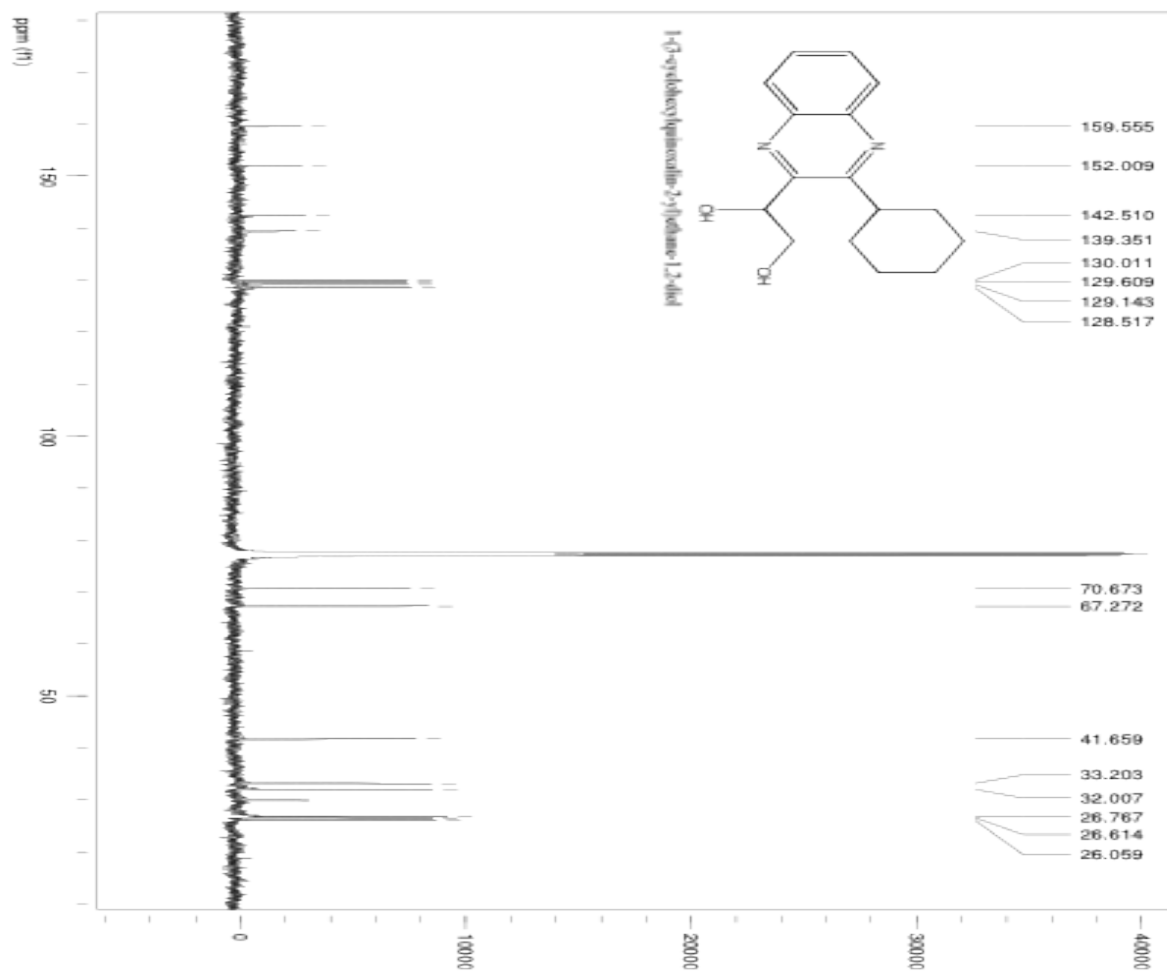
===== CHANNEL f1 =====
NUC1 13C
P1 11.50 usec
PL1 0.00 dB
SFO1 399.7324685 MHz

F2 - Processing parameters
SI 32768
SF 399.7300000 MHz
WDW EM
SSB 0
LB 0.30 Hz
GB 0
PC 2.00



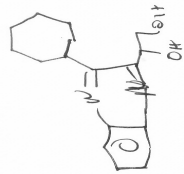
1-(3-cyclohexylquinoxalin-2-yl)ethane-1,2-diol (S42):





1-(3-cycloheptylquinoxaline-2-yl)ethane-1,2-diol:

User Name smith
Group sintim
Sample Label cycloheptyl_quinox



Expected M = 286

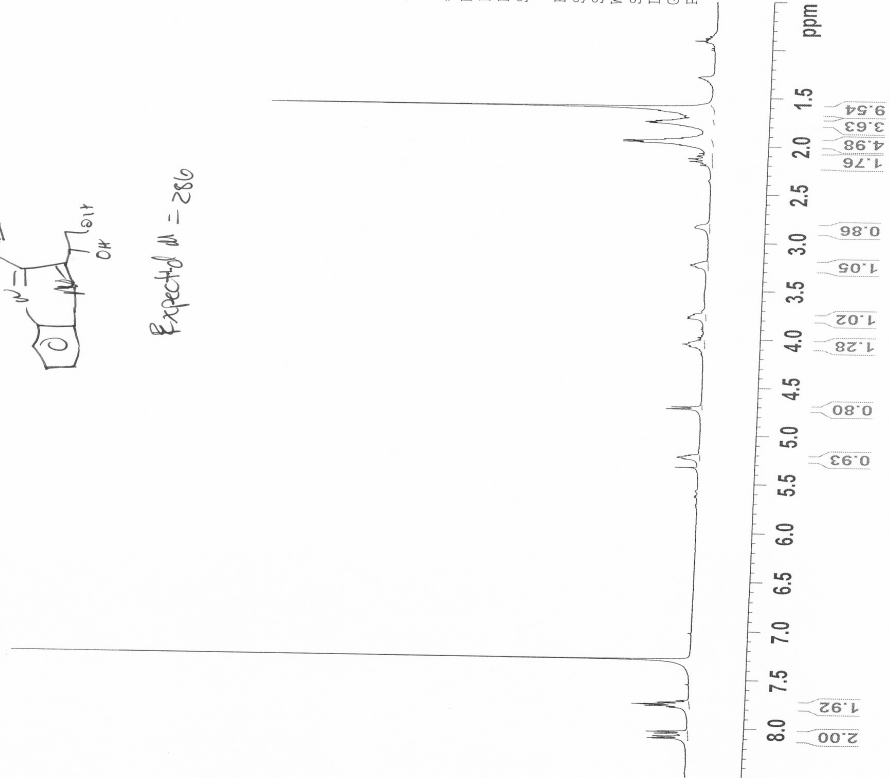
Current Data Parameters
NAME 23-smith-0505
EXPNO 10
PROCNO 1

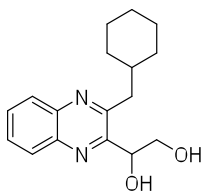
F2 - Acquisition Parameters
Date 20100506
Time 0.25

INSTRUM spect
PROBHD 5 mm QNP 1H/1
PULPROG zg30
TD 38392
SOLVENT COCL3
NS 64
DS 2
SWH 7575.758 Hz
FIDRES 0.192317 Hz
AQ 2.5999219 sec
RG 362
DW 66.000 usec
DE 6.00 usec
TE 295.4 K
D1 1.50000000 sec
TD0 1

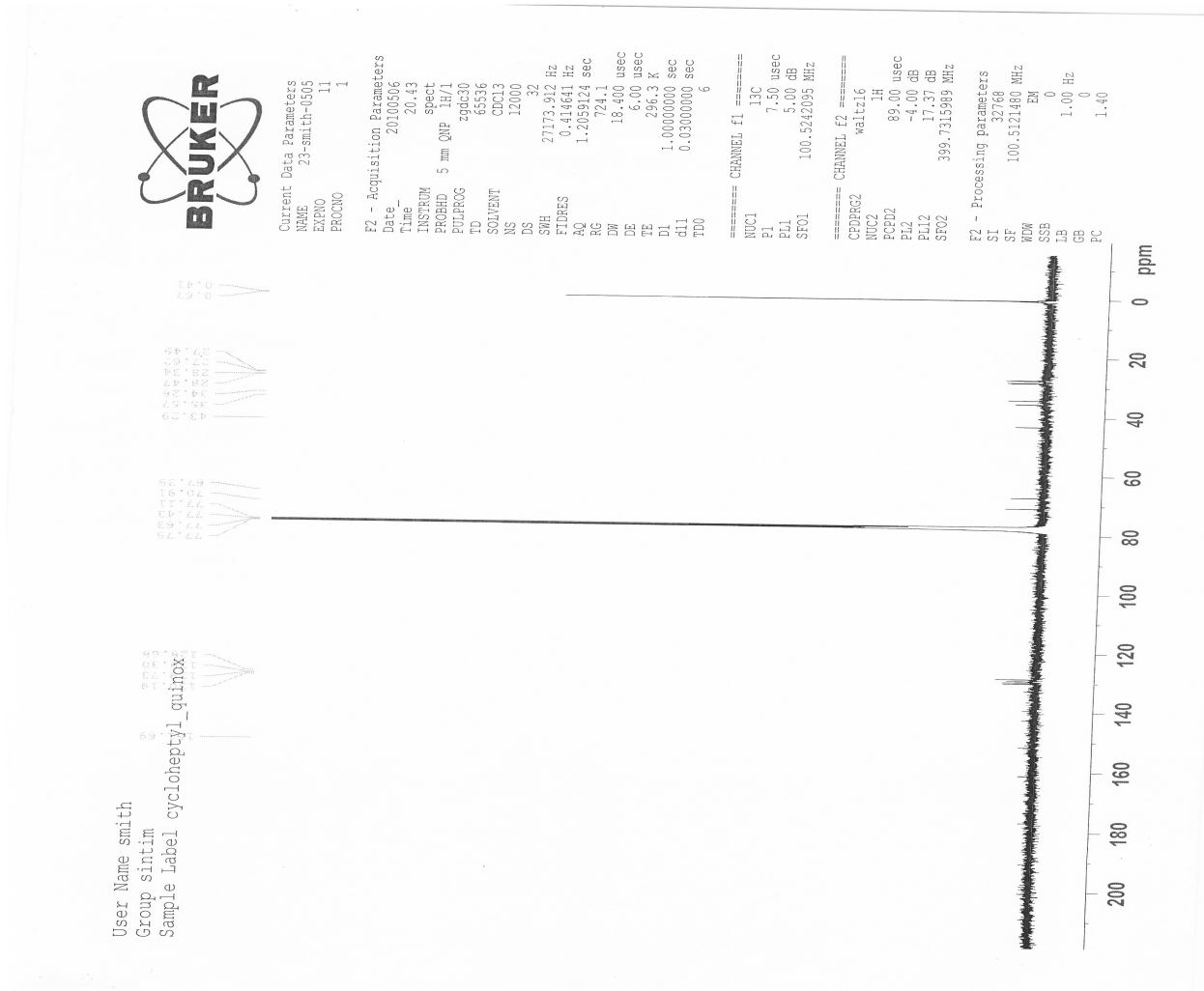
==== CHANNEL F1 =====
NUC1 1H
P1 9.50 usec
PL1 -3.00 dB
SFO1 399.7324685 MHz

F2 - Processing parameters
SI 32768
SF 399.7300000 MHz
WDW EM
SSB 0
LB 0.30 Hz
GB 0
PC 2.00





1-(3-(cyclohexylmethyl)quinoxalin-2-yl)ethane-1,2-diol:



User Name smith
Group sirtim
Sample Label ch2_cyclohexy



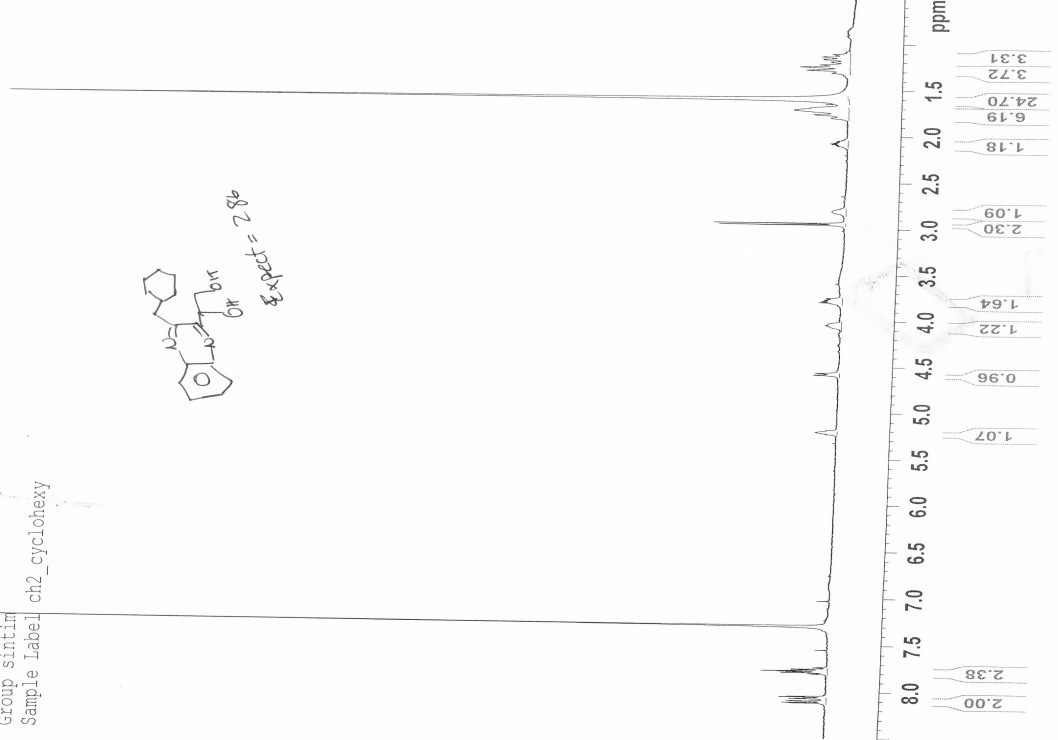
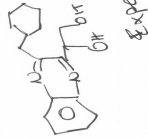
Current Data Parameters
NAME Zl-smith-0505
EXPNO 10
PROCNO 1

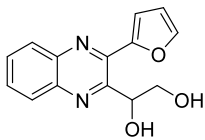
F2 - Acquisition Parameters

Date_ 20100505
Time_ 9.41
INSTRUM spect
PROBHD 5 mm QNP 1H/1
PULPROG zg30
TD 39392
SOLVENT CDCl3
NS 64
DS 2
SWH 7575.758 Hz
FIDRES 0.132317 Hz
AQ 2.5999219 sec
RG 362
DW 66.000 usec
DE 6.00 usec
TE 295.2 K
D1 1.5000000 sec
TDO 1

==== CHANNEL f1 =====
NUC1 1H
P1 9.50 usec
PL1 -3.00 dB
SFO1 399.7324685 MHz

F2 - Processing parameters
SI 32768
SF 399.7300000 MHz
WDW EM
SSB 0
LB 0.30 Hz
GB 0
PC 2.00





1-(3-(furan-2-yl)quinoxalin-2-yl)ethane-1,2-diol (S46):



Current Data Parameters
NAME ch2_cyclohexyl_quinox
EXPNO 2
PROCNO 999

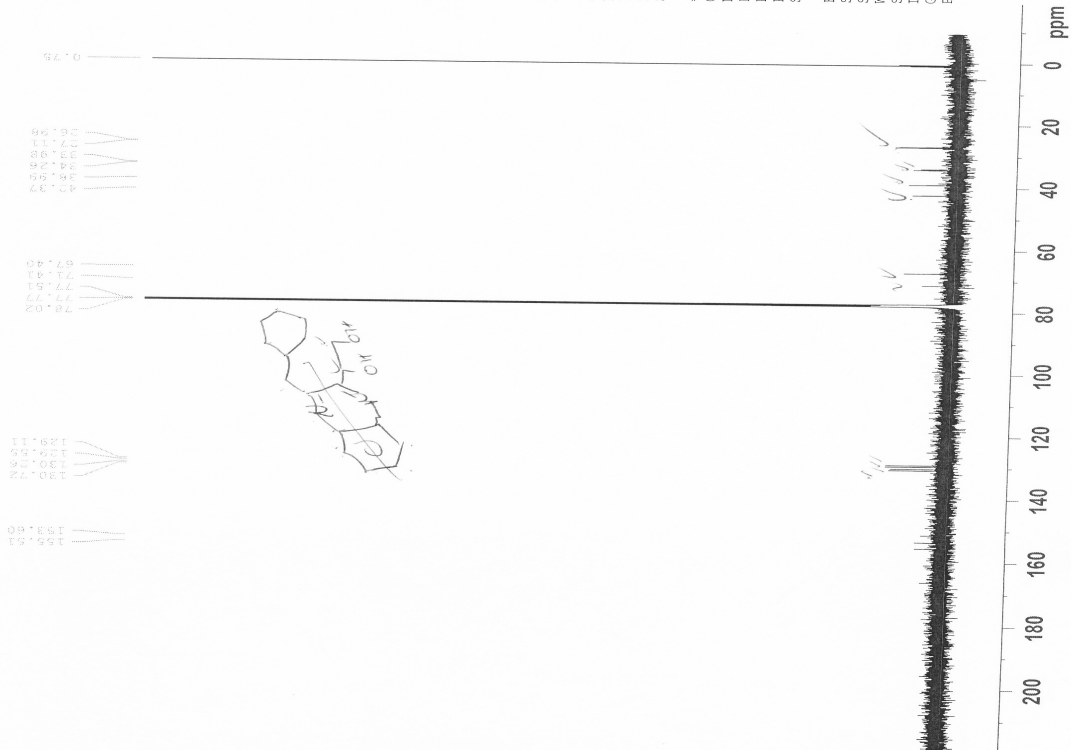
F2 - Acquisition Parameters

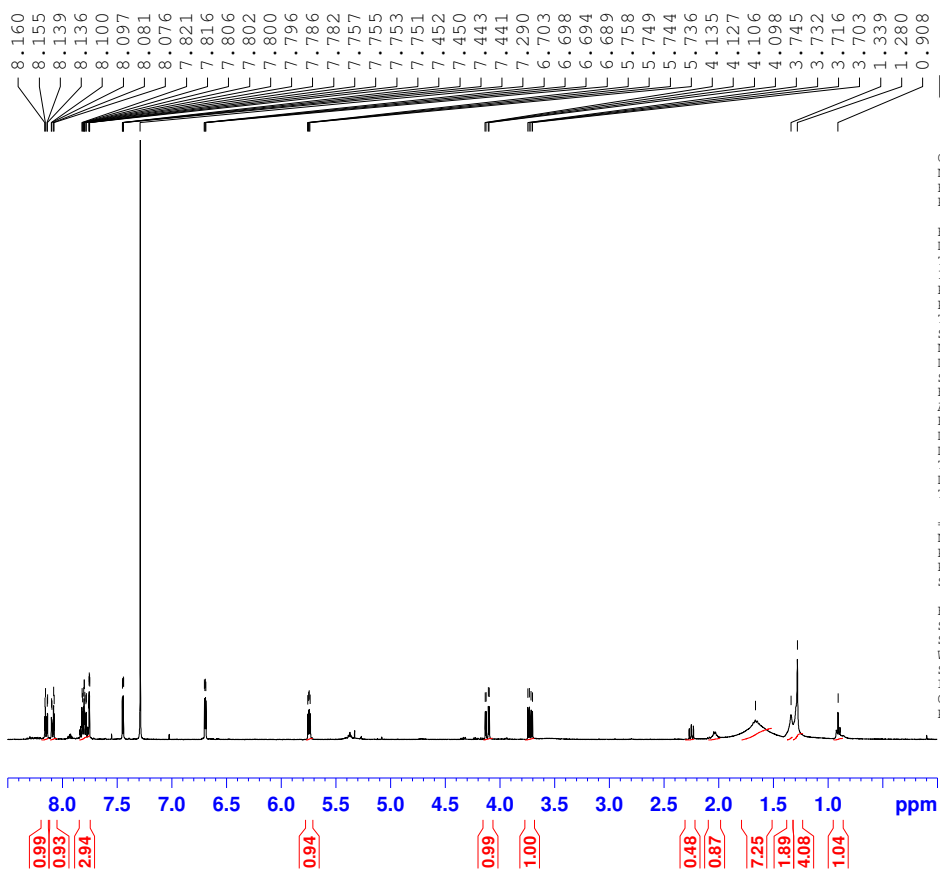
Date 20100605
Time 14:27
INSTRUM spect
PROBHD 5 mm BBO2 new
PULPROG zgpg30
TD 65536
SOLVENT CDCl3
NS 6144
DS 16
SWH 32679.738 Hz
FIDRES 0.458653 Hz
AQ 1.0027508 sec
RG 91195.2
DM 15.300 usec
DE 6.50 usec
TE 298.4 K
D1 1.00000000 sec
d11 0.03000000 sec
TD0 1

===== CHANNEL f1 =====
NUC1 13C
P1 12.50 usec
PL1 3.00 dB
SFO1 125.762839 MHz

===== CHANNEL f2 =====
CPDPRG2 waltz16
NUC2 1H
PCPD2 60.00 usec
PL2 0.00 dB
PL12 17.80 dB
SFO2 500.1325007 MHz

F2 - Processing parameters
SI 32768
SF 125.767638 MHz
WDW EM
SSB 0
LB 0.00 Hz
GB 0
PC 1.40



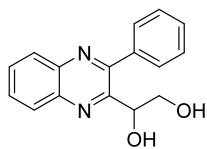
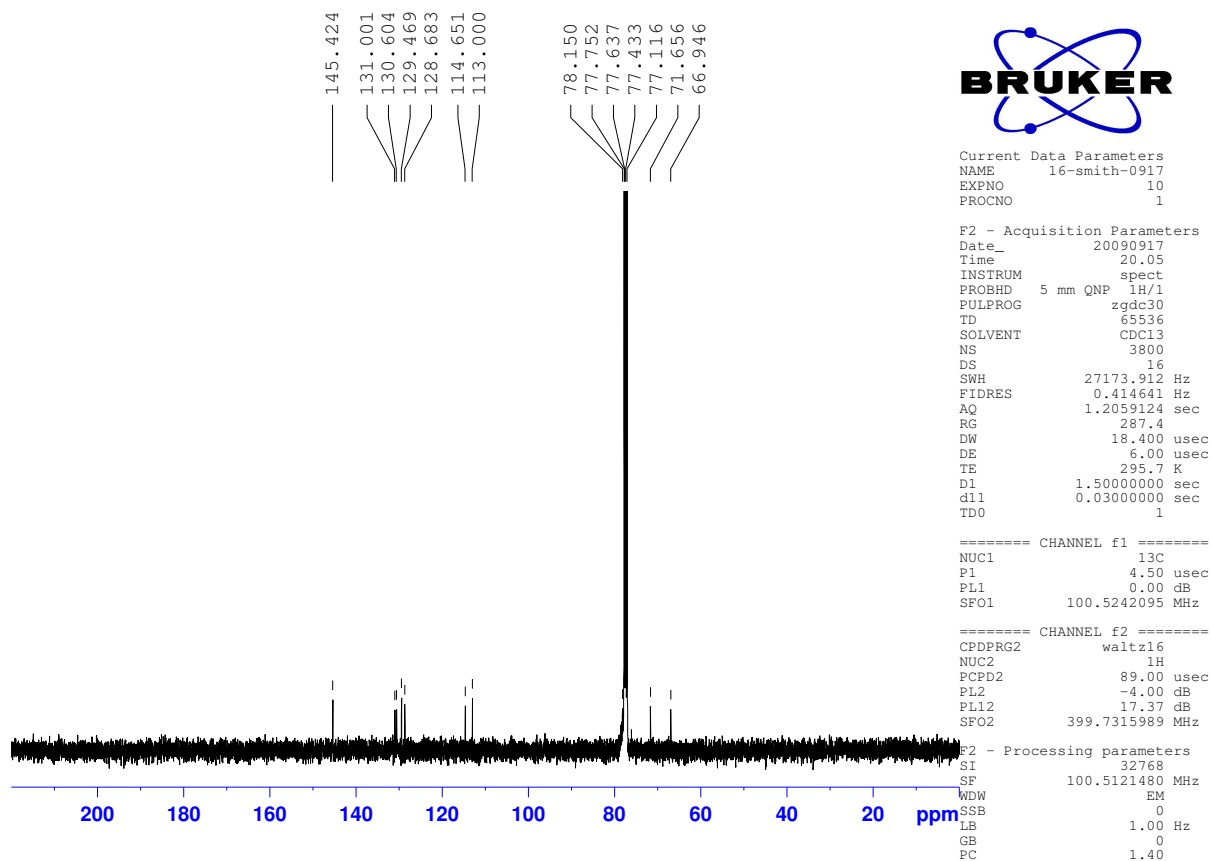


Current Data Parameters
 NAME 16-smith-0916
 EXPNO 10
 PROCNO 1

F2 - Acquisition Parameters
 Date_ 20090916
 Time 16.41
 INSTRUM spect
 PROBHD 5 mm QNP 1H/1
 PULPROG zg30
 TD 39392
 SOLVENT CDCl3
 NS 64
 DS 2
 SWH 7575.758 Hz
 FIDRES 0.192317 Hz
 AQ 2.5999219 sec
 RG 574.7
 DW 66.000 usec
 DE 6.00 usec
 TE 294.9 K
 D1 1.5000000 sec
 TD0 1

===== CHANNEL f1 =====
 NUC1 1H
 P1 10.00 usec
 PL1 -4.00 dB
 SFO1 399.7324685 MHz

F2 - Processing parameters
 SI 32768
 SF 399.7300000 MHz
 WDW EM
 SSB 0
 LB 0.30 Hz
 GB 0
 PC 2.00



1-(3-phenyl-quinoxalin-2-yl)-ethane-1,2-diol (S45):

User Name smith
Group sintim
Sample Label phenyl_quinoxaline

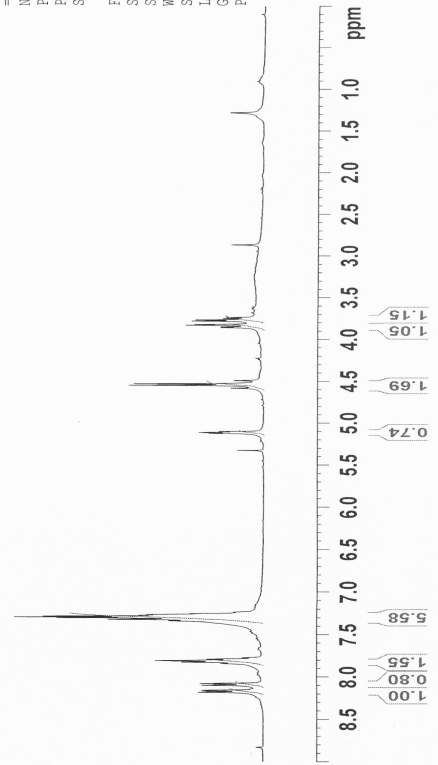


Current Data Parameters
NAME 34-smith-1119
EXPNO 10
PROCNO 1

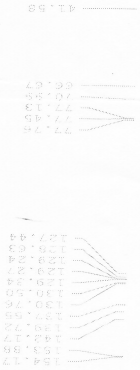
F2 - Acquisition Parameters
Date_ 20101119
Time 16.15
INSTRUM spect
PROBHD 5 mm QNP 1H/1
PULPROG zg30
TD 39392
SOLVENT CDCl3
NS 64
DS 2
SWH 7575.758 Hz
FIDRES 0.192317 Hz
AQ 2.5999219 sec
RG 287.4
DW 66.000 usec
DE 6.00 usec
TE 295.8 K
D1 1.50000000 sec
TDO 1

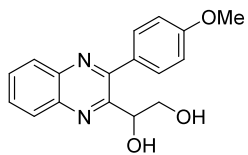
==== CHANNEL F1 =====
NUC1 1H
PL 11.50 usec
PL1 0.00 dB
SFO1 399.7324685 MHz

F2 - Processing parameters
SI 32768
SF 399.7300000 MHz
WDW EM
SSB 0
LB 0.30 Hz
GB 0
PC 2.00

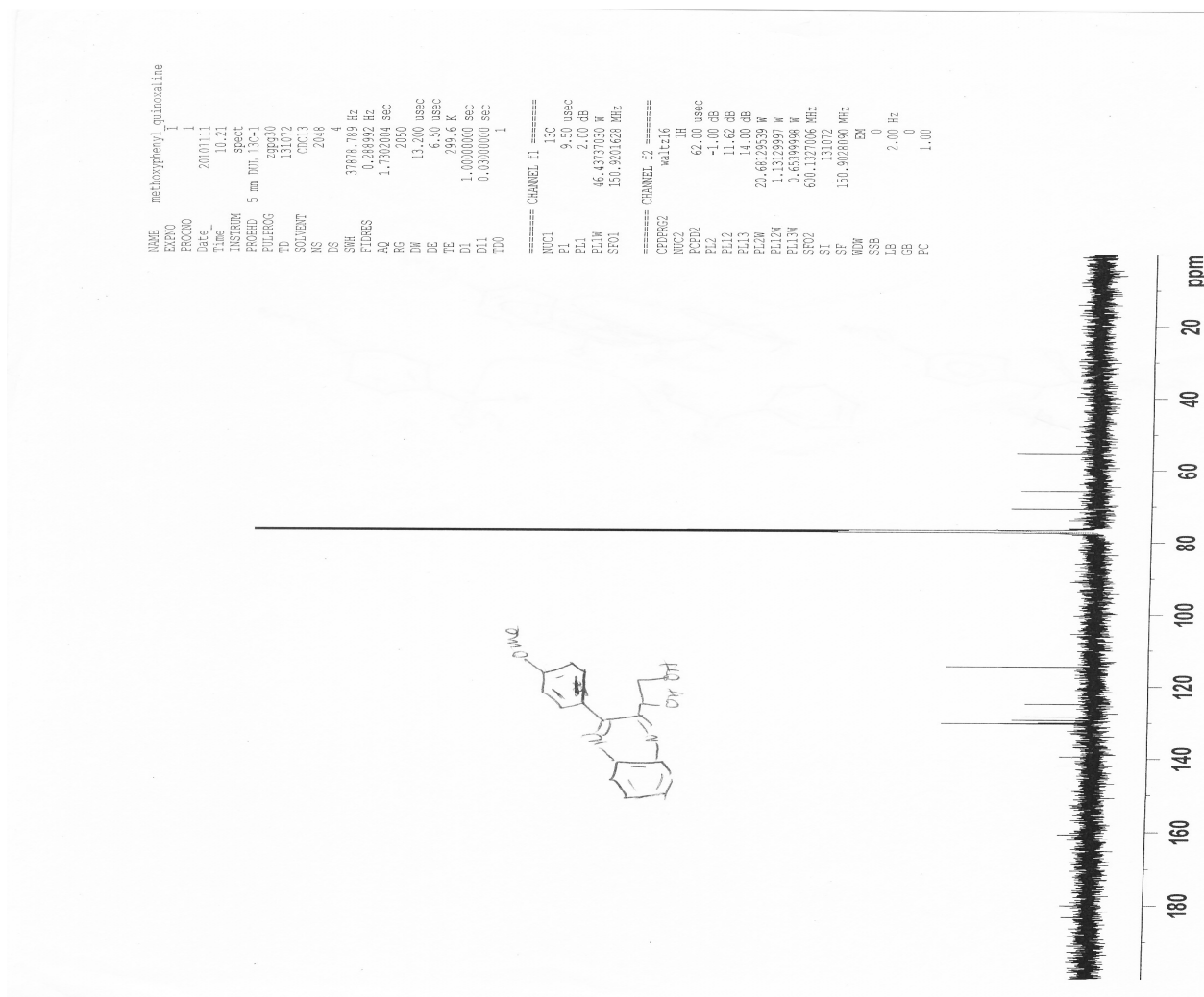


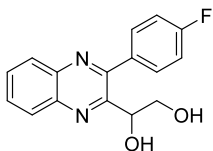
User Name smith
 Group sintim
 Sample Label phenyl_quinoxaline



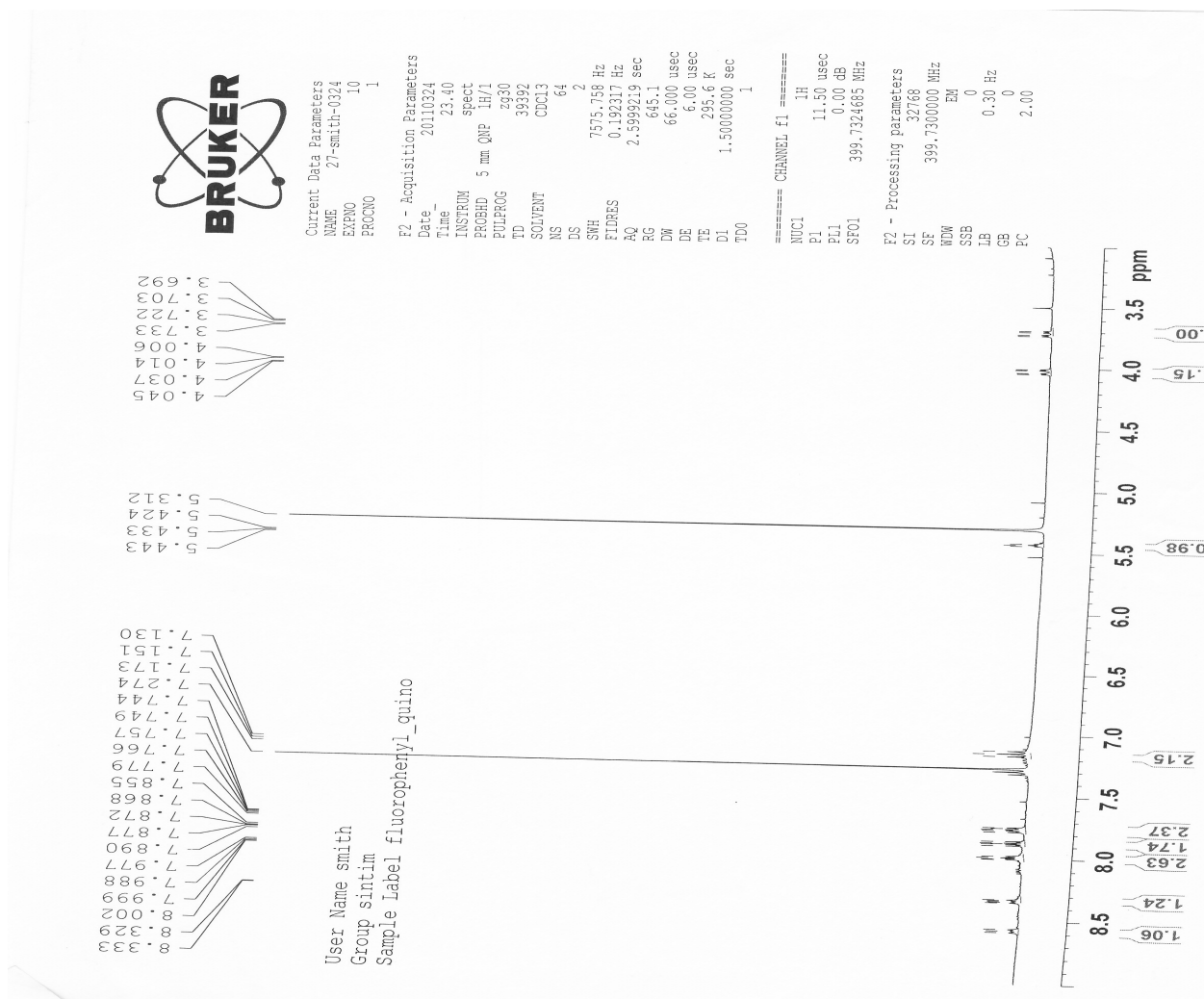


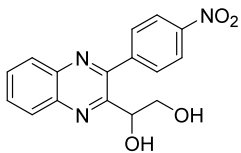
1-(3-methoxyphenyl-quinoxalin-2-yl)-ethane-1,2-diol (S47):



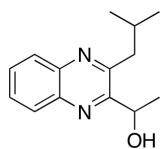
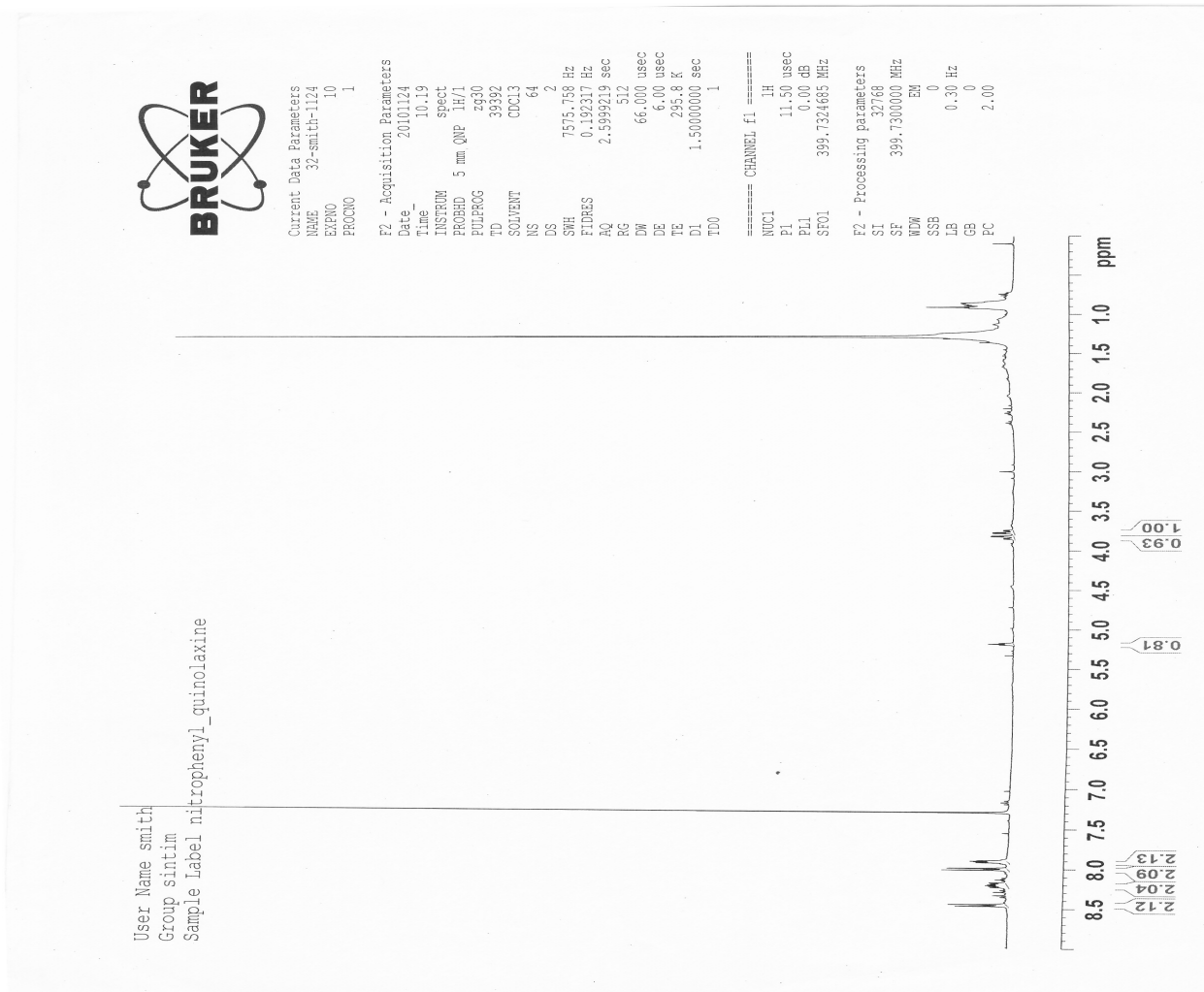


1-(3-fluorophenyl-quinoxalin-2-yl)-ethane-1,2-diol (S48):

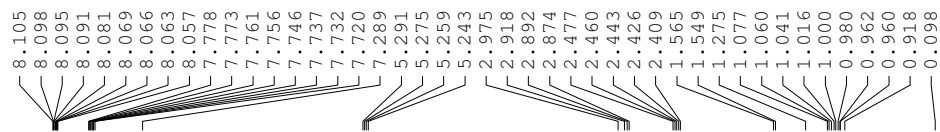




1-(3-nitrophenyl-quinoxalin-2-yl)-ethane-1,2-diol (S49):



1-(3-isobutylquinoxalin-2-yl) ethanol:



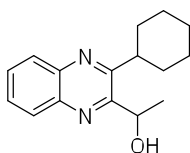
User Name smith
 Group sintim
 Sample Label deoxisobut_quin

Current Data Parameters
 NAME 8-smith-1214
 EXPNO 10
 PROCNO 1

F2 - Acquisition Parameters
 Date_ 20091214
 Time 10.21
 INSTRUM spect
 PROBHD 5 mm QNP 1H/1
 PULPROG zg30
 TD 39392
 SOLVENT CDCl3
 NS 64
 DS 2
 SWH 7575.758 Hz
 FIDRES 0.192317 Hz
 AQ 2.5999219 sec
 RG 64
 DW 66.000 usec
 DE 6.00 usec
 TE 295.0 K
 D1 1.5000000 sec
 TD0 1

===== CHANNEL f1 =====
 NUC1 1H
 P1 10.00 usec
 PL1 -4.00 dB
 SFO1 399.7324685 MHz

F2 - Processing parameters
 SI 32768
 SF 399.7300000 MHz
 WDW EM
 SSB 0
 LB 0.30 Hz
 GB 0
 PC 2.00



1-(3-cyclohexylquinoxalin-2-yl) ethanol:

8.096
8.089
8.087
8.081
8.075
8.071
8.058
8.053
8.041
8.040
8.034
7.742
7.737
7.727
7.717
7.712
7.290
5.304
5.288
5.265
2.912
1.988
1.960
1.908
1.896
1.880
1.868
1.863
1.855
1.848
1.837
1.829
1.754
1.748
1.571
1.555
1.492
1.485
1.462
1.442
1.314
1.298
1.288
1.279



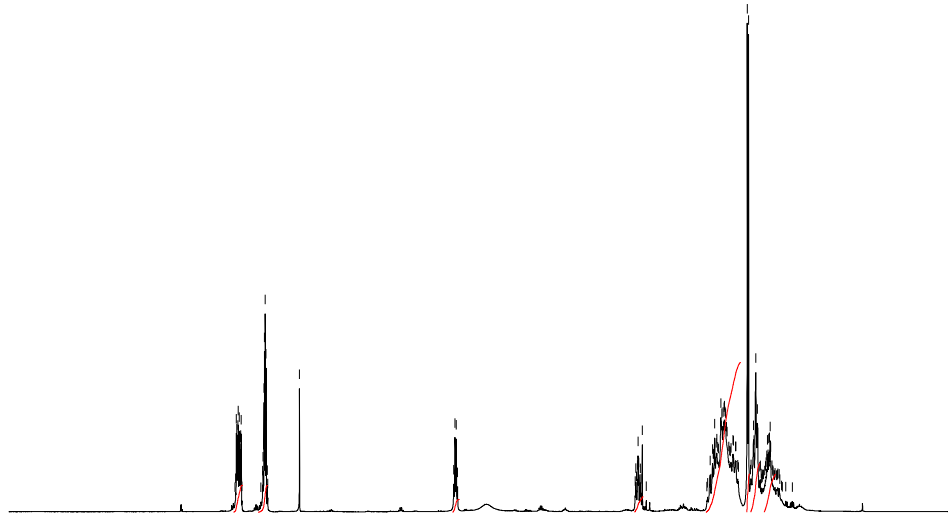
User Name smith
Group sintim
Sample Label deoxycyclohex_quin

Current Data Parameters
NAME 7-smith-1214
EXPNO 10
PROCNO 1

F2 - Acquisition Parameters
Date_ 20091214
Time 10.02
INSTRUM spect
PROBHD 5 mm QNP 1H/1
PULPROG zg30
TD 39392
SOLVENT CDC13
NS 64
DS 2
SWH 7575.758 Hz
FIDRES 0.192317 Hz
AQ 2.5999219 sec
RG 128
DW 66.000 usec
DE 6.00 usec
TE 295.0 K
D1 1.50000000 sec
TD0 1

===== CHANNEL f1 =====
NUC1 1H
P1 10.00 usec
PL1 -4.00 dB
SFO1 399.7324685 MHz

F2 - Processing parameters
SI 32768
SF 399.7300000 MHz
WDW EM
SSB 0
LB 0.30 Hz
GB 0
PC 2.00



10 9 8 7 6 5 4 3 2 1 0 ppm

1.97 2.00
0.94
1.14
10.96 2.83 3.58 2.81

User Name smith
Group sintim
Sample Label METHYL_DIPROPIONATE

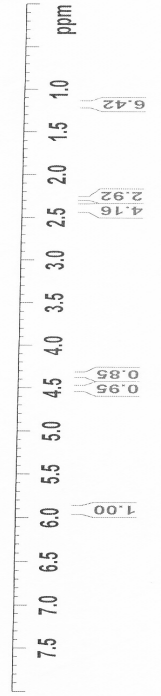


Current Data Parameters
NAME 24-smith-0429
EXPMO 10
PROCNO 1

F2 - Acquisition Parameters
Date_ 20100429
Time_ 22.03
INSTRUM spect
PROBHD 5 mm QNP 1H/1
PULPROG zg30
TD 32768
SOLVENT CDCl3
NS 64
DS 2
SWH 7575.758 Hz
FIDRES 0.192317 Hz
AQ 2.599219 sec
RG 128
DM 66.000 usec
DE 6.00 usec
TE 295.6 K
DL 1.5000000 sec
TDO 1

===== CHANNEL f1 =====
NUC1 1H
P1 9.50 usec
PL1 -3.00 dB
SFO1 399.7324685 MHz

F2 - Processing parameters
SI 32768
SF 399.7300000 MHz
WDW EM
SSB 0
LB 0.30 Hz
GB 0
PC 2.00



User Name smith
Group sintim
Sample Label METHYL_DIPROPIONATE



Current Data Parameters
NAME 24-smith-0429
EXPNO 11
PROCNO 1

F2 - Acquisition Parameters
Date_ 20100430
Time 23.04
INSTRUM spect
PROBHD 5 mm QNP 1H/1
PULPROG zgpg30
TD 65536
SOLVENT CDCl3
NS 3800
DS 16
SWH 27173.912 Hz
FIDRES 0.414641 Hz
AQ 1.2059124 sec
RG 574.7
DM 18.400 usec
DE 6.00 usec
TE 296.1 K
D1 1.50000000 sec
d11 0.03000000 sec
TD0 1

==== CHANNEL F1 =====
NUC1 13C
P1 7.50 usec
PL1 5.00 dB
SFO1 100.6242095 MHz

==== CHANNEL F2 =====
CPDPRG2 waltz16
NUC2 1H
PCPD2 89.00 usec
PL2 -4.00 dB
PL12 17.37 dB
SFO2 399.7315989 MHz

F2 - Processing parameters
SI 32768
SF 100.6121480 MHz
WDW EM
SSB 0
LB 1.00 Hz
GB 0
PC 1.40



9.11
8.84
8.57
8.30
8.03
7.76
7.49
7.22
6.95
6.68
6.41
6.14
5.87
5.60
5.33
5.06
4.79
4.52
4.25
3.98
3.71
3.44
3.17
2.90
2.63
2.36
2.09
1.82
1.55
1.28
1.01
0.74
0.47
0.20
0.00



User Name smith
Group sintim
Sample Label METHYL_DIBUTYRATE

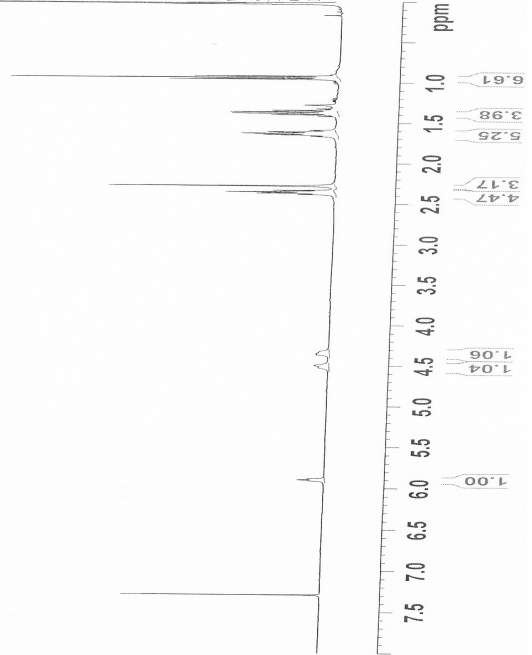


Current Data Parameters
NAME 25-smith-0429
EXPERO 10
PROCNO 1

F2 - Acquisition Parameters
Date 20100429
Time 22.17
INSTRUM spect
PROBHD 5 mm QNP 1H/1
PULPROG zgpg30
TD 32768
SOLVENT CDCl3
NS 64
DS 2
SWH 7575.738 Hz
FIDRES 0.19217 Hz
AQ 2.5999219 sec
RG 181
DM 66.000 usec
DE 6.00 usec
TE 295.5 K
D1 1.5000000 sec
T00 1

===== CHANNEL f1 =====
NUC1 1H
P1 9.50 usec
PL1 -3.00 dB
SFO1 399.732465 MHz

F2 - Processing parameters
SI 32768
SF 399.7300000 MHz
WDW EM
SSB 0
LB 0.30 Hz
GB 0
PC 2.00



User Name smith
 Group sintim
 Sample Label METHYL_DIBUTYRATE



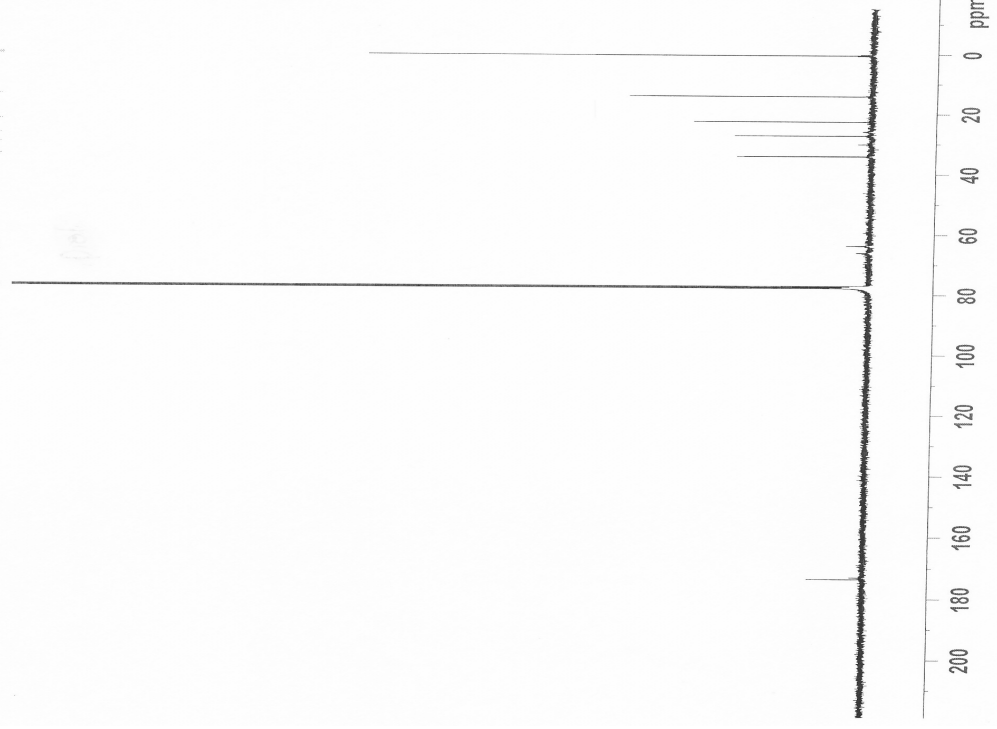
Current Data Parameters
 NAME 25-sm1lb-0429
 EXPNO 11
 PROCNO 1

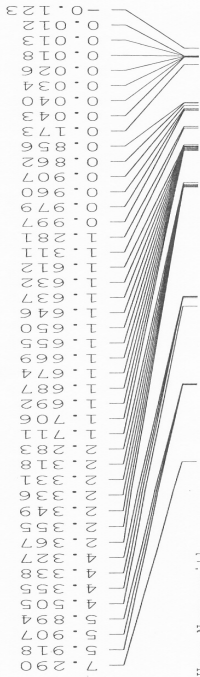
F2 - Acquisition Parameters
 Date_ 20100501
 Time_ 2.09
 INSTRUM spect
 PROBRD 5 mm QNP 1H/1
 PULPROG zgpg30
 TD 65536
 SOLVENT CDCl3
 NS 3800
 DS 16
 SWH 27173.912 Hz
 FIDRES 0.4114641 Hz
 AQ 1.2059124 sec
 RG 724.1
 DW 18.400 usec
 DE 6.00 usec
 TE 296.1 K
 D1 1.50000000 sec
 d11 0.03000000 sec
 TDO 1

==== CHANNEL f1 =====
 NU01 13C
 P1 7.50 usec
 PL1 5.00 dB
 SFO1 100.5242095 MHz

==== CHANNEL f2 =====
 CPDPRG2 waltz16
 NU02 1H
 PCPD2 89.00 usec
 PL2 -4.00 dB
 PL12 17.37 dB
 SFO2 399.713989 MHz

F2 - Processing parameters
 SI 32768
 SF 100.5121480 MHz
 KW 0
 SSB 0
 LB 1.00 Hz
 GB 0
 PC 1.40





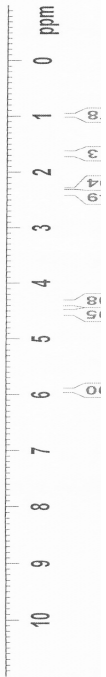
User Name smith
Group sintim
Sample Label METHYL_DIVALERATE

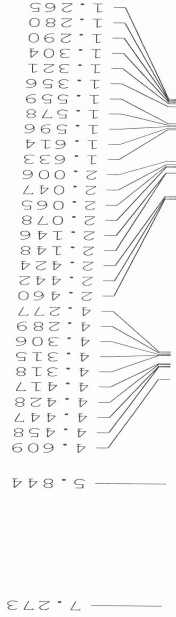
Current Data Parameters
NAME 26-smith-0429
EXPNO 10
PROCNO 1

F2 - Acquisition Parameters
Date_ 20100429
Time 22.30
INSTRUM spect
PROBHD 5 mm QNP 1H/1
PULPROG zg30
TD 39392
SOLVENT CDCl3
NS 64
DS 2
SWH 7575.758 Hz
FIDRES 0.192317 Hz
AQ 2.5999219 sec
RG 203.2
DW 66.000 usec
DE 6.00 usec
TE 295.5 K
D1 1.50000000 sec
TD0 1

==== CHANNEL f1 =====
NUC1 1H
P1 9.50 usec
PL1 -3.00 dB
SFO1 399.1324685 MHz

F2 - Processing parameters
SI 32768
SF 399.1300000 MHz
WDW EM
SSB 0
LB 0.30 Hz
GB 0
PC 2.00





User Name smith
Group sintim
Sample Label hexyl_diacetate



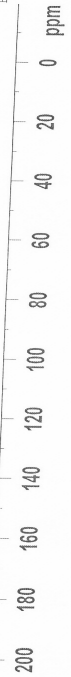
Current Data Parameters
NAME 12-smith-0216
EXNO 11
PROCNO 1

F2 - Acquisition Parameters
Date 201100216
Time 19.57
INSTRUM spect
PROBHD 5 mm QNP 1H/1
PULPROG zgpg30
TD 65536
SOLVENT CDCl3
NS 1300
DS 32
SNUF 27173.912 Hz
FIDRES 0.41641 Hz
AQ 1.2059124 sec
RG 287.4
DM 18.400 usec
DE 6.00 usec
TE 295.6 K
D1 1.5000000 sec
d11 0.0300000 sec
TD0 1

===== CHANNEL f1 =====
NUC1 13C
P1 4.50 usec
PL1 0.00 dB
SFO1 100.6242095 MHz

===== CHANNEL f2 =====
CPDPRG2 waltz16
NUC2 1H
PCPD2 89.00 usec
PL2 -4.00 dB
PL12 17.37 dB
SFO2 399.7315989 MHz

F2 - Processing parameters
SI 32768
SF 100.6121480 MHz
WDW EM
SSB 0
LB 1.00 Hz
GB 0
PC 1.40



User Name smith
Group sintim
Sample Label hexyl_propionate



Current Data Parameters
NAME 34-smith-0311
EXPRO 10
PROCNO 1

F2 - Acquisition Parameters

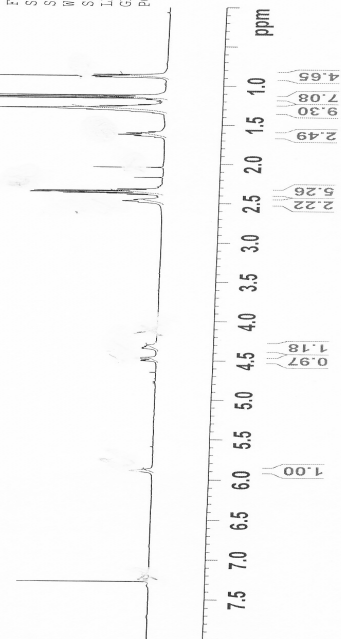
Date_ 20100311
Time_ 18.14
INSTRUM spect
PROBHD 5 mm QNP 1H/1
PULPROG zg30
TD 32768
SOLVENT CDCl3
NS 64
DS 2
SWH 7515.758 Hz
FIDRES 0.192317 Hz
AQ 2.5999219 sec
RG 37
DM 66.000 usec
DE 6.00 usec
TE 285.2 K
D1 1.5000000 sec
TDO 1

===== CHANNEL f1 =====

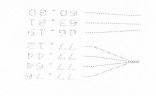
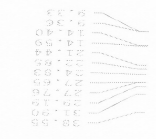
NUC1 1H
P1 9.50 usec
PL1 -3.00 dB
SFO1 399.7324685 MHz

F2 - Processing parameters

SI 32768
SF 399.7300000 MHz
WDW EM
SSB 0
LB 0.30 Hz
GB 0
PC 2.00



User Name smith
Group sintim
Sample Label hexyl_propionate



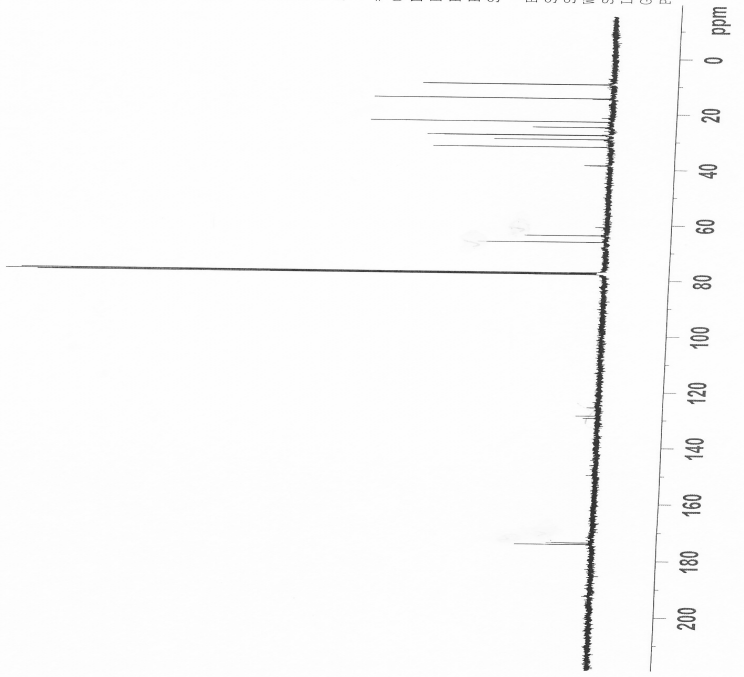
Current Data Parameters
NAME 34-sm1h-0311
EXPNO 11
PROCNO 1

F2 - Acquisition Parameters
Date_ 20100311
Time 18.49
INSTRUM spect
PROBHD 5 mm QNP 1H/1
PULPROG zgpg30
TD 65536
SOLVENT CDCl3
NS 900
DS 4
SWH 27173.912 Hz
FIDRES 0.414641 Hz
AQ 1.2059124 sec
RG 724.1
DW 18.400 usec
DE 6.00 usec
TE 295.8 K
D1 1.0000000 sec
d11 0.0300000 sec
TD0 1

==== CHANNEL f1 =====
NUC1 13C
P1 7.50 usec
PL1 5.00 dB
SFO1 100.5242095 MHz

==== CHANNEL f2 =====
CPDPRG2 waltz16
NUC2 1H
PCPD02 89.00 usec
PL2 -4.00 dB
PL12 17.37 dB
SFO2 399.7315899 MHz

F2 - Processing parameters
SI 32768
SF 100.5121480 MHz
WDW EN
SSB 0
LB 1.00 Hz
GB 0
PC 1.40



User Name smith
Group sintim
Sample Label hexyl_butylrate



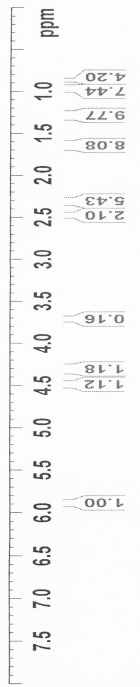
Current Data Parameters
NAME 35-smith-0311
EXPNO 10
PROCNO 1

F2 - Acquisition Parameters
Date_ 20100311
Time 19.04

INSTRUM spect
PROBHD 5 mm QNP 1H/1
PULPROG zg30
TD 39992
SOLVENT CDCl3
NS 64
DS 2
SWH 7575.758 Hz
FIDRES 0.190317 Hz
AQ 2.399219 sec
RG 45.3
DW 66.000 usec
DE 6.00 usec
TE 295.2 K
D1 1.5000000 sec
TD0 1

==== CHANNEL f1 =====
NUC1 1H
P1 9.50 usec
PL1 -3.00 dB
SFO1 399.7324685 MHz

F2 - Processing parameters
SI 32768
SF 399.7300000 MHz
WDW EM
SSB 0
LB 0.30 Hz
GB 0
PC 2.00





User Name smith
Group sintim
Sample label hexyl_butyrate



Current Data Parameters
NAME 35-smith-0311
EXPERNO 11
PROCNO 1

F2 - Acquisition Parameters
Date 20100311
Time 19.39
INSTRUM spect
PROBHD 5 mm QNP 1H/1
PULPROG zgpg30
TD 65536
SOLVENT CDCl3
NS 900
DS 4
SWH 27173.912 Hz
FIDRES 0.414641 Hz
AQ 1.2059124 sec
RG 645.1
DM 18.400 usec
DE 6.00 usec
TE 295.8 K
D1 1.0000000 sec
d11 0.0300000 sec
T00 1

===== CHANNEL f1 =====
NUC1 13C
P1 7.50 usec
PL1 5.00 dB
SFO1 100.5242095 MHz

===== CHANNEL f2 =====
CPDPRG2 waltz16
NUC2 1H
PCPD2 89.00 usec
PL2 4.00 dB
PL12 17.37 dB
SFO2 399.7315989 MHz

F2 - Processing parameters
SI 32768
SF 100.5121480 MHz
WDW EM
SSB 0
LB 1.00 Hz
GB 0
PC 1.40



User Name smith
Group sintim
Sample Label hexyl_valerate

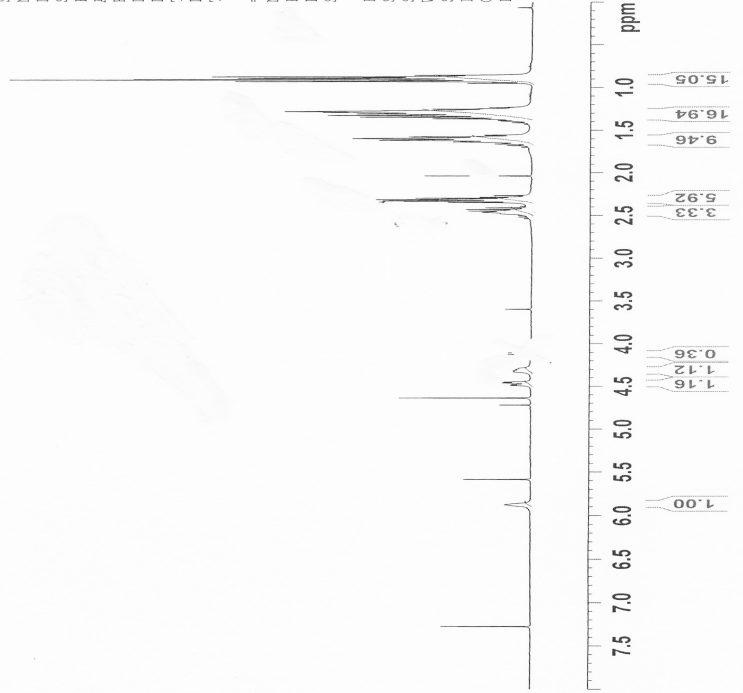


Current Data Parameters
NAME 36-smith-0311
EXPNO 10
PROCNO 1

F2 - Acquisition Parameters
Date_ 20100311
Time 19:52
INSTRUM spect
PROBHD 5 mm QNP 1H/1
PULPROG zg30
TD 39392
SOLVENT CDCl3
NS 64
DS 2
SWH 7515.768 Hz
FIDRES 0.192317 Hz
AQ 2.5999219 sec
RG 40.3
DM 66.000 usec
DE 6.00 usec
TE 295.3 K
D1 1.5000000 sec
TD0 1

===== CHANNEL f1 =====
NUC1 1H
P1 9.50 usec
PL1 -3.00 dB
SFO1 399.7324685 MHz

F2 - Processing parameters
SI 32768
SF 399.7300000 MHz
WDW EM
SSB 0
LB 0.30 Hz
GB 0
PC 2.00



User Name smith
Group sintim
Sample Label hexyl_valerate



Current Data Parameters
NAME 36-smith-0311
EXPNO 11
PROCNO 1

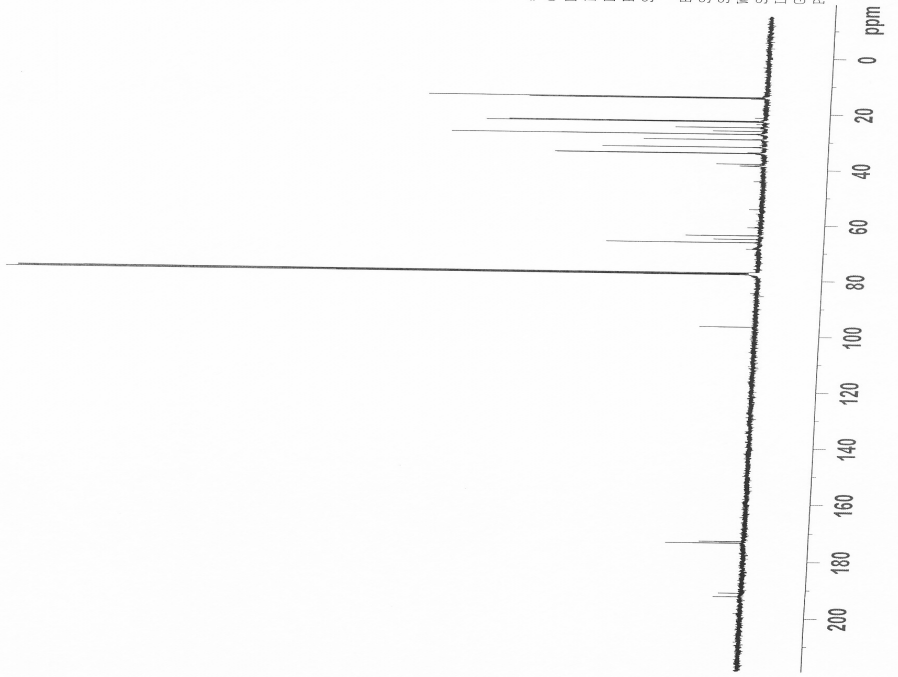
F2 - Acquisition Parameters
Date_ 20100311
Time 20.27

INSTRUM spect
PROBHD 5 mm QNP 1H/1
PULPROG zgpg30
TD 65536
SOLVENT CDCl3
NS 900
DS 4
SWH 27173.912 Hz
FIDRES 0.418641 Hz
AQ 1.2059124 sec
RG 645.1
DW 18.400 usec
DE 6.00 usec
TE 295.8 K
D1 1.40000000 sec
d11 0.03000000 sec
TDO 1

==== CHANNEL f1 =====
NUC1 13C
P1 7.50 usec
PL1 5.00 dB
SFO1 100.5242095 MHz

==== CHANNEL f2 =====
CPDPRG2 waltz16
NUC2 1H
PCPD2 89.00 usec
PL2 -4.00 dB
PL12 17.37 dB
SFO2 399.7315899 MHz

F2 - Processing parameters
SI 32768
SF 100.5121800 MHz
WDW EM
SSB 0
LB 1.00 Hz
GB 0
PC 1.40



User Name smith
Group sintim
Sample Label dipropionate_methyl - D30

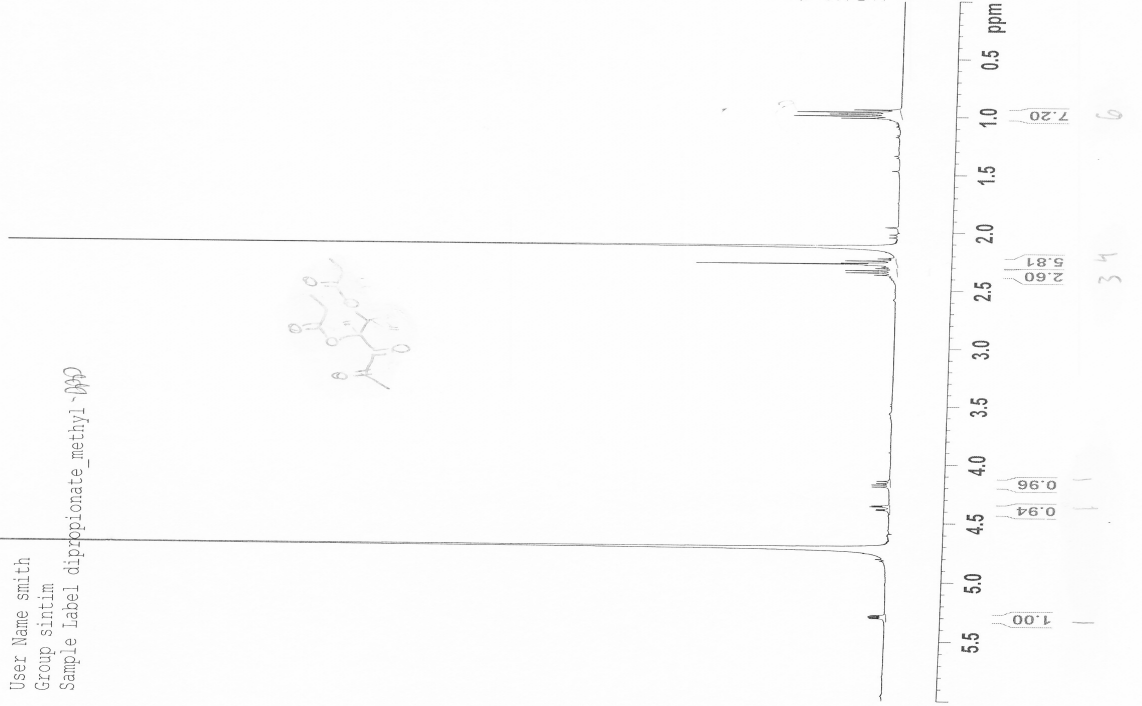
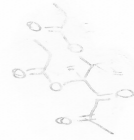


Current Data Parameters
NAME 17-smith-0504
EXNO 10
PROCNO 1

F2 - Acquisition Parameters
Date 20100504
Time 15:06
INSTRUM spect
PROBHD 5 mm QNP 1H/1
PULPROG zg30
TD 39382
SOLVENT D2O
NS 64
DS 2
SWH 7575.758 Hz
FIDRES 0.192317 Hz
AQ 2.5999219 sec
RG 128
DM 66.000 usec
DE 6.00 usec
TE 295.2 K
D1 1.5000000 sec
TD0 1

===== CHANNEL f1 =====
NUC1 1H
P1 9.50 usec
PL1 -3.00 dB
SFO1 399.7324685 MHz

F2 - Processing parameters
SI 32768
SF 399.7300000 MHz
WDW EM
SSS 0
LB 0.30 Hz
GB 0
PC 2.00



User Name smith
Group sintim
Sample Label dipropionate_methyl



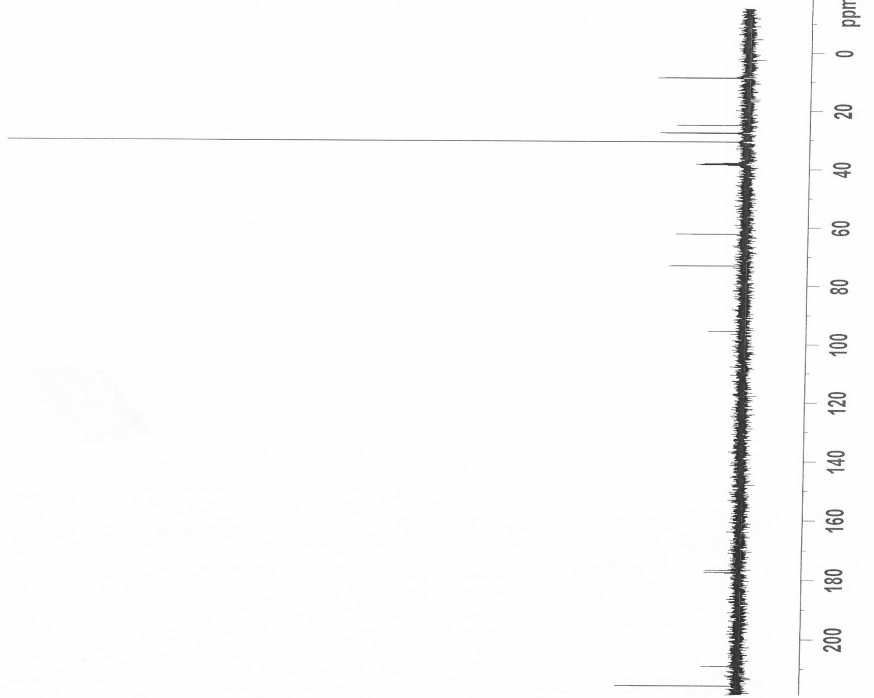
Current Data Parameters
NAME 17-smith-0504
EXENO 11
PROCNO 1

F2 - Acquisition Parameters
Date 20100504
Time 20.39
INSTRUM spect
PROBHD 5 mm QNP
PULPROG zgpg30
TD 65536
SOLVENT D2O
NS 3800
DS 16
SWH 27173.912 Hz
FIDRES 0.414641 Hz
AQ 1.2059124 sec
RG 2580.3
DM 18.400 usec
DE 6.00 usec
TE 296.2 K
D1 1.5000000 sec
d11 0.0300000 sec
TDO 1

==== CHANNEL f1 =====
NUC1 13C
P1 7.50 usec
PL1 5.00 dB
SFO1 101.5242095 MHz

==== CHANNEL f2 =====
CPCPRG2 waltz16
NUC2 1H
PCPD2 89.00 usec
PL2 -4.00 dB
PL12 17.37 dB
SFO2 399.7315989 MHz

F2 - Processing parameters
SI 32768
SF 100.5121480 MHz
WDW EM
SSB 0
LB 1.00 Hz
GB 0
PC 1.40



User Name smith
Group sintim
Sample Label methyl_dibutyrate - DMF

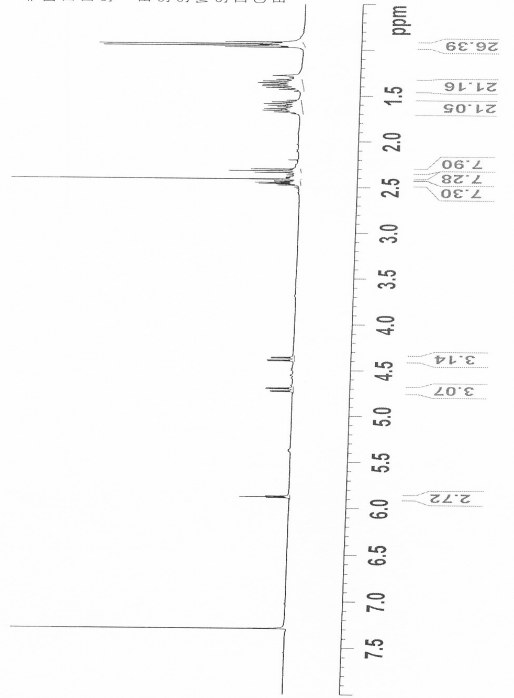


Current Data Parameters
NAME 24-smith-0505
EXPNO 10
PROCNO 1

F2 - Acquisition Parameters
Date_ 20100506
Time 0.38
INSTRUM spect
PROBHD 5 mm QNP 1H/1
PULPROG zg30
TD 3932
SOLVENT CDCl3
NS 64
DS 2
SWH 7575.758 Hz
FIDRES 0.192317 Hz
AQC 2.599219 sec
RG 256
DW 66.000 usec
DE 6.00 usec
TE 295.4 K
D1 1.5000000 sec
TD0 1

==== CHANNEL f1 =====
NUC1 1H
P1 9.50 usec
PL1 -3.00 dB
SFO1 399.732465 MHz

F2 - Processing parameters
SI 32768
SF 399.730000 MHz
AQM EM
SSB 0
LB 0.30 Hz
GB 0
PC 2.00



User Name smith
Group sintim
Sample Label methyl_dibutryate `020



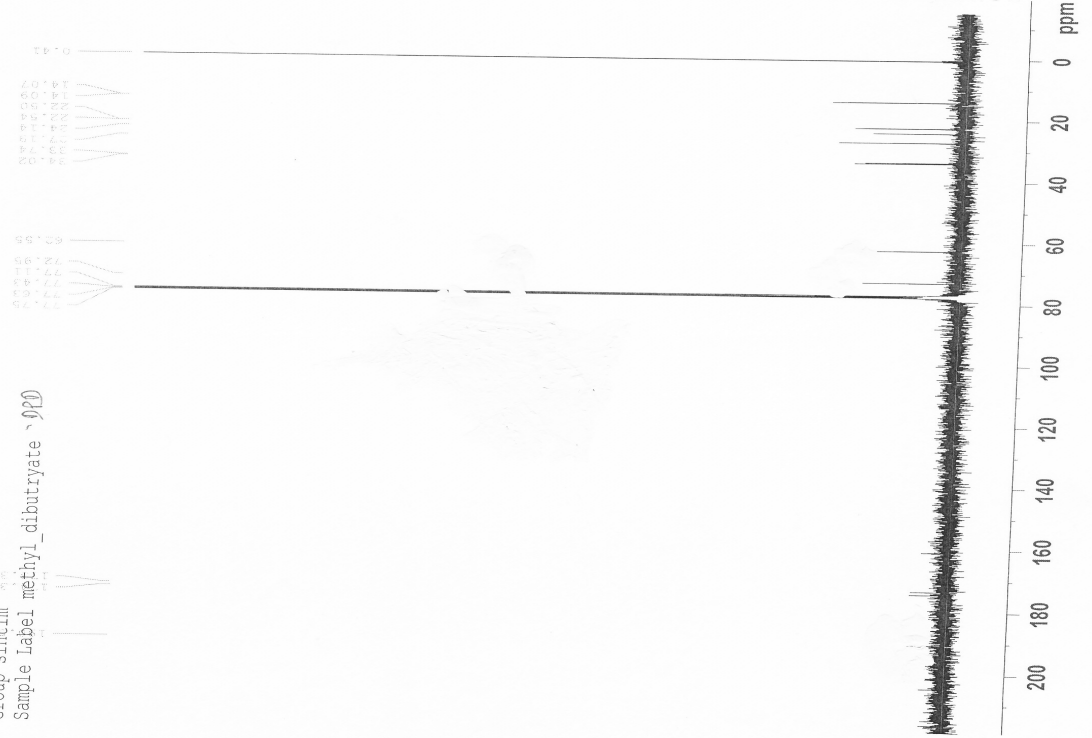
Current Data Parameters
NAME 24-smith-0505
EXNO 11
PROCNO 1

F2 - Acquisition Parameters
Date_ 20100506
Time 11.08
INSTRUM spect
PROBHD 5 mm QNP 1H/1
PULPROG zgpg30
TD 65536
SOLVENT CDCl3
NS 1300
DS 32
SWH 27113.912 Hz
FIDRES 0.414621 Hz
AQ 1.2059124 sec
RG 456.1
DW 18.400 usec
DE 6.00 usec
TE 295.8 K
D1 1.50000000 sec
d11 0.03000000 sec
TD0 1

==== CHANNEL F1 =====
NUC1 13C
P1 7.50 usec
PL1 5.00 dB
SF01 100.5242095 MHz

==== CHANNEL F2 =====
CPDPRG2 waltz16
NUC2 1H
PCPD2 89.00 usec
PL2 4.00 dB
PL12 17.37 dB
SF02 399.7315989 MHz

F2 - Processing parameters
SI 32768
SF 100.5121480 MHz
WDW EN
SSB 0
LB 1.00 Hz
GB 0
PC 1.40



User Name smith
Group sintim
Sample label methyl_divalerate

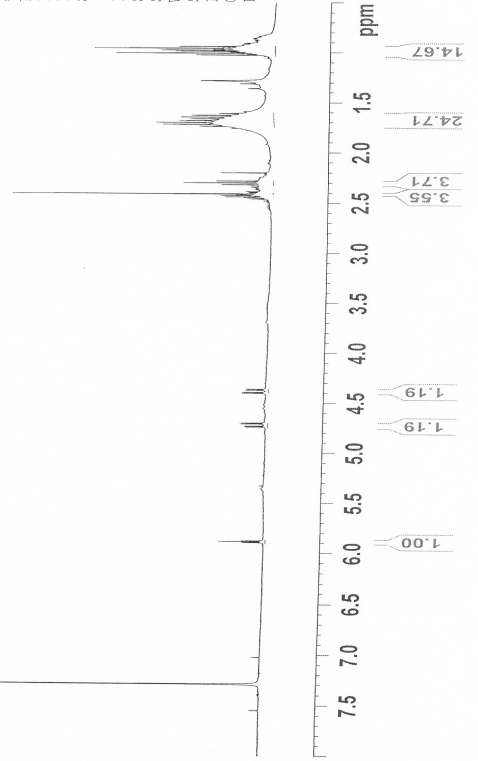


Current Data Parameters
NAME 25-smith-0505
EXPERNO 10
PROCNO 1

F2 - Acquisition Parameters
Date_ 20100506
Time_ 0.52
INSTRUM spect
PROBHD 5 mm QNP 1H/1
PULPROG zg30
TD 39392
SOLVENT CDCl3
NS 64
DS 2
SWH 7575.758 Hz
FIDRES 0.192317 Hz
AQ 2.5999219 sec
RG 362
DM 66.000 usec
DE 6.000 usec
TE 295.3 K
D1 1.50000000 sec
TDO 1

==== CHANNEL f1 =====
NUC1 1H
P1 9.50 usec
PL1 -3.00 dB
SFO1 399.7324685 MHz

F2 - Processing parameters
SI 32768
SF 399.7300000 MHz
WDW EM
SSB 0
LB 0.30 Hz
GB 0
PC 2.00





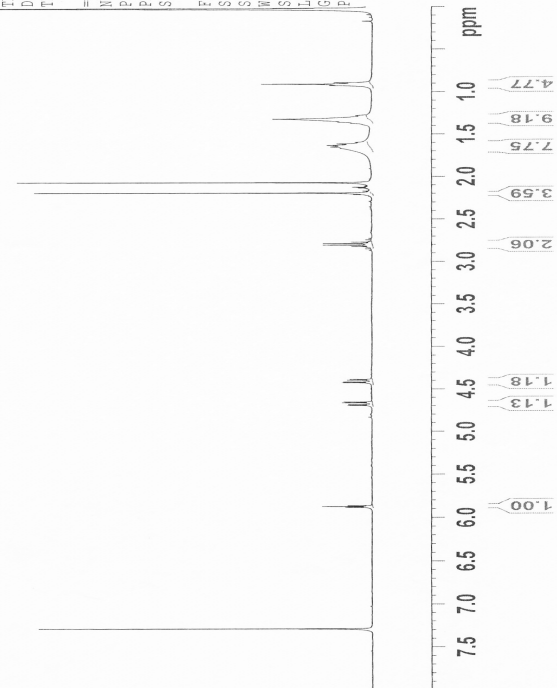
User Name smith
Group sintim
Sample Label hexyl_diacetate_dpd

Current Data Parameters
NAME 37-smith-0527
EXENO 20
PROCNO 1

F2 - Acquisition Parameters
Date_ 20100927
Time_ 15:30
INSTRUM spect
PROBHD 5 mm QNP 1H/1
PULPROG zg30
TD 32768
SOLVENT CDCl3
NS 64
DS 2
SWH 7575.758 Hz
FIDRES 0.192317 Hz
AQ 2.5899219 sec
RG 362
RW 66.000 usec
DE 6.00 usec
TE 295.3 K
D1 1.50000000 sec
TD0 1

==== CHANNEL f1 =====
NUC1 1H
P1 9.50 usec
PL1 -1.00 dB
SFO1 399.7324685 MHz

F2 - Processing parameters
SI 32768
SF 399.7300000 MHz
WDW EM
SSB 0
LB 0.30 Hz
GB 0
PC 2.00





User Name smith
 Group simtim
 Sample Label hexyl_diacetate_dpd



Current Data Parameters
 NAME 37-smith-0527
 EXPNO 21
 PROCNO 1

F2 - Acquisition Parameters
 Date 20100527
 Time 19:29
 INSTRUM spect
 PROCNO 5 mm QNP 1H/1
 PULPROG zgpg30
 TD 65536
 SOLVENT CDCl3
 NS 3800
 DS 16
 SWH 27173.912 Hz
 FIDRES 0.411641 Hz
 AQ 1.2059124 sec
 RG 512
 DW 18.400 usec
 DE 6.00 usec
 TE 296.2 K
 D1 1.50000000 sec
 d11 0.03000000 sec
 TDO 1

==== CHANNEL f1 =====
 NU01 13C
 PL 7.50 usec
 PL1 5.00 dB
 SF01 100.5242095 MHz
 ===== CHANNEL f2 =====
 CPDPRG2 waltz16
 NU02 1H
 PL2 89.00 usec
 PL2 -4.00 dB
 PL12 17.37 dB
 SF02 399.7315969 MHz

F2 - Processing parameters
 SI 32768
 SF 100.5121480 MHz
 WHW EM
 SSB 0
 LB 1.00 Hz
 GB 0
 PC 1.40



User Name smith
Group sintim
Sample Label hexyl_dipropionate_dpd



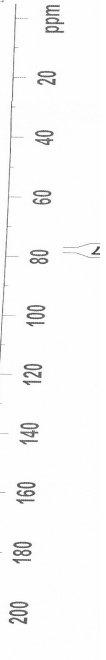
Current Data Parameters
NAME 39-smith-0537
EXPERNO 21
PROCNO 1

F2 - Acquisition Parameters
Date_ 20100527
Time_ 22.38
INSTRUM spect
PROBHD 5 mm QNP 1H/1
PULPROG zgpg30
TD 65536
SOLVENT CDCl3
NS 3800
DS 16
SWH 27173.912 Hz
FIDRES 0.414641 Hz
AQ 1.2059124 sec
RG 406.4
DA 18.400 usec
DE 6.00 usec
TE 296.1 K
DL 1.5000000 sec
d11 0.0300000 sec
TD0 1

===== CHANNEL f1 =====
NUC1 13C
P1 7.50 usec
PL1 5.00 dB
SFO1 100.6242095 MHz

===== CHANNEL f2 =====
CPDPRG2 waltz16
NUC2 1H
PCPD2 89.00 usec
PL2 -4.00 dB
PL12 17.37 dB
SFO2 399.731989 MHz

F2 - Processing parameters
SI 32768
SF 100.5121480 MHz
WDW EM
SSB 0
LB 1.00 Hz
GB 0
PC 1.40



User Name smith
Group sintim
Sample Label hexyl_dibutyrate_dbd

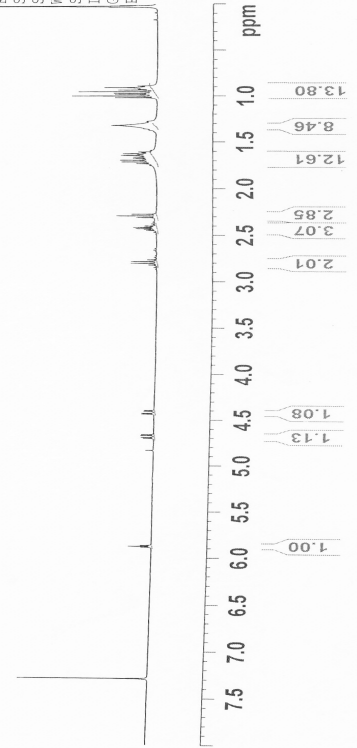


Current Data Parameters
NAME 39-smith-0527
EXPNO 20
PROCNO 1

F2 - Acquisition Parameters
Date 20100527
Time 16.01
INSTRUM spect
PROBHD 5 mm QNP 1H/1
PULPROG zg30
TD 39392
SOLVENT CDCl3
NS 64
DS 2
SWH 7575.758 Hz
FIDRES 0.192317 Hz
AQ 2.5999219 sec
RG 287.4
DW 66.000 usec
DE 6.00 usec
TE 295.4 K
D1 1.5000000 sec
TDO 1

===== CHANNEL f1 =====
NUC1 1H
P1 9.50 usec
PL1 -3.00 dB
SFO1 399.7324685 MHz

F2 - Processing parameters
SI 32768
SF 399.7300000 MHz
WDW EM
SSB 0
LB 0.30 Hz
GB 0
PC 2.00



User Name smith
Group sintim
Sample Label hexyl_dibutyrate_dpd



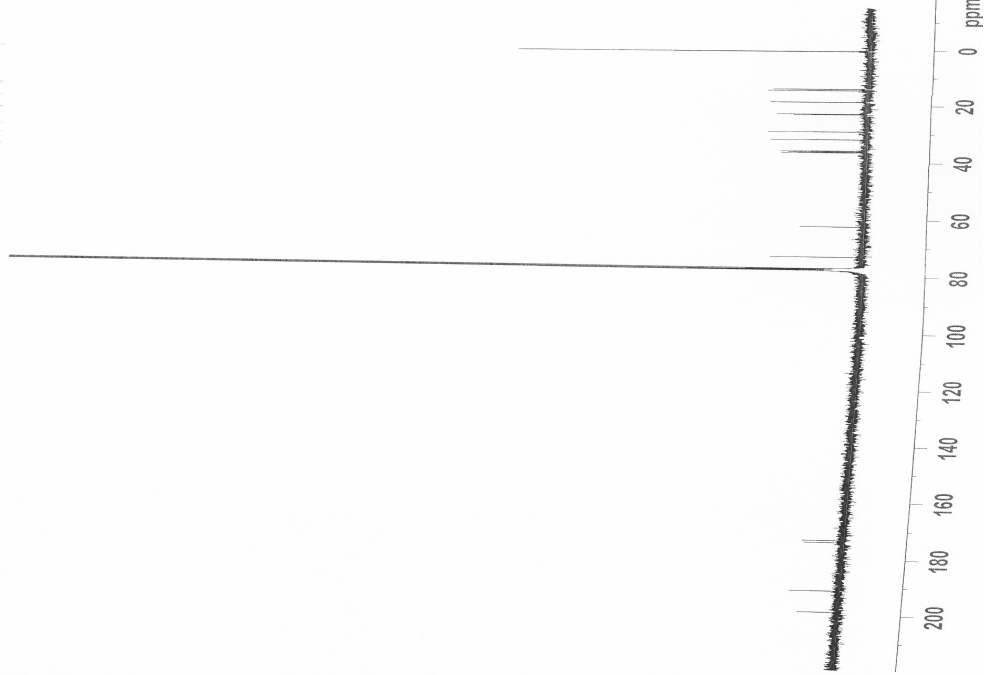
Current Data Parameters
NAME 39-smith-0527
EXPERNO 21
PROCNO 1

F2 - Acquisition Parameters
Date_ 20100528
Time 1.45
INSTRUM spect
PROBHD 5 mm QNP 1H/1
PULPROG zgpg30
TD 65536
SOLVENT CDCl3
NS 3800
DS 16
SWH 27173.912 Hz
FIDRES 0.419441 Hz
AQ 1.2059724 sec
RG 912.3
DM 18.400 usec
DE 6.00 usec
TE 296.0 K
D1 1.50000000 sec
d11 0.03000000 sec
TDO 1

===== CHANNEL f1 =====
NUC1 13C
P1 7.50 usec
PL1 5.00 dB
SFO1 100.5242095 MHz

===== CHANNEL f2 =====
CPDPRG2 waltz16
NUC2 1H
PCPD2 89.00 usec
PL2 -4.00 dB
PL12 17.37 dB
SFO2 399.7315989 MHz

F2 - Processing parameters
SI 32768
SF 100.5121460 MHz
ADW EM
SSB 0
LB 1.00 Hz
GB 0
PC 1.40



User Name smith
Group sintim
Sample Label hexyl_divalerate_dpd

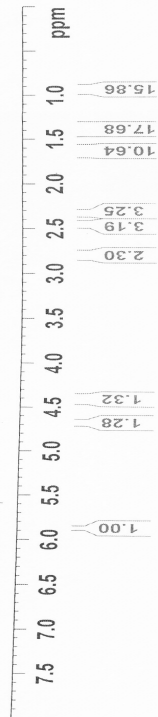


Current Data Parameters
NAME 40-smith-0327
EXPRO 20
PROCNO 1

F2 - Acquisition Parameters
Date 20100527
Time 16.20
INSTRUM spect
PROBHD 5 mm QNP 1H/1
PULPROG zg30
TD 39392
SOLVENT CDCl3
NS 64
DS 2
SWH 7575.758 Hz
FIDRES 0.192317 Hz
AQ 2.5999219 sec
RG 228.1
DM 66.000 usec
DE 6.00 usec
TE 295.4 K
D1 1.5000000 sec
TDO 1

==== CHANNEL f1 =====
NUC1 1H
P1 9.50 usec
PL 0
FLL 3.00 dB
SFO1 399.7324695 MHz

F2 - Processing parameters
SI 32768
SF 399.7300000 MHz
WDW EM
SSB 0
LB 0.30 Hz
GB 0
PC 2.00





References

1. Arias, C. A.; Murray, B. E., Antibiotic-Resistant Bugs in the 21st Century- A Clinical Super-Challenge. *New Engl. J. Med.* **2009**, *360* (5), 439-443.
2. Clatworthy, A. E.; Pierson, E.; Hung, D. T., Targeting virulence: a new paradigm for antimicrobial therapy. *Nat. Chem. Biol.* **2007**, *3* (9), 541-548.

3. (a) Sintim, H. O.; Smith, J. A. I.; Wang, J.; Nakayama, S.; Yan, L., Paradigm shift in discovering next-generation anti-infective agents: targeting quorum sensing, c-di-GMP signaling and biofilm formation in bacteria with small molecules. *Future Med. Chem.* **2010**, *2* (6), 1005-1036; (b) Cegelski, L.; Marshall, G. R.; Eldridge, G. R.; Hultgren, S. J., The biology and future prospects of antivirulence therapies. *Nat. Rev. Microbiol.* **2008**, *6* (1), 17-27.
4. (a) Waters, C. M.; Bassler, B. L., Quorum Sensing: Cell-to Cell Communication in Bacteria. *Annu. Rev. Cell Dev. Biol.* **2005**, *21*, 319-346; (b) Parker, C. T.; Sperandio, V., Cell-to-cell signalling during pathogenesis. *Cell. Microbiol.* **2009**, *11* (3), 363-369; (c) Asad, S.; Opal, S. M., Bench-to-bedside review: Quorum sensing and the role of cell-to-cell communication during invasive bacterial infection. *Critical Care* **2008**, *12* (6), 236.
5. Antunes, L. C. M.; Ferreira, R. B. R.; Buckner, M. M. C.; Finlay, B. B., Quorum sensing in bacterial virulence. *Microbiology* **2010**, *156*, 2271-2282.
6. (a) Costerton, J. W., Bacterial Biofilms: A Common Cause of Persistent Infections. *Science* **1999**, *284* (5418), 1318-1322; (b) Fux, C.; Costerton, J.; Stewart, P.; Stoodley, P., Survival strategies of infectious biofilms. *Trends Microbiol.* **2005**, *13* (1), 34-40.
7. Parsek, M.; Greenberg, E., Sociomicrobiology: the connections between quorum sensing and biofilms. *Trends Microbiol.* **2005**, *13* (1), 27-33.
8. Camilli, A.; Bassler, B. L., Bacterial Small-Molecule Signaling Pathways. *Science* **2006**, *311*, 1113-1116.
9. Koch, B.; Lijefors, T.; Persson, T.; Nielsen, J.; Kjelleberg, S.; Givskov, M., The LuxR receptor: the sites of interaction with quorum-sensing signals and inhibitors. *Microbiology* **2005**, *151*, 3589-3602.
10. Geske, G. D.; O'Neill, J. C.; Blackwell, H. E., Expanding dialogues: from natural autoinducers to non-natural analogues that modulate quorum sensing in Gram-negative bacteria. *Chem. Soc. Rev.* **2008**, *37* (7), 1432.
11. Ng, W.-L.; Bassler, B. L., Bacterial Quorum-Sensing Network Architectures. *Annu. Rev. Genet.* **2009**, *43* (1), 197-222.
12. Reading, N. C.; Sperandio, V., Quorum sensing: the many languages of bacteria. *FEMS Microbiol. Lett.* **2006**, *254* (1), 1-11.
13. Lowery, C. A.; Salzameda, N. T.; Sawada, D.; Kaufmann, G. F.; Janda, K. D., Medicinal Chemistry as a Conduit for the Modulation of Quorum Sensing. *J. Med. Chem.* **2010**, *53* (21), 7467-7489.
14. (a) Yang, F.; Wang, L.; Wang, J.; Dong, Y.; Hu, J.; Zhang, L., Quorum quenching enzyme activity is widely conserved in the sera of mammalian species. *FEBS Lett.* **2005**, *579* (17), 3713-3717; (b) Sio, C. F.; Otten, L. G.; Cool, R. H.; Diggle, S. P.; Braun, P. G.; Bos, R.; Daykin, M.; Camara, M.; Williams, P.; Quax, W. J., Quorum quenching by an N-acyl homoserine lactone acylase from *Pseudomonas aeruginosa* PAO1. *Infect. Immun.* **2006**, *74* (3), 1673-1682; (c) Bokhove, M.; Jimenez, P. N.; Quax, W. J.; Dijkstra, B. W., The quorum-quenching N-acyl homoserine lactone acylase PvdQ is an Ntn-hydrolase with an unusual substrate-binding pocket. *Proc. Natl. Acad. Sci.* **2009**; (d) Pustelny, C.; Albers, A.; Büldt-Karentzopoulos, K.; Parschat, K.; Chhabra, S. R.; Cámara, M.; Williams, P.; Fetzner, S., Dioxygenase-Mediated Quenching of Quinolone-Dependent Quorum Sensing in *Pseudomonas aeruginosa*. *Chem. Biol.* **2009**, *16* (12), 1259-1267.

15. Rasmussen, T. B.; Skindersoe, M. E.; Bjarnsholt, T.; Phipps, R. K.; Christensen, K. B.; Jensen, P. O.; Andersen, J. B.; Koch, B.; Larsen, T. O.; Hentzer, M.; Eberl, L.; Hoiby, N.; Givskov, M., Identity and effects of quorum-sensing inhibitors produced by *Penicillium* species. *Microbiology* **2005**, *151* (Pt 5), 1325-1340.
16. Brackman, G.; Defoirdt, T.; Miyamoto, C.; Bossier, P.; Van Calenbergh, S.; Nelis, H.; Coenye, T., Cinnamaldehyde and cinnamaldehyde derivatives reduce virulence in *Vibrio* spp. by decreasing the DNA-binding activity of the quorum sensing response regulator LuxR. *BMC Microbiol.* **2008**, *8* (1), 149.
17. Manefield, M.; Rasmussen, T. B.; Hentzer, M.; Andersen, J. B.; Steinberg, P.; Kjelleberg, S.; Givskov, M., Halogenated furanones inhibit quorum sensing through accelerated LuxR turnover. *Microbiology* **2002**, *148*, 1119-1127.
18. (a) Hentzer, M.; Riedel, K.; Rasmussen, T. B.; Heydorn, A.; Andersen, J. B.; Parsek, M. R.; Rice, S. A.; Eberl, L.; Molin, S.; Hoiby, N.; Kjelleberg, S.; Givskov, M., Inhibition of quorum sensing in *Pseudomonas aeruginosa* biofilm bacteria by a halogenated furanone compound. *Microbiology* **2002**, *148*, 87-102; (b) Janssens, J. C. A.; Steenackers, H.; Robijns, S.; Gellens, E.; Levin, J.; Zhao, H.; Hermans, K.; De Coster, D.; Verhoeven, T. L.; Marchal, K.; Vanderleyden, J.; De Vos, D. E.; De Keersmaecker, S. C. J., Brominated Furanones Inhibit Biofilm Formation by *Salmonella enterica* Serovar Typhimurium. *Appl. Environ. Microbiol.* **2008**, *74* (21), 6639-6648.
19. Defoirdt, T.; Miyamoto, C. M.; Wood, T. K.; Meighen, E. A.; Sorgeloos, P.; Verstraete, W.; Bossier, P., The natural furanone (5Z)-4-bromo-5-(bromomethylene)-3-butyl-2(5H)-furanone disrupts quorum sensing-regulated gene expression in *Vibrio harveyi* by decreasing the DNA-binding activity of the transcriptional regulator protein luxR. *Environ. Microbiol.* **2007**, *9* (10), 2486-2495.
20. Zang, T.; Lee, B. W. K.; Cannon, L. M.; Ritter, K. A.; Dai, S.; Ren, D.; Wood, T. K.; Zhou, Z. S., A naturally occurring brominated furanone covalently modifies and inactivates LuxS. *Biorg. Med. Chem. Lett.* **2009**, *19* (21), 6200-6204.
21. More, M. I.; Finger, L. D.; Stryker, J. L.; Fuqua, C.; Eberhard, A.; Winans, S. C., Enzymatic synthesis of a quorum-sensing autoinducer through use of defined substrates. *Science* **1996**, *272* (5268), 1655-1658.
22. Singh, V., Femtomolar Transition State Analogue Inhibitors of 5'-Methylthioadenosine/S-Adenosylhomocysteine Nucleosidase from *Escherichia coli*. *J. Biol. Chem.* **2004**, *280* (18), 18265-18273.
23. Gutierrez, J. A.; Crowder, T.; Rinaldo-Matthis, A.; Ho, M.-C.; Almo, S. C.; Schramm, V. L., Transition state analogs of 5'-methylthioadenosine nucleosidase disrupt quorum sensing. *Nat. Chem. Biol.* **2009**, *5* (4), 251-257.
24. Eberhard, A.; Widrig, C. A.; Mcbath, P.; Schineller, J. B., Analogs of the Autoinducer of Bioluminescence in *Vibrio-Fischeri*. *Arch. Microbiol.* **1986**, *146* (1), 35-40.
25. Geske, G. D.; O'Neill, J. C.; Miller, D. M.; Mattmann, M. E.; Blackwell, H. E., Modulation of Bacterial Quorum Sensing with Synthetic Ligands: Systematic Evaluation of N-Acylated Homoserine Lactones in Multiple Species and New Insights into Their Mechanisms of Action. *J. Am. Chem. Soc.* **2007**, *129* (44), 13613-13625.
26. Geske, G. D.; Wezeman, R. J.; Siegel, A. P.; Blackwell, H. E., Small Molecule Inhibitors of Bacterial Quorum Sensing and Biofilm Formation. *J. Am. Chem. Soc.* **2005**, *127*, 12762-12763.

27. (a) Smith, K. M.; Bu, Y. G.; Suga, H., Induction and inhibition of *Pseudomonas aeruginosa* quorum sensing by synthetic autoinducer analogs. *Chem. Biol.* **2003**, *10* (1), 81-89; (b) Smith, K. M.; Bu, Y. G.; Suga, H., Library screening for synthetic agonists and antagonists of a *Pseudomonas aeruginosa* autoinducer. *Chem. Biol.* **2003**, *10* (6), 563-571.
28. (a) Castang, S.; Chantegrel, B.; Deshayes, C.; Dolmazon, R.; Gouet, P.; Haser, R.; Reverchon, S.; Nasser, W.; Hugouvieux-Cotte-Pattat, N.; Doutheau, A., N-sulfonyl homoserine lactones as antagonists of bacterial quorum sensing. *Biorg. Med. Chem. Lett.* **2004**, *14* (20), 5145-5149; (b) Persson, T.; Hansen, T. H.; Rasmussen, T. B.; Skinderso, M. E.; Givskov, M.; Nielsen, J., Rational design and synthesis of new quorum-sensing inhibitors derived from acylated homoserine lactones and natural products from garlic. *Org. Biomol. Chem.* **2005**, *3* (2), 253-262.
29. (a) Lyon, G. J.; Mayville, P.; Muir, T. W.; Novick, R. P., Rational design of a global inhibitor of the virulence response in *Staphylococcus aureus*, based in part on localization of the site of inhibition to the receptor-histidine kinase, AgrC. *Proc. Natl. Acad. Sci. USA* **2000**, *97* (24), 13330-13335; (b) Chan, W.; Coyle, B.; Williams, P., Virulence regulation and quorum sensing in staphylococcal infections: Competitive AgrC antagonists as quorum sensing inhibitors. *J. Med. Chem.* **2004**, 4633-4641.
30. Lyon, G. J.; Wright, J. S.; Muir, T. W.; Novick, R. P., Key Determinants of Receptor Activation in the agr Autoinducing Peptides of *Staphylococcus aureus*. *Biochemistry* **2002**, *41*, 10095-10104.
31. George, E. A.; Novick, R. P.; Muir, T. W., Cyclic Peptide Inhibitors of Staphylococcal Virulence Prepared by Fmoc-Based Thiolactone Peptide Synthesis. *J. Am. Chem. Soc.* **2008**, *130* (14), 4914-4924.
32. (a) Muh, U.; Schuster, M.; Heim, R.; Singh, A.; Olson, E. R.; Greenberg, E. P., Novel *Pseudomonas aeruginosa* quorum-sensing inhibitors identified in an ultra-high-throughput screen. *Antimicrob. Agents Chemother.* **2006**, *50* (11), 3674-3679; (b) Muh, U.; Hare, B. J.; Duerkop, B. A.; Schuster, M.; Hanzelka, B. L.; Heim, R.; Olson, E. R.; Greenberg, E. P., A structurally unrelated mimic of a *Pseudomonas aeruginosa* acyl-homoserine lactone quorum-sensing signal. *Proc. Natl. Acad. Sci. USA* **2006**, *103* (45), 16948-16952.
33. Rasko, D. A.; Moreira, C. G.; Li, D. R.; Reading, N. C.; Ritchie, J. M.; Waldor, M. K.; Williams, N.; Taussig, R.; Wei, S. G.; Roth, M.; Hughes, D. T.; Huntley, J. F.; Fina, M. W.; Falck, J. R.; Sperandio, V., Targeting QseC signaling and virulence for antibiotic development. *Science* **2008**, *321* (5892), 1078-1080.
34. Swem, L. R.; Swem, D. L.; Wingreen, N. S.; Bassler, B. L., Deducing Receptor Signaling Parameters from In Vivo Analysis: LuxN/AI-1 Quorum Sensing in *Vibrio harveyi*. *Cell* **2008**, *134* (3), 461-473.
35. Swem, L. R.; Swem, D. L.; O'Loughlin, C. T.; Gatmaitan, R.; Zhao, B.; Ulrich, S. M.; Bassler, B. L., A Quorum-Sensing Antagonist Targets Both Membrane-Bound and Cytoplasmic Receptors and Controls Bacterial Pathogenicity. *Mol. Cell* **2009**, *35* (2), 143-153.
36. Schauder, S.; Shokat, K.; Surette, M. G.; Bassler, B. L., The LuxS family of bacterial autoinducers: biosynthesis of a novel quorum-sensing signal molecule. *Mol. Microbiol.* **2001**, *41* (2), 463-476.

37. Chen, X.; Schauder, S.; Potier, N.; Van Dorsselaer, A.; Pelczar, I. n.; Bassler, B. L.; Hughson, F. M., Structural identification of a bacterial quorum-sensing signal containing boron. *Nature* **2002**, *415*, 545-549.
38. Miller, S. T.; Xavier, K. B.; Campagna, S. R.; Taga, M. E.; Semmelhack, M. F.; Bassler, B. L.; Hughson, F. M., Salmonella typhimurium Recognizes a Chemically Distinct Form of the Bacterial Quorum-Sensing Signal AI-2. *Mol. Cell* **2004**, *15* (5), 677-687.
39. Taga, M. E.; Miller, S. T.; Bassler, B. L., Lsr-mediated transport and processing of AI-2 in Salmonella typhimurium. *Mol. Microbiol.* **2003**, *50* (4), 1411-1427.
40. Xavier, K. B.; Bassler, B. L., Regulation of uptake and processing of the quorum-sensing autoinducer AI-2 in Escherichia coli. *J. Bacteriol.* **2005**, *187* (1), 238-248.
41. Xavier, K. B.; Miller, S. T.; Lu, W. Y.; Kim, J. H.; Rabinowitz, J.; Pelczar, I.; Semmelhack, M. F.; Bassler, B. L., Phosphorylation and processing of the quorum-sensing molecule autoinducer-2 in enteric bacteria. *ACS Chem. Biol.* **2007**, *2* (2), 128-136.
42. Xavier, K. B. B., B.L., Interference with AI-2-mediated bacterial cell-cell communication. *Nature* **2005**, *437*, 750-753.
43. Novak, E. A.; Shao, H.; Daep, C. A.; Demuth, D. R., Autoinducer-2 and QseC Control Biofilm Formation and In Vivo Virulence of Aggregatibacter actinomycetemcomitans. *Infect. Immun.* **2010**, *78* (7), 2919-2926.
44. Pereira, C. S.; McAuley, J. R.; Taga, M. E.; Xavier, K. B.; Miller, S. T., Sinorhizobium meliloti, a bacterium lacking the autoinducer-2 (AI-2) synthase, responds to AI-2 supplied by other bacteria. *Mol. Microbiol.* **2008**, *70* (5), 1223-1235.
45. Surette, M. G.; Miller, M. B.; Bassler, B. L., Quorum sensing in Escherichia coli, Salmonella typhimurium, and Vibrio harveyi: A new family of genes responsible for autoinducer production. *Proc. Natl. Acad. Sci. USA* **1999**, *96* (4), 1639-1644.
46. (a) Henke, J. M.; Bassler, B. L., Quorum sensing regulates type III secretion in Vibrio harveyi and Vibrio parahaemolyticus. *J. Bacteriol.* **2004**, *186* (12), 3794-3805; (b) Meighen, E. A., Bacterial Bioluminescence - Organization, Regulation, and Application of the Lux Genes. *FASEB J.* **1993**, *7* (11), 1016-1022.
47. (a) Neiditch, M. B.; Federle, M. J.; Miller, S. T.; Bassler, B. L.; Hughson, F. M., Regulation of LuxPQ receptor activity by the quorum-sensing signal autoinducer-2. *Mol. Cell* **2005**, *18* (5), 507-518; (b) Freeman, J. A.; Bassler, B. L., A genetic analysis of the function of LuxO, a two-component response regulator involved in quorum sensing in Vibrio harveyi. *Mol. Microbiol.* **1999**, *31* (2), 665-677.
48. Lilley, B. N.; Bassler, B. L., Regulation of quorum sensing in Vibrio harveyi by LuxO and Sigma-54. *Mol. Microbiol.* **2000**, *36* (4), 940-954.
49. Lenz, D. H.; Mok, K. C.; Lilley, B. N.; Kulkarni, R. V.; Wingreen, N. S.; Bassler, B. L., The small RNA chaperone Hfq and multiple small RNAs control quorum sensing in Vibrio harveyi and Vibrio cholerae. *Cell* **2004**, *118* (1), 69-82.
50. Pompeani, A. J.; Irgon, J. J.; Berger, M. F.; Bulyk, M. L.; Wingreen, N. S.; Bassler, B. L., The Vibrio harveyi master quorum-sensing regulator, LuxR, a TetR-type protein is both an activator and a repressor: DNA recognition and binding specificity at target promoters. *Mol. Microbiol.* **2008**, *70* (1), 76-88.

51. Higgins, D. A.; Pomianek, M. E.; Kraml, C. M.; Taylor, R. K.; Semmelhack, M. F.; Bassler, B. L., The major *Vibrio cholerae* autoinducer and its role in virulence factor production. *Nature* **2007**, *450* (7171), 883-886.
52. Sun, J. B.; Daniel, R.; Wagner-Dobler, I.; Zeng, A. P., Is autoinducer-2 a universal signal for interspecies communication: a comparative genomic and phylogenetic analysis of the synthesis and signal transduction pathways. *BMC Evol. Biol.* **2004**, *4*, -.
53. Rickard, A. H.; Palmer Jr, R. J.; Blehert, D. S.; Campagna, S. R.; Semmelhack, M. F.; Eglund, P. G.; Bassler, B. L.; Kolenbrander, P. E., Autoinducer 2: a concentration-dependent signal for mutualistic bacterial biofilm growth. *Mol. Microbiol.* **2006**.
54. McNab, R.; Ford, S. K.; El-Sabaeny, A.; Barbieri, B.; Cook, G. S.; Lamont, R. J., LuxS-based signaling in *Streptococcus gordonii*: Autoinducer 2 controls carbohydrate metabolism and biofilm formation with *Porphyromonas gingivalis*. *J. Bacteriol.* **2003**, *185* (1), 274-284.
55. Shao, H.; Lamont, R. J.; Demuth, D. R., Autoinducer 2 is required for Biofilm growth of *Aggregatibacter* (*Actinobacillus*) *actinomycetemcomitans*. *Infect. Immun.* **2007**, *75* (9), 4211-4218.
56. Yoshida, A.; Ansai, T.; Takehara, T.; Kuramitsu, H. K., LuxS-based signaling affects *Streptococcus mutans* biofilm formation. *Appl. Environ. Microbiol.* **2005**, *71* (5), 2372-2380.
57. Taga, M. E.; Semmelhack, J. L.; Bassler, B. L., The LuxS-dependent autoinducer AI-2 controls the expression of an ABC transporter that functions in AI-2 uptake in *Salmonella typhimurium*. *Mol. Microbiol.* **2001**, *42* (3), 777-793.
58. Ohtani, K.; Hayashi, H.; Shimizu, T., The luxS gene is involved in cell-cell signalling for toxin production in *Clostridium perfringens*. *Mol. Microbiol.* **2002**, *44* (1), 171-179.
59. Holmes, K.; Tavender, T. J.; Winzer, K.; Wells, J. M.; Hardie, K. R., AI-2 does not function as a quorum sensing molecule in *Campylobacter jejuni* during exponential growth in vitro. *BMC Microbiol.* **2009**, *9*, -.
60. Auger, S.; Krin, E.; Aymerich, S.; Gohar, M., Autoinducer 2 affects biofilm formation by *Bacillus cereus*. *Appl. Environ. Microbiol.* **2006**, *72* (1), 937-941.
61. Sela, S.; Frank, S.; Belausov, E.; Pinto, R., A mutation in the luxS gene influences *Listeria monocytogenes* biofilm formation. *Appl. Environ. Microbiol.* **2006**, *72* (8), 5653-5658.
62. Ali, S. A.; Benitez, J. A., Differential response of *Vibrio cholerae* planktonic and biofilm cells to autoinducer 2 deficiency. *Microbiol. Immunol.* **2009**, *53* (10), 582-586.
63. Brackman, G.; Celen, S.; Baruah, K.; Bossier, P.; Van Calenbergh, S.; Nelis, H. J.; Coenye, T., AI-2 quorum-sensing inhibitors affect the starvation response and reduce virulence in several *Vibrio* species, most likely by interfering with LuxPQ. *Microbiology* **2009**, *155* (12), 4114-4122.
64. Li, X.; Han, Y.; Yang, Q.; Zhang, X. H., Detection of quorum sensing signal molecules and mutation of luxS gene in *Vibrio ichthyenteri*. *Res. Microbiol.* **2010**, *161* (1), 51-57.
65. Kim, S. Y.; Lee, S. E.; Kim, Y. R.; Kim, C. M.; Ryu, P. Y.; Choy, H. E.; Chung, S. S.; Rhee, J. H., Regulation of *Vibrio vulnificus* virulence by the LuxS quorum-sensing system. *Mol. Microbiol.* **2003**, *48* (6), 1647-1664.

66. Zhang, M.; Sun, K.; Sun, L., Regulation of autoinducer 2 production and luxS expression in a pathogenic *Edwardsiella tarda* strain. *Microbiology-Sgm* **2008**, *154*, 2060-2069.
67. Doherty, N.; Holden, M. T. G.; Qazi, S. N.; Williams, P.; Winzer, K., Functional analysis of luxS in *Staphylococcus aureus* reveals a role in metabolism but not quorum sensing. *J. Bacteriol.* **2006**, *188* (8), 2885-2897.
68. Xu, L.; Li, H. L.; Vuong, C.; Vadyvaloo, V.; Wang, J. P.; Yao, Y. F.; Otto, M.; Gao, Q., Role of the luxS quorum-sensing system in biofilm formation and virulence of *Staphylococcus epidermidis*. *Infect. Immun.* **2006**, *74* (1), 488-496.
69. Li, M.; Villaruz, A. E.; Vadyvaloo, V.; Sturdevant, D. E.; Otto, M., AI-2-dependent gene regulation in *Staphylococcus epidermidis*. *BMC Microbiol.* **2008**, *8*, -.
70. Pecharki, D.; Petersen, F. C.; Scheie, A. A., LuxS and expression of virulence factors in *Streptococcus intermedius*. *Oral Microbiol. Immunol.* **2008**, *23* (1), 79-83.
71. Ahmed, N. A. A. M.; Petersen, F. C.; Scheie, A. A., AI-2 quorum sensing affects antibiotic susceptibility in *Streptococcus anginosus*. *J. Antimicrob. Chemother.* **2007**, *60* (1), 49-53.
72. Tannock, G. W.; Ghazally, S.; Walter, J.; Loach, D.; Brooks, H.; Cook, G.; Surette, M.; Simmers, C.; Bremer, P.; Dal Bello, F.; Hertel, C., Ecological behavior of *Lactobacillus reuteri* 100-23 is affected by mutation of the luxS gene. *Appl. Environ. Microbiol.* **2005**, *71* (12), 8419-8425.
73. Lebeer, S.; De Keersmaecker, S. C. J.; Verhoeven, T. L. A.; Fadda, A. A.; Marchal, K.; Vanderleyden, J., Functional analysis of luxS in the probiotic strain *Lactobacillus rhamnosus* GG reveals a central metabolic role important for growth and Biofilm formation. *J. Bacteriol.* **2007**, *189* (3), 860-871.
74. Dove, J. E.; Yasukawa, K.; Tinsley, C. R.; Nassif, X., Production of the signalling molecule, autoinducer-2, by *Neisseria meningitidis*: lack of evidence for a concerted transcriptional response. *Microbiology-Sgm* **2003**, *149*, 1859-1869.
75. Shen, F. F.; Hobley, L.; Doherty, N.; Loh, J. T.; Cover, T. L.; Sockett, R. E.; Hardie, K. R.; Atherton, J. C., In *Helicobacter pylori* auto-inducer-2, but not LuxS/MccAB catalysed reverse transsulphuration, regulates motility through modulation of flagellar gene transcription. *BMC Microbiol.* *10*, 15.
76. Schneider, R.; Lockett, C. V.; Johnson, D.; Belas, R., Detection and mutation of a luxS-encoded autoinducer in *Proteus mirabilis*. *Microbiology-Sgm* **2002**, *148*, 773-782.
77. Hubner, A.; Revel, A. T.; Nolen, D. M.; Hagman, K. E.; Norgard, M. V., Expression of a luxS gene is not required for *Borrelia burgdorferi* infection of mice via needle inoculation. *Infect. Immun.* **2003**, *71* (5), 2892-2896.
78. Hardie, K. R.; Heurlier, K., Establishing bacterial communication by 'word of mouth': LuxS and autoinducer 2 in biofilm development. *Nat. Rev. Microbiol.* **2008**, *6*, 635-643.
79. Vendeville, A.; Winzer, K.; Heurlier, K.; Tang, C. M.; Hardie, K. R., Making 'sense' of metabolism: autoinducer-2, LUXS and pathogenic bacteria. *Nat. Rev. Microbiol.* **2005**, *3* (5), 383-396.
80. Parveen, N.; Cornell, K. A., Methylthioadenosine/S-adenosylhomocysteine nucleosidase, a critical enzyme for bacterial metabolism. *Mol. Microbiol.* **2011**, *79* (1), 7-20.

81. Heurlier, K.; Vendeville, A.; Halliday, N.; Green, A.; Winzer, K.; Tang, C. M.; Hardie, K. R., Growth Deficiencies of *Neisseria meningitidis* pfs and luxS Mutants Are Not Due to Inactivation of Quorum Sensing. *J. Bacteriol.* **2009**, *191* (4), 1293-1302.
82. De Keersmaecker, S. C. J.; Varszegi, C.; van Boxel, N.; Habel, L. W.; Metzger, K.; Daniels, R.; Marchal, K.; De Vos, D.; Vanderleyden, J., Chemical synthesis of (S)-4,5-dihydroxy-2,3-pentanedione, a bacterial signal molecule precursor, and validation of its activity in *Salmonella typhimurium*. *J. Biol. Chem.* **2005**, *280* (20), 19563-19568.
83. Duan, K. M.; Dammel, C.; Stein, J.; Rabin, H.; Surette, M. G., Modulation of *Pseudomonas aeruginosa* gene expression by host microflora through interspecies communication. *Mol. Microbiol.* **2003**, *50* (5), 1477-1491.
84. Tavender, T. J.; Halliday, N. M.; Hardie, K. R.; Winzer, K., LuxS-independent formation of AI-2 from ribulose-5-phosphate. *BMC Microbiol.* **2008**, *8* (1), 98.
85. (a) Alfaro, J. F.; Zhang, T.; Wynn, D. P.; Karschner, E. L.; Zhou, Z. S., Synthesis of LuxS Inhibitors Targeting Bacterial Cell-Cell Communication. *Org. Lett.* **2004**, *6* (18), 3043-3046; (b) Gopishetty, B.; Zhu, J.; Rajan, R.; Sobczak, A. J.; Wnuk, S. F.; Bell, C. E.; Pei, D., Probing the Catalytic Mechanism of S-Ribosylhomocysteinase (LuxS) with Catalytic Intermediates and Substrate Analogues. *J. Am. Chem. Soc.* **2009**, *131* (3), 1243-1250.
86. Lowery, C. A.; McKenzie, K. M.; Qi, L.; Meijler, M. M.; Janda, K. D., Quorum sensing in *Vibrio harveyi*: probing the specificity of the LuxP binding site. *Biorg. Med. Chem. Lett.* **2005**, *15* (9), 2395-2398.
87. Frezza, M.; Soulère, L.; Balestrino, D.; Gohar, M.; Deshayes, C.; Queneau, Y.; Forestier, C.; Doutheau, A., Ac2-DPD, the bis-(O)-acetylated derivative of 4,5-dihydroxy-2,3-pentanedione (DPD) is a convenient stable precursor of bacterial quorum sensing autoinducer AI-2. *Biorg. Med. Chem. Lett.* **2007**, *17* (5), 1428-1431.
88. Frezza, M.; Balestrino, D.; Soulère, L.; Reverchon, S.; Queneau, Y.; Forestier, C.; Doutheau, A., Synthesis and Biological Evaluation of the Trifluoromethyl Analog of (4S)-4,5-Dihydroxy-2,3-pentanedione (DPD). *Eur. J. Org. Chem.* **2006**, *2006* (20), 4731-4736.
89. Frezza, M.; Soulère, L.; Queneau, Y.; Doutheau, A., A Baylis-Hillman/ozonolysis route towards (\pm) 4,5-dihydroxy-2,3-pentanedione (DPD) and analogues. *Tetrahedron Lett.* **2005**, *46* (38), 6495-6498.
90. Lowery, C. A.; Park, J.; Kaufmann, G. F.; Janda, K. D., An Unexpected Switch in the Modulation of AI-2-Based Quorum Sensing Discovered through Synthetic 4,5-Dihydroxy-2,3-pentanedione Analogues. *J. Am. Chem. Soc.* **2008**, *130*, 9200-9201.
91. Ni, N.; Choudhary, G.; Li, M.; Wang, B., Pyrogallol and its analogs can antagonize bacterial quorum sensing in *Vibrio harveyi*. *Biorg. Med. Chem. Lett.* **2008**, *18* (5), 1567-1572.
92. Ni, N.; Chou, H.; Wang, J.; Li, M.; Lu, C.; Tai, P.; Wang, B., Identification of boronic acids as antagonists of bacterial quorum sensing in *Vibrio harveyi*. *Biochem. Biophys. Res. Commun.* **2008**, *369* (2), 590-594.
93. Ni, N. T.; Choudhary, G.; Li, M. Y.; Wang, B. H., A new phenothiazine structural scaffold as inhibitors of bacterial quorum sensing in *Vibrio harveyi*. *Biochem. Biophys. Res. Commun.* **2009**, *382* (1), 153-156.

94. Semmelhack, M. F.; Campagna, S. R.; Hwa, C.; Federle, M. J.; Bassler, B. L., Boron Binding with the Quorum Sensing Signal AI-2 and Analogues. *Org. Lett.* **2004**, *6* (15), 2635-2637.
95. Meijler, M. M.; Hom, L. G.; Kaufmann, G. F.; McKenzie, K. M.; Sun, C.; Moss, J. A.; Matsushita, M.; Janda, K. D., Synthesis and Biological Validation of a Ubiquitous Quorum-Sensing Molecule. *Angew. Chem. Int. Ed.* **2004**, *43*, 2106-2108.
96. Semmelhack, M. F.; Campagna, S. R.; Federle, M. J.; Bassler, B. L., An Expedient Synthesis of DPD and Boron Binding Studies. *Org. Lett.* **2004**, *7* (4), 569-572.
97. Smith, J. A. I.; Wang, J.; Mau-Nguyen, S.-M.; Lee, V.; Sintim, H. O., Biological screening of a diverse set of AI-2 analogues in *Vibrio harveyi* suggests that receptors which are involved in synergistic agonism of AI-2 and analogues are promiscuous. *Chem. Commun.* **2009**, 7033-7035.
98. (a) Arndt, F., Diazomethane. *Organic Syntheses* **1943**, *2*, 165-167; (b) Scott, L. T., Sumpter, C.A., Diazo ketone cyclization onto a benzene ring: 3,4-dihydro-1(2H)-azulenone. *Org. Synth.* **1990**, *69*, 180-7.
99. Wenkert, E., McPherson, C.A., Condensations of Acyldiazomethanes with Aldehydes, Ketones, and Their Derivatives. *J. Am. Chem. Soc.* **1972**, *94* (23), 8084-8090.
100. Jiang, N., Wang, J., DBU-promoted condensation of acyldiazomethanes to aldehydes and imines under catalytic conditions. *Tetrahedron Lett.* **2002**, *43*, 1285-1287.
101. Roy, V.; Smith, J. A. I.; Wang, J.; Stewart, J. E.; Bentley, W. E.; Sintim, H. O., Synthetic Analogs Tailor Native AI-2 Signaling Across Bacterial Species. *J. Am. Chem. Soc.* **2010**, *132*, 11141-11150.
102. Bassler, B. L.; Greenberg, E. P.; Stevens, A. M., Cross-species induction of luminescence in the quorum-sensing bacterium *Vibrio harveyi*. *J. Bacteriol.* **1997**, *179* (12), 4043-4045.
103. Neiditch, M. B.; Federle, M. J.; Pompeani, A. J.; Kelly, R. C.; Swem, D. L.; Jeffrey, P. D.; Bassler, B. L.; Hughson, F. M., Ligand-induced asymmetry in histidine sensor kinase complex regulates quorum sensing. *Cell* **2006**, *126* (6), 1095-1108.
104. Jobling, M. G.; Holmes, R. K., Characterization of hapR, a positive regulator of the *Vibrio cholerae* HA protease gene hap, and its identification as a functional homologue of the *Vibrio harveyi* luxR gene. *Mol. Microbiol.* **1997**, *26* (5), 1023-1034.
105. Croxatto, A.; Chalker, V. J.; Lauritz, J.; Jass, J.; Hardman, A.; Williams, P.; Camara, M.; Milton, D. L., VanT, a homologue of *Vibrio harveyi* LuxR, regulates serine, metalloprotease, pigment, and biofilm production in *Vibrio anguillarum*. *J. Bacteriol.* **2002**, *184* (6), 1617-1629.
106. McCarter, L. L., OpaR, a homolog of *Vibrio harveyi* LuxR, controls opacity of *Vibrio parahaemolyticus*. *J. Bacteriol.* **1998**, *180* (12), 3166-3173.
107. Lee, D. H.; Jeong, H. S.; Jeong, H. G.; Kim, K. M.; Kim, H.; Choi, S. H., A consensus sequence for binding of SmcR, a *Vibrio vulnificus* LuxR homologue, and genome-wide identification of the SmcR regulon. *J. Biol. Chem.* **2008**, *283* (35), 23610-23618.
108. Fidopiastis, P. M.; Ruby, E. G., LitR, a newly described transcriptional activator homologue, regulates symbiotic light organ colonization by *Vibrio fischeri*. *Abstracts of the General Meeting of the American Society for Microbiology* **2001**, *101*, 503.

109. Waters, C. M.; Bassler, B. L., The *Vibrio harveyi* quorum-sensing system uses shared regulatory components to discriminate between multiple autoinducers. *Genes Dev.* **2006**, *20* (19), 2754-2767.
110. Ganin, H.; Tang, X.; Meijler, M. M., Inhibition of *Pseudomonas aeruginosa* quorum sensing by AI-2 analogs. *Biorg. Med. Chem. Lett.* **2009**, *19* (14), 3941-3944.
111. Miller, J., *Experiments in molecular genetics*. Cold Spring Harbor. Cold Spring Harbor Laboratory, N.Y.: 1972.
112. Xue, T.; Zhao, L. P.; Sun, H. P.; Zhou, X. X.; Sun, B. L., LsrR-binding site recognition and regulatory characteristics in *Escherichia coli* AI-2 quorum sensing. *Cell Res.* **2009**, *19* (11), 1258-1268.
113. (a) Backhed, F.; Ley, R. E.; Sonnenburg, J. L.; Peterson, D. A.; Gordon, J. I., Host-bacterial mutualism in the human intestine. *Science* **2005**, *307* (5717), 1915-20; (b) Grice, E. A.; Kong, H. H.; Conlan, S.; Deming, C. B.; Davis, J.; Young, A. C.; Bouffard, G. G.; Blakesley, R. W.; Murray, P. R.; Green, E. D.; Turner, M. L.; Segre, J. A., Topographical and temporal diversity of the human skin microbiome. *Science* **2009**, *324* (5931), 1190-2; (c) Keller, L.; Surette, M. G., Communication in bacteria: an ecological and evolutionary perspective. *Nat Rev Microbiol* **2006**, *4* (4), 249-58.
114. Davies, D.; Parsek, M.; Pearson, J.; Iglewski, B.; Costerton, J.; Greenberg, E., The involvement of cell-to-cell signals in the development of a bacterial biofilm. *Science* **1998**, 295-298.
115. Costerton, J.; Stewart, P.; Greenberg, E., Bacterial biofilms: A common cause of persistent infections. *Science* **1999**, 1318-1322.
116. Chun, C. K., Inactivation of a *Pseudomonas aeruginosa* quorum-sensing signal by human airway epithelia. *Proc. Natl. Acad. Sci.* **2004**, *101* (10), 3587-3590.
117. Zhu, J. G.; Pei, D. H., A LuxP-based fluorescent sensor for bacterial autoinducer II. *ACS Chem. Biol.* **2008**, *3* (2), 110-119.
118. Shah, K., Orthogonal chemical genetic approaches for unraveling signaling pathways. *IUBMB Life* **2005**, *57* (6), 397-405.